Drosophila Information Service

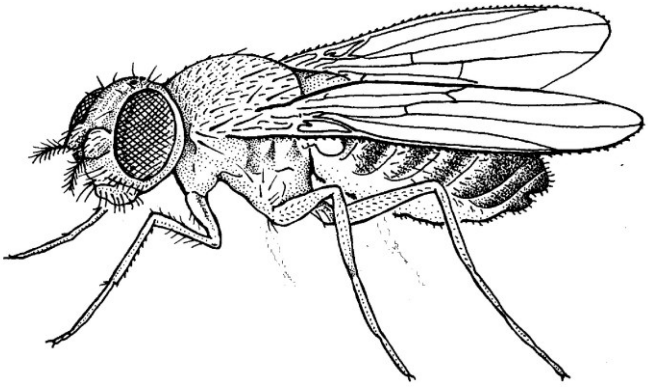

Number
105

December 2022

Prepared at the
Department of Biology
University of Oklahoma
Norman, OK 73019 U.S.A.

Preface

Drosophila Information Service (often called "DIS" by those in the field) was first printed in March, 1934. For those first issues, material contributed by *Drosophila* workers was arranged by C.B. Bridges and M. Demerec. As noted in its preface, which is reprinted in Dros. Inf. Serv. 75 (1994), Drosophila Information Service was undertaken because, "An appreciable share of credit for the fine accomplishments in *Drosophila* genetics is due to the broadmindedness of the original *Drosophila* workers who established the policy of a free exchange of material and information among all actively interested in *Drosophila* research. This policy has proved to be a great stimulus for the use of *Drosophila* material in genetic research and is directly responsible for many important contributions." Since that first issue, DIS has continued to promote open communication.

Except for the special issues that contained mutant and stock information now provided in detail by FlyBase and similar material in the annual volumes, all issues are now freely-accessible from our web site: www.ou.edu/journals/dis. For rare early issues that exist as aging typed or mimeographed copies, some notes and announcements have not yet been fully brought on line. But we intend to fill in those gaps for historical purposes in the future. Printed copies of recent annual issues can be obtained from www.lulu.com.

We continue to encourage all researchers to consider submitting articles that use *Drosophila* for teaching as well as articles that report new techniques, research results, and interesting new mutations. In the interests of honoring the long-standing philosophy of open exchange of ideas, we sometimes accept articles that have unusual or limited perspectives. We thank the many contributors from around the world who sent material for this issue, and we invite your submissions for future annual issues as well as any suggestions you have for maintaining this as a useful *Drosophila* research community resource.

James N. Thompson, jr., Editor
David Ross Boyd Professor of Biology
Department of Biology
University of Oklahoma, Norman

Jenna J. Hellack, Associate Editor
Department of Biology, Emeritus
University of Central Oklahoma, Edmond
Department of Biology, Adjunct Professor
University of Oklahoma, Norman

Contributions and Inquiries should be sent to:

James N. Thompson, jr., Department of Biology, University of Oklahoma, Norman, OK 73019; Phone: (405) 325-2001 or (405) 325-4821, FAX (405) 325-6202, email: jthompson@ou.edu

Printed copies of the recent volumes can be ordered from www.lulu.com.

List of Contributions

General Announcements

Research Notes

Other Reports

Research Notes

Mutagenic activities of seeds of *Hyoscyamus niger* L. in somatic cells of *Drosophila in vivo* conditions.

Uysal, H.,* and Ş. Lokumcu. Department of Biology, Faculty of Science, Atatürk University, 2540, Erzurum, Turkey; *Corresponding author; E-mail: hauysal@atauni.edu.tr

Introduction

It is known that many of the drugs used for centuries due to their medicinal and recreational properties are of herbal origin. Apart from solving health problems, these psychoactive plants taken into the body cause temporary changes in mood, perception, and behavior, leading to addiction (Uysal and Bayam, 2021). *Hyoscyamus niger* L., belonging to the Solanaceae family, is a cosmopolitan plant species with these features. *H. niger,* which is widespread in the world and our country, is also an important medicinal plant used in the treatment of diseases. This plant species has calming, stimulating, and pain-relieving effects. It is especially preferred in Tibetan medicine as an antitumor, anthelmintic, and antipyretic, and in Chinese medicine as a stomachache, stomach cramps, and cough suppressant (Begum *et al.*, 2010). According to Hong *et al.* (2010), it is also used in the treatment of renal colic due to stones in the urinary tract.

However, when the seeds and leaves of *H. niger* are taken into the body in high amounts by humans, symptoms such as dry mouth, constipation, behavioral disorder, and hallucinations occur (Erkal *et al.*, 2006; Alizadeh *et al.*, 2014). It was reported in a case report that a 23-year-old and 32-week pregnant woman had complaints such as nausea, vomiting, speech disorder, and tachycardia as a result of accidentally consuming the *H. niger* plant instead of lettuce (Karadaş *et al.*, 2012). Similarly, Collak *et al.* (2015) stated in a case report that a 7-year-old girl had complaints such as inconsistent behavior, dry mouth, and vision problems as a result of accidentally consuming *H. niger*.

In another study, it was investigated whether methanol extracts prepared from flowers, stems, and leaves of *H. niger* were lethal on the larvae of *Culex* spp. and the flower, leaf, and stem extracts were found to be larvicidal, respectively (Baharshahi *et al.*, 2017). In another study by Behravan *et al.* (2017), methanol extracts prepared from the root, stem, leaves, and flowers of *H. niger* were applied to the larvae of *Anopheles* spp. According to the data obtained, the flower extract was found to have the highest insecticidal effect. It was also found that the extract prepared from the seeds of *H. niger* caused a lethal effect on *Lucillia sericata* larvae (Akkol *et al.*, 2020).

In the present study, it was investigated whether water (HN_{wtr}) and methanol (HN_{met}) extracts of *H. niger*, which causes different symptoms in case of intentional or unintentional use among the public, and have larvicidal and insecticidal effects in animal organisms, have genotoxic effects or not, in *Drosophila* by the somatic mutation and recombination test (SMART).

Material and Method

The plant used in the study

H. niger, used in the study, was collected from Pasinler town of Erzurum province (geographical position; 40.023718 N, 41.593414 E) during the flowering period. The seeds of this plant were left to dry at room temperature (22-24°C) and in a dark environment without sunlight.

Drosophila *strains and laboratory condition*

In our study, *mwh (mwh/mwh)* and *flr^3 (flr^3 /In (3LR) TM3, BdS*) mutant strains of *Drosophila* have been used. These mutant strains carry determinant genes. Of these determinant genes, the *flare (flr^3*, 3-38.8)

gene forms dulled, point-like hair instead of the normal long and straight feathers on the wings. Since the *flare* gene in its homozygote state causes lethal effects in the embryonic stage, it is used together with the stabilizing *TM3* chromosome to protect individuals from the embryonic lethal effects of the *flare* gene and to suppress the recombination. The other determinant gene *mwh* (*mwh,* 3-0.3) shows itself by causing the wing hair to come out as three or more from the same cell.

These mutant strains had been maintained for many years in the Genetic Research Laboratory at the Department of Biology, Ataturk University, Erzurum/Türkiye. All control and application groups were kept in our laboratory heated-cooled ovens (25 ± 1°C), %60 relative humidity, and a permanent dark environment in a Standard Drosophila Medium (SDM) composed of maize flour, agar, sucrose, dried yeast, and propionic acid.

Adult individuals of both mutant strains were crossed into separate culture flasks to obtain offspring (Uysal *et al.,* 2006). F_1 individuals obtained following metamorphosis were collected in 4-hour periods for 3 days and males and females were kept in separate bottles. Then, trans-heterozygous individuals were obtained by crossing *flr*^{3} female and *mwh* male. The genotypic representation of the crosses is as follows:

P: *flr*^{3} */In (3LR) TM3, BdS* ♀♀ × *mwh/mwh* ♂♂

Performing the somatic mutation and recombination test (SMART) and evaluating the results

For this test, distilled water and 1% DMSO, the solvent of plant extracts, were used as the negative control group, and ethyl methanesulfonate (EMS), known to be genotoxic, as the positive control group. Apart from the control groups, different concentrations (10, 20, 30, and 40 ppm) of herbal extracts (HN_{wtr} and HN_{met}) were added to the culture bottles containing *Drosophila* Instant Medium (DIM), and application groups were formed. Then, 100 trans-heterozygous larvae were placed in the nutrient medium of the control and treatment groups, separately. Adult individuals obtained from trans-heterozygous larvae completing metamorphosis were divided into two groups according to their wing phenotypes normal and serrate winged. Then, normal and serrate wing preparations belonging to each group were prepared separately. The wings in all the preparations of the control and treatment groups were examined and it was examined whether mutant clones were formed. Mutant clones observed in the treatment groups of plant extracts were counted and recorded. Mutant clones are also classified as small single spot (SSS), large single spot (LSS), and twin clones (Graf *et al.,*1984).

The statistical analysis

Statistical analysis of the results obtained from the SMART method was performed with the Microsta computer program. The results of the original and alternative hypotheses calculated with Microsta were evaluated according to the multiple-decision procedure of Frei and Würgler (1988).

Preparation of methanol extract

The seeds of *H. niger*, which were dried at room temperature, were weighed 25 g, then kept in 200 ml of methanol for 24 hours and filtered with filter paper. *H. niger* methanol extract (HN_{met}) was obtained by using a soxhlet extractor at 50°C to separate methanol from this filtrate. This extract was stored in a sterile glass bottle at +4°C until used.

Preparation of water extract

Pure water at 60-80°C was added to the *H. niger* seeds placed in an Erlenmeyer flask and it was waited for this temperature to decrease to 21-24°C. Then, the water in the filtrate was removed by the lyophilization method. This extract (HN_{wtr}) was stored in a sterile bottle at -18°C in the refrigerator.

Results

As a result of our experimental study, 9 SSS and 2 LSS were observed in the DMSO negative control group, while only 8 SSS were observed in the distilled water control group. In the EMS-positive control group, 27 SSS, 11 LSS, and 8 twin spots were seen, respectively. According to the data obtained from the EMS positive control group, the clone induction frequency was calculated as 1.94 (Table 1). When the

negative control groups (distilled water and DMSO) were compared with the EMS positive control group, the results were found to be statistically positive and effective (+).

It was observed that the number of mutant clones increased in all HN_{wtr} treatment groups compared to the DMSO control group (Table 1). While 12 SSS and 3 LSS were observed for the normal wing phenotype (*mwh/flr*^{3}) in the 10 ppm HN_{wtr} application group, 16 SSS and 4 LSS were observed in the 40 ppm application. The data obtained for 10 ppm were found to have a statistically insignificant effect (i). Although the number of mutant clones increased in the 40 ppm application group, only a statistically positive effect (+) was determined for total *mwh* spots and total spots (Table 1). In serrate wing phenotype (*mwh/TM3*), values close to the DMSO control group were obtained for mutant clones, and these results were found to be statistically insignificant (i) (Table 1). Mutant clones were also observed in the serrate wing phenotype (*mwh/TM3*) depending on HN_{wtr} treatment. However, since the number of mutant clones was almost the same as the DMSO control groups, it was found to be statistically insignificant (i).

Table 1. Wing spot test data obtained after exposure to HN_{wtr}.

Application groups (ppm)	Number of wings	SSS (1-2 cell)			LSS (>2cell)			Twin spots			Total *mwh* spots			Total spots			CIF
		No	Fr.	D	No	Fr.	D	No	Fr.	D	No	Fr.	D	No	Fr.	D	
Normal wing (*mwh/flr*^{3})																	
Control (distilled water)	80	8	(0.10)		0	(0.00)		0	(0.00)		8	(0.10)		8	(0.10)		0,40
DMSO (%1)	80	9	(0.11)	i	2	(0.02)	i	0	(0.00)	-	11	(0.13)	i	11	(0.13)	i	0,56
EMS (1 ppm)	80	27	(0.33)	+	11	(0.13)	+	8	(0.10)	+	38	(0.47)	+	46	(0.57)	+	1,94
10 ppm	80	12	(0.15)	i	3	(0.03)	i	0	(0.00)	-	15	(0.18)	i	15	(0.18)	i	0,76
20 ppm	80	13	(0.16)	i	3	(0.03)	i	0	(0.00)	-	16	(0.20)	i	16	(0.20)	i	0,81
30 ppm	80	15	(0.18)	i	3	(0.03)	i	0	(0.00)	-	18	(0.22)	+	18	(0.22)	+	0,92
40 ppm	80	16	(0.20)	i	4	(0.05)	i	0	(0.00)	-	20	(0.25)	+	20	(0.25)	+	1,02
Serrate wing (*mwh/TM3*)																	
Control (distilled water)	80	6	(0.07)		0	(0.00)					6	(0.07)		6	(0.07)		0.30
DMSO (%1)	80	8	(0.10)	i	1	(0.01)	i				9	(0.11)	i	9	(0.11)	i	0.46
EMS (1 ppm)	80	20	(0.25)	+	6	(0.07)	+	Balancer chromosome *TM3* does not carry the *flr*^{3} mutation			26	(0.32)	+	26	(0.32)	+	1.33
10 ppm	80	5	(0.06)	i	0	(0.00)	-				5	(0.06)	i	5	(0.06)	i	0.25
20 ppm	80	6	(0.07)	i	0	(0.00)	-				6	(0.07)	i	6	(0.07)	i	0.30
30 ppm	80	7	(0.08)	i	0	(0.00)	-				7	(0.08)	i	7	(0.08)	i	0.35
40 ppm	80	8	(0.10)	i	1	(0.01)	i				9	(0.11)	i	9	(0.11)	i	0.46

No: Number of clones, Fr: Frequency, D: statistical analysis according to Frei and Würgler (1988); +: positive; –: negative; i: inconclusive; m: multiplication factor; probability levels $\alpha = \beta = 0.05$, CIF: Frequency of clone formation per 10^5 cell.

HN_{met} extract applied at different doses also caused an increase in the number of mutant clones in the normal wing phenotype *(mwh/flr*^{3}*)*. While only 9 SSS and 2 LSS were observed in the DMSO control group, 13 SSS and 6 LSS mutant clones were observed in the highest HN_{met} application group (40 ppm). Although the number of SSS mutant clones increased in all treatment groups, this was found to be statistically insignificant (i). As seen in Table 2, the number of LSS mutant clones also increased compared to the DMSO control group. However, this increase was found to be positive (+) effective only in the 40 ppm application group. In the serrate wing phenotype (*mwh/TM3*), mutant clone results obtained from all HN_{met} treatment groups were close to the DMSO control group (Table 2). Therefore, statistical evaluations were found to be insignificant (i).

Table 2. Wing spot test data obtained after exposure to HN_{met}.

Application groups (ppm)	Number of wings	SSS (1-2cell)			LSS (>2 cell)			Twin spots			Total *mwh* spots			Total spots			CIF
		No	Fr.	D	No	Fr.	D	No	Fr.	D	No	Fr.	D	No	Fr.	D	
Normal wing (*mwh/flr*^{3})																	
Control (distilled water)	80	8	(0.10)		0	(0.00)		0	(0.00)		8	(0.10)		8	(0.10)		0.40
DMSO (%1)	80	9	(0.11)	i	2	(0.02)	i	0	(0.00)	-	11	(0.13)	i	11	(0.13)	i	0.56
EMS (1 ppm)	80	27	(0.33)	+	11	(0.13)	+	8	(0.10)	+	38	(0.47)	+	46	(0.57)	+	1.94
10 ppm	80	12	(0.15)	i	1	(0.01)	i	0	(0.00)	-	13	(0.16)	i	13	(0.16)	i	0.66
20 ppm	80	12	(0.15)	i	4	(0.05)	i	0	(0.00)	-	16	(0.20)	i	16	(0.20)	i	0.81
30 ppm	80	13	(0.16)	i	3	(0.03)	i	2	(0.02)	i	16	(0.20)	i	18	(0.22)	+	0.81
40 ppm	80	13	(0.16)	i	6	(0.07)	+	1	(0.01)	i	19	(0.23)	+	20	(0.25)	+	0.97
Serrate wing (*mwh/TM3*)																	
Control (distilled water)	80	6	(0.07)		0	(0.00)					6	(0.07)		6	(0.07)		0.30
DMSO (%1)	80	8	(0.10)	i	1	(0.01)	i				9	(0.11)	i	9	(0.11)	i	0.46
EMS (1 ppm)	80	20	(0.25)	+	6	(0.07)	+	Balancer chromosome *TM3* does not carry the *flr*^{3} mutation			26	(0.32)	+	26	(0.32)	+	1.33
10 ppm	80	4	(0.05)	i	0	(0.00)	-				4	(0.05)	i	4	(0.05)	i	0.20
20 ppm	80	6	(0.07)	i	0	(0.00)	-				6	(0.07)	i	6	(0.07)	i	0.30
30 ppm	80	7	(0.08)	i	0	(0.00)	-				7	(0.08)	i	7	(0.08)	i	0.35
40 ppm	80	8	(0.10)	i	0	(0.00)	-				8	(0.10)	i	8	(0.10)	i	0.40

No: Number of clones, Fr: Frequency, D: statistical analysis according to Frei and Würgler (1988); +: positive; –: negative; i: inconclusive; m: multiplication factor; probability levels $\alpha = \beta = 0.05$, CIF: Frequency of clone formation per 10^5 cell.

Discussion

The use of plants to eliminate health problems in humans is considered among the traditional treatment methods. *H. niger,* which spreads in large areas, is also used by people as a bladder relaxant, antispasmodic, anticarcinogenic, anticholinergic, and sedative. Due to such effects, it is considered a "medicinal plant". In some Central European countries, this plant species is also used in the treatment of neurodegenerative diseases such as Parkinson's, Alzheimer's, and dementia (Banjari *et al*., 2018).

However, *H. niger* can be toxic when consumed unconsciously. It is also used as a recreational drug due to its narcotic effect. In a case report, it was stated that a 65-year-old woman had complaints such as drowsiness, tachycardia, and hallucinations as a result of accidental consumption by *H. niger* (Shams *et al.*, 2017). It can also cause dizziness, nausea, and even vomiting. Again, a 65-year-old woman who consumed *H. niger* seeds against hemorrhoids had behavioral disorders, self-talk, and insomnia complaints (Atay and Seçkin, 2011). In a study conducted by Bayam and Uysal (2021), it was observed that the extracts of this plant increased the micronucleus frequency in human lymphocyte cells. It was observed that cellular viability was lost when the extract prepared from the aerial parts of *H. niger* was applied to different cancer cell lines (Ismeel, 2011). In the present study, it was determined that water and methanol extracts of *H. niger* caused somatic mutations in *D. melanogaster* by stimulating the genotoxic effect. We think that the increase in mutant clones observed in the wings of *D. melanogaster* is due to the alkaloids found in both extracts of *H. niger* (Table 1 and Table 2). The alkaloids found in *H. niger* lead to the formation of reactive oxygen species (ROS), which cause damage to biomolecules. Oxidative stress that may occur due to ROS may also cause genotoxic effects and somatic mutations.

References: Akkol, E.K., M. Ilhan, E. Kozan, F.T.G. Dereli, M. Sak, and E. Sobarzo-Sanchez 2020, Plants 9 (5): 1-10; Alizadeh, A., M. Moshiri, J. Alizadeh, and M. Balali-Mood 2014, Avicenna Journal of Phytomedicine 4 (5): 297-311; Atay, I.M., and D. Seçkin 2011, Journal of Academic Emergency Medicine Case Reports 2 (2): 48-50; Baharshahi, A., M. Vaezi-Kakhki, B. Mahdavi, and M.R. Behravan 2017, Pars Journal of Medical Sciences 14 (4): 25-32; Banjari, I., T. Marcek, S. Tomic, and V.Y. Waisundara 2018, Mini

Review 5 (95): 1-9; Begum, S., B. Saxena, M. Goyal, R. Ranjan, V.B. Joshi, C.V. Rao, S. Krishnamurthy, and M. Sahai 2010, Fitoterapia 81 (3): 178-184; Behravan, M.R., A. Baharshahi, M. Vaezi-Kakhki, and A. Naghizadeh 2017, Archives of Hygiene Sciences 6 (3): 288-293; Collak, Z., D. Kara, E.U. Karaman, F. Karakoc, and A. Collak 2015, Journal of Advances in Medicine and Medical Research 11 (6): 1-3; Erkal, H., Y. Özyurt, and Z. Arıkan 2006, Turkish Journal of Geriatrics 9 (3): 188-191; Frei, H., and F.E. Würgler 1988, Mutation Research 203: 297-308; Graf, U., F.E. Würgler, A.J. Katz, H. Frei, H. Juon, C.B. Hall, and P.G. Kale 1984, Environmental and Molecular Mutagenesis 6: 153-188; Hong, M.L.K., A. Bhatt, N. Shuping, and C.L. Keng 2010, Journal of Medicinal Plants Research 4 (24): 2710-2718; Ismeel, A.O., 2011, Cytogenetic and cytotoxic studies on the effect of phytoinvestigated active compounds of *Hyoscyamus niger*. Doctoral Thesis, University of Al-Nahrian, Baghdat, Iraq; Karadaş, S., A. Güler, M. Şahin, and L. Behçet 2012, Van Tıp Dergisi 19 (1): 36-38; Shams, T.A., S. Gosselin, and R. Chuang 2017, Toxicology Communications 1 (1): 37-40; Uysal, H., and H. Bayam 2021, Journal of TUBAV Science 14 (2): 1-12; Uysal, H., T. Şişman, and H. Aşkın 2006, *Drosophila* Biyolojisi ve Çaprazlama Yöntemleri. Atatürk Üniversitesi Yayınları, ISBN: 975-442-111-0.

Stigmasterol-induced acute and chronic toxicity, one of the plant sterols, in *Drosophila melanogaster* Oregon-R wild strain by *in vivo* longevity test.

Uysal, H. Genetic Research Laboratory**,** Department of Biology, Faculty of Science, Atatürk University, 25240 Erzurum,Türkiye; Email: hauysal@atauni.edu.tr

Introduction

Bioactive components found in plant organisms are secondary metabolites that have various functions in plant growth and development. Secondary metabolites impart plant-specific color, taste, and odor characteristics. In addition, these metabolites provide protective properties for plants against bacteria, viruses, fungi, and pests.

Bioactive substances are compounds with different chemical functions and structures. According to their structures, they are divided into some subgroups such as carotenoids, phenolic compounds, flavonoids, stilbenes, glucosinolates, lignans, organosulfur compounds, and plant sterols (Uyar and Sürücüoğlu, 2010). Plant sterols/stanols (phytosterols), one of these groups, are compounds similar to cholesterol found in almost all plants (Kyçyk *et al.,* 2016). Sterols are synthesized and stored as secondary metabolites and have no nutritional value. However, they are also defined as a group of bioactive compounds in steroid structure that show beneficial effects for health when consumed with daily nutrition.

Plant sterols are found naturally in silverberry oil, corn oil, olive oil, soybean oil, cereals, legumes, nuts, vegetables, and fruits (Li, 2006). It is used as a bioactive compound in functional foods (functional foods are foods produced by the use of one or more of a wide variety of bioactive factors) due to its cholesterol-lowering properties, especially in terms of human health. Plant sterols are also used in medicine and cosmetics for different purposes (Ostlund *et al*., 2003). Studies have shown that there are more than 200 types of phytosterols. Campesterol, cholesterol, brasicasterol, ergosterol, sitosterol, sitostanol and stigmasterol are the main phytosterols (Pennington and Douglas, 2005). One of the plant sterols, stigmasterol is also a kind of triterpene. The chemical structure of stigmasterol (Synonyms: Stigmasterin, Wulzen factor, Stigmasta-5,22-dien-3β- ol, $C_{29}H_{48}O$) is given in Figure 1.

Bioactive components are compounds that can directly react with free radicals and prevent them from reacting with other cell components (Nie *et al.,* 2001). However, these components can also act as enzyme inhibitors, inhibitors of receptor activity, and gene expression (Kris-Etherton *et al.,* 2004).

In this study, whether stigmasterol (STG) one of the phytosterols, is a biotoxic agent in acute and chronic applications, depending on the dose-time interaction, was investigated by *in vivo* longevity test using the wild strain of *Drosophila melanogaster* Oregon-R.

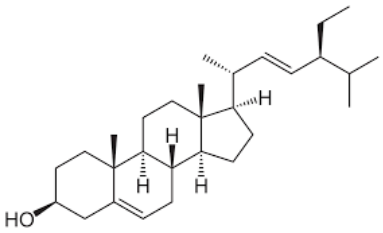

Figure 1. The chemical structure of stigmasterol.

Materials and Methods

Organisms used in experiments and the application of STG to adults ♀♀ and ♂♂ *individuals*

The Oregon-R strain (Diptera: Drosophilidae) of *D. melanogaster* used in our experiments is a wild-type strain and has been an inbred homogeneous stock in the Genetics Research Laboratory of Atatürk University, Faculty of Science, Department of Biology for many years. Adult individuals of this strain have long wings, brown body color, and red and round eyes (Uysal *et al.,* 2006).

Two separate sets of experiments were prepared for the acute and chronic application of STG. STG (Cas no.: 83-48-7, Purity: 98.0%) was added to Standard Drosophila Medium (SDM: containing agar, sugar, yeast, cornmeal, and propionic acid as a mold inhibitor) at different concentrations (50, 100, 200, and 400 ppm) for both acute and chronic applications. In addition, dimethyl sulfoxide (DMSO), the solvent of STG, was also used as a control group. In control and application groups, viable individuals were transferred to fresh media twice a week and the dead individuals were counted and recorded. This experimental procedure was continued until the last individual died. All culture tubes were placed in the incubators at the temperature of 25 ± 1°C and having 40-60% of relative humidity.

Applications were made separately for male and female populations and started with 100 female and 100 male individuals. For this purpose, preliminary stocks were created by crosses in culture bottles containing fresh SDM to obtain the same old individuals to be used in applications. An average of 100 individuals were collected for each group from the same old (1-3 days old) unmated ♀♀ and ♂♂ flies emerging from the pupa. Collected individuals were placed in empty culture bottles and starved for 2 hours before application.

Experiments were made in triplicate. In acute applications, individuals were exposed to SDM+STG for only three days. In chronic applications, individuals were treated with SDM+STG continuously and the applications were continued until the last individual died. To be able to determine the statistical significance of the results, Duncan's one-way range test was applied. The differences between groups were considered significant at $p < 0.05$ level.

Results and Discussion

Based on data from acute and chronic applications, the maximum lifespan in the female population was 79 days for the control group (appl. no 1) containing only SDB and 76 days for the control group containing DMSO (appl. no 2). In the male population, this period was determined as 76 days for both control groups (appl. no 1-2) (Table 1). In acute STG applications, the maximum lifespan in the female population was 73 days to 64 days in the lowest (50 ppm) and highest applications (400 ppm), respectively. In the male population, it decreased from 70 days to 55 days. Again in this treatment group, the mean lifespan was found to be 48.85 ± 1.95 days in the DMSO control group (appl. no 2) in the female population and 48.32 ± 2.22 days in the male population. However, these values were considerably shortened in both male and female populations due to increasing STG concentration. The maximum life span was 40.09 ± 1.51 days in the highest acute application group (400 ppm) for the female population, while it was 34.36 ± 1.26 days for the male population. Statistical evaluations of control and application groups are given in Table 1. The regression

level due to the acute STG application was also found to be R: -0.342 for the female population and R: -0.485 for the male population (Table 1).

Table 1. Maximum and mean lifespan of male and female populations of *D. melanogaster* and the probability levels between acute STG application groups (n = 100 per group).

Acute STG Application						
Application groups	Female Population			Male Population		
	Maximum Life span	Mean Life span ± SE	*P* <	Maximum Life span	Mean life span ± SE	*P* <
Control (1)	79	49.16 ±1.99		76	48.48±2.24	
DMSO (2)	76	48.85 ±1.95	1-4,5,6*	76	48.32±2.22	1-3,4,5,6*
50 ppm (3)	73	48.49 ±1.77	2-4,5,6* 3-4,5,6*	70	44.92±1.65	2-3,4,5,6* 3-4,5,6*
100 ppm (4)	70	44.44 ±1.63	4-6*	64	41.80±1.57	4-6*
200 ppm (5)	67	41.44± 1.64	R: -0.342	58	36.94±1.40	R: -0.485
400 ppm (6)	64	40.09 ±1.51		55	34.36±1.26	

SE: Standard error *: The difference between the groups is significant at the $p < 0.05$ level, R: Regression level

Table 2. Maximum and mean lifespan of male and female populations of *D. melanogaster* and the probability levels between chronic STG application groups (n = 100 per group).

Chronic STG Application						
Application groups	Female Population			Male Population		
	Maximum lifespan	Mean life span ± SE	*P* <	Maximum Life span	Mean life span ± SE	*P* <
Control (1)	79	49.16 ± 1.99		76	48.48 ±2 .24	
DMSO (2)	76	48.85 ± 1.95	1-4,5,6*	76	48.32 ± 2.22	1-3,4,5,6*
50 ppm (3)	67	47.17 ± 1.54	2-4,5,6* 3-4,5,6*	61	43.24 ± 1.59	2-3,4,5,6* 3-4,5,6*
100 ppm (4)	64	42.16 ± 1.68	4-6*	55	36.28 ± 1.45	4-6*
200 ppm (5)	61	39.25 ± 1.54	R: -0.330	52	32.56 ± 1.44	R: - 0.410
400 ppm (6)	58	36.94 ± 1.44		49	32.53 ± 1.15	

SE: Standard error *: The difference between the groups is significant at the $p < 0.05$ level, R: Regression level

Similar results were also seen in the chronic STG application groups (Table 2, appl. no 3-6). As in acute application, increased STG concentration in chronic application caused a shortening effect on lifespan. At the lowest (50 ppm) and highest chronic STG applications (400 ppm), the maximum lifespan for the female population decreased from 67 days to 58 days, respectively. In the male population, these values were determined as 61 and 49 days (Table 2). The mean lifespan for the female population also decreased from 47.17 ± 1.54 (appl. no 3) to 36.94 ± 1.44 (appl. no 6.) days. These values were determined as 43.24 ± 1.59

(appl. no 3) and 32.53 ± 1.15 (application no 6.) days in the male population. According to the data obtained, the regression level due to chronic STG application was also calculated. These values were found to be R: -0.330 for the female population and R: - 0.410 for the male population (Table 2).

Lifespan varies by species. According to Galor and Moav (2006), "the expected lifespan" for living things is a statistical measure that reveals how long an organism lives on average. In all living things, whether primitive or advanced, cells and tissues age from birth. During mitosis, which provides growth, development, and regeneration, the "telomeric repeat sequences" in DNA shorten. In other words, with each division of the cell, the length of the telomere shortens and cellular division becomes impossible. According to the "telomere length theory" of aging, cells age with a decrease in telomere length with each division.

According to another view, genetic coding errors due to mutations in the gene(s) related to lifespan are endogenous causes of aging. While genetic code errors generally cause aging in the natural life process, they can sometimes accelerate aging based on environmental stress factors.

Aging is a continuous biological process. In this process, the decrease in physiological capacity and exposure to environmental stresses cause an increase in free radicals formed as a result of aerobic metabolism. All these factors accelerate aging and increase the risk of death in the living (Uysal *et al*., 2009). This leads to the aging of the population. Especially free radicals in the organism damage DNA, protein, lipid, and other molecules in the cell, negatively affecting gene expression and cell division cycles (Wallace, 1992). Another negative cellular interaction initiated by free radicals is lipid peroxidation. Lipid peroxidation leads to disruption of the cell membrane transport system and intracellular and extracellular ion balance. As a result, with the increase of intracellular calcium concentration, proteases are activated. These events induce cell damage and cell senescence (Gensler and Bernstein, 1981).

One of the cell organelles where free radicals are effective is mitochondria. Compared to nuclear DNA, mtDNA is less conserved; therefore, it is more easily affected by radicals and various mutations occur (Şekeroğlu and Şekeroğlu, 2009). Less energy is produced by the accumulation of damages in mtDNA. For all these reasons, mitochondria are also accepted as a cause of cell aging (Conti, 2008). Cellular damage also plays an important role in the pathogenesis of aging and aging-related diseases, especially in humans (Burtis and Ashwood, 1999).

In the present study, the only variable in optimum living conditions that will affect hemostasis for *D. melanogaster* is STG added to SDM. As seen in Table 1 and Table 2, increasing STG concentration shortened the maximum and mean lifespan compared to the control groups ($p < 0.05$). Therefore, the shortening of lifespan that can be seen in male and female populations can also be considered "population aging" in our opinion. In particular, we predict that "damage at the cellular level that may occur due to free radicals" may affect the lifespan.

References: Burtis, C.A., and E.R. Ashwood 1999, Tietz Textbook of Clinical Chemistry, W.B. Saunders Company, Philadelphia, Pennsylvania; Conti, B., 2008, Cel. Mol. Life. Sci. 65: 1626-1630; Galor, O., and O. Moav 2006, DEGIT Conference Papers c011_062; Gensler, H.L., and H. Bernstein 1981, Q. Rev. Biol. 56(3): 279-303; Kris-Etherton, P.M., M. Lefevre, G.R. Beecher, M.D. Gross, C.L. Keen, and T.D. Etherton 2004, Annu. Rev. Nutr. 24: 511-38; Kyçyk, O., M.P. Aguilera, J.J. Gaforio, A. Jiméneza, and G. Beltrán 2016, J. Sci. Food Agric. 96(12): 4143-4150; Li, T.S.C., 2006, Food Chem. 101(4): 1633-1639; Nie, G., T. Wei, S. Shen, and B. Zhao 2001, Meth. Enzymol. 335: 232-244; Ostlund, R.E., S.B. Racette, and W.F. Stenson 2003, Am. J. Clin. Nutr. 77(6): 1385-1589; Pennington, J.A.T., and J.S. Douglas 2005, Food Values of Portions Commonly Used, 18th ed.; Şekeroğlu, Z.A., and V. Şekeroğlu 2009, Turkish J. Sci. Rev. 2(2): 69-74; Uyar, B.B., and M.S. Sürücüoğlu 2010, J. Nutr. and Diet 38(1-2): 69-76; Uysal, H., T. Şişman, and H. Aşkın 2006, Drosophila *Biology and Crossover Methods* (Extended 2nd Edition), Atatürk Univ. Press, Erzurum, Türkiye, 53 pp.; Uysal, H., D. Altun, and A. Aslan 2009, TÜBAV 2(3): 271-276; Wallace, D.C., 1992, Science 256: 628- 632.

Analyzing intra- and interchromosomal associations between ubiquitously distributed inversions in *Drosophila bipectinata*.

Singh, Gurvachan, and A.K. Singh. Genetics Laboratory, Department of Zoology, Banaras Hindu University, Varanasi- 221 005, India.

Abstract

Drosophila bipectinata is one of the prominent species of genus *Drosophila* distributed in the major parts of Indian subcontinent. Its taxonomic and genetical characteristics have been superbly investigated by various researchers. There are three well-identified inversions, which have common occurrence all along its distribution area. The distribution of these inversions in seven natural populations of India was studied to observe genetic differentiation among the populations. The data available regarding the association between linked and unlinked inversions were used to see whether such associations are random or non-random. The results reveal random association of inversions, whether they are present on the same chromosome or different chromosomes. It is therefore evident that intra- and inter-chromosomal associations of different chromosome inversions exist in linkage equilibrium in natural populations of *D. bipectinata*. The probable reasons for such type of association have been briefly discussed in this article. Key words**:** *Drosophila bipectinata,* Linkage equilibrium, Intra- and Interchromosomal associations, Chromosome inversions.

Introduction

The linked genes with little distance between them are likely to get inherited to further generations together, whereas, unlinked genes or linked genes having larger distances between them segregate independently. This genetical phenomenon may decide the fate of such genes either being persistent in the population or being feebly present. The occurrence of certain gene combinations in excess over others in the population leads to linkage disequilibrium. The incidence of linkage disequilibrium is mainly attributed to forces like differential selection, suppression of crossing over, genetic drift, and genetic hitch-hiking. The phenomenon of linkage disequilibrium has been studied in different species of *Drosophila* (Hill and Robertson, 1968; Charlesworth and Charlesworth, 1973; Langley *et al.,* 1974; Langley *et al.,* 1977; Ohta, 1982; Singh and Singh, 1989; Zapata and Alvarez, 1992; Rodriguez *et al.,* 2001; Kumar and Singh, 2013, 2014). Initially chromosome inversions spotted in the polytene chromosomes were the favorite markers to observe this phenomenon, but later enzyme loci and segments of DNA and SNPs were also used for this kind of studies. The role of natural selection and genetic drift have been cited to result in linkage disequilibrium in natural populations of *Drosophila* (Lewontin, 1974; Hill and Robertson, 1968; Ohta, 1982).

Inversion polymorphism in association with allozymes has been substantially analysed in *Drosophila* (Zapata and Alvarez, 1992; Kamping and Delden, 1999; Rodriguez *et al.,* 2000; Iriarte *et al.,* 2002; Rodriguez-Trelles, 2003). Rodriguez *et al.* (2001) studied gametic disequilibrium between second chromosome polymorphic arrangements and seven linked loci in seven populations of *D. buzzatii* from Argentina and reported significant and consistent associations across populations for *Est-1, Est-2, Aldox,* and *Xdh*. Norman and Prakash (1980) chose *D. persimilis* to test the inter-allelic associations between amylase locus and naturally occurring inversions of its third chromosome. They observed that the $Amy^{1.09}$ allele occurs at a high frequency with Whitney (WT) arrangement, whereas other common gene arrangements occur with $Amy^{1.00}$. Non-random association between allozyme loci *Mdh-2, Lo-5,* and gene arrangements Ui+a+s and Ur+a in natural population of Ttibingen in *D. subobscura* was observed by Pinsker *et al.* (1978). Similar study performed by Rodriguez *et al.* (2001) and Barker *et al.* (1986) in *D. buzzatii* for chromosomal arrangements and linked allozyme loci revealed linkage disequilibrium between inversions and enzyme loci. Rodriguez *et*

al. (2001) explained that restriction of recombination in heterokaryotypes could be the main reason for linkage disequilibrium between inversion and the enzyme loci located inside the rearranged segments.

D. bipectinata belongs to the *Drosophila bipectinata* species complex of the *ananassae* subgroup of the *melanogaster* species group. Chromosomal polymorphism in this species has been documented by several population geneticists (Bock, 1971a, b; Bock and Wheeler, 1972; Gupta and Panigrahy, 1990; Das and Singh, 1992; Singh and Singh, 2001; Koop and Barmina, 2005; Banerjee and Singh, 2017; Singh and Singh, 2020, 2021). This species is one of the prevalently occurring species of *bipectinata* species complex that has its wide distribution almost perennially in south Indian states and seasonally dominating one during July to September in north Indian states. Its population genetical studies on chromosomal (inversion) and allozyme polymorphism have been one of the major areas of investigation by Indian workers (Jha and Rahman, 1972; Gupta and Panigrahy, 1990; Banerjee and Singh, 1996; Singh and Banerjee, 2016; Banerjee and Singh, 2017; Singh and Singh, 2016, 2018, 2020, 2021). In this paper, we are reporting intra- and interchromosomal associations between inversion loci to test linkage disequilibrium in *D. bipectinata.*

Materials and Methods

D. bipectinata flies were collected from seven different places of India. The places were Moradabad (MBD) and Varanasi (VNS) from north India and Madurai (MDR), Rameshwaram (RMM), Trivandrum (TVM), Kanayakumari (KKR), and Nagarcoil (NGC) from south India. Isofemale lines were established from the females collected from these geographical areas to get their third instar larvae. To prepare polytene chromosomes from the third star larva, the lacto-aceto orcein method was used. Thus, a third instar larva randomly selected from an isofemale line was dissected in insect saline (0.67%) under the stereo-binocular to separate out its salivary glands. The glands were then transferred onto a clean glass slide, treated with fixative (acetic acid and methanol in the ratio of 1:1) for about thirty seconds, and then subjected to LWA (lactic acid-1: water-2: acetic acid-3) for about five seconds. The glands were then stained in 2% lacto-aceto-orcein for half an hour. Finally, the stained glands were washed (in 45% acetic acid) and squashed in mountant (lactic acid and 60% acetic acid in 1:1 ratio) by pressing the glands covered with glass cover. The specific inversion locus was identified based on its banding sequence. Quantitative data on the frequencies of different genotype combinations were analyzed to obtain the number of various intra- and interchromosomal associations in the seven populations of *D. bipectinata*. Under the assumption of random combination of genotypes, their expected numbers were calculated from the marginal totals of R × C contingency table. Since each locus was expressed in three karyotypic forms, in total, nine genotypic combinations for a pair of inversion loci could be ascertained.

Results and Discussion

During the karyotypic observation of a specific inversion locus, three distinct combinations are likely to be observed, *i.e*., ST/ST, ST/IN, and IN/IN, where ST stands for standard gene arrangement and IN for inversion arrangement. Thus, due to presence of three karyotypes (ST/ST, ST/IN, and IN/IN) for an inversion locus, one would be able to observe total nine associations between the two inversions, either located independently on the same chromosome or at different chromosomes. Thus, the data which we could procure for the population genetical study on *D. bipectinata* (Singh and Singh, 2021) was used to see intra- as well as interchromosomal associations between the inversions. Intrachromosomal associations between commonly occurring inversions of right (In(C)2R) and left arms (In(D)2L) of second chromosome in seven natural populations of *D. bipectinata* is presented in Table 1. The chi-square analysis done through R × C contingency table reveals insignificant difference between observations and expectations for all the seven populations indicating lack of intrachromosomal associations between the linked inversions.

A similar procedure to analyze interchromosomal associations between the second and third chromosome cosmopolitan inversions was also attempted. The association tested between 2L (In(D)2L) and 3L (In (H)3L) inversion loci and between 2R (In(C)2R) and 3L (In (H)3L) inversion loci in seven natural populations of *D. bipectinata* is depicted in Table 2 and 3, respectively. Out of seventeen such cases, we could observe the existence of interchromosomal associations in only two cases (NGC and KKR) giving a gross clue

Table 1. Intra-chromosomal associations between right and left arms of second chromosome in seven natural populations of D. bipectinata.

Karyotypic combinations		Populations						
2R	2L	MBD	VNS	MDR	RMM	TVM	NGC	KKR
ST/ST	ST/ST	29 (29.75)	26 (26.71)	24 (25.26)	29 (28.39)	28 (29.91)	37 (38.71)	28 (26.71)
ST/ST	ST/In(D)2L	4 (3.43)	6 (5.50)	5 (3.94)	2 (3.07)	7 (5.51)	9 (8.06)	4 (5.66)
ST/ST	In(D)2L /In(D)2L	1 (0.85)	1 (0.79)	1 (0.79)	2 (1.53)	1 (1.57)	4 (3.23)	2 (1.61)
ST/In(C)2R	ST/ST	5 (4.38)	6 (5.66)	6 (5.05)	7 (7.74)	8 (6.46)	9 (7.74)	4 (5.50)
ST/In(C)2R	ST/In(D)2L	0 (0.50)	1 (1.17)	0 (0.78)	2 (0.84)	0 (1.19)	1 (1.61)	3 (1.17)
ST/In(C)2R	In(D)2L /In(D)2L	0 (0.12)	0 (0.16)	0 (0.15)	0 (0.41)	1 (0.34)	0 (0.65)	0 (0.33)
In(C)2R /In(C)2R	ST/ST	1 (0.88)	2 (1.52)	2 (1.68)	1 (0.86)	2 (1.65)	2 (1.55)	1 (0.78)
In(C)2R /In(C)2R	ST/In(D)2L	0 (0.10)	0 (0.33)	0 (0.26)	0 (0.09)	0 (0.29)	0 (0.32)	0 (0.17)
In(C)2R /In(C)2R	In(D)2L /In(D)2L	0 (0.03)	0 (0.05)	0 (0.05)	0 (0.05)	0 (0.08)	0 (0.12)	0 (0.05)
	χ2	0.94	1.10	1.88	2.73	4.01	2.03	4.52

d.f. = 4; *p<0.05

that there is absence of even interchromosomal associations between the unlinked inversions. The results of this study on intrachromosomal associations between chromosome inversions of 2R and 2L revealed the occurrence of random distribution of all possible genotypic combinations in all the seven populations that might be due to substantial amount of crossing over between the concerned inversion loci and the different combinations having equal survival efficiency. Similar analysis for interchromosomal associations between 2L and 3L and between 2R and 3L chromosome inversions specify the occurrence of random distribution of all possible combinations and rule out the role of epistatic interaction, which is one of the major forces causing linkage disequilibrium (Das and Singh, 1992; Singh and Singh, 1989).

Acknowledgments: Financial support in the form of research fellowship to GS from University Grants Commission, New Delhi (India) and ICMR, New Delhi is thankfully acknowledged.

References: Banerjee, P., and B.N. Singh 2017, J. Genet. 96: 97-107; Banerjee, R., and B.N. Singh 1996, Cytobios 87: 31-43; Bock, I.R., 1971a, Univ. Texas Publ. 6: 273-280; Bock, I.R., 1971b, Chromosoma 34: 206-229; Barker, J.S.F., 1979, Theor. Popul. Biol. 16: 323-346; Bock, IR., and M.R. Wheeler 1972, Texas Univ. Publ. 7213: 1-102; Charlesworth, B., and D. Charlesworth 1973, Genetics 73: 351-359; Dobzhansky, T., and A.H. Sturtevant 1938, Genetics 23: 28–64; Dobzhansky, T., 1970, Columbia University Press, New York; Gupta, J.P., and K.K. Panigrahy 1990, Genetica 82: 45-49; Hill, W.G., and A. Robertson 1968, Theor. Appl. Genet. 38: 226-231; Jha, A.P., and S.M.Z. Rahman 1972, Chromosoma 37: 445-454; Kopp, A., and O. Barmina 2005, Genet. Res. 85: 23-46; Kumar, S., and A.K. Singh 2013, Dros. Inf. Serv. 96: 52-54; Kumar, S., and. A.K. Singh 2004, Genetika 46: 227–234; Langley, C.H., K. Ito, and R.A. Voelker 1977, Genetics 86: 447-454; Langley, C.H., 1977, Springer-Verlag, NY, USA, 19: 265-273; Langley, C.H., Y.N. Tobari, and K. Kojima 1974, Genetics 8: 921-936; Lewontin, R.C., 1974, Columbia University Press, New York; Matsuda, M., Y. Tomimura, and Y.N. Tobari 2005, Genetica 125: 69-78; Ohta, T., 1982, Proc.

Table 2. Inter-chromosomal associations between two inversion loci of 2L and 3L in seven natural populations of *D. bipectinata.*

Karyotypic combinations		Populations						
2L	3L	MBD	VNS	MDR	RMM	TVM	NGC	KKR
ST/ST	ST/ST	32 (32.83)	28 (28.28)	24 (26.95)	31 (30.97)	32 (33.15)	45 (42.67)	28 (29.07)
ST/ST	ST/ In(H)3L	4 (3.70)	6 (6)	5 (4.21)	3 (3.34)	7 (6.11)	5 (7.84)	7 (6.16)
ST/ST	In(H)3L /In(H)3L	1 (0.92)	2 (1.71)	1 (0.84)	2 (1.67)	2 (1.74)	4 (3.48)	2 (1.78)
ST/In(D)2L	ST/ST	2 (1.75)	4 (3.92)	6 (5.05)	5 (5.16)	4 (4.04)	3 (5.53)	4 (3.14)
ST/In(D)2L	ST/ In(H)3L	0 (0.20)	1 (0.83)	0 (0.79)	1 (0.56)	1 (0.74)	4 (1.02)	0 (0.67)
ST/In(D)2L	In(H)3L /In(H)3L	0 (0.05)	0 (0.23)	0 (0.16)	0 (0.28)	0 (0.21)	0 (0.45)	0 (0.19)
In(D)2L /In(D)2L	ST/ST	1 (0.88)	1 (0.78)	0 (0.84)	1 (0.86)	1 (0.80)	1 (0.79)	1 (0.78)
In(D)2L /In(D)2L	ST/ In(H)3L	0 (0.10)	0 (1.67)	0 (0.13)	0 (0.09)	0 (0.14)	0 (0.15)	0 (0.17)
In(D)2L /In(D)2L	In(H)3L /In(H)3L	0 (0.03)	0 (0.05)	0 (0.03)	0 (0.04)	0 (0.04)	0 (0.06)	0 (0.05)
$\chi 2$		0.53	2.03	1.88	0.88	0.57	12.14*	1.7

d.f. = 4; *p<0.05

Table 3. Inter-chromosomal associations between inversion loci of 2R and 3L in seven natural populations of *D. bipectinata.*

Karyotypic combinations		Populations						
2R	3L	MBD	VNS	MDR	RMM	TVM	NGC	KKR
ST/ST	ST/ST	31 (31.45)	30 (29.14)	23 (23.65)	28 (28.29)	32 (33.06)	43 (44.35)	30 (30.76)
ST/ST	ST/ In(H)3L	5 (4.62)	5 (6)	6 (5.71)	8 (7.74)	8 (70.41)	10 (8.87)	7 (6.33)
ST/ST	In(H)3L /In(H)3L	1 (0.92)	1 (0.86)	2 (1.63)	1 (0.86)	2 (1.78)	2 (1.80)	0 (0.90)
ST/In(C)2R	ST/ST	2 (1.7)	3 (4.04)	6 (5.34)	5 (3.84)	4 (3.14)	6 (4.83)	3 (3.23)
ST/In(C)2R	ST/ In(H)3L	0 (0.25)	2 (0.83)	1 (1.28)	0 (1.05)	0 (0.68)	0 (0.96)	0 (0.66)
ST/In(C)2R	In(H)3L /In(H)3L	0 (0.05)	0 (0.12)	0 (0.37)	0 (0.12)	0 (0.17)	0 (0.19)	1 (0.09)
In(C)2R /In(C)2R	ST/ST	1 (0.85)	1 (0.81)	0 (0.76)	0 (0.76)	1 (0.79)	1 (0.80)	1 (0.80)

In(C)2R /In(C)2R	ST/ In(H)3L	0 (0.12)	0 (1.67)	0 (0.18)	1 (0.21)	0 (0.17)	0 (0.16)	0 (0.16)
In(C)2R /In(C)2R	In(H)3L /In(H)3L	0 (0.03)	0 (0.02)	0 (0.05)	0 (0.02)	0 (0.04)	0 (0.03)	0 (0.02)
χ^2		0.568	4.11	1.61	5.30	1.7	1.93	11.04*

d.f. = 4; *p<0.05

Nat. Acad. Sci. USA. 79: 1940–1944; Rodriguez, C., R. Piccinali, E. Levy, and E. Hasson 2001, J. Hered. 92: 382-391; Singh, A.K., and B.N. Singh 1989, Naturalia 14: 19-29; Singh, A.K., 2018, Ind. Jour. Sci. Res. 08: 169-178; Singh, B.N., and P. Banerjee 2016, Proc. Indian Natl. Sci. Acad. 82: 99–115; Singh, B.N., 2019, Current Science 117: 761-775; Singh, G., and A.K. Singh 2018, J. Exp. Zool. India 21: 29-33; Singh, G., and A.K. Singh 2020, J. Sci. Res. B H U 64: 85-89; Singh, G., and A.K. Singh 2021, J. Genet. 100: 42; Tomimura, Y., M. Matsuda, and Y.N. Tobari 2005, Genome 48: 487–502; Zapata, C., and G. Alvarez 1992, Evolution 46: 1900-1917.

Random distribution of pupae in the wild type and disease model stocks (park^{1} and park^{13}) of *Drosophila melanogaster.*

Das, Ankita, and Arvind Kuma Singh. Department of Zoology, Institute of Science, Banaras Hindu University, Varanasi-221 005, INDIA; *aksbhu23@rediffmail.com*

Introduction

Drosophila is an excellent model organism to study its pre-adult and adult behavior. The pupation site preference by the third instar larva is a prominent marker for studying the post embryonal or pre-adult behavior in case of *Drosophila* species (Mensua, 1967). Selection of pupation height is one of the key factors that impacts on the survival of the pupae (Sokal *et al*., 1960; Markow, 1979; Singh and Pandey, 1991). Several abiotic and biotic factors like sex, larval density, moisture, temperature, developmental time, and density of population can influence the site of pupation in *Drosophila* (Pandey and Singh, 1992). Pupation site varies both intra- and interspecifically within populations (Markow, 1979; Singh and Pandey, 1991). Studies have reported that the genetic factors also influence the pupation site preference of the *Drosophila* larvae (Sokal *et al*., 1960).

Parkinson disease (PD) is a common neurological disorder that generally strikes in the old age (Bekris and Zabetian, 2010). Dopaminergic neuronal loss and accumulation of proteins, commonly known as lewy bodies, are the salient features of Parkinson's disease (Feany and Bender, 2000). A few genes have been linked to familial PD, such as SNCA, LRRK2, PARK7, PINK1, or PRKN gene (Hardy, 2010). As a result of mutations in Parkin, PD occurs as a second most commonly occurring neurological problem. Parkin gene is located at the 6q25.2-27 positions of human chromosome (Dawson and Dawson, 2010). It is an autosomal recessive type of mutation. Presently, *Drosophila* flies are used to understand the intricacies of Parkinson's disease as its ortholog genes are also present in *Drosophila* flies and the mutational changes in them trigger physiological changes similar to human (Soriano and Paricio, 2011).

In the present research note, we are reporting the pupation height preference by the third instar larvae of *D. melanogaster* belonging to three genetically different lines. One of the lines is wild type laboratory stock, Oregon-R, whereas the other two are Parkinson disease model flies, park^{1} and park^{13}. Our objective of the present study was to observe the pupation site preference of the wild type and two Parkinson disease flies, park^{1} and park^{13}.

Materials and Methods-

Three stocks, Oregon R, park[1] (Bloomington stock center no. 34747), and park[13] (Bloomington stock center no. 79210) of *Drosophila melanogaster* were used in this study. These stocks were maintained on culture medium containing maize powder, agar-agar, yeast, brown sugar, propionic acid and nipagin. All the experiments were performed at constant laboratory temperature (24±1° Celsius) keeping 12-hour light and dark conditions.

The food vials used in the experiments were of the same height (8.0 cm) and diameter (4.0 cm) and the food poured in them was of equal amount that occupied 1.0 cm height from the bottom of the vials. The upper surface of the food in the vial was demarcated as 0.0 cm and the pupation height of an individual was considered from this end. Each vial was marked in five divisions above the food, where each division measured 1.0 cm.

10 pairs of virgin females and males of each strain were introduced in the food vials to get the next generation. Parental flies were discarded from the culture vials after 4 days. The observation was made on the tenth day by measuring the height of each pupa from the food surface for all the three strains. We analyzed our data by introducing two major statistical tests: one by applying two-way ANOVA to observe whether wild type strain and disease model strains (park[1] and park[13]) show differences in their pupation preference (average pupation height) and among the varying heights (rows constructed based on varying heights). Beside this, coefficient of variation and R × C chi-square tests was also employed.

Table1. Distribution of pupae at varying heights in different strains of *D. melanogaster.*

Height (in cm)	Oregon-R	park[1]	park[13]
1	13	2	8
2	54	29	15
3	20	51	13
4	6	6	3
5	0	50	6
Mean ± S.E	18.6 ± 9.45	27.6 ± 10.4	9 ± 2.2

Results

Data regarding pupation height and distribution of pupae in varying parts of the vials is shown in the Table 1. The mean pupation height of Oregon-R, park[1], park[13] is 18.0 ± 9.46 cm, 27.6 ± 10.42 cm, and, 9.0 ± 2.21 cm, respectively. The two-way ANOVA subjected on these data is presented in Table 2. Results of this analysis clearly show that there is non-significant difference among the average heights of pupation among the three different stocks ($F = 1.51$; d.f. = 2,8; $p > 0.28$). Among the five divisions, based on heights, there also existed non-significant difference ($F = 1.55$; d.f. = 4,8; $p > 0.28$). Coefficient of variation helps to measure the extent of variation in the distribution of pupae in different stocks. This statistical analysis indicates that there is maximum variation in wild type stock followed by park[1]. When the same data were subjected to R × C contingency table to analyze that whether larvae pupate randomly in different columns and rows, it was found that the larvae settle in non-random distribution pattern in varying heights in all the three strains ($p < 0.001$). Figure 1 depicts the distribution of pupae at different heights in the food vials. Perusal of the three pie charts (Figure 1) displays that the maximum number of third instar larvae prefer to settle for pupation at a range between two to three centimeters of height.

Table 2. Two-way ANOVA depicting the level of significance among rows (heights) and columns (strains).

Source of Variation	*SS*	*df*	*MS*	*F*	*P-value*	*F crit*
Rows	1771.6	4	442.9	1.546709	0.2775	3.837853
Columns	865.2	2	432.6	1.510739	0.277588	4.45897
Error	2290.8	8	286.35			
Total	4927.6	14				

Discussion

The pre-adult behavior has been shown to be influenced by genotype, environment, and genotype by environment interactions in *Drosophila* (Santos *et al*., 1994; Matzkin *et al*., 2011). In the present study, we did not find significant difference in three genetically different strains of *D. melanogaster*. This denotes that there is no effect of genetic mutation (parkin gene) on average pupation height when compared with wild type strain, *i.e*., Oregon-R. Further, the maximum congregation of pupae in a specific height of all the three strains is an indication that the third instar larvae have preference for pupation site. Thus, this brief preliminary study helps us to infer that the Parkinson like symptoms may be restricted to the adult stage of fly life. There are no effects of Parkinson disease seen in pre-adult of park larvae in terms of locomotive behavior and pupation site preference.

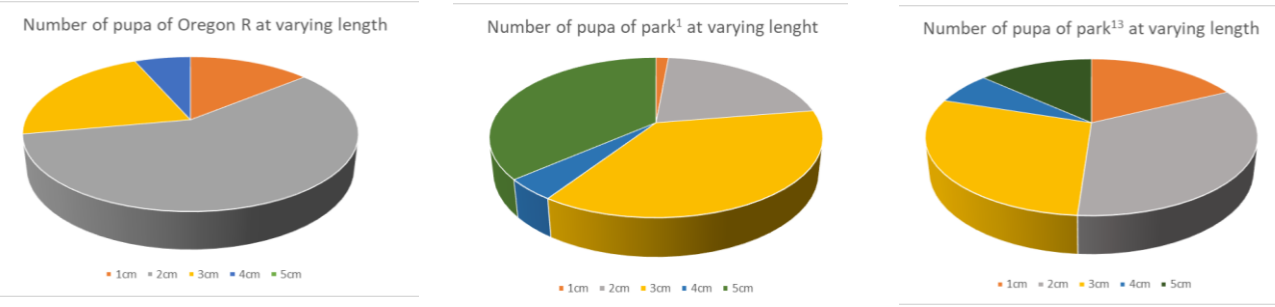

Figure 1. Pie chart showing the distribution of pupae at different height in Oregon-R, Park[1], and Park[13] strains of *D. melanogaster.*

Acknowledgment: The authors are thankful to Prof. J.K. Roy of the department for providing the park[1] and park[13] lines of *Drosophila melanogaster* used in the present experiments. Financial support in the form of JRF (Junior Research Fellowship) from University Grants Commission (UGC), New Delhi to Ankita Das is thankfully acknowledged.

References: Bekris, L.M., I.F. Mata, and C.P. Zabetian 2010, J. Geriatr. Psychiatry Neurol. 23: 228-242; Dawson, T.M., and V.L. Dawson 2010, Mov. Disord. 25: S32-S39; Feany, M., and W. Bender 2000, Nature 404: 394–398; Hardy, J., 2010, Neuron 0896-6273; Markow, T.A., 1979, Beh. Genet. 9: 209-217; Matzkin, L.M, S. Jhonson, C. Paight, and T.A Markow 2013, PLos One e59530; Mensua, J., 1967, Dros. Inf. Serv. 42: 76; Pandey, M., and B.N. Singh 1991, Dros. Inf. Serv. 70: 170-171; Pandey, M., and B.N. Singh 1992, Dros. Inf. Serv. 71: 258-259; Singh, B.N., and M. Pandey 1991, Indian J. Exp. Biol. 29: 926-929; Sokal, R.R., P.R. Erhlich, P.E. Hunder and G. Schlager 1960, Ann. Ent. Soc. Amer. 53: 174-182; Santos, M., K. Fowler, and L. Partridge 1994, Heredity 72: 515-521; Soriano Verónica Muñoz and Nuria Paricio 2011, Parkinson's Disease 520640-14.

Timing of Bownes stage five embryos in *Drosophila pseudoobscura*.

Wright*, Dynisty, and Stephen W. Schaeffer. Eberly College of Science, The Pennsylvania State University, University Park, Pennsylvania [dze12@psu.edu].

Abstract

Bownes (1975) characterized embryonic development in *Drosophila melanogaster* by delineating easily recognizable phases of the process based on the developmental and internal movements of cell layers. These described stages have allowed the dissection of the genetics of important phases of *D. melanogaster* development (Zusman and Wieschaus, 1985). Hug *et al.* (2017) showed that Bownes stage five embryos are

the best stage for collecting embryos to study the evolution of chromatin architecture, because it is the stage when zygotic gene expression has begun. Because embryonic development was characterized in *D. melanogaster,* it is not clear when this stage occurs in other *Drosophila* species. Specifically, we were interested in knowing when the optimal time to collect Bownes stage five embryos is for *D. pseudoobscura* to allow for the analysis of the evolution of topologically associated domains (TADs) within this species (Wright and Schaeffer, 2022). TADs are self-interacting domains within the A (open chromatin) and B (closed chromatin) compartments that show preferential internal chromatin interactions towards size, structure, and proteins involved in their formation (Hong and Kim, 2017; Le and Laub, 2016; Szabo *et al.*, 2019). To understand the best time to collect Bownes stage five embryos in *D. pseudoobscura*, we collected embryos every thirty minutes over a five-and-a-half-hour period. We used statistical analysis to estimate the mean and variance of stage five embryo frequencies to differentiate among individual time points. We found that the best time to collect the maximum number of stage five embryos was at four and a half hours, which occurs at a time that is 1.3× longer than in *D. melanogaster* and would have been predicted based on the longer egg-to-larval hatch time in *D. pseudoobscura*.

Introduction

Embryogenesis in Drosophila melanogaster

Bownes stage embryos are defined based on the development and internal morphological movements of cell layers in *D. melanogaster* (Bownes, 1975). Studies in *D. melanogaster* show that Bownes stage five is the best developmental stage for collecting embryos (Cartwright and Lott, 2020; Crews, 2015; Karr *et al.*, 1985; Kuhn *et al.*, 2015; Prayitno *et al.*, 2019; Tran *et al.*, 2016), because this is the phase when zygotic gene expression has begun, which can allow methods such as HiC to infer aspects of chromatin architecture, such as topologically associate domains (TADs) (Hug *et al.*, 2017). Embryonic development in *D. melanogaster* has been characterized by distinct stereotypic phases that occur over an 18-hour period culminating in the hatching of first instar larvae (Bownes, 1975). Bownes (1975) described 14 stages of embryonic development. Within those stages, Bownes stage five in *D. melanogaster* occurs after approximately three hours (Bownes, 1975).

Bownes Stage Embryos in D. pseudoobscura

In *D. pseudoobscura*, we assume that zygotic gene activation occurs in Bownes stage five, since the stages are morphologically similar to that of *D. melanogaster*. However, it is unknown when these embryos can be collected because the timing of embryonic stages has not yet been clearly defined in *D. pseudoobscura*. In this study, we asked several questions: 1. When is the best time to collect Bownes stage five embryos in *D. pseudoobscura*? 2. Does variation in times influence the number of embryos on any given day? and 3. Is the timing of embryonic development in *D. pseudoobscura* similar to *D. melanogaster*? In an effort to map TAD boundaries and bodies in the Tree Line gene arrangement of *D. pseudoobscura,* we wanted to determine when to collect Bownes stage five embryos to contrast TAD structure with the previously analyzed Arrowhead arrangement (Liao *et al.*, 2021). Because *D. melanogaster* takes three hours to reach Bownes stage five, we hypothesize that *D. pseudoobscura* will take longer, because the time from egg laying to larval hatch is 24 hours (Markow *et al.*, 2008) *versus* 18 hours in *D. melanogaster* (Bownes, 1975).

Methods

Counting Bownes Stage Embryos

Flies were reared on a 15 × 60 mm petri plate of apple agar inside an embryo collection cage (Genessee Scientific Catalog No. 59-100). The apple agar was prepared as described by (Karpen, 2009). A yeast solution (for eggs) was spread across the apple agar, and 0.25 g yeast paste (for adult flies) was prepared and added to each plate.

Fresh adult flies were placed in embryo collection chambers and left for 48 hours to begin producing offspring. Adult flies were moved into new collection chambers, and embryos were collected at 30-minute time intervals (starting at 30 minutes and ending at 5.5 hours). Embryos were collected from each plate and dechorionated in 50% bleach, as described by Karpen (2009), and transferred to slides for visualization at

100× power. The slide was separated into four equal quadrants, and two of the four were counted and doubled, estimating the numbers for the whole slide. The two quadrants were randomly selected for all experiments, and then those two quadrants were fixed for every trial. In our trials, quadrants 1 and 4 were randomly selected and were used to estimate the number of embryos for all slides and trials. An approximation was done, because there could be thousands of embryos across all four quadrants. A total of 24 replicate trials were used for each time period at 18°C.

Statistical Analysis of Time Points

We computed the proportion of Bownes stage embryos with $\hat{p} = x/n$ (where *n* is the total number of observed embryos and *x* is the number of embryos in Bownes stage five) for each of the 24 trials or the embryos at each time point. For example, for trial one at 2 hours, there were 61 larvae, with 1 in Bownes stage five giving a proportion of 2%. We then computed the mean proportions in each time point $\mu_t = \sum_{i=1}^{24} \hat{p}_{it}/24$ (where t is the time points), and estimated the variance (Figure 1).

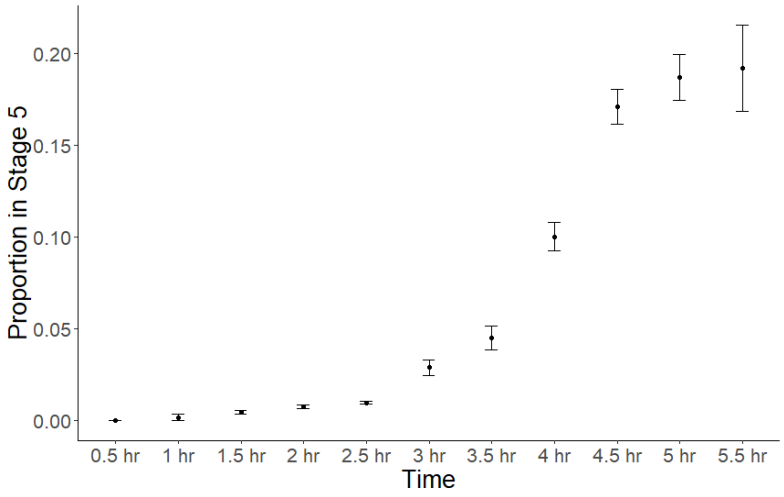

Figure 1. Proportion of Embryos in Bownes Stage Five. Proportions of embryos in stage five were counted and plotted based on their time from 0.5 to 5.5 hours.

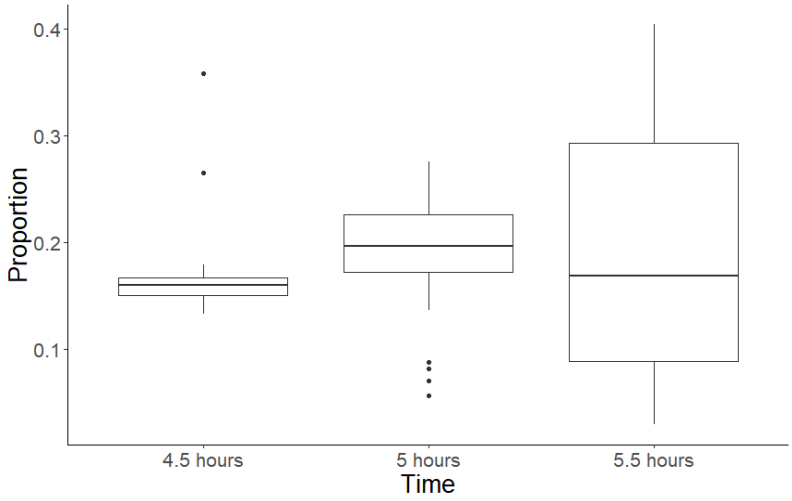

Figure 2. Proportion of Highest Time Points. Boxplots of the proportions of the three highest time points. Boxplots show the amount of variation within the time points.

Results

Bownes stage five embryos occur at different times in different species and occur faster or slower depending on the temperature that the embryos are reared (Kuntz and Eisen, 2014). To understand when the peak of Bownes stage five embryos occurred in *D. pseudoobscura*, we counted the number of Bownes stage five embryos at 11 different time points separated by 30-minute intervals over a total of five and a half hours. After four and a half hours, the proportions began to asymptote. In particular, 4.5, 5, and 5.5 have approximately the same proportion (Figure 1). Those three time points maximize the number of Bownes stage five embryos before it begins to decrease.

To understand which proportions had the least amount of variation for Bownes stage five embryo collection, we created a box plot of the last three time points. The variation increases over the three time points, with 4.5 hours being the lowest variation among them (Figure 2).

Discussion

We collected *D. pseudoobscura* embryos over a five-hour time period to determine the optimal time to collect Bownes stage five embryos. We show that the fraction of stage five embryos starts to asymptote at around 4.5 hours. We suggest that 4.5 hours is the optimal time to collect stage five embryos in *D. pseudoobscura*. Collecting after 4.5 hours leads to increasing numbers of embryos in Bownes stage six and above. The egg-to-larval hatch time of *D. pseudoobscura* is 1.33 times longer than in *D. melanogaster*, 24 *versus* 18 hours, respectively. We estimate that stage five of embryogenesis occurs 1.5 times later in *D. pseudoobscura* than in *D. melanogaster* (4.5 versus 3.0 hours). These data suggest that one could estimate the times of the comparable embryonic stages of *D. melanogaster* in *D. pseudoobscura* by assuming that the timing will be 1.33 to 1.5 times longer than that of *D. melanogaster*.

Acknowledgments: We would like to thank Penn State research funds to S.W.S. that supported this research.

Data: The data for this research can be found here: https://github.com/dynisty18/Embryo-Staging-in-Drosophila-pseudoobscura.git

References: Bownes, M. 1975; Cartwright, E.L., and S.E. Lott 2020, Genetics 216(3): 805-821. https://escholarship.org/content/qt0m79q8rr/qt0m79q8rr.pdf?t=qmgowc; Crews, S.M., 2015, Vanderbilt University; Hong, S., and D. Kim 2017, Nucleic Acids Research 45(18): 10403-10414. https://doi.org/10.1093/nar/gkx738; Hug, C.B., A.G. Grimaldi, K. Kruse, and J.M. Vaquerizas 2017, Cell 169(2): 216-228. e219; Karpen, G.H., 2009, Cold Spring Harbor Protocols 2009(7), pdb. prot5254; Karr, T.L., Z. Ali, B. Drees, and T. Kornberg 1985, Cell 43(3): 591-601; Kuhn, H., R. Sopko, M. Coughlin, N. Perrimon, and T. Mitchison 2015, Development 142(22): 3869-3878; Kuntz, S.G., and M.B. Eisen 2014, PLoS Genet. 10(4): e1004293. https://doi.org/10.1371/journal.pgen.1004293; Le, T.B., and M.T. Laub 2016, The EMBO Journal 35(14): 1582-1595. https://doi.org/https://doi.org/10.15252/embj.201593561; Liao, Y., X. Zhang, M. Chakraborty, and J. Emerson 2021, Genome research 31(3): 397-410; Markow, T., S. Beall, and L. Matzkin 2008, Journal of Evolutionary Biology 22: 430-434. https://doi.org/10.1111/j.1420-9101.2008.01649.x; Prayitno, K., T. Schauer, C. Regnard, and P.B. Becker 2019, EMBO reports, 20(8): e48138. https://www.ncbi.nlm.nih.gov/pmc/articles/PMC6680166/pdf/EMBR-20-e48138.pdf; Szabo, Q., F. Bantignies, and G. Cavalli 2019, Science advances 5(4): eaaw1668; Tran, M., V. Tsarouhas, and A. Kegel 2016, Biol. Open 5(7): 928-941. https://doi.org/10.1242/bio.019000; Wright, D., and S.W. Schaeffer 2022, Philosophical Transactions of the Royal Society B: Biological Sciences 377(1856): 20210206. https://doi.org/doi:10.1098/rstb.2021.0206; Zusman, S.B., and E.F. Wieschaus 1985, Developmental Biology 111(2): 359-371.

The multi sex chromosome system in *Colocasiomyia xenalocasiae* (Drosophilinae).

Watabe, H.[1], and M. Yafuso[2]. [1]The Hokkaido University Museum, Hokkaido University, Sapporo, Japan; [2]Uema 1-2-21, Naha, Japan; E-mail: watabe@air.ocn.ne.jp

A large number of chromosomal researches have hitherto been made in the family Drosophilidae (Clayton, 1998; Clayton and Guest, 1986; Clayton and Wheeler, 1975; Morelli *et al.,* 2022), and contributed to understandings of karyotype evolution in various taxonomic groups (*cf*., Throckmorton,1982). The preparation of mitotic chromosomes is made with neuroblasts of larvae, and chromosome studies have been restricted mostly to the genus *Drosophila*, especially in three subgenera: *Drosophila*, *Siphlodora*, and *Sophophora*, because of its ease of maintenance in the laboratory rearing (Clayton and Guest, 1986; Yamada *et*

al., 1993). Another reason is that the species discrimination is nearly impossible in pre-adult stages in the wild.

The flower-visiting genus *Colocasiomyia* de Meijere is an exceptional case, since its members use flowers of specific groups of host plants in the families Araceae, Arecaceae, and Magnolianceae, as breeding resources. In Okinawa of southern Japan, a pair of *Colocasiomyia* species, C. *xenalocasiae* and *C. alocasiae*, are synhospitalic on inflorescences of *Alocasia odora* C. Koch. The former uses mostly its pistillate region (lower part of the spadix) for oviposition, while the latter does its staminare region (upper), with partly overlaps in transitional region (intermediate) between them. Further, larvae of these two species can be easily discriminated by morphology and distribution patterns of spracles and spicules on the body surfaces (Yafuso,1983). We examined karyotypes of two *Colocasiomyia* species, and here report a unique example of the multi sex chromosome system.

Full flower periods of *Alocasia odora* are mainly in March and April in Okinawa, and we collected flowers in the campus of Ryukyu University in Nishihara town, carried them to the laboratory, and picked up *Colocasiomyia* larvae from the respective regions of the spadix. Neural ganglia from 3rd instar larvae were incubated for about 45 min in a 0.1 mg/ml colchicine solution, fixed with aceto-methanol, stained with 4% Giemsa solution, and then air-dried (Watabe, 1998). Metaphase configurations were taken by an analog camera (Olympus PM-6) and then saved as digital figures using a film-scanner (Nikon APS IX 240). More than 50 (usually 100) metaphase plates were observed in each species.

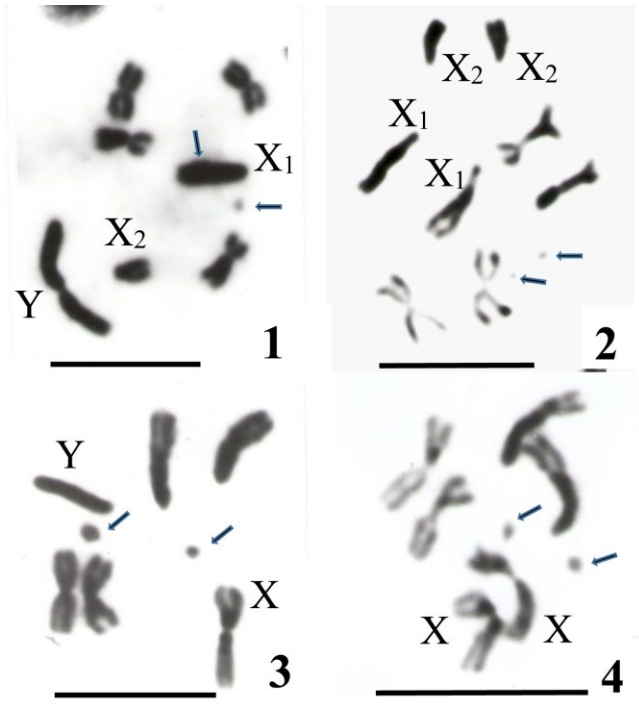

Figures 1-4. Mitotic chromosomes of *Colocasiomyia xenalocasiae* (1, 2) and *C. alocasiae*. Arrows represent micro-chromosomes, and one of a pair of micro-chromosomes in Figure 1 is overlapped mostly with X_1. Bars = 10 μm.

Figures 1-4 show metaphase chromosomes of *C. xenalocasiae* (♂ in Figure 1, ♀ in Figure 2) and *C. alocasiae* (♂ in Figure 3, ♀ in Figure 4). Males of *C. xenalocasiae* possessed 2n = 9, consisting of 1 pair of metacentric autosomes (V-shaped), 1 pair of sub-metacentric autosomes (J-shaped), 1 pair of micro-chromosomes (marked with arrow; Dot-shaped), and 3 un-paired chromosomes. In comparison of chromosomal constitutions between males and females, 3 un-paired chromosomes in males were considered to be a large acrocentric X (= X_1 in Figure 1; Rod-shaped), a short acrocentric X (X_2) and a large metacentric Y. Nuclear plates of *C. xenalocasiae* females had 2n = 10, with 1 pair of metacentric autosomes, 1 pair of sub-metacentric autosomes, 2 pairs of acrocentric X, and a pair of micro-chromosomes. Nuclear plates of *C. alocasiae* showed 2n = 8 (1R, 2V, 1D), consisting of 1 pair of acrocentric chromosomes, 2 pairs of metacentric chromosomes, and 1 pair of micro-chromosomes (Figures 3-4). Both X and Y were metacentric.

In the family Drosophilidae, a great majority of the species have the XX/XY system, and a few the XO/XX (Clayton, 1998; Watabe 1998). The multi sex chromosome system was found only in *Drosophila miranda*, a North American member of the *obscura* species group of the subgenus *Sophophora*, (Dobzhansky, 1923; Dobzhansky and Powell,1975). Since *C. xenalocasiae* and *D. miranda* are distantly related to each other in the phylogeny of drosophilid flies, it is reasonable to assume that the $X_1X_2Y/X_1X_1X_2X_2$ system might have emerged independently during the process of the karyotype evolution within the respective taxonomic groups. The genus *Colocasiomyia* is distributed in the Oriental region, and its new members have been recently discovered from Southeast Asia, some of which are closely related to *C. xenalocasiae* (Takano *et al.,*

2021). Presumably the multi sex chromosome system might have resulted from fissions of the X chromosome, and a further analysis is needed to clarify the origin of the sex chromosome system presently found in *C. xenalocasiae* and to trace the following karyotype evolution within the genus *Colocasiomyia* (Morelli *et al.,* 2022).

References: Clayton, F.E., 1998, Dros. Inf. Serv. 81: 5-125; Clayton, F.E., and M.R. Wheeler 1975, Handbook of Genetics 3: 471-512; Clayton, F.E., and W.C. Guest 1986, *The Biology and Genetics of* Drosophila 3e: 1-38; Dobzhansky, T., 1935, Genetics 20: 377-391; Dobzhansky, T., and J.R. Powell 1975, *Handbook of Genetics* 3: 537-587; Morelli, M.W., H. Blackmon, and C.E. Hjelmen 2022, Frontiers in Ecology and Evolution 10: 1-6; Takano, K.T., J. Gao, Y. Hu, N. Li, M. Yafuso, A. Suwito, R. Repin, R.A.S. Pingga, P.A. Meleng, C.H.K. Iang, L. Chong, and M.J. Toda 2021, Zootaxa 5079: 1-70; Throckmorton, L.H., 1982, *The Biology and Genetics of* Drosophila 3b: 227-296; Watabe, H., 1998, Entomological Science 1: 309-311; Yafuso, M., 1983, Kontyu, Tokyo 51: 520-527; Yamada, K., Y. Hu, and H. Watabe 1993, La Kromosoma II 71-72: 2429-2432.

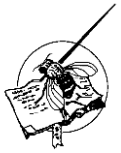

Making "brushes" in *D. melanogaster* by disabling *Notch*.

Held, Lewis I., Jr., and Jason J. Shin. Department of Biological Sciences, Texas Tech University, Lubbock, Texas 79409.

Over the eons, evolution has equipped males with various contraptions to out-compete their fellow suitors in the quest for mates (Emlen, 2008), and flies are no exception (Rice *et al*., 2018). The most salient such gadget in flies is the "sex comb"—a row of curved bristles on the forelegs that helps males grasp females during attempted copulations (Kopp, 2011). Every rookie student of genetics learns that the sex comb is an easy way to sort males from female *D. melanogaster*. A less-well-known device is the "sex brush"—a Velcro®-like patch of wavy bristles on the forelegs that might be used in a similar way to grip the female abdomen (Tanaka *et al*., 2022). Brushes evolved separately from sex combs in a few clades of the family Drosophilidae, including the *D. immigrans* group.

In their study of brush-bearing species Tanaka *et al.* (2022) conjectured that the brushes evolved from transverse rows ("t-rows") that decorate the forelegs in males and females of most species in this family (Figure 1). Such rows are used to wipe dust from the eyes (Szebenyi, 1969). The authors argued that a mutation(s) arose which let bristle cells be compacted at the maximal density permitted by the process of "lateral inhibition." That mechanism enforces bristle spacing intervals (Simpson, 1990). We sought to test this idea by interfering with the time course of lateral inhibition itself to see whether we could elicit brushes in a species that lacks them—viz., *D. melanogaster*. Indeed, we were able to induce brush-like lawns of bristles by disabling the *Notch* gene that mediates lateral inhibition throughout the nervous system (Held, 2002a).

The *Notch* signaling pathway is an ancient mode of cellular communication across the metazoan spectrum (Held, 2017). Unlike the other cardinal pathways, it requires cell contact instead of using diffusible morphogens at a distance, although nonadjacent cells can manage to touch one another via filopodial extensions that span several cell diameters (de Joussineau *et al*., 2003). Homozygous *Notch*-null individuals die as embryos, but they can be rescued by using the temperature-sensitive allele $l(1)N^{ts1}$ and exposing those mutants to restrictive temperature only during later stages of development. The definitive analysis of such stages was conducted by Shellenbarger and Mohler (1978). They found many temperature-sensitive periods (TSPs).

Two types of TSPs affect bristles. For any given set of bristles the first TSP increases bristle number, but it is inevitably followed by a TSP where those very same bristles vanish. Subsequent studies revealed why (Held, 2002a). *Notch* plays two different roles in bristle development. First, it lets bristle cells block nearby skin cells from becoming bristles—the process of lateral inhibition (Simpson, 1990). Disabling *Notch* at this time releases the skin cells from inhibition, so extra bristles arise. Later, *Notch* assigns different identities (shaft *vs*. socket *vs*. neuron *vs*. sheath) to mitotic offspring of the bristle progenitor cell (Hartenstein and

Posakony, 1990). Suppressing *Notch* during this second phase converts shaft and socket cells into neurons that lie beneath the epidermis, hence deleting bristles from the cuticular surface.

We decided to focus on the *D. melanogaster* tibia instead of the basitarsus (ta1) or ta2, where brushes are located in *D. immigrans*. Why? Tibial t-rows are straighter than basitarsal ones, so misalignments are more easily detected. Second, most t-row bristles lack bracts, while basitarsal t-rows possess them. Bracts are tiny protrusions that are induced by bristle cells (del Álamo *et al*., 2002; Held, 2002b), and they would have complicated our analysis by limiting the maximal possible bristle density. Finally, we chose to use females instead of males because their larger tibias allowed us to map subregions within the t-row area that manifest different TSPs.

Materials and Methods

We used the fly stock w^a *l(1)*N^{ts1} *rb* to disable *Notch* at various times. We raised these mutant flies at the permissive temperature of 18°C throughout their larval period. We then collected batches of ~36 white prepupae at 2-hour intervals for later exposure to the restrictive temperature (31°C). The brevity of the white prepupal stage makes it ideal for synchronizing individuals (Ashburner, 1989). We divided each batch into 3 cohorts (~12 pupae each) so that we could expose them to different pulse lengths. For each batch, we gave one cohort a 1-hour pulse, another a 2-hour pulse, and the third a 4-hour pulse. We found that the longest pulse (4 hours) elicited the strongest phenotypes, so we confined our further investigation to those cohorts. The actual durations of time before pulsing were passed at 18°C, but the standard temperature for assessing age-dependent effects is 25°C. Development is slowed by a factor of two at 18°C relative to 25°C (Held, 1990), so the ages in Figure 2 were computed by halving the time at 18°C to express the stage as "hAP^{25}"—*i.e*. hours after pupariation as if they were developing at 25°C.

Flies were cultured on Ward's *Drosophila* Instant Medium supplemented with live yeast. Specimens were preserved in 70% ethanol. Fly legs were dissected, mounted in Faure's medium (Lee and Gerhart, 1973), and photographed with a Nikon microscope at 200× magnification. Our normal mounting procedure had to be modified because t-rows reside on the inner (anterior-ventral) surface of the tibia and cannot be seen in their entirety when the "knee" joint (between femur and tibia) is intact. The bend in that joint (or the tibia-tarsus joint) typically forces the leg to lay flat with its anterior surface up, its ventral surface down, and t-rows obscured in side view. To remedy this constraint, we cut each tibia from its knee joint and its tarsus before immersing it in a drop of Faure's. We then sandwiched the tibia between an upper (round) and lower (rectangular) cover slip and pressed gently on the upper cover slip with a pair of blunt forceps while rolling the tibia in whatever direction was necessary until the t-rows lay uppermost.

Results and Discussion

The *achaete* gene enables ordinary epidermal cells to become bristle cells (Held, 2002a). On the legs, *achaete* is mainly expressed in "proneural" stripes that span each leg segment, and those stripes eventually resolve into longitudinal rows (Joshi *et al*., 2006). However, this is not true for the t-rows. Instead, *achaete* is expressed uniformly throughout the entire chevron-shaped region that precedes the t-rows at around 6 hAP^{25} (Shroff *et al*., 2007). Evidently, every skin cell in this area has the potential to become a bristle cell, but does not normally do so, because this pool of equivalent cells is whittled down to a much smaller subset by lateral inhibition. That repressive process is orchestrated by the *Notch* pathway (Simpson, 1990). In the absence of *Notch* function we might expect every cell to become a bristle, in which case the region should make a brush resembling the one on the foreleg basitarsus of a *D. immigrans* male (Figure 1a).

By exposing *l(1)*N^{ts1} mutants to a 4-hour heat pulse at various times from 0 to 18 hAP^{25}, we were able to induce extra bristles in the tibial t-row area at any age from about 1 to 11 hAP^{25} (Figure 2). As the pupal age advanced from 1 to 11 hAP^{25}, extra bristles appeared in a broad wave from distal to proximal, starting at t-row d1 and ending around t-row d5. The maximal effect was seen at 7 or 8 hAP^{25} when the majority of epidermal cells in the t-row area became bristles.

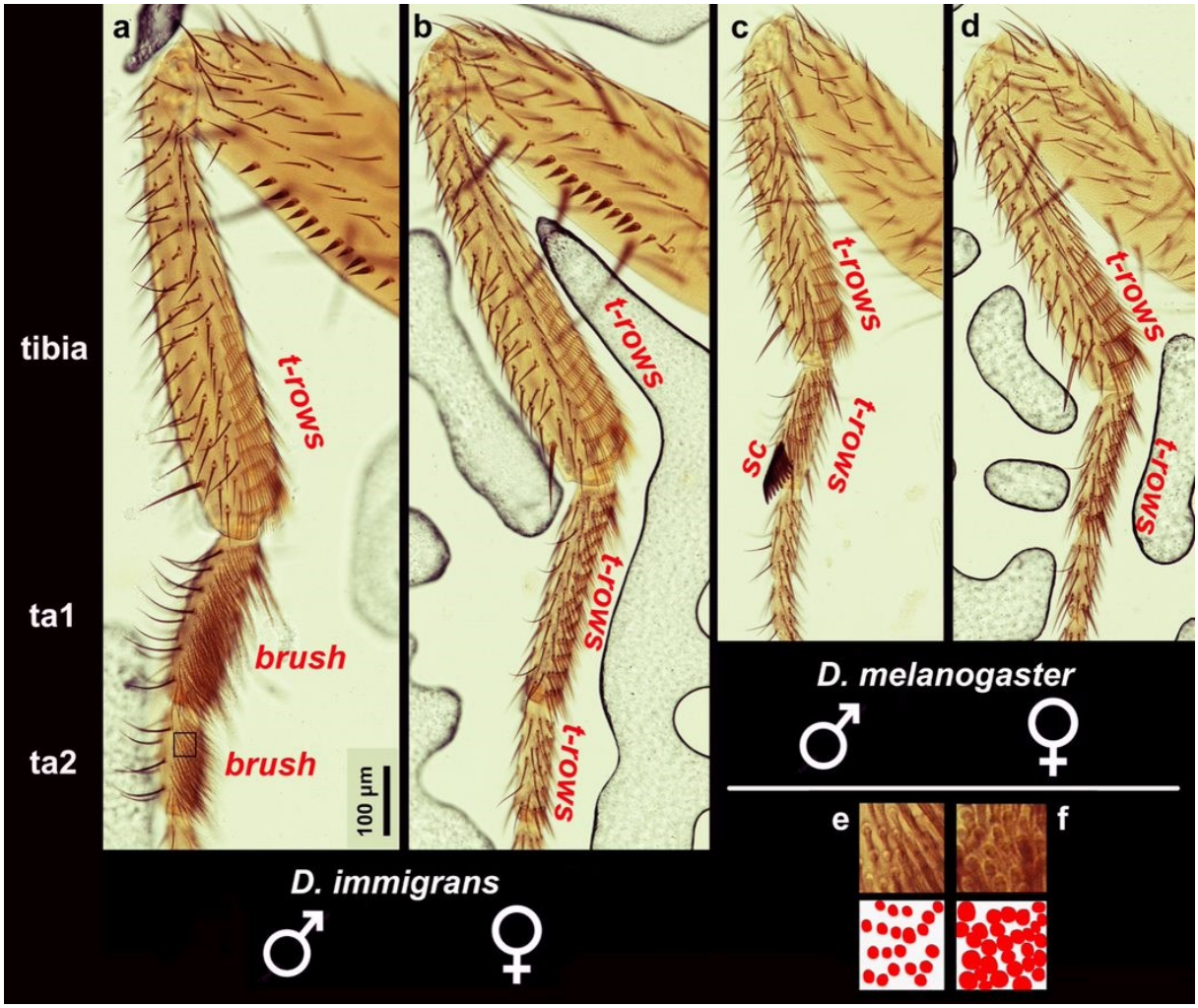

Figure 1. Forelegs (anterior surface) of a wild-type *D. immigrans* male (**a**) and female (**b**) and a wild-type *D. melanogaster* male (**c**) and female (**d**), all at the same magnification (scale bar in **a**). Leg segments include the tibia, first tarsal segment (ta1; a.k.a. "basitarsus"), and second tarsal segment (ta2). Each panel also shows the distal half of the femur (upper right), where *D. immigrans* has a row of "thorn" bristles that *D. melanogaster* lacks. All four legs have transverse rows (t-rows) of yellow bristles on the tibia and basitarsus, except the *D. immigrans* male, which has a "brush" at that location on its basitarsus and ta2, though the proximal end of its basitarsus manifests a few t-rows (Rice *et al*., 2018). The *D. melanogaster* male has a sex comb (sc) of dark, curved bristles on its basitarsus in addition to t-rows. The *D. immigrans* male foreleg is actually a left leg, as are both of the *D. melanogaster* legs, but all three images were flipped horizontally (to appear as right legs) for the sake of uniformity and consistency with Figure 2. Some bristles were deflected during mounting. Bubbles are artifacts. **e**, **f**. Enlarged insets from ta2 in **a** of this figure and from 10hAP^{25} of Figure 2, both of which contain ~20 bristles. Below the inserts are "pepperoni" diagrams of socket silhouettes. Note that *D. immigrans* sockets are not maximally close-packed (**e**), whereas *D. melanogaster* sockets do typically abut one another (**f**).

Such close-packed arrays look remarkably like the brush of a *D. immigrans* male. Therefore, our results are consistent with the hypothesis of Tanaka *et al*. (2022) regarding the evolution of brushes from t-rows via mutations that facilitate bristle crowding. However, even our most extreme *Notch*-null phenotypes fail to completely mimic the *D. immigrans* brush because bare swaths remain in our confluent lawns, possibly due to the wave of TSP sensitivity. Moreover, the bristles of a *D. immigrans* brush are usually separated by

one or two skin cells (Tanaka *et al*., 2022), whereas the sockets of our densest arrays often abut one another with no spaces in between (Figure 1f), though skin cells with tiny apical surfaces could conceivably be squeezed between adjacent sockets.

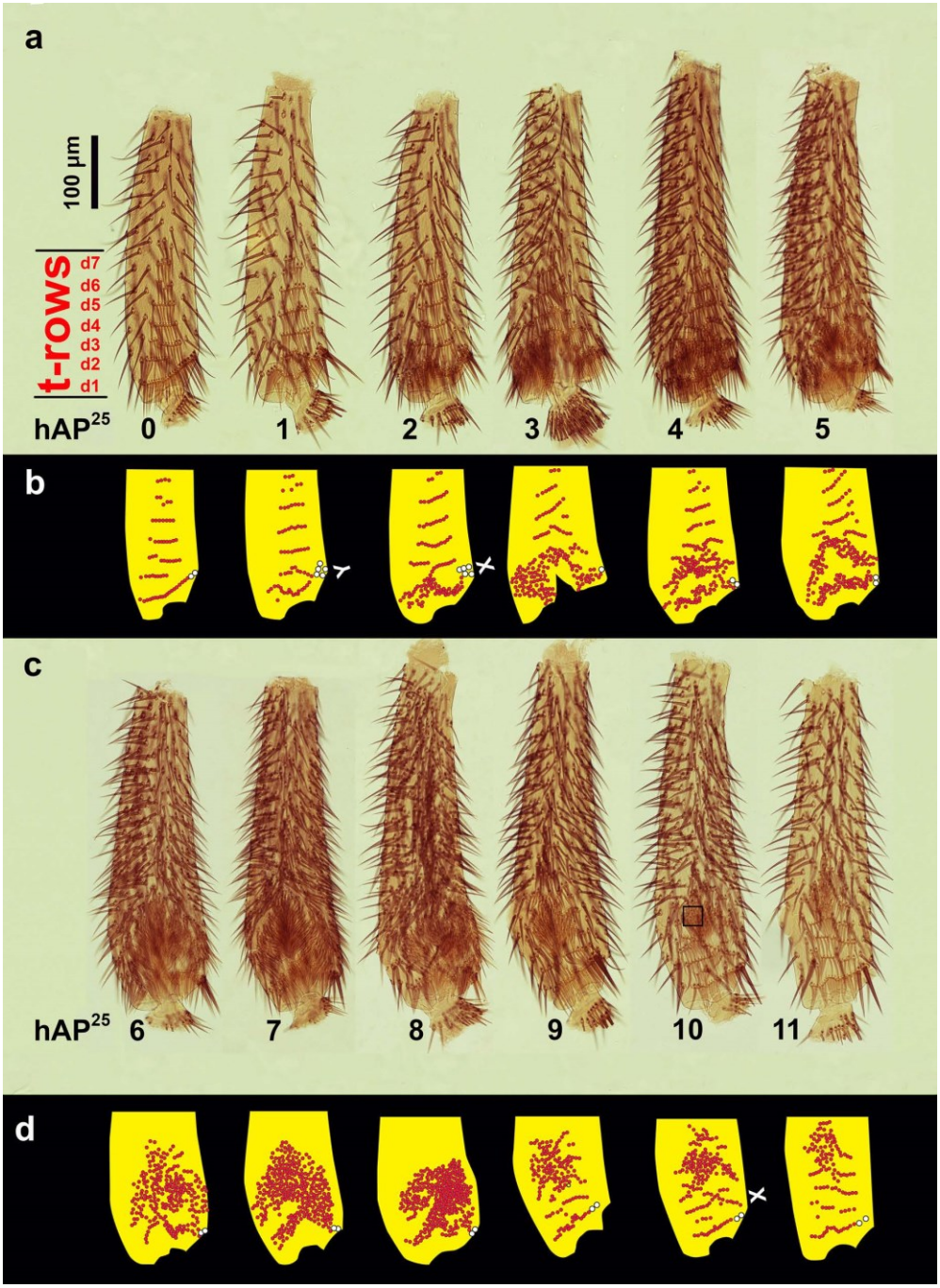

Figure 2. **a**, **c**. Representative examples of tibias from cohorts of w^a $l(1)N^{ts1}$ *rb* female *D. melanogaster* exposed to a 4-hour pulse of 31°C, beginning at the ages indicated by numbers below. The abbreviation "hAP^{25}" denotes the age (in hours after pupariation) when we began the heat pulse, based on the pace of development at 25°C (see Materials and Methods). For ease of comparison, left tibias (2, 4, 5, 7, 8, 9, and 10) were flipped horizontally to look like right tibias. The t-rows are numbered from distal to proximal (d1-d7), although the number of rows varies from individual to individual and even can differ on the left *vs*. right sides of the same fly. The tibia that was heat-pulsed at 0 hAP^{25} looks wild-type; it offers a standard of comparison for the normal (un-treated) phenotype. Inset in 10 hAP^{25} is enlarged in Figure 1f. Many bristles got deflected from their normal proximal-distal orientations when the tibia was squeezed between cover slips in order to roll it into a favorable orientation during slide mounting (see Materials and Methods). Anterior-ventral surface is uppermost and in focus in all photos. **b**, **d**. Schematic diagrams of the distal tibia (traced yellow shape), with the positions of all t-row bristle sockets indicated by solid circles, except for the enlarged bristles at the ventral end of t-row d1 (hollow circles), which appear to be homologous to the apical bristle of the midleg. Bristles belonging to t-rows are distinguishable from other bristles based on their yellowish color, their shape, and usually their lack of a bract. Xs and Ys denote branched t-rows that presumably arose via fusion of adjacent

rows. Note the brush-like lawns in the t-row areas of tibias heat-pulsed at 6, 7, and 8 hAP^{25}. At pupal ages from 12 to 18 hAP^{25} (not shown) bristles vanish progressively from distal to proximal. This extra-to-missing-bristle sequence agrees with the TSP timeline of Shellenbarger and Mohler (1978), who studied thoracic bristles. The edge of the 3 hAP^{25} tibia was torn during mounting.

If the mutations that led to Drosophilid brushes did occur by tuning the *Notch* pathway, then this tuning may have stopped short of reducing *Notch* to a null level. Alternatively, t-row bristle cells might differ *qualitatively* (instead of *quantitatively*) from brush bristle cells in (1) their mobility in the skin (Tanaka *et al*., 2022), (2) their ability to find and bind one another (see Atallah *et al*., 2009, for how this occurs in the sex comb), and (3) the level of "stickiness" required to form chains (Tanaka *et al*., 2009). The capacity of t-row sockets to form tight lattices (Figure 1f) suggests that they are adhesive around their entire circumference, not just on their lateral surfaces. If so, then there must be safeguards to prevent accidental clumping in normal flies. The sporadic occurrence of X- or Y-shaped intersections (Figure 2) may represent instances where these safeguards malfunction. X- and Y-shaped junctions are also seen when the EGFR pathway is disabled (Held, 2002c). In both situations (*Notch* and EGFR), the defects are typically unilateral (*i.e*., left or right leg but not both)—a "fluctuating asymmetry" which implies that such errors are stochastic, rather than genetic (Dongen, 2006).

Previous attempts to mimic evolutionary alterations by developmental interventions have likewise been only partly successful—*e.g*., efforts to modify the sex comb (Lee *et al*., 2011). The lesson from the latter study and from other "phenocopy" endeavors (Landauer, 1959) is that evolution typically tinkers with anatomy by tweaking multiple genes, rather than a single one. In order to create leg brushes, other kinds of mutations (aside from *Notch*) must have altered the t-row bristles themselves so as to make them thinner, curlier, and/or hooked to assist in grasping. We did not see any such changes in bristle morphology in our experiments. That is, t-row bristles looked the same, regardless of whether they were aligned in rows or packed into a quasi-brush.

Acknowledgments: The fly stock used for disabling *Notch*—w^a *l(1)*N^{ts1} *rb*—was kindly supplied by Clifton Poodry, and the *D. immigrans* stock came from the Austin Stock Center. Helpful comments on the manuscript were provided by Joel Atallah, Artyom Kopp, Nicolas Malagon, Gavin Rice, Kohtaro Tanaka, and Jeffrey Thomas. Technical assistance was furnished by Vien Le.

References: Ashburner, M., 1989, Drosophila: *A Laboratory Handbook*. Cold Spring Harbor Press; Atallah, J., N.H. Liu, P. Dennis, A. Hon, D. Godt, and E.W. Larsen 2009, Evol. Dev. 11: 191-204; de Joussineau, C., J. Soulé, M. Martin, C. Anguille, P. Montcourrier, and D. Alexandre 2003, Nature 426: 555-559; Dongen, S.V., 2006, J. Evol. Biol. 19: 1727-1743; Emlen, D.J., 2008. Annu. Rev. Ecol. Evol. Syst. 39: 387-413; Hartenstein, V., and J.W. Posakony 1990, Dev. Biol. 142: 13-30; Held, L.I., Jr., 1990, Roux's Arch. Dev. Biol. 199: 31-47; Held, L.I., Jr., 2002a, *Imaginal Discs: The Genetic and Cellular Logic of Pattern Formation*. New York, Cambridge Univ. Press; Held, L.I., Jr., 2002b, Mechs. Dev. 117: 225-234; Held, L.I., Jr., 2002c, Dros. Inf. Serv. 85: 17-19; Held, L.I., Jr,. 2017, *Deep Homology? Uncanny Similarities of Humans and Flies*. New York, Cambridge Univ. Press; Joshi, M., K.T. Buchanan, S. Shroff, and T.V. Orenic 2006, Dev. Biol. 293: 64-76; Kopp, A., 2011, Evol. Dev. 13: 504-522; Landauer, W., 1959, Experientia 15: 409-412; Lee, J., J.N. Malagon, and E. Larsen 2011, J. Undergrad. Life Sci. 5: 28-31; Lee, L.-W., and J.C. Gerhart 1973, Dev. Biol. 35: 62-82; Rice, G., O. Barmina, K. Hu, and A. Kopp 2018, Evol. Dev. 20: 78-88; Shellenbarger, D.L., and J.D. Mohler 1978, Dev. Biol. 62: 432-446; Shroff, S., M. Joshi, and T.V. Orenic 2007, Mechs. Dev. 124: 43-58; Simpson, P., 1990, Development 109: 509-519; Szebenyi, A.L., 1969, Anim. Behav. 17: 641-651; Tanaka, K., O. Barmina, and A. Kopp 2009, PNAS 106 (12): 4764-4769; Tanaka, K., O. Barmina, A. Thompson, J.H. Massey, B.Y. Kim, S. Suvorov, and A. Kopp 2022, Dev. Genes Evol. 232: 89-102.

Cap 'n' collar helps EGFR to align t-rows.

Held, Lewis I., Jr.[1], J. Nicolas Malagon[2], and Jason J. Shin[1]. [1]Department of Biological Sciences, Texas Tech University, Lubbock, Texas 79409; [2]Canadian Mennonite University, 500 Shaftesbury Blvd, Winnipeg, MB, Canada R3P 2N2.

Looking like icicles on windowsills (Figure 1a), the transverse rows ("t-rows) of bristles on the forelegs of *D. melanogaster* present a tantalizing geometrical problem: how do they line up? Twenty years ago, evidence was adduced that the Epidermal Growth Factor Receptor (EGFR) pathway is involved, since disabling the EGF receptor itself upsets this rigid order (Held, 2002c). At that time, this result seemed paradoxical, because the EGFR pathway was thought to only act via diffusible signals (Held, 2002a): why should adjacent t-row bristle cells need to "shout" over distances greater than one cell diameter? Subsequently, one member of the bristle cell lineage—the socket cell—was found to use a protrusion of its cell membrane to convey EGFR ligands directly to an adjacent cell so as to induce that cell to form a bract (Peng *et al*., 2012). Hence, the EGFR pathway can transmit *contact*-mediated, as well as *diffusion*-mediated, cellular signals.

Nevertheless, a mystery remained: *how* do cells use the EGFR pathway to create t-rows? An intriguing clue surfaced in 2015 when Tamada and Zallen (2015) showed that the *cap 'n' collar* (*cnc*) gene cooperates with the EGFR pathway to align cells into perfectly square arrays. Such arrays occur in the pharyngeal part of the ventral midline in the *D. melanogaster* embryo. Could *cnc* be acting similarly in the foreleg to corral epidermal cells into forming t-rows? To investigate this possibility we raised and lowered *cnc* expression to see what effect these changes might have on t-rows. We did find t-row misalignments in the latter case. However, the extent of these effects is too small for *cnc* to be playing as key a role for t-rows as it plays in the embryo. Moreover, we carefully inspected epidermal cells residing between t-rows in the pupal epidermis but failed to see the kinds of square arrays at those locations that prevail at the embryo's midline.

Materials and Methods

Genotypes and starter stocks for the analysis of the EGFR pathway are described in Held (2002b), and that published article should be consulted for details. In particular, we used the genotype $Egfr^{ts1a}$ *cn bw*/$Egfr^{CO}$ to disable the EGF receptor at various times: $Egfr^{ts1a}$ is a temperature-sensitive allele (active at 18°C but inactive at 29°C), whereas $Egfr^{CO}$ is a null allele. Development is slowed by a factor of 2 at 18°C and sped up by a factor of 0.86 at 29°C, so we adjusted pupal ages to the standard 25°C development rate ("hAP^{25}") by dividing 18°C ages by 2 and multiplying 29°C ages by 1.16 (Held, 1990).

Two types of *Gal4* drivers were used: *Distal-less* (*Dll*)-*Gal4*, which is expressed in the tarsus and distal tibia, and *scabrous* (*sca*)-*Gal4*, which is active in all bristle cells. To probe the role of *cnc*, we used two different *UAS* stocks: *UAS-cncC* and *UAS-cncC-RNAi* for our GOF and LOF analyses, respectively. *UAS-cncC-RNAi* was inserted on both the 2nd and 3rd chromosomes as a way of maximally reducing *cnc* expression (Sykiotis and Bohmann, 2008).

The ubi-*D*Ecad::GFP construct was generated by Oda and Tsukita (2000). For live imaging, pupae were mounted and recorded following the protocol described by Atallah *et al*. (2009). Developing tibias were imaged with a Zeiss laser 510 scanning confocal microscope at 25°C with a 40× objective, using Zeiss LSM Browser software. The time interval was 30 minutes, and the z-stacks had a 3-μm step size.

Flies were raised on Ward's *Drosophila* Instant Medium augmented with Baker's yeast and preserved in 70% ethanol. Fly legs were mounted in Faure's fluid (Lee and Gerhart, 1973) and photographed with a Nikon microscope at 200× magnification. Because tibial t-rows lie on the inner (anterior-ventral) surface, they could not be seen fully when legs were dissected by our normal protocol of sandwiching legs between cover

slips. To solve this problem, we used blunt forceps to press on the top cover slip and push it a few mm orthogonal to the tibial axis until the tibia rolled to an ideal angle.

Abbreviations: DER$^+$, *Drosophila* EGF Receptor; GOF, gain of function; LOF, loss of function; hAP, hours after pupariation; TSP, temperature-sensitive period. The symbol ">" is a shorthand for linking a *Gal4* to its *UAS*—*e.g.*, "*sca>DER*$^+$ denotes *sca-Gal4:UAS-DER*$^+$.

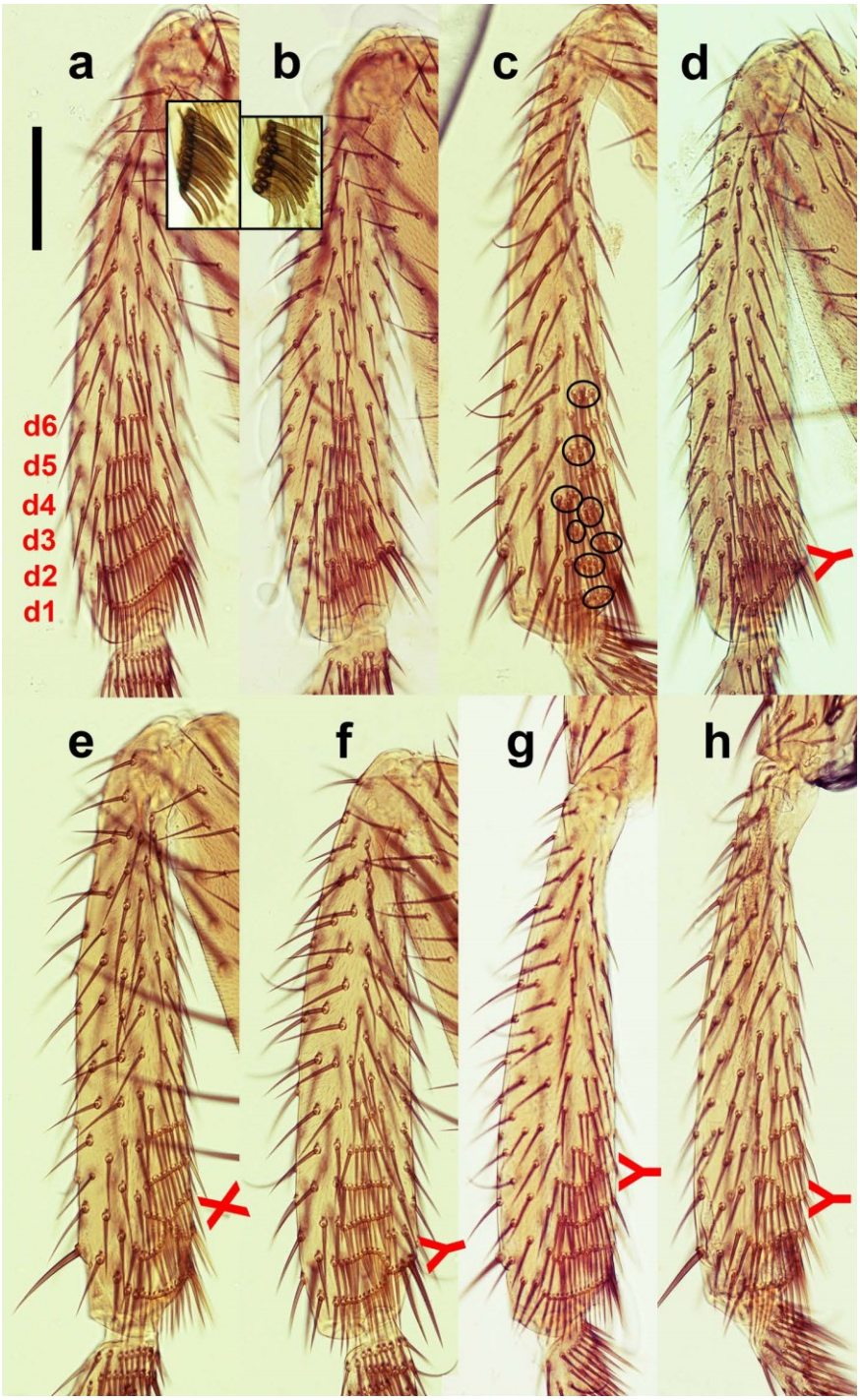

Figure 1. "Rogue's gallery" of tibial t-row phenotypes exhibited by EGFR pathway genotypes. **a**. Normal arrangement of t-rows, as illustrated by an *Egfr*^{ts1a}/*Egfr*^{CO} (LOF) fly upshifted (18°C to 29°C) at 20 hAP^{25}, which is after the TSP when EGFR acts, so there is no impact on the pattern. The t-rows are numbered from distal to proximal (d1-d6), though the number of rows fluctuates from fly to fly. Note the two enlarged, dark bristles at one end of d1—a consistent feature. *Inset:* sex comb from a fly in the same upshifted cohort. Note its linear arrangement of bristle sockets. **b**. *Egfr*^{ts1a}/*Egfr*^{CO} (LOF) fly upshifted at 2 hAP^{25}, which precedes the TSP when EGFR acts. *Inset:* sex comb from a fly in the same upshifted cohort. Jumbled comb teeth are typical for flies upshifted around this time. Such zigzags also occur for *Dll>argos* and *sca>argos*, with milder disruptions seen for *Star*^{5671}. For consistency, this left tibia was flipped horizontally to look like the right tibias in all other panels. **c**, **d**. *Egfr*-GOF flies, whose t-row disruptions resemble *Egfr*-LOF phenotypes (**b**). **c**. *Dll>DER*$^+$ fly. Clumps of bristles, which are common in other genotypes as well, are circled. **d**. *sca>DER*$^+$ fly. A Y-shaped junction exists between d1 and d2, though it is hard to see amidst the jumbled bristles in those rows. The proportion of the tibia occupied by t-rows is much smaller in **d** than in **c**—a consistent trend for these genotypes—but we have no idea why this should be so. **e-h**. X- or Y-shaped unions of t-rows in various EGFR pathway mutants—marked by the "X" or "Y" to the right of the junction—but unburdened by the kind of clumping in **d**. **e**. *Egfr*^{ts1a}/*Egfr*^{CO} (LOF) fly downshifted at 18 hAP @29°C (= 21 hAP^{25}). The distal end of

this tibia was pictured in Figure 1d of Held (2002c). **f**. *Egfr*^{ts1a}/*Egfr*^{CO} (LOF) fly downshifted at 14 hAP @29°C (= 16 hAP[25]). **g**. *Star*^{5671}/*CyO* fly. The frequency of Y-shaped junctions in such flies was 13% (2/24 legs). **h**. *sca>argos* fly. The Y shapes in g and h have short stems and long branches (bordering on a "V" condition), in contrast to the Y shapes in **d** and **f**, where the stem is somewhat longer. In all panels, the femur-tibia "knee" joint is at the top, and all tibias were from males, except **c**, **d**, and **h** (females). Scale bar (**a**) = 100 μm. For abbreviations, see Materials and Methods.

Table 1. Effects of EGFR pathway genes on t-row alignment (versus bract development).*

Genotype	EGFR	Effect on bracts	Effect on t-rows	Figure
Egfr^{ts1a}/*Egfr*^{CO}	LOF	Missing	Clumps and X-or-Y junctions; depending on shift time	Fig. 1b, e-f
Dll>DER^{+}	GOF	Missing	Clumps (100% of legs) and Y junctions (21% of legs)	Fig. 1c
sca>DER^{+}	GOF	Missing	Clumps (100% of legs) and X (8%) or Y (71%) junctions	Fig. 1d
Star^{5671}/*CyO*	LOF	Missing	Clumps (96% of legs) and Y junctions (13% of legs)	Fig. 1g
Star^{5671}/*Ras1*^{e1B}	LOF	Missing	Clumps (100% of legs) and Y junctions (8% of legs)	
Dll>argos	LOF	Missing	Clumps (88% of legs) and Y junctions (71% of legs)	
sca>argos	LOF	Missing	Clumps (83% of legs) and X (13%) or Y (25%) junctions	Fig. 1h
Dll>mSpi	GOF	No effect	No effect	
sca>mSpi	GOF	No effect	No effect	
Dll>sSpi	GOF	Extra	No effect	
sca>sSpi	GOF	Extra	No effect	
*hs-Ras** shock	GOF	Extra	Chaos, but no X-or-Y junctions.	

*Data on bracts (column 3) are from Held (2002b). LOF and GOF changes in the EGFR pathway (column 2) cause missing or extra bracts respectively, except for *mSpi* (both drivers, no effect) and *DER*$^{+}$ (both drivers, missing instead of extra). Fewer extra bracts were seen with *Dll* > *sSpi* and *sca* > *sSpi* than with other constructs, which might explain why the impact on t-rows was likewise muted. Sample sizes per genotype = 24 legs, except last row, where we exposed activated-*Ras* (*hs-Ras**) flies to heat shocks at one-hour intervals from 13 to 24 hAP[25] and examined 12 legs per time point (=144 legs). The failure to find X or Y junctions (< 1%) among those specimens was surprising. In every case, Y-shaped intersections exceeded X-shaped ones, which were much more rare. The "Y" designation also includes minimal "V" cases where the joined t-rows only share a single (terminal) bristle (see Figs. 2 and 3), hence eliminating the stem of the Y.

Results and Discussion

Insect bristles differ from mammalian hairs insofar as they form well-organized patterns. Of course, there are exceptions to this rule—*e.g*., the prominent rows of whiskers on a cat's face. In general, evenly spaced repeated elements are extremely common in organisms (Held, 1992). Less common, however, are alignments of tandem elements with no intervening intervals at all. Such a situation prevails in the sex comb of *D. melanogaster*, whose evolution and development have been studied intensively (Kopp, 2011). The sex comb is a modified t-row (Tokunaga, 1962) that rotates from a horizontal to a vertical orientation during metamorphosis (Atallah *et al*., 2009). In that posture it serves a new role (grasping the female during courtship) that deviates from the ancient task of the t-rows (Kopp, 2011), which is to brush dust from the eyes (Szebenyi, 1969). For both of these functions, it makes sense to pack the bristles into a tight, linear array.

Ever since 2002 we have known that the EGF receptor is somehow involved in t-row development (Held, 2002c). When the receptor is chronically disabled (LOF) or chronically overexpressed (GOF), there is fragmentation, intersection, and merging of t-rows, as well as misalignment and clumping of the bristles therein (Figure 1b-d). The similarity of these LOF and GOF phenotypes suggests a "Goldilocks" explanation—namely, the dosage of the receptor may be critical, and deviations (up or down) from its ideal ("just right") set point unleashes chaos. Despite that chaos, the number of t-row bristles remains relatively normal, unlike the drastic increase in bristle density that is seen when the Notch receptor is disabled (Held and Shin, 2022). By fine-tuning the timing of EGF receptor expression, it is possible to reduce the chaos to a simpler phenotype where adjacent rows intersect in X- or Y-shaped junctions (Figure 1e, f).

We wondered whether other components of the EGFR pathway—aside from the receptor itself—are capable of generating comparable phenotypes. For that purpose we examined t-rows of mounted specimens that we had used in our prior study of bract induction (Held, 2002b). For virtually every genotype that had an impact on bract induction, we also found an effect of some sort on t-row development. Those effects are inventoried in Table 1, and typical phenotypes are presented in Figure 1.

The most common phenotypes were bristle clumps ranging from (1) individual bristles nestled into a crevice between adjacent bristles in otherwise normal t-rows to (2) clusters of close-packed bristles within t-rows that are fragmented, fused, or otherwise disrupted (Figure 1c). The next most common defects were X- or Y-shaped junctions linking adjacent t-rows (Figure 1d-h). To assess how often such aberrations occur in normal flies, we inspected the left and right forelegs of 100 Oregon R wild-type males. We found no clumps nor X-or-Y connections at all, indicating a baseline frequency less than 0.5% for each kind of deviation. Hence, these outcomes must be due to some (as yet unknown) function of the EGFR pathway, rather than to an aggravation of incidental (subliminal?) tendencies that are inherent in wild-type flies.

Argos is a secreted inhibitor of the EGFR pathway, so we expected to see a chaotic phenotype *for argos*-GOF flies akin to chronic EGFR deprivation (Figure 1b), but *argos*-GOF legs have relatively few clumps of bristles, regardless of whether their t-rows intersect or not. When the *argos* gene is overexpressed *via* either a *sca-Gal4* or *Dll-Gal4* driver, the resulting legs exhibited a higher frequency of X- or Y-shaped junctions than when we altered the EGF receptor itself: 38% (9/24) legs for *sca>argos* and 71% (17/24) legs for *Dll>argos* (Figure 1h), *versus* only 25% (6/24) legs for $Egfr^{ts1a}/Egfr^{CO}$ flies shifted from 29°C to 18°C at various times from 14 to 21 hAP^{25} (Figure 1e, f). Why is excess Argos so effective at instigating intersections? We presume that bristle cells whose EGFR is disabled become sticky around their entire surface, rather than just on their lateral sides. The same may be true for the *Notch* pathway (Held and Shin, 2022).

After having surveyed various components of the EGFR pathway for their ability to perturb t-rows (Table 1, Figure 1), we felt ready to investigate whether, and if so to what extent, the *cnc* gene might be involved in t-row development. To that end we manipulated *cnc* expression by driving *UAS-cncC* (GOF) or *UAS-cncC-RNAi* (LOF) constructs throughout the tibia and tarsus (*Dll*-Gal4) or in incipient bristle cells (*sca*-Gal4). If *cnc* were as instrumental in aligning t-rows as it is in aligning cells along the embryonic ventral midline, then we expected to see massive changes in t-row alignment under LOF conditions. We used the *cncC* isoform instead of *cncA* or *cncB* (McGinnis *et al.*, 1998), because it encodes the full-length homolog of the mammalian *Nrf2* gene, whose role has been studied extensively (Sykiotis and Bohmann, 2008). No *cncC* mRNA is detected in imaginal discs (*ibid.*), but *cncC* could still be playing a role at lower levels.

Neither the *sca>cncC* nor the *sca>cncC-RNAi* F_1 offspring of our *Gal4* X *UAS* crosses showed bristle abnormalities, so we focused instead on using our *Dll-Gal4* driver to force expression in the tibia and tarsus. Because *cnc* is vital for embryonic development, we decided to use the $Gal80^{ts}$ trick to bypass the embryonic period (McGuire *et al*., 2004). We collected eggs from *Dll-Gal4/CyO; Gal80*^{ts} mothers (mated with *UAS* males) at room temperature (22°C) for 2-day periods, then placed the vials at 18°C for 2 more days (until the F_1 finished embryogenesis), whereupon we transferred the vials to a 30°C incubator for the remainder of development. After F_1 flies eclosed, we were surprised to see no *Dll>cncC* or *Dll>cncC-RNAi* F_1 (non-Curly) flies among them … until we examined the food and found that those flies had hatched but fallen and stuck to the food due to the absence of functional claws.

Dll>cncC (GOF) and *Dll>cncC-RNAi* (LOF) flies exhibit similar leg phenotypes not only in terms of absent or non-useable claws, but also insofar as their tarsi are shorter due to fusions of their ta2-ta3 and ta4-ta5

segments (Figure 2). Shortened tarsi are also typical of flies whose EGFR pathway has been disabled by mutations in its component genes (Campbell, 2002) such as *argos* (Figure 2e). Hence, one possible explanation for the *Dll>cncC-RNAi* (LOF) phenotype is that *cnc* is cooperating with the EGFR pathway akin to how it works in the embryo (Tamada and Zallen, 2015). If so, then disabling *cnc* might dismantle the collaboration, resulting in a canonical EGFR-LOF phenotype.

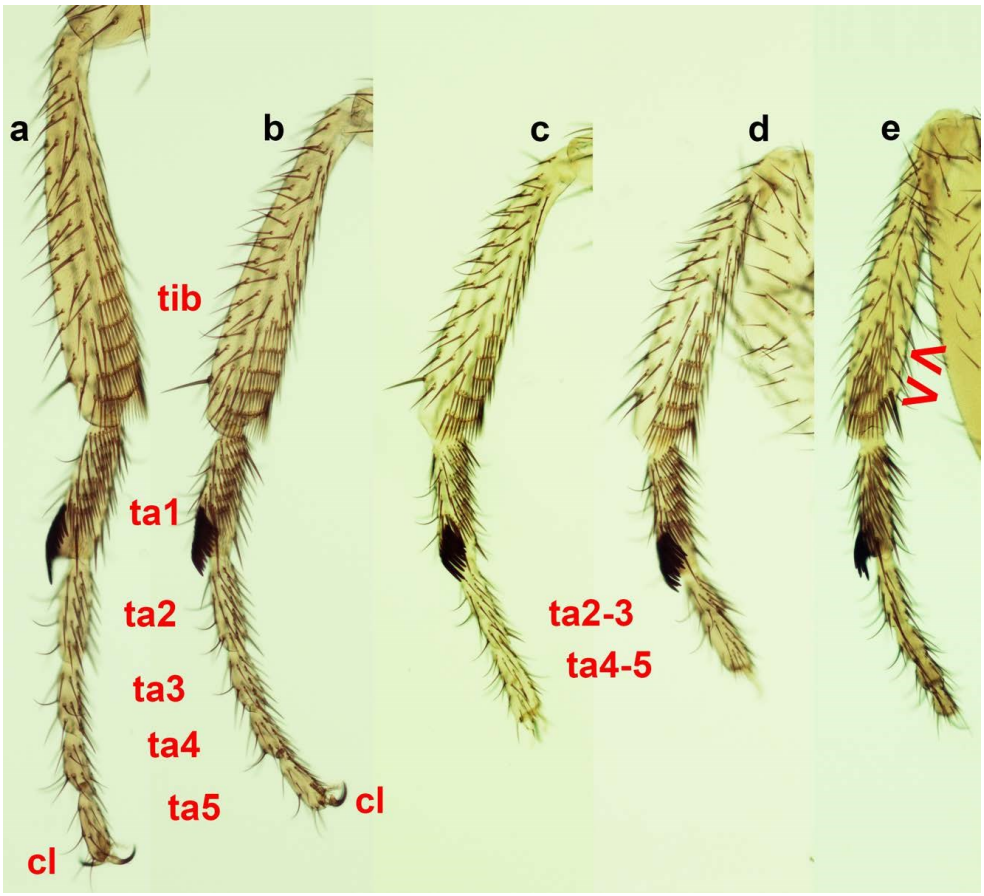

Figure 2. **a**, **b**. Control *Dll>cncC* (GOF, **a**) and *Dll>cncC-RNAi* (LOF, **b**) flies raised entirely at 18°C, which is permissive for $Gal80^{ts}$ (McGuire *et al*., 2004). Leg segments (tibia and tarsal segments 1-5) are labeled, as are claws (cl). **c**, **d**. Experimental *Dll >cncC* (GOF) and *Dll>cncC-RNAi* (LOF) flies raised at non-permissive temperature (30°C) following the embryonic period. The tarsi are shorter due to pairwise fusions of tarsal segments (ta2-3 and ta4-5), and the claws are either absent entirely (**d**) or deformed (**c** has a single straight claw). The t-rows in **a-d** look relatively normal. **e**. *Dll >argos* (EGFR-LOF) fly for comparison. It has all 5 tarsal segments, but they are shorter, and it lacks claws. This leg is also noteworthy, because of two pairs of osculating t-rows (V shapes) pointing in opposite directions on its tibia (see Figure 3f, g). The distal V harbors a t-row fragment in its "jaws," whereas the upper V is empty inside. This specimen constitutes one of the most complex examples of t-row interconnections that we found. To conform with other figures, images of left legs in **a**, **c**, and **e** were flipped to look like right legs.

Further parallels between *cncC*-LOF (our results) and EGFR-LOF (earlier work; Table 1) are also consistent with this notion of a *cnc*-EGFR confederation. Notably, the *cncC*-LOF genotype yields Y-shaped junctions of t-rows (Figure 3) that mimic those of EGFR-LOF (Figure 1). Among 100 forelegs examined, we found 9 Y configurations (9%), which is close to that of $Star^{5671}/Ras1^{e1B}$ (8%) and $Star^{5671}/CyO$ (13%), though far short of *Dll>argos* (71%) and *sca>argos* (25%). Moreover, 42% of *cncC*-LOF sex combs (N = 50) manifest the same sorts of zigzag disruptions that are typical of EGFR-LOF sex combs (Figure 1b inset). *cncC*-LOF also exhibits clumped bristles, but the frequency (31%; N = 100) is much less than the range for EGFR-LOF (83-100%), and all but 5 of the 31 "clumps" just involve single bristles nestling into the crevice between adjacent bristles of a t-row. Hence, the *cncC*-LOF genotype goes farther than any EGFR-LOF construct in fostering Y junctions in the absence of bristle clumping. This uncoupling suggests that X-or-Y intersections may differ in their etiology from bristle clumping, calling into question whether stickiness around the socket perimeter can explain both effects.

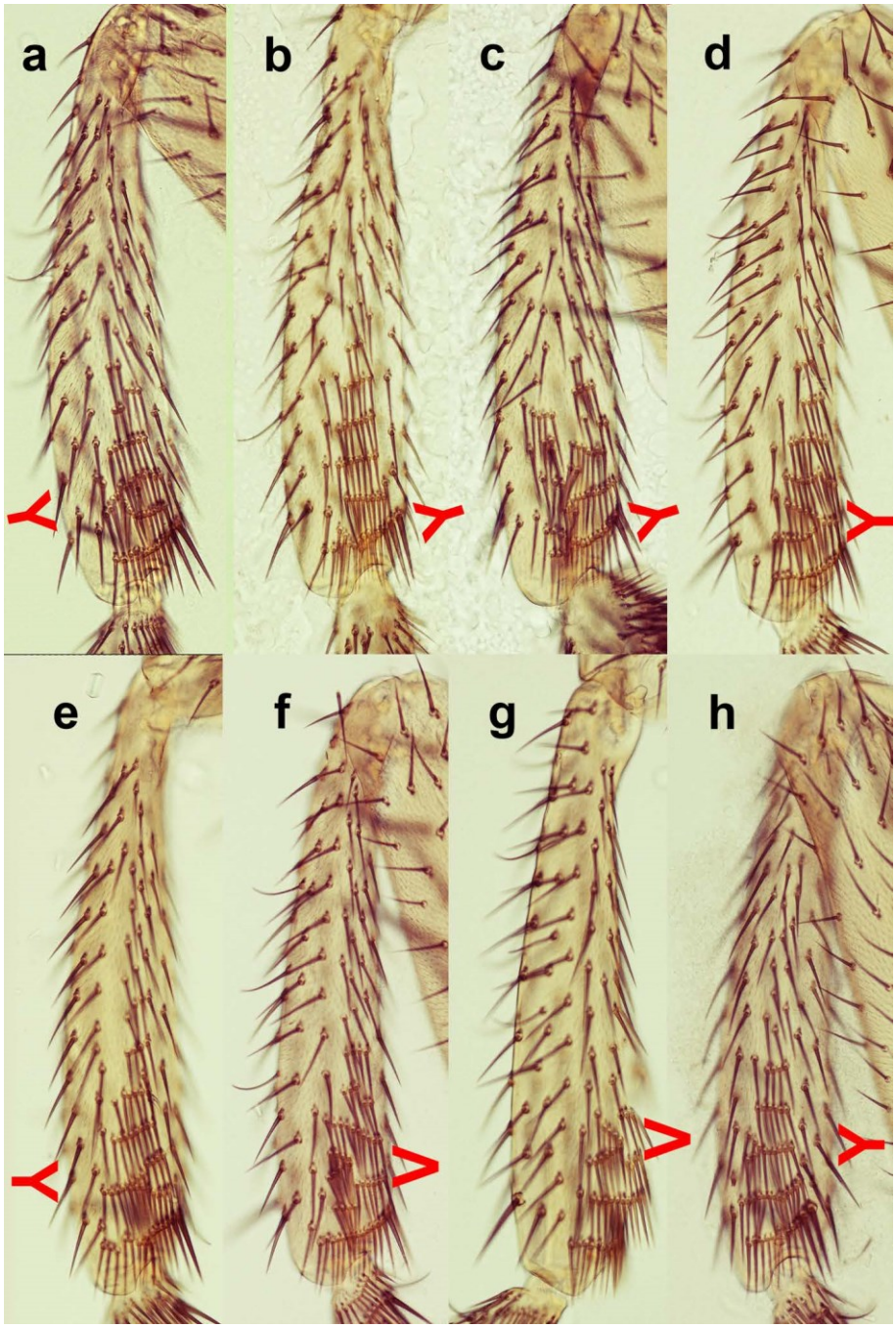

Figure 3. Tibias of *Dll>cncC-RNAi* (LOF) flies raised at 30°C following the embryonic period, which display Y- or V-shaped intersections of t-rows. "V" configurations (**f**, **g**) are a degenerate version of a Y where the stem of the Y is reduced to one bristle. Y shapes in **a**, **d**, and **e** have a short stem and long branches, while those in **b**, **c** and **h** have a long stem and short branches. In conformity with other figures, images of left legs in **a**, **b**, and **d**-**g** were flipped to look like right legs.

At the level of bristle patterns the *Dll>cncC* (GOF) and *Dll>cncC-RNAi* (LOF) flies have almost nothing in common: (1) no X-or-Y-shaped intersections arose among 100 *Dll>cncC* (GOF) forelegs, (2) only 4% of those legs displayed "clumps" and all of them involved single bristles, and (3) virtually all *Dll>cncC* (GOF) sex combs were as straight as a wild-type comb. How then are we to explain the similarity of their tarsi in terms of stunted growth, segmental fusions, and missing claws? Conceivably, an excess of Cnc protein might have the same effect as a dearth thereof (the Goldilocks phenomenon), but a simpler explanation is available. Flooding the tarsus with transcription factors (Ubx or Scr) throughout the larval period can cause drastic truncations as an artifactual side-effect (Held *et al*., 2018), and Cnc is also a transcription factor. Thus, the tarsal similarities in Figure 2 may be deceptively superficial.

Given the trivial effects of *cncC*-GOF and the less-than-drastic effects of *cncC*-LOF on bristle pattern, we must conclude that our infatuation with square arrays was misguided. If t-rows really rely on square arrays like those at the embryonic midline, then *cncC*-LOF should have melted t-rows into total chaos, but it did not. Are there no square arrays at all in the t-row area? It is not easy to follow changes in cell shape in that zone during metamorphosis because the t-row side of the leg mostly faces the body wall and hence is hard to observe in a single focal plane. However, one of us (J.N.M.) managed to surmount these difficulties to record a movie of tibial epidermis when the t-rows are forming (see Materials and Methods) by using a ubiquitously

expressed cadherin-GFP construct to make cell membranes fluoresce (Oda and Tsukita, 2001). Figure 4 is one still frame from that movie. It shows that the epidermal cells between t-rows are hexagonally shaped, not square, and a remarkably similar geometry is visible between the t-rows of *D. pruinosa* (Figure 4B of Tanaka *et al*., 2022), and cells next to the sex comb (a modified t-row) are mostly hexagonal as well (Doerksen *et al*., 2022). Given the ubiquity of these (non-square) cell shapes it is perhaps no wonder that *cnc* turns out to not be essential for t-row spacing.

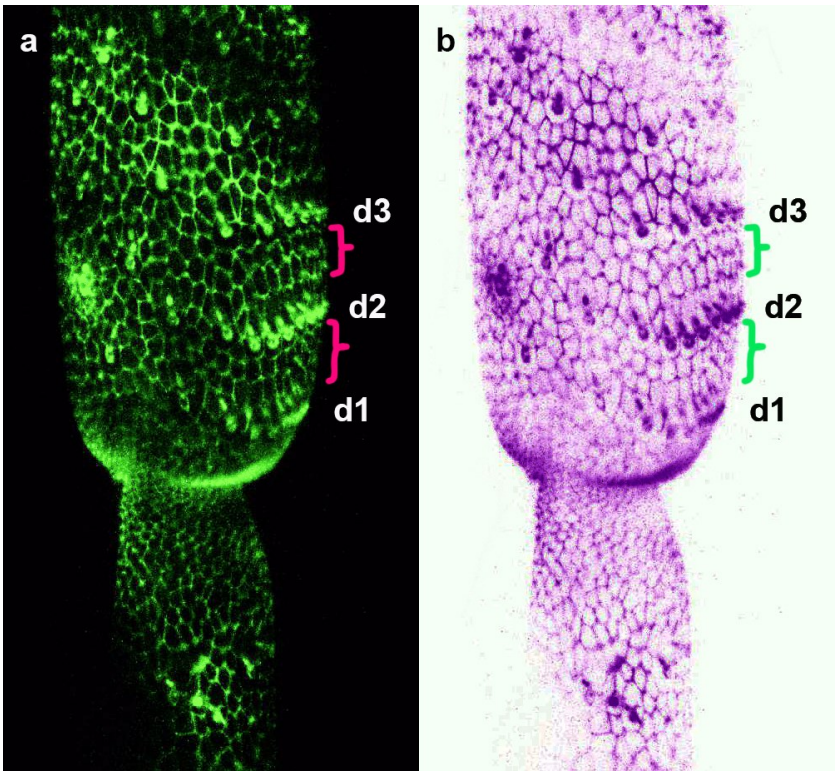

Figure 4. Distal tibia of a right foreleg (anterior view) of a living *D. melanogaster* pupa during the stage when t-rows are forming. Three t-rows are labeled (d1-d3). **a**. Freeze frame of movie. Cell boundaries are visible via a ubiquitously expressed DE-Cadherin-green fluorescent protein (GFP) construct. **b**. Inverted image of **a**, where cell boundaries may be easier to discern. Note the hexagonal (not square) shapes of epidermal cells between the t-rows.

Nevertheless, the mystery of the Xs and Ys remains. Clearly the wild-type *cnc* gene and the EGFR pathway are mutually involved in suppressing such intersections … but how? A possible clue is offered by Peng *et al*.'s (2012) discovery that socket cells induce bracts by extending lamellipodia with an EGFR signal. Socket cells are also critical for t-rows (Held and Harrington, 2022), so they might use comparable protrusions to align bristles. Peng *et al*.'s tendrils are too short to span the gap between t-rows, and they act too late (24 hAP^{25}), but to our knowledge no one has yet looked at the right place (t-row area) and time (16-21 hAP^{25} based on X-or-Y shapes after $Egfr^{ts1a}$ downshifts; Figure 1e, f) to see whether Peng *et al*.'s lamellipodia are longer at earlier stages. This idea is appealing because tibial t-rows develop in distal-to-proximal order (Held and Harrington, 2022), so any protrusions from early t-rows to later ones would have to aim proximally—the same direction in which bristles induce bracts.

Other types of cellular protrusions (aside from lamellipodia) can mediate morphogenesis (*e.g*., cytonemes; Ramirez-Weber and Kornberg, 1999), but some of them are harder to detect histologically than others. Given the ability of basal filopodia to align scale cells on moth wings (Nardi and Magee-Adams, 1986) and the homology of scales with bristles (Zhou *et al*., 2009), it would be worth looking for these "epidermal feet" as well. Scale rows get refined into parallel files that are eerily reminiscent of tibial t-rows in the fly. The paradox here is that *inter*-t-row signaling should be repulsive, while *intra*-t-row signaling should be attractive (adhesive), and it is hard to envision the EGFR pathway being used for both functions at the same time.

Acknowledgments: The *UAS-cncC* and *UAS-cncC-RNAi* stocks were constructed by Sykiotis and Bohmann (2008) and generously supplied by Jen Becker in Matt Rand's lab at the University of Rochester. Useful comments on the manuscript were kindly provided by Artyom Kopp and Jeff Thomas. Technical assistance was furnished by Lia Harrington.

References: Atallah, J., N.H. Liu, P. Dennis, A. Hon, D. Godt, and E.W. Larsen 2009, Evol. Dev. 11: 191-204; Campbell, G., 2002, Nature 418: 781-785; Doerksen, A., M. Mulder, S. Ingram, D. Nelson, J.

Defehr, E. Reimer, J. Atallah, and J.N. Malagon 2022, microPub. *Biology*; Held, L.I., Jr. 1992, *Models for Embryonic Periodicity*. Basel, Karger; Held, L.I., Jr. 2002a. *Imaginal Discs: The Genetic and Cellular Logic of Pattern Formation*. New York, Cambridge Univ. Press; Held, L.I., Jr. 2002b, Mechs. Dev. 117: 225-234; Held, L.I., Jr. 2002c, Dros. Inf. Serv. 85: 17-19; Held, L.I., Jr., and L.G. Harrington 2022, 105: 32-37; Held, L.I., Jr., S.C. McNeme, and D. Hernandez 2018, Dros. Inf. Serv. 101: 25-32; Held, L.I., Jr., and J.J. Shin 2022. Dros. Inf. Serv. 105: 20-24; Kopp, A., 2011, Evol. Dev. 13: 504-522; McGinnis, N., E. Ragnhildstveit, A. Veraksa, and W. McGinnis 1998, Development 125: 4553-4564; McGuire, S.E., Z. Mao, and R.L. Davis 2004, Sci. STKE 2004 (220): p16; Nardi, J.B., and S.M. Magee-Adams 1986, Dev. Biol. 116: 265-277; Oda, H. and S. Tsukita 2001, J. Cell Sci. 114: 493-501; Peng, Y., C. Han, and J.D. Axelrod 2012, Dev. Cell 23: 507-518; Ramirez-Weber, F.-A., and T.B. Kornberg 1999, Cell 97: 599-607; Sykiotis, G.P., and D. Bohmann 2008, Dev. Cell 14: 76-85; Szebenyi, A.L., 1969, Anim. Behav. 17: 641-651; Tanaka, K., O. Barmina, A. Thompson, J.H. Massey, B.Y. Kim, S. Suvorov, and A. Kopp 2022, Dev. Genes Evol. 232: 89-102; Tokunaga, C., 1962, Dev. Biol. 4: 489-516; Zhou, Q., L. Yu, X. Shen, Y. Li, W. Xu, Y. Yi, and Z. Zhang 2009, Genetics 183: 619-627.

Socket cells, not shaft cells, align t-rows and sex combs.

Held, Lewis I., Jr., and Lia G. Harrington. Department of Biological Sciences, Texas Tech University, Lubbock, Texas 79409.

The exoskeleton of an insect shields it from harm but inhibits its ability to feel things. Flies solve this "coat of armor" problem by deploying touch-sensitive bristles throughout their cuticle at fairly regular intervals. The precision of these bristle arrays in some parts of the fly surface is astounding, most notably on the legs, where transverse rows of bristles function as brushes for grooming (Szebenyi, 1969). Those "t-rows" are parallel single files of bristles that run transverse to the leg's main axis, looking a lot like the chevrons on a sergeant's sleeve. In some species of *Drosophila*, evolution has modified one or more t-rows on the basitarsus to craft a "sex comb" of thicker, darker bristles (Tokunaga, 1962) that males use to grasp females during courtship (Ng and Kopp, 2008). Sex combs have been the subject of intense investigation from both an evolutionary (Kopp, 2011) and a developmental (Tanaka *et al.*, 2009) perspective, but we still do not know exactly how the cells of the t-rows and sex comb go about assembling themselves into such intricate patterns.

Each mechanosensory bristle organ contains four cells: a cell that makes the shaft, a cell that makes the socket, a neuron, and a cell that forms a sheath around the neuron. All of them are descended from a common sensory organ precursor (SOP) that undergoes successive mitoses (Held, 2002). The question that we pose here is: Which of these cells lets bristles form chains? In principle, it should be easy to answer this question. All that would be necessary is to delete one or more of the cell types in the bristle lineage and see if t-rows and sex combs can still form. A similar riddle was recently solved vis-à-vis which cell type is responsible for inducing a bract. In that case all of the experimental evidence pointed to the socket cell (Peng and Axelrod, 2012). By using the same approach as in that previous study, we arrived at a similar conclusion—*viz*., that the socket cell also seems to be responsible (at an earlier stage than bract induction) for corralling bristle cells into t-rows and into a sex comb.

Materials and Methods

To suppress sockets, we injected Mitomycin C into pupae at a concentration of 0.1 mg/ml at various times after pupariation. Details on the protocol can be found in Held (1990), where the specimens used in the present investigation were preserved. In that earlier paper we also studied socket inhibition by the mutation *l(1)63*, but a re-examination revealed that that it erases more bristles entirely (both socket and shaft) on the foreleg than on the midleg, which was the focus of our 1990 paper. Because these bald patches interfered with our ability to analyze the t-row area, *l(1)63* proved less useful than Mitomycin C for assessing the ability of

shaft cells to form t-rows, so we decided not to include any data from those mutant legs in the present manuscript.

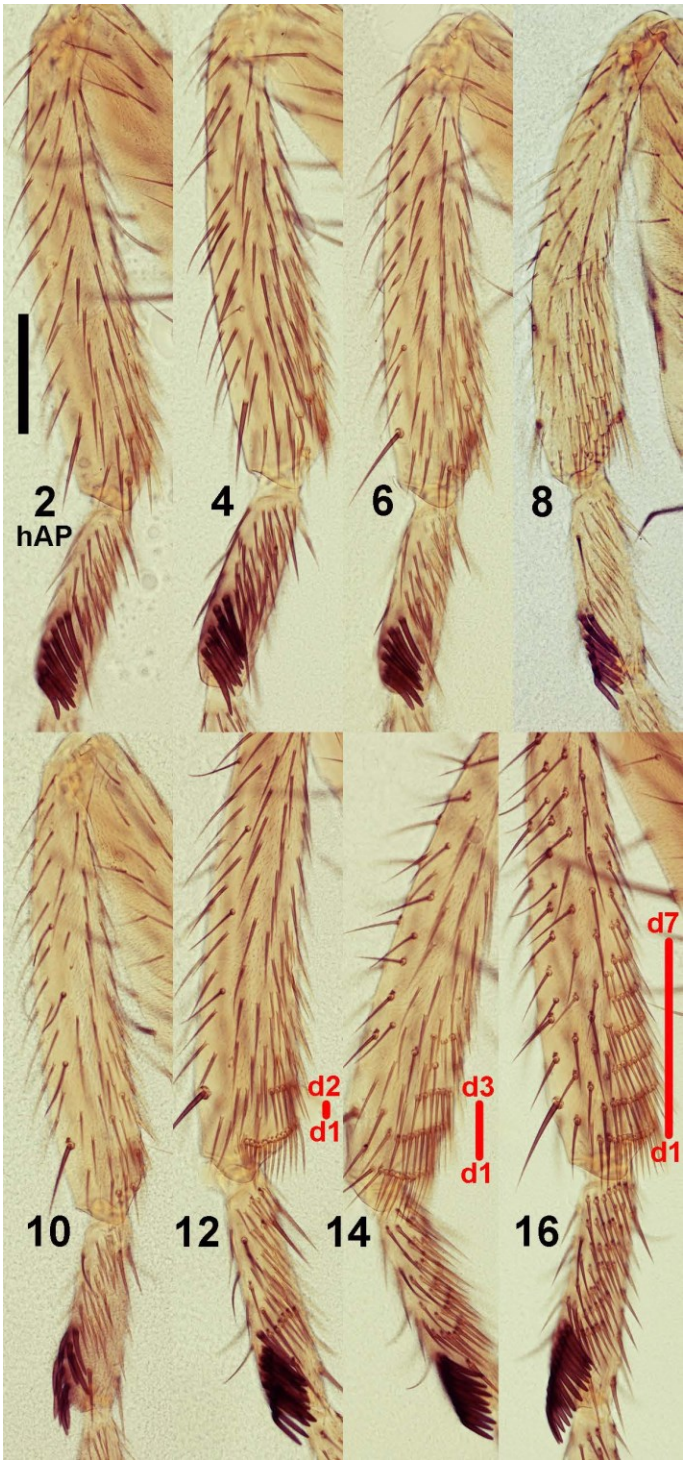

Figure 1. Effects of Mitomycin C injection on the male foreleg tibia and basitarsus. Numbers denote ages (in hAP^{25}) when pupae were injected. Photos are of representative specimens per cohort (N = 6 forelegs examined per time point). Until 12 hAP^{25} tibial bristles lack sockets and fail to organize into recognizable t-rows, and sex comb teeth are dissociated from one another in a loose zigzag array. At 12 hAP^{25} the two distalmost t-rows (d1 and d2) appear, followed at later time points by more proximal t-rows until 16 hAP^{25} when the full complement of t-rows is reached (indicated by vertical bars). From 12 hAP^{25} on, the average number of teeth rose slightly from 10 to 12, and the size of the tibia and basitarsus also increased. To conform with other figures, the images for 2, 6, 8, 10 hAP^{25} were flipped horizontally to appear as right (*vs*. left) legs. Scale bar (upper left) = 100 μm.

To suppress shafts, we used two approaches. First, we examined a *shaven*^{depilate} (*sv*^{de}) stock from the Bloomington Stock Center (#662): *sv*^{de}/Dp(2;4) *ey*^{D}, *ey*^{D}. Second, we disabled the gene *numb*, which encodes shaft identity (see text) by using a *UAS-numb-RNAi* construct (#35045) that we expressed in the tibia and tarsus via a *Distal-less* (*Dll*)-*Gal4* driver. To bypass the embryonic stage when *numb* is vital, we toggled *Gal4*'s gene's expression to a null state at 18°C via a temperature-sensitive *Gal80*^{ts} transgene (see McGuire *et al.*, 2004) and then released *Gal4* from this silencing by shifting larvae to 30°C before pupariation. Flies develop slower at 18°C and faster at 30°C, so we normalized ages in hours after pupariation to the standard 25°C developmental rate ("hAP^{25}"). Conversion factors were 0.5 (18° → 25°) and 1.16 (30° → 25°).

Flies were raised on Ward's *Drosophila* Instant Medium plus Baker's yeast and preserved in 70% ethanol. Fly legs were mounted in Faure's fluid (Lee and Gerhart, 1973) between cover slips and photographed with a Nikon microscope. We used blunt forceps to press on the top cover slip to roll the tibia a few mm orthogonal to its axis so as to turn it to an ideal angle for viewing the t-rows.

Results and Discussion

When Tobler (1969) injected *D. melanogaster* larvae with Mitomycin C, he found that this anti-cancer drug eliminated sockets from bristles all over the whole body, except on the abdomen (Tobler and Burckhardt, 1971), leaving only the shaft portion of each bristle intact. The effects on t-rows and sex comb were dramatic: t-rows dissolved into a chaotic forest of shafts, and the bristles ("teeth") of the sex comb failed to line up in a single file (his Figure 2), although the sex comb was still able to rotate fully (see Atallah *et al.*, 2009). A later study by Walt and Tobler (1978) showed that the socket cell is still present in Mitomycin-injected flies, but it is disabled—not only insofar as it cannot form a socket but also insofar that it cannot induce a bract (see Peng and Axelrod, 2012).

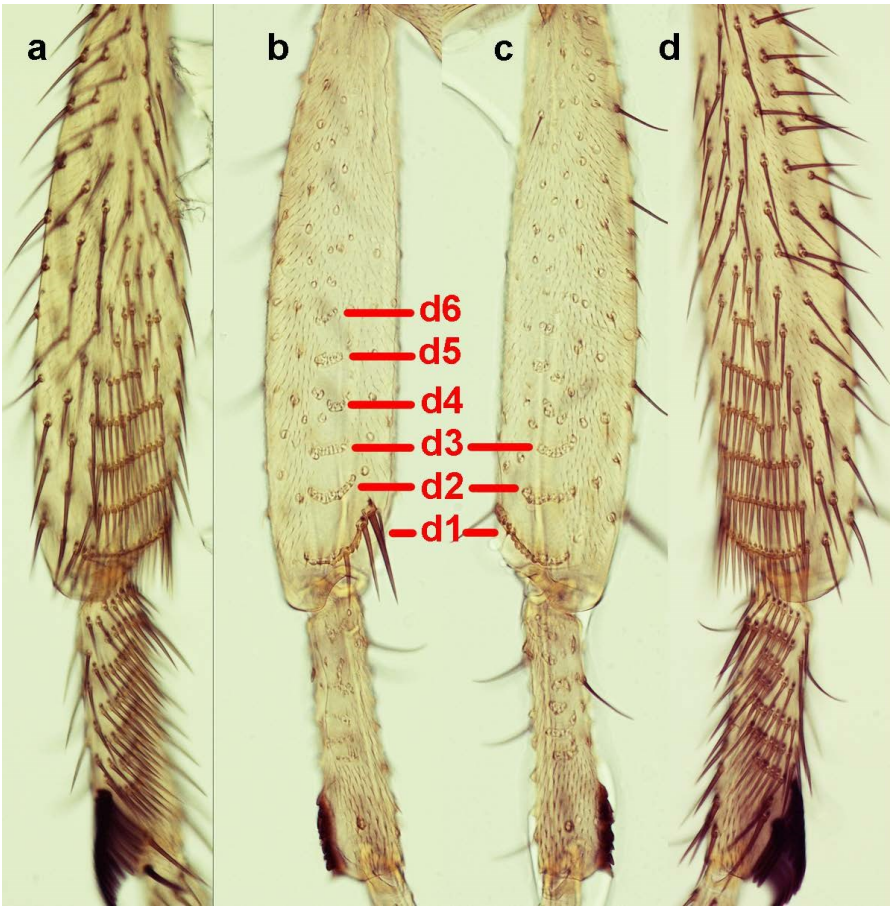

Figure 2. Middle panels: right (**b**) and left (**c**) forelegs of a representative male sv^{de} homozygote (N = 12 males examined), showing the ability of socket cells to form t-rows without any apparent assistance from shaft cells. The right leg displays six t-rows (d1-d6), while the left one has only three (d1-d3), and all of these rows are devoid of shafts except for d1. Such "fluctuating asymmetry" is indicative of a stochastically unstable process (Dongen, 2006). The bristles of the sex combs have rudimentary, pigmented shafts, so no conclusion can be drawn about the role of socket cells alone in sex comb alignment. Flanking panels: right (**a**) and left (**d**) forelegs of a typical male sv^{de}/ey^{D} heterozygote from the same generational pool of siblings as **b** and **c** (raised under identical conditions), whose t-rows look wild-type. However, the sex combs are slightly enlarged due to the ey^{D} mutation.

We wanted to ascertain the latest stage when Mitomycin C injections could produce these defects, so we used his injection protocol during the pupal period at 2-hour intervals from 2 to 24 hAP^{25}. We obtained the same disorganized phenotype that he did for time points 2, 4, 6, 8, and 10 hAP^{25} (Figure 1), but by 12 hAP^{25} we began to see sockets and t-rows appear from the distal end of the tibia, gradually extending proximally until by 16 hAP^{25} the tibia acquired a wild-type state. The sex comb followed the same time course with half the forelegs at 12 hAP^{25} (transition point) being straight and the other half displaying zigzag disruptions. From these results we conclude that (1) a functional socket cell is needed for proper t-row and sex comb alignment, and (2) the shaft cell cannot align such bristles on its own. However, the sex comb does not need sockets in order to rotate. It is also clear from our data that the t-rows arise in a distal-to-proximal wave, rather than all at once; Held and Shin (2022) provide corroboration for this conclusion.

Having shown that the socket cell is necessary for t-row and sex comb alignment, we next wished to see whether it is sufficient. In 1973 Tobler *et al.* studied two mutants that suppress shafts but retain sockets:

Hairless^{2} and *sv*^{de}, but *Hairless*^{2} has negligible effects on t-row and sex comb bristles, so we focused our investigation solely on *sv*^{de}.

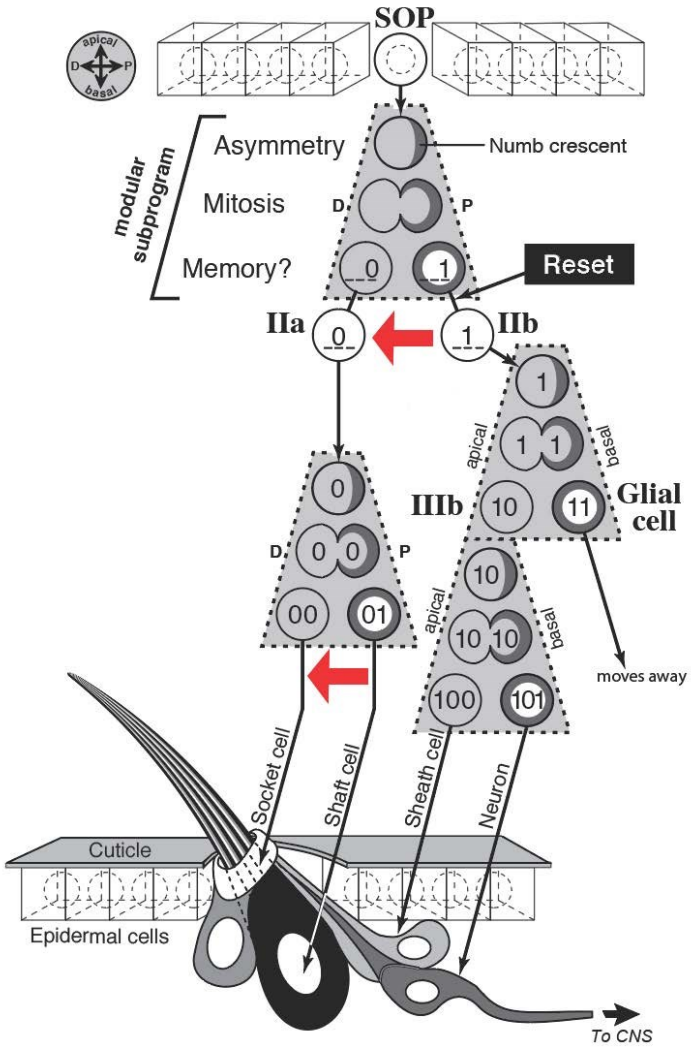

Figure 3. Differentiative divisions of a bristle SOP. Modified (with permission) from Held (2002). "1" and "0" denote presence or absence, respectively, of Numb protein following segregation of the Numb crescent during each mitosis, with the final combinatorial states providing a binary code. This code dictates cell fate. For example, the code for a socket cell is "0, 0." "P" and "D" are proximal and distal for leg bristles (*vs.* thoracic bristles whose anterior-posterior axis was depicted in the original diagram). Thick arrows show presumed effects (identity shifts) caused by using *UAS-numb-RNAi* to block *numb* expression during the indicated mitoses. Converting a IIb cell into a IIa cell (upper thick arrow) should result in a twinned external bristle (2 shafts, 2 sockets). Further conversion of a shaft cell into a socket cell (lower thick arrow) should produce 4 socket cells at that site, with no other cell types present.

Some ambiguity exists about whether a shaft cell is actually present in *sv*^{de} bristle organs that lack overt shafts. Walt and Tobler (1978) assert that it is absent based on histology at an ultrastructural level (*i.e.*, transmission electron microscopy), but a later study by Kavaler *et al.* (1999) which used stronger alleles of *sv* at the *D-Pax2* locus suggests that the shaft cell may be present (at least at earlier stages) based on genetic markers for cell identity.

We examined the forelegs of a dozen homozygous *sv*^{de} flies from a balanced stock of heterozygous *sv*^{de} /*ey*^{D} individuals. Panels b and c in Figure 2 show the right and left forelegs of a single *sv*^{de} male to convey the range (and bilateral asymmetry) of the phenotypes we witnessed. The right leg (b) of this specimen has a full complement of t-rows (d1-d6), whereas its left leg (c) displays fewer bona fide rows (d1-d3). All of these rows (except d1 where some shafts exist) formed with sockets alone, thus arguing that socket cells are sufficient for t-row alignment, though rows above d2 tend to have fewer sockets than expected. The sex comb is another matter entirely. Its bristles all have rudimentary shafts (as can be inferred from the dark pigmentation), so we cannot assess the sufficiency of sockets for sex comb development.

Given the possibility of residual shaft cell function in *sv*^{de} flies, we looked for a way to guarantee a complete absence of shaft cells by using the gene *numb*, which encodes the four cell identities (shaft cell,

socket cell, neuron, and sheath cell) that descend from the SOP (Rhyu *et al.*, 1994). The only cell that never expresses *numb* in any of its mitotic ancestors is the socket cell (Held, 2002). Hence, we should be able to convert the other three cells into socket cells by blocking *numb* expression during the SOP's differentiative mitoses (Figure 3). To achieve that suppression we used *Dll-Gal4* to drive expression of *UAS-numb-RNAi* in the tibia and tarsus.

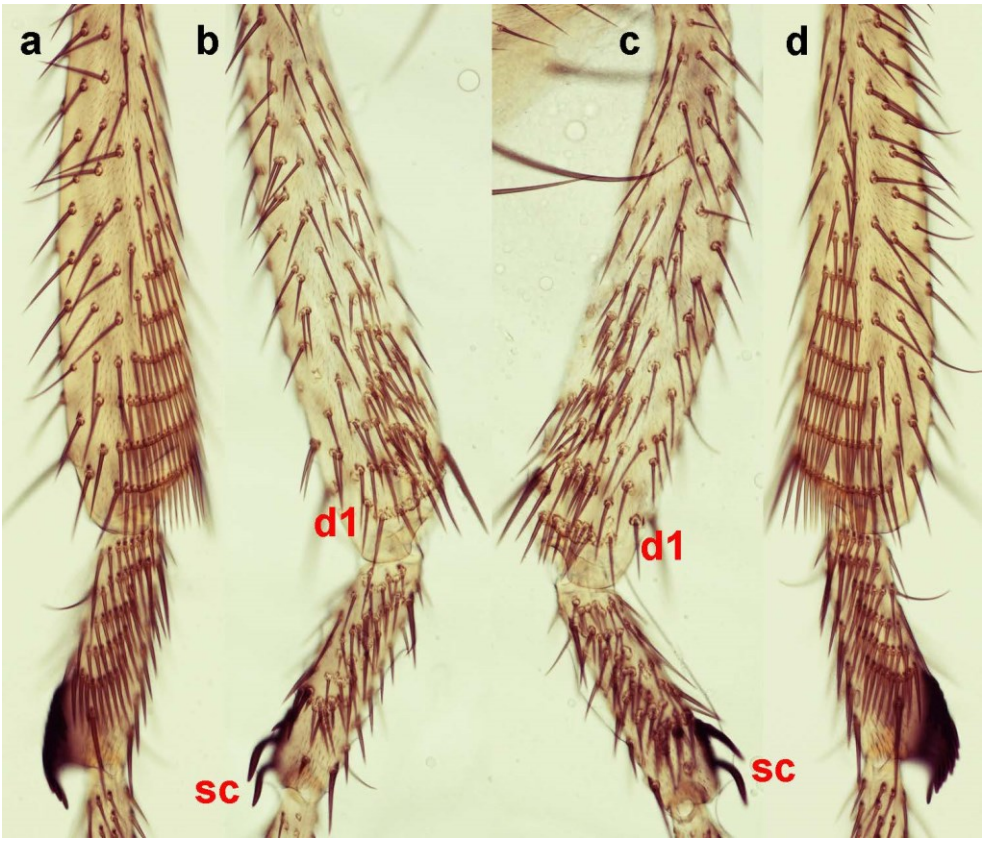

Figure 4. Middle panels: right (**b**) and left (**c**) forelegs from a *Dll-Gal4/UAS-numb-RNAi; Gal80^{ts}/+* male that was shifted to 30°C before pupariation (N = 12 males examined). The distalmost t-row (d1) of the right leg (**b**) consists almost entirely of socket cells, which have managed to form a straight line with little or no assistance from shaft cells. The distalmost t-row (d1) of the left leg (**c**) appears to be a jumble of ordinary bristles and enlarged sockets. Elsewhere on the tibias are many cases of twinned bristles, which appear to have been induced by a IIb→IIa conversion (see Figure 3) without any subsequent conversion of shaft→socket. The sex combs (sc) of both legs appear to have undergone conversion of shafts to sockets, except for ~2 teeth each. Flanking panels: right (**a**) and left (**d**) forelegs of a control male of the same genotype as **b** and **c** but raised only at the permissive temperature of 18°C. Its t-rows look wild-type.

Because *numb* is vital for embryonic development, we used the *Gal80^{ts}* transgene to bypass the embryonic period (McGuire *et al.*, 2004). We collected eggs from *Dll-Gal4/CyO; Gal80^{ts}* mothers (mated with *UAS-numb-RNAi* males) at room temperature (22°C) for 2-day periods, then placed in vials at 18°C for 3, 5, 7, or 9 more days, at which point we transferred the vials (containing larvae but no pupae) to a 30°C incubator for the remainder of development. Only the vial with the oldest larvae at time of upshift (9 days at 18°C) yielded sufficient F_1 adults for analysis. From that cohort we mounted the legs of a dozen non-Curly (*Dll-Gal4/UAS-numb-RNAi; Gal80^{ts}/+*) F_1 males.

We saw frequent cases of twinned bristles (indicative of solitary IIb→IIa conversions), but quadruple sockets (IIb→IIa plus shaft→socket) were less common, perhaps due to an inability of the *UAS-numb-RNAi* to overcome both hurdles of endemic *numb* transcription. The organization of the t-rows was commonly disrupted. The forelegs of one interesting specimen are shown in Figure 4 (b, c). The distalmost t-row of its right foreleg consists almost entirely of socket cells, yet it has aligned itself fairly normally, and most sex comb teeth of this fly appear to have been converted to sockets, yet the sex combs are straight. These results

are consistent with our inference that socket cells, not shaft cells, are critical for aligning both t-rows and sex combs.

Acknowledgments: Useful comments on the manuscript were kindly provided by Artyom Kopp. Technical assistance was furnished by Lien Ngo.

References: Atallah, J., N.H. Liu, P. Dennis, A. Hon, D. Godt, and E.W. Larsen 2009, Evol. Dev. 11: 191-204; Dongen, S.V., 2006, J. Evol. Biol.19: 1727-1743; Held, L.I., Jr. 1990, Roux's Arch. Dev. Biol. 199: 31-47; Held, L.I., Jr. 2002, *Imaginal Discs: The Genetic and Cellular Logic of Pattern Formation*. New York, Cambridge Univ. Press; Held, L.I., Jr., and J.J. Shin 2022. Dros. Inf. Serv. 105: 20-24; Kavaler, J., W. Fu, H. Duan, M. Noll, and J.W. Posakony 1999, Development 126: 2261-2272; Kopp, A., 2011, Evol. Dev. 13: 504-522; Ng, C.S., and A. Kopp 2008, Behav. Genet. 38: 195-201; Peng, Y., C. Han, and J.D. Axelrod 2012, Dev. Cell 23: 507-518; Rhyu, M.S., L.Y. Jan, and Y.N. Jan 1994, Cell 76: 477-491; Szebenyi, A.L., 1969, Anim. Behav. 17: 641-651; Tanaka, K., O. Barmina, and A. Kopp 2009. PNAS 106(12): 4764-4769; Tobler, H., 1969, Experientia 25: 213-214; Tobler, H., and H. Burckhardt 1971, Experientia 27: 189-191; Tobler, H., V. Rothenbühler, and R. Nöthiger 1973, Experientia 29: 370-371; Tokunaga, C., 1962, Dev. Biol. 4: 489-516.

Molecular evolution of the GstD1 protein with alkaloid interaction in cactophilic *Drosophila* species.

dos Santos[1*], Adriano Silva, Silvana Giuliatti[1], Dora Yovana Barrios-Leal[1], and Maura Helena Manfrin[1,2]. [1]Postgraduate, Department of Genetics, Faculty of Medicine of Ribeirão Preto, University of São Paulo, Ribeirão Preto, Brazil; [2]Department of Biology, Faculty of Philosophy, Sciences and Letters of Ribeirão Preto, University of São Paulo, Brazil.

Abstract

Genetic mutations in codons can result in changes in amino acids and properties in proteins, which contribute to the diversification of phenotypes and interactions of organisms with the environment. The *Drosophila*-cactus model encompasses seven cactophilic species of the *Drosophila buzzatii* cluster (*Drosophila repleta* group), with distribution in South America, and important candidates to study genetics, ecology, and adaptation. These organisms show phenotypic changes (viability, developmental time, reproductive system, and wing morphology) and differential gene expression (*e.g*., detoxification genes such as *GstD1*) when larvae develop into necrotic tissues in different cactus host species. This *GstD1* gene (630 bp) is an important candidate in the adaptation process in *Drosophila*. We obtained seven complete coding sequences for *GstD1*, with representatives of closely related species in the *D. buzzatii* cluster. Variations in codons of *GstD1*, with the meaning of positive and purifying selection, were found among the *Drosophila* species. Our data indicated four positive selection signals with changes in amino acids positioned within or close to active sites in proteins. The GstD1 enzymes present different values of interaction energy with the alkaloid mescaline. Our results indicate that changes in GstD1 may contribute to protein interactions with chemical substrates, and we discuss the effects concerning the ecology of *Drosophila* species. Keywords: *Drosophila*; GstD1; molecular evolution; docking; physiology; host cactus.

Introduction

The *Drosophila buzzatii* cluster (*Drosophila repleta* group) is attractive in studies with the *Drosophila*-cactus model as it is promising for understanding gene functions and evolutionary biology, which is a monophyletic group composed of seven cactophilic species: *Drosophila buzzatii*, *Drosophila koepferae*, *Drosophila antonietae*, *Drosophila serido*, *Drosophila gouveai*, *Drosophila seriema*, and *Drosophila borborema* (Manfrin *et al.,* 2001; Manfrin and Sene, 2006; Santos *et al.,* 2009; Franco *et al.,* 2010). This

group comprises the biological characteristics: the organisms must develop in necrotic tissue of cacti (Pereira *et al.,* 1983; Manfrin *et al.,* 2006); distribution in open areas in South America (Manfrin *et al.,* 2006; Barrios-Leal *et al.,* 2019); constant selection pressure with cactus chemical barriers, such as alkaloid groups, which is potentially toxic to *Drosophila* development (Kircher *et al.,* 1967; Soto *et al.,* 2014).

Chemical factors such as alkaloid contents in cacti, for example, mescaline and trichocerein, are related to changes in survival, developmental time, and wing morphology in *D. buzzatii* (Padró *et al.,* 2018; Soto *et al.,* 2014). Interestingly, differences in expression levels of detoxification-related genes in larvae that developed in their secondary host *Trichocereus terscheckii* cacti compared to their primary host *Opuntia suphurea*, with overexpression of *Gst* genes in the host plant change in the cactophilic fly *Drosophila buzzatii* (cluster *Drosophila buzzatii*) (Matzkin, 2014; Panis *et al.,* 2016).

The Glutathione S-Transferase (GST) superfamily is interesting for studies due to its diversification by processes that include gene duplication and loss, change in codons, amino acid substitution, and differential regulation (Low *et al.,* 2007; Saisawang *et al.,* 2012). The GSTs enzymes have roles in physiological processes, protection against oxidative stress, hormonal biosynthesis, and detoxification (Saisawang *et al.,* 2012). One of the GSTs enzymes, Glutathione S-Transferase D1 (GstD1), has received attention for its metabolic detoxification function, such as in pesticides (dichloro-diphenyl-trichloroethane) (Low *et al.,* 2007), cytotoxic compounds (4-hydroxynonenal) (Saisawang *et al.,* 2012), and allelochemical substances from plants involved in the use of the host by herbivorous insects (Gloss *et al.,* 2014).

Matzkin, (2008) reported seven non-synonymous substitutions, with two differences in the active site pocket of the GstD1 enzyme (Leu-7-Gln and His-39-Gln), in cactophilic flies (*D. arizonae* and *D. mojavensis*) that developed differently in plant tissues of cactus species. The interactions of flies with decaying pieces of cactus involve potentially toxic organic compounds, with constant selection in organisms to resist these components in breeding sites (Matzkin, 2008; Panis *et al.,* 2016).

Considering the association of flies with cacti to investigate the pattern of evolution of *GstD1* gene in *D. buzzatii* cluster species, we analyzed selective changes in *GstD1* codons and physicochemical properties of amino acids. Additionally, we evaluated the interaction of the enzyme GstD1 with a chemical molecule (mescaline) found in different cacti, and that has been used in other research of models drosophila-cacti (Soto *et al.,* 2014; Padró *et al.,* 2018), with evaluating the relationship to the survival of *Drosophila*.

Material and Methods

2.1 Biological samples and sequences

We analyzed seven species of the *Drosophila buzzatii* cluster samples: *D. koepferae*, *D. antonietae*, *D. serido*, *D. gouveai*, *D. borborema*, and *D. seriema* (Table S1). DNA extraction was performed with a sample representative of each species of the *D. buzzatii* cluster, according to the protocol of DNeasy® tissue kit (QIAGEN Inc., Hilden, Germany). Only for the species *D. buzzatii*, the sequence of *GstD1* was obtained from the genome (scaffold 305: 1573-2228), available at http://dbuz.uab.cat/welcome.php. Two pairs of primers for amplification and sequencing of the *GstD1* gene were designed based on sequences available in GenBank (access EU079442.1 and EU079471.1), following forward and reverse primers: 1 – F 5' – MATGGYTGACTTCTAYTAYC - 3' and R 5' –TTCTCGTACCACTTGTTCACGTTNKCR - 3'; 2 – F 5' – CCCGAGTTCGTGAAGATCAAYCCNCA - 3' and R 5' –GGCTYAWTCGAAGTAYTTCTTG - 3'. The amplifications were performed in 20 µL reaction with 50-75 ng of DNA, 2.0 mM $MgCl_2$+ buffer, 2.0 mM dNTPs, 0.4 µM of each primer and 0.5 U *Taq* polymerase. The PCR conditions were one step of 94°C for 1 min 30 sec, 35 cycles of 94°C for 30 sec, 46°C for 30 sec, and 72°C for 2 min, with a final extension of 72°C for 10 min.

DNA sequencing reactions we performed with the BigDye Terminator Cycle Sequencing Ready Reaction kit protocol (Perkin-Elmer, Foster City, CA, USA), with runs on the ABI Prism 377 sequencer (Applied Biosystems, Foster City, CA, USA), and quality assessment using Phred (Ewing and Green, 1998). Alignments were performed in ClustalW Multiple Alignment 1.8 (Thompson *et al.,* 1994) and sequence editing using BioEdit 7.1.9 (Hall, 1999). Heterozygous sites (double peaks in chromatograms) were inferred using the Chromas program. Thus, a second sequencing reaction was performed to confirm the double peaks.

2.2 Phylogenetic analyses

To compare the phylogenetic structure, we analyzed sequences of *GstD1* of 11 species of *Drosophila*. As outgroups, we use the cactophilic species *D. mojavensis*, *D. arizonae* and *D. navojoa*, and *D. virilis* as non-cactophilic.

The phylogenetic hypothesis using *GstD1* sequences was estimated by Bayesian Inference (BI) tree in MrBayes v.3.1.2 (Huelsenbeck, 2001). The General Time Reversible (GTR+G) model of nucleotide substitution was determined as the best fit model in jModeltest v.2.1.2 (Posada, 1998) for both genes. The convergence and stability of the parameters were verified using Tracer v.1.6 (effective sample size, ESS ≥ 200) (Rambaut *et al.,* 2018) and visualized as a consensus tree using FigTree v.1.3.1.

2.3 Selection signal analysis

To evaluate the codon selection and amino acids properties, analyzes were performed using the structure topology inferred for the DNA sequences with the Maximum Likelihood (ML) method in MEGA v.6.0 (Tamura *et al.,* 2013). In the first step, comparisons between the sequences of the nuclear gene *GstD1* were analyzed using the ratio (ω) between the rate of non-synonymous substitutions (dN) by synonymous substitutions (dS) (ω = dN/dS) (Doron-Faigenboim *et al.,* 2005), using the Selecton Server (Available at http://selecton.tau.ac.il/). We analyzed the models M8 (beta, ω ≥ 1, proportions p1 = 1-p0) (Yang *et al.,* 2000), M8a (beta, ω = 1) (Swanson *et al.,* 2003), and M7 (beta) (Yang *et al.,* 2000). The values of ω < 1, ω = 1, and ω > 1 represent signs of purifying, neutral and positive selection, respectively. Statistical significance was assessed using the X^2 test, assuming 2 degrees of freedom and $P < 0.05$.

The second step, the selective influence assessment of 31 physical-chemical properties of amino acid residues of GstD1, was evaluated according to McClellan and McCracken (2001) in TreeSAAP v.3.2 (Woolley *et al.,* 2003). This analysis uses a gradient of categories to classify changes in amino acid residues in property between conservative (C1 to C5) and destabilizing (C6 to C8), with structural and functional consequences. Scores assessed using $P < 0.05$, $P < 0.01$ and $P < 0.001$.

2.4 Structure modeling analyses

All complete coding sequences (CDs) of *GstD1* were translated into amino acid residues using the EMBOSS Transeq (available at https://www.ebi.ac.uk/Tools/st/emboss_transeq/) using the codon table pattern. The three-dimensional structure of the GstD1 protein was modeled by homology using Modeller 9v.7 (Sali *et al.,* 1995), using the protein model in *Drosophila melanogaster* (access to the Protein Data Bank: 3MAK), to obtain the structure 3D of *D. mojavensis*, and in the species of the cluster *D. buzzatii*.

Protein models were evaluated using the Ramachandran Plot Analysis (Available at http://mordred.bioc.cam.ac.uk/~rapper/rampage.php.) (Lovell *et al.,* 2003). Protein structure alignment using Chimera v.1.14 (Pettersen *et al.,* 2004). The constitution of the active sites of GstD1 (G and H) was analyzed using metaPocket v.2.0 (Huang, 2009).

Molecular docking was evaluated with the interaction of the G site in GstD1 with mescaline (PubChem access: 4076; 3,4,5-Trimethoxyphenethylamine) using the PyRx program (Wolf, 2009), with independent runs (Pagadala *et al.,* 2017). Inferences with negative interaction energy values (Kcal/mol) suggest a better ligand position in the binding site (Pagadala *et al.,* 2017). Finally, changes in ligand and protein interactions and hydrophobic forces were manually analyzed and visualized using PyMOL v.2.3 (DeLano, 2018).

Results

3.1 Phylogenetic analysis

The 630 base pairs of *GstD1* coding region, single exon, were obtained for species of *D. buzzatii* cluster. The BI tree based on *GstD1* sequences recovered the monophyly of the *D. buzzatii* cluster (Fig. 1; Bayesian Posterior Probabilities, BPP = 1). For the *GstD1* BI tree, a polytomy defined the intra-cluster relationship with a branch for *D. buzzatii*, another one for *D. koepferae*, and two well-supported clades: one encompassing *D. antonietae* and *D. serido* as sister species (BPP = 1.0), and other with *D. gouveai*, *D. borborema* and *D. seriema* (BPP = 0.94), with the last two sister taxa (BPP = 1.0) (Fig.1).

3.2 Selection test

The selective changes in DNA sequences were evaluated using the rate of synonym substitutions (dS) and the rates of non-synonyms (dN) at each codon site. Sites with positive selections were located in the sequences of the *GstD1* gene in DNA molecules obtained from flies of the *D. buzzatii* cluster species. Positive selection is evident in six codons (positions 2, 117, 133, 171, 191, and 209) (dN/dS > 1) (see Table 1). We found positive selection for the heterozygous site at codon 117 (C > T) (changed Leu to Val) in *D. seriema*. The substitution in codon 117 results in an amino acid change (Leu-117-Val) within the G-site for *D. serido* and *D. koepferae*. The substitution at codons 171, 191, and 209 resulted in amino acid changes within the H-site in *D. gouveai*. The substitution in codon 2 is close to the active sites in all species (Figure 2).

Table 1. Results of positive selection in codons (Selecton) of *GstD1* gene sequences, which is presented in *Drosophila* species, codon position, ω values, amino acid residues, and confidence interval. Val = valine; Thr = threonine; Lys = lysine.

Species	Codon position	ω values	Amino acid residues	Active site	Confidence interval
D. gouveai, *D. koepferae*, *D. seriema*, *D. serido*, *D. borborema* and *D. antonietae*.	2	1.6	Val	-	0.13, 4.9
D. serido and *D. koepferae*	117	4.8	Val	Site G*	0.46, 4.9
D. gouveai, *D. serido*, *D. antonietae*, *D. buzzatii* and *D. koepferae*	133	2.5	Thr	-	0.13, 4.9
All species in the cluster	171	3.0	Lys	Site H*	0.46, 4.9
All species in the cluster	191	2.8	Thr	Site H*	0.13, 4.9
D. borborema, *D. serido* and *D. antonietae*	209	4.6	Lys	Site H*	0.46, 4.9

Note. * Selective change in active site for some species of *Drosophila*.

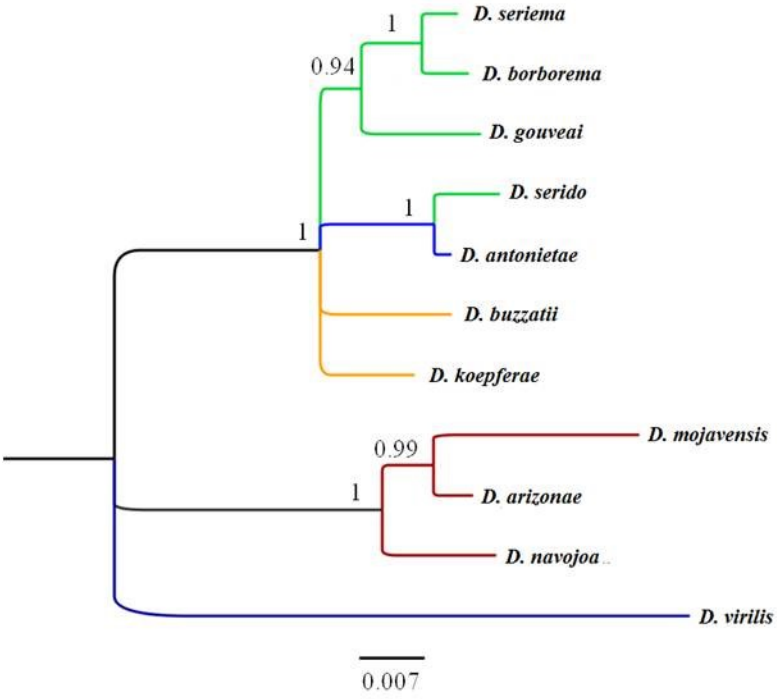

Figure 1. Bayesian phylogenetic hypothesis for the *Drosophila* species based on *GstD1* DNA sequences. The colored branches are exclusive to *D. koepferae* and *D. buzzatii* (orange), *D. antonietae* (blue), *D. serido*, *D. gouveai*, *D. borborema*, and *D. seriema* (green). For the external group, *D. navojoa*, *D. arizonae*, and *D. mojavensis* (red), and *D. virilis* (blue or grey). *Drosophila virilis* was used as an external group, which uses other foods, not cactus specialists. The internal nodes of the tree were organized with a posterior probability (PP 0,8), located next to each branch. The scale bar represents genetic distances calculated.

We identified ten physicochemical alterations, with changes at thirteen amino acid sites, in GstD1 (Table 2). These data were compared for the goodness of fit and statistical differences in the proportions of amino acid substitutions with an analysis of evolutionary processes. Variations in the second codon (Val-2-Ala) suggest a purifying selection in *D. buzzatii*.

We identified three positive selection signals in codons that result in physicochemical variations in amino acid of GstD1, such as substitutions: Val-2-Ala in *D. buzzatii*, Asp-3-Ala in *D. gouveai*, Val-19- Ala in *D. serido* and *D. antonietae*, and Ala/Pro-178 -Glu for species *D. buzzatii* cluster (Figure S1).

Table 2. Protein level results (TreeSAAP) to physicochemical properties, categories, amino acid sites and Z-scores for positive selection of GstD1 protein.

Property	Category	Amino acid residue	Z-scores
Total non-bonded energy	8	151a 158, 187e 191	27,483***
Composition	6	171	5,046***
Turn tendencies	6	178	2,638**
Helical contact area	6	151 a 156, 164e 171	13,996***
Alpha-helical tendences	6	16a 168	11,888***
Beta-structure tendencies	6	2, 3, 19 and 137	1,878*
Isoelectric point	6	160, 164, 166 and 178	-1,677*
Solvent accessible reduction ratio	6	2, 3 and 139	-1,904*
Short and medium range non bonded energy	6	152 a 168	10,97***
Chromatographic index	6	172 to 175	-2,218*

Note. Statistical significance is represented by $p < 0.05$*, $p < 0.01$** and $p < 0.001$***. Only amino acids with selection signal were show in the table.

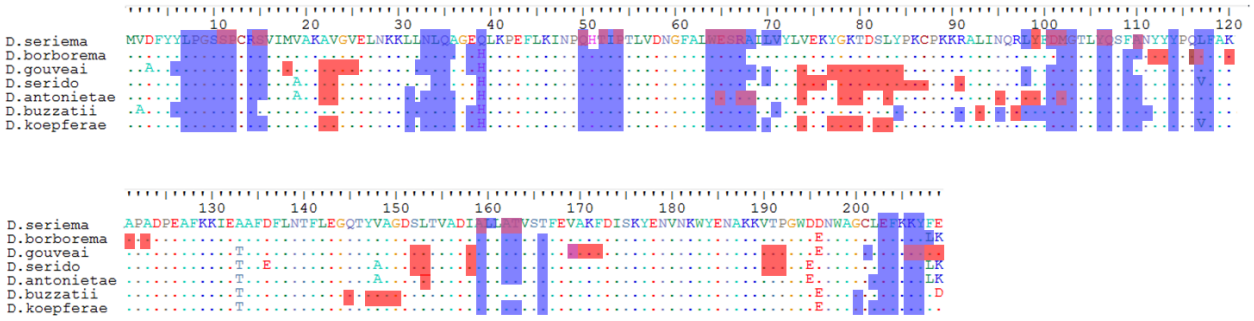

Figure 2. Multiple alignments of the primary structures of the GstD1 proteins of the *D. buzzatii* cluster species. The N-terminal region comprises amino acid residues 1-79, and the C-terminal comprises residues 86-208. The residues that make up the active sites G, in blue color, and H, in red color, were estimated. The magenta sites represent the residues with possible double functions at the active sites.

3.3 Molecular modeling and docking

The primary protein of GstD1, the species of *D. buzzatii* cluster, is composed of 209 amino acid residues, with a secondary structure comprising nine α-helices and four β-sheets (Figure 3), and the tail has amino acid residue substitutions in the cactophilic species (Figure 1). The N-terminal domain contains three α-helices and four β-sheets, and the C-terminal domain contains six α-helices in the GstD1 protein. The C-terminal region is more variable than the N-terminal (Figure 2). The structure of the GstD1 proteins ranged from 0.18 Å to 0.26 Å in flies (Figure S2).

The number of amino acid residues in site G changed from 40-aa, as in *D. serido*, to 51-aa in *D. buzzatii*. *Drosophila serido*, *D. antonietae*, and *D. buzzatii* showed the highest number of amino acid changes in the GstD1 protein (Figure 2). The number of amino acid residues for the H-site in *D. buzzatii* cluster varied from 7-aa, as *D. serido*, to 22-aa in *D. buzzatii*.

The complex between the GstD1 proteins and the mescaline ligand results in differences in interaction energy. Low interaction energy values were between -5.9 Kcal/mol and -5.6 Kcal/mol, in *D. seriema*, *D. gouveai*, and *D. kopeferae* (Figure 4). Interaction energy values were -5.3 Kcal/mol in *D. antonietae* and *D. borborema*. The highest energy values of interactions were calculated between -5.1 and -4.8 Kcal/mol, in *D serido* and *D. buzzatii*, respectively. Molecular surface changes near the G-site of the GstD1 protein, and properties of amino acids, indicate an adjustment of hydrophobic properties for *D. seriema*, *D. gouveai*, and *D. koepferae*, with a slight gain in portions with less hydrophobic properties close to the G-site, and a slight decrease in *D. buzzatii* (Figure 5).

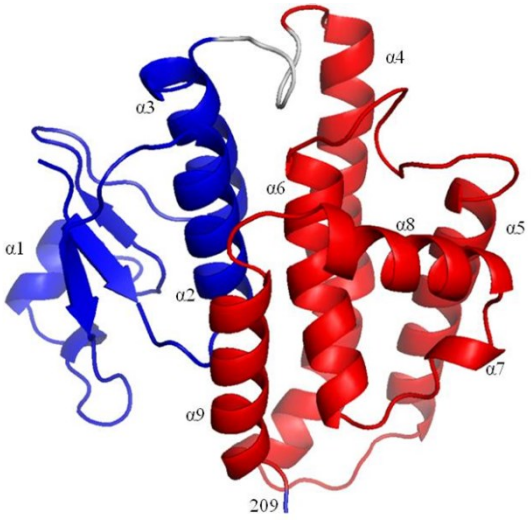

Figure 3. *In silico* prediction of the GstD1 protein, with the visualization of α-helices and β-sheets structures, with the representation of the N-terminal (blue color) and C-terminal (red color) regions. Residue 209 (highlighted in blue) corresponds to the tail of the protein.

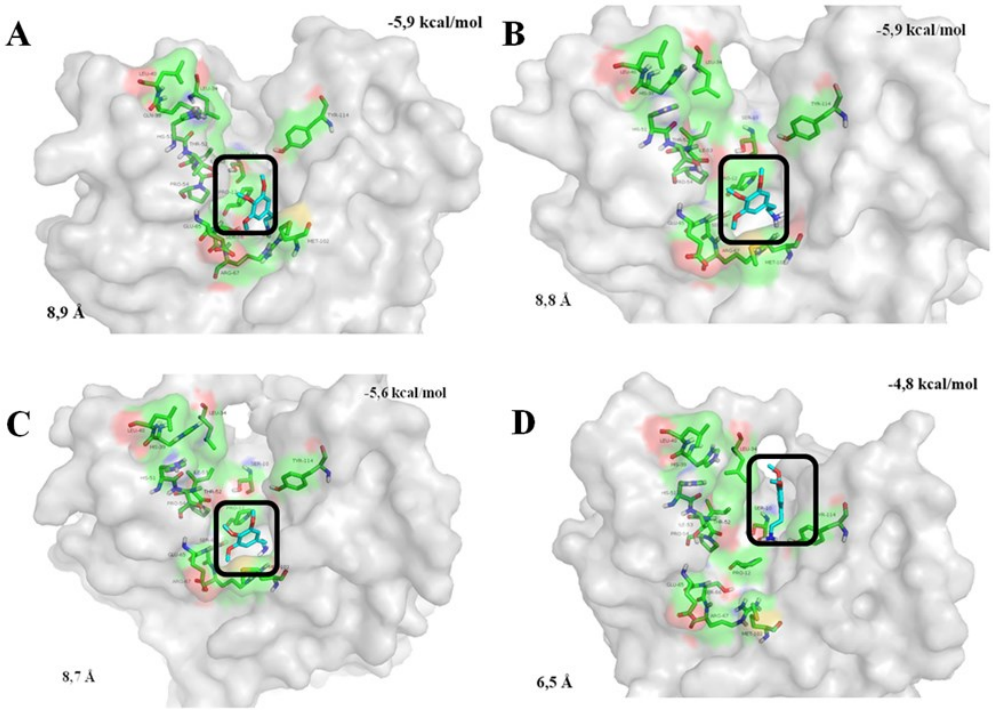

Figure 4. Molecular docking of the GstD1 protein with the mescaline ligand for *D. seriema* (A), *D. gouveai* (B), *D. koepferae* (C), and *D. buzzatii* (D). The protein is presented in gray, the G-site with its amino acid residues in green, red, and blue, and the ligand in blue and red. The values of interaction energy (top, right side) and distance between residue 10 and the ligand (bottom, left side) are shown.

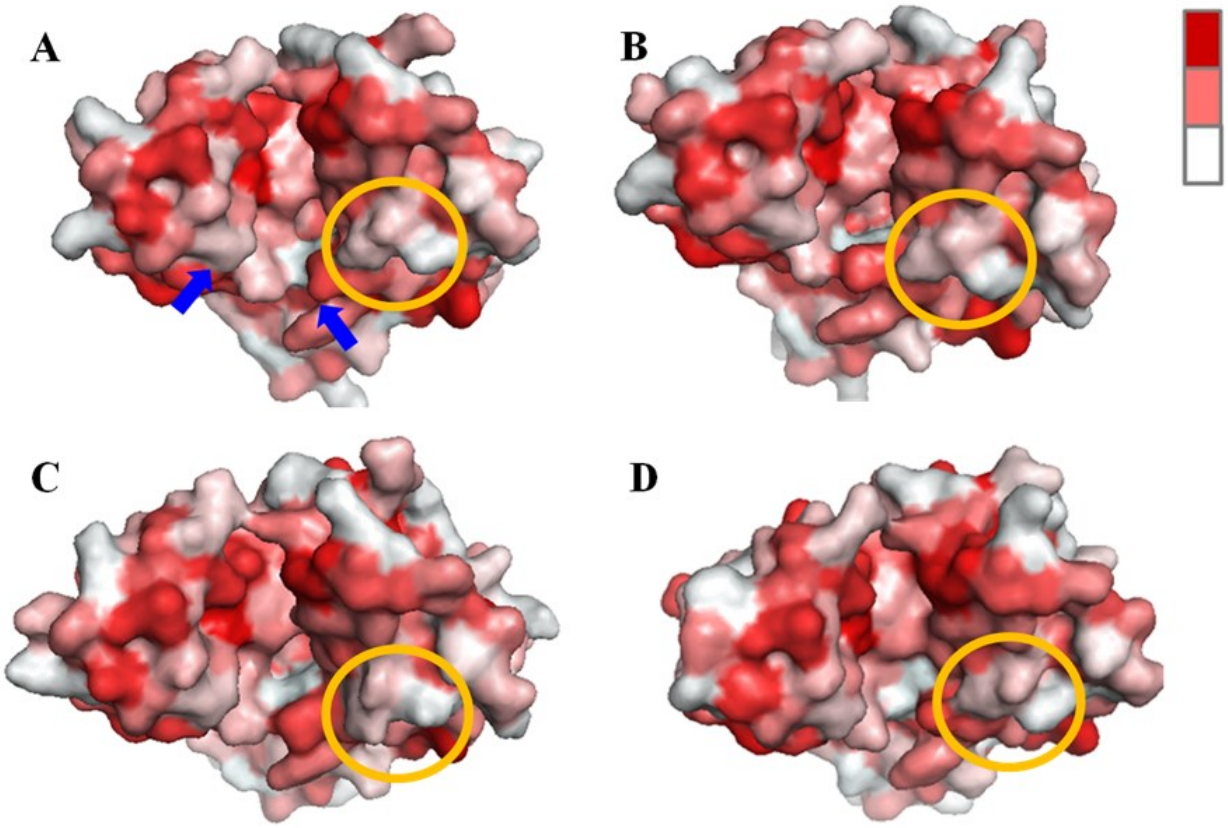

Figure 5. *In silico* model of the global surface of the GstD1 protein, with representation of hydrophobic regions in red and regions with less hydrophobic properties in pink and white. In visualization the proteins of *D. seriema* (A), *D. koepferae* (B), *D. gouveai* (C), and *D. buzzatii* (D), with indication of a subtle change in hydrophobic portions (yellow circle). The blue arrows indicate the basal region of the G site. The scale of hydrophobic properties represented by regions in red and regions with less hydrophobic properties in pink and white (upper part, right side).

Discussion

Based on data on genes, genomes, and phenotypes in the *Drosophila*-cactus model organism has allowed the evaluation of evolutionary processes, such as adaptive selection events. This process involves the interaction of flies with cacti that result in changes in phenotypic traits of viability, developmental and reproduction time, metabolism, and detoxification (Markow, 2019; Soto *et al.,* 2014; Panis *et al.,* 2016). The *GstD1* gene contains phylogenetic information for the *Drosophila buzzatii* cluster, previous corroborating studies with *Esterase-5*, *Period*, and mt*COI* (Manfrin *et al.,* 2001; Santos *et al.,* 2009; Franco *et al.,* 2010). However, our results indicate differences in molecular evolution in *GstD1*, with positive and purifying selection processes. Finally, we found differences in the physicochemical composition of the GstD1 proteins and the interaction of the protein with the alkaloid in the *D. buzzatii* cluster flies.

4.1 Selection and protein structure and function

Our results identified substitution at codon 2 (Val to Ala), with purification selection at *GstD1*, in *Drosophila buzzatii* species. Based on the amino acids chemical structure and function characteristics (Betts

and Russell, 2003), the change in the second amino acid suggests a loss of β-sheet conformation and solvent accessibility in GstD1. Allied to this fact, we observed a subtle hydrophobic region in the GstD1 protein of *D. buzzatii* in contrast to the other proteins in the *D. buzzatii* cluster species (Figure 4). Information indicates that hydrophobic regions may imply intermolecular interactions in proteins, with the function of decreasing the interaction of the protein with soluble compounds (Eisenhaber, 1996, 1999). We hypothesize that the change in the hydrophobic portions of GstD1 may affect the accessibility of proteins with soluble substances in *D. buzzatii*.

Positive selection in *gustatory receptor* (*Gr*) and *odorant receptor* (*Or*) nuclear genes suggest a role in transmembrane communication in cells in the adaptation process between *Drosophila*-cactus (Diaz *et al.,* 2018), which are similar to our data with *GstD1*. Substitution in the codon 171-Lys found in the *D. buzzatii* cluster (see Table 1) can affect the interaction with toxic compounds. The 171-Lys residue was associated with a better docking binding between GstD1 and the DDT compound in *D. melanogaster* (Low *et al.,* 2007). Data suggest that the Gly-171-Lys substitution did not evolve in response to DDT selection; one hypothesis is that this substitution may affect the kinetics of DDTase activity or other activities, in *D. mojavensis* (Matzkin *et al.,* 2006). In this context, the substitution in amino acid 171-lys may represent changes in the enzymatic activity of GstD1, and contribute to the interaction of the enzyme with chemical environments.

Positive selection in codon 117 is related to the change from Leu-117-Val residue in *D. serido* and *D. koepferae*, on G-site, in GstD1 (see Table 1). The valine residue has a Cβ branch linked to two non-hydrogen substituents and represents a gain in volume and chemical interaction with a group of lipids (Betts and Russell, 2003). Conformational changes in residues 117-Val and 118-Phe have been reported as important to DDT binding in *D. melanogaster* (Low *et al.,* 2010). Positive selection signal at codon 116-Thr, which has been suggested to have evolved in the bonding of substrates in the adaptation process in different chemical environments in fly *Drosophila hexastigama* (López-Olmos *et al.,* 2017). These factors suggest changes in *D. serido* and *D. koepferae* that can improve the activity of GstD1 in metabolic processes.

4.3 Molecular docking

Our molecular docking results showed lower interaction energy between the G-site of GstD1 with mescaline, in *D. seriema*, *D. gouveai*, and *D. koepferae*, showed intermediate values for *D. antonietae* and *D. borborema*, and higher value for *D. buzzatii* and *D. serido*. Mescaline is an alkaloid widely distributed in tissues of different cacti genera, such as *Trichocereus*, *Opuntia* (Turner and Heyman, 1960; Cruse, 1973; Shulgin, 1979; Panis *et al.,* 2016), *Gymnocalycium*, *Turbinicarpus* (Starha 1996, 1999), *Pereskia* (Turra *et al.,* 2007), *Lophophora* (Shulgin, 1979). The difference in the interaction energy of the GstD1 protein with mescaline may be related to an adaptive process in resource exploitation. One factor is that the energy value is associated with the sling-protein interactions, which indicates the stability of the complex, and the lower the energy in the interaction corresponds to a better fit of the interaction, and possibly with implications for the biological activity of proteins (Tripathi *et al.,* 2013). This indicates that the interactions of GstD1 proteins with mescaline may represent different values in stability and chemical interaction.

Study by Panis *et al*. (2016) indicate *D. koepferae* preferentially uses *T. terscheckii*, which has a concentration of 0.4 mg of the alkaloid mescaline (Panis *et al.,* 2016), which corroborate our data that indicate an improved interaction of GstD1 with mescaline. In contrast, *D. buzzatii* preferentially uses *O. sulphurea*, which contains 0.05 mg of this alkaloid (Panis *et al.,* 2016). We found a high energy value for the interaction of the GstD1 protein with this compound. Our results indicate that flies need physiological adjustments or metabolize with the concentration of mescaline in cactus tissues, corroborating the study by Panis *et al*. (2016). However, amounts of mescaline alkaloids have not been reported in tissues from other cacti. A future perspective will be to investigate the ecological associations in populations of cactophilic *Drosophila* with different host cacti species, with wide distribution in different biomes.

Conclusions

The complexity of chemical groups in plants can be a barrier in exchanging hosts for phytophagous insects (Becerra, 1997), which demands an adjustment in the insect detoxification system, such as P450s, UGTs, ADH, Esterases, and Gsts, in cactophilic *Drosophila* (Matzkin, 2014; Panis *et al.,* 2016). Our data

indicate that GstD1 has a position with positive selection in active sites of the enzyme, with subtle physicochemical changes, and difference in protein-alkaloid interaction energy in the cactophilic species of the *D. buzzatii* cluster.

Table S1. Biological samples for species, location and number of individuals (N) for the study of *Glutathione S-Transferase D1* (*GstD1*) gene, and Genbank Access Number (Accessions).

Species and Location	N GstD1	GstD1 Accessions
Drosophila buzzatii	1	MW805280
Drosophila koepferae Famantina, Argentina (B26) (SUYDB60)	1	MW805281
Drosophila serido Bom Jesus, Rio Grande do Norte, Brazil (R38) Mucugê, Minas Gerais, Brazil (N45)	1	MW805284
Drosophila seriema Santana do Riacho, Minas Gerais, Brazil (N58)	**1**	MW805283
Cachoeira Ferro Doido, Bahia, Brazil (N42)		MW805286
Drosophila antonietae Sertãozinho, São Paulo, Brazil (R71) N61C5	1	MW805286
Drosophila gouveai Petrolina, Pernambuco, Brazil (N36) N36	1	MW805282
Drosophila borborema Casa Nova, Bahia, Brazil (R41) N47	1	MW805285
Drosophila mojavensis MJBC95 **enmu97**	1	EU079442.1
Drosophila arizonae RVSD17 **1271_14**	1	EU079471.1
Drosophila navojoa **NAV12**	1	EU079446.1
NAV.A828b ***Drosophila virilis***	1	XM 002054301.2
Vi-L160		

Acknowledgments: The authors were funded by the Universidade de São Paulo (USP) and Coordenação de Aperfeiçoamento de Pessoal de Nível Superior (CAPES) (CAPES 88882.378679/2019-1 to A.S.S.; PNPD/CAPES, 88882.317598/2019-01 to D.Y. B.L.), Conselho Nacional de Desenvolvimento

Científico e Tecnológico (CNPq) (447697/2014-5 to M.H.M.), and Fundação de Amparo à Pesquisa do Estado de São Paulo (FAPESP) (03/05031-0; 2011/51652-2 to M.H). The team of the Laboratory of Evolutionary Genetics, Faculdade de Filosofia, Ciências e Letras de Ribeirão Preto-USP-SP, for their assistance in the part of molecular biology, statistical analysis and scientific discussions.

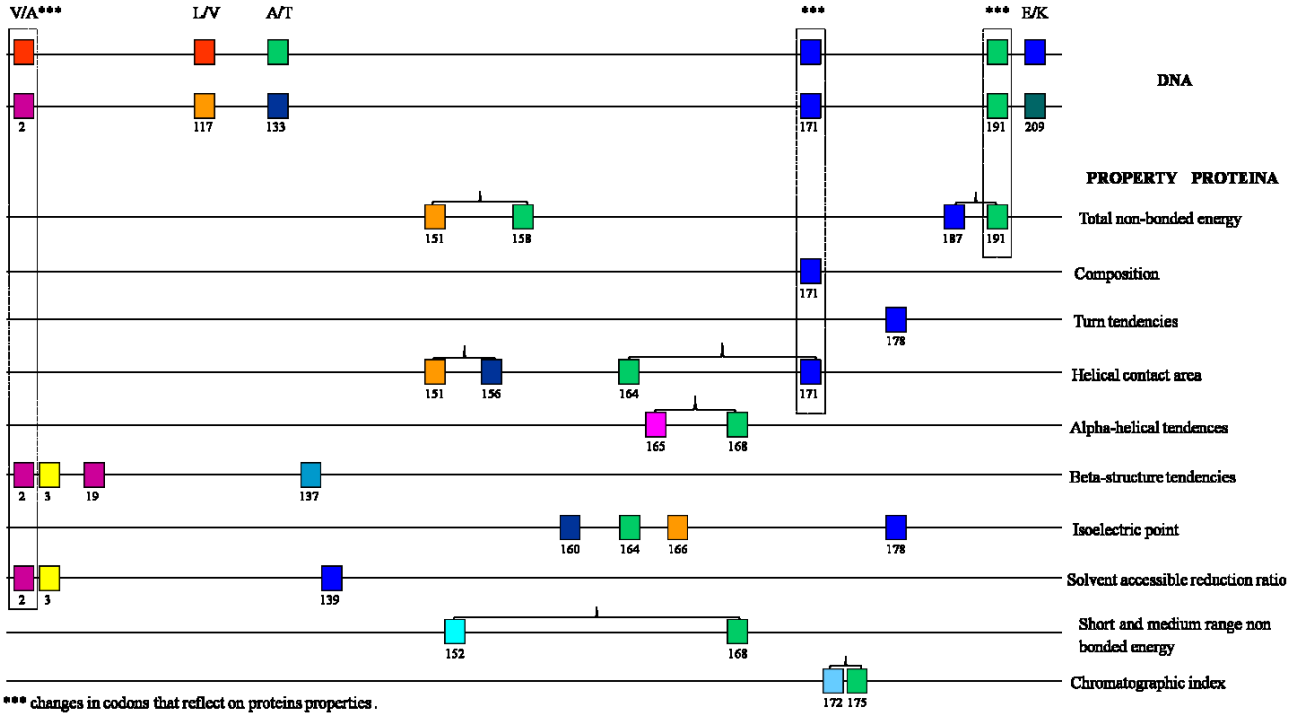

Figure S1. Scheme with codon selection signals and changes in physicochemical properties of GstD1 proteins.

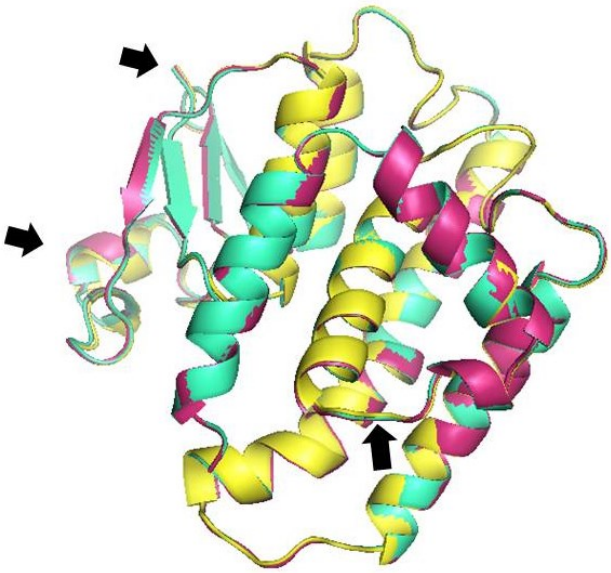

Figure S2. Multiple alignments, in the program Chimera v.1.14, between the seven tertiary proteins GstD1 of the species of the *D. buzzatii* cluster. Structural change measures between *D. buzzatii* (template) with *D. koepferae* (0.203 Å), *D. gouveai* (0.237 Å), *D. seriema* (0.189 Å), *D. serido* (0.226 Å), *D. borborema* (0.262 Å), and *D. antonietae* (0.235 Å). The colors yellow, violet, and blue correspond to the grouping of *D. koepferae*, *D. gouveai*, *D. seriema*, *D. serido*, *D. borborema*, and *D. antonietae*, and *D. buzzatii* in gray. Structural changes indicated by black arrows.

References: Barrios-Leal, D.Y., J. Neves-da-Rocha, and M.H. Manfrin 2019, J. Hered. 10: 22-33. https://doi.org/10.1093/jhered/esy042; Becerra, J.X., 1997, Science 276: 253-256. https://doi: 10.1126/science.276.5310.21; Betts, M.J., and R.B. Russell 2003, In: *Bioinformatics for Geneticists*. (Barners, M.R., and I.C. Gray, Eds.). Wiley, New York, pp. 289-316. https://doi.org/10.1002/0470867302.ch14; Cruse, R.R., 1973, Econ. Bot. 27: 210-230. https://doi.org/10.1007/BF02872991; DeLano, W., 2018, The PyMOL Molecular Graphics System. Available in: http://www.pymol.org. (accessed 20 January 2018); Diaz, F., C.W. Allan, and L.M. Matzkin 2018, BMC Evol. Biol. 18: 1-13. https://doi.org/10.1186/s12862-018-1250-x; Doron-Faigenboim, A., A. Stern, I. Mayrose, E. Bacharach, and T. Pupko 2005, Bioinformatics. 21: 2101-2103. https://doi.org/10.1093/bioinformatics/bti259; Eisenhaber, F., 1996, Protein Sci. 5: 1676-1686. https://doi.org/10.1002/pro.5560050821; Eisenhaber, F., 1999, Perspect. Drug Discov. Des. 17: 27-42. https://doi.org/10.1023/A:1008766422140; Ewing, B., and P. Green 1998, Genome Res. 08: 186-194. https://doi.org/10.1101/gr.8.3.186; Franco, F.F., E. Silva-Bernardi, F.M. Sene, E. Hasson, and M.H. Manfrin 2010, J. Zool. Syst. Evol. Res. 48: 322-331. https://doi.org/10.1111/j.1439-0469.2010.00564.x; Gloss, A.D., D.G. Vassão, A.L. Hailey, A.C. Nelson-Dittrich, K. Schramm, M. Reichelt, T.J. Rast, A. Weichsel, M.G. Cravens, J. Gershenzon, W.R. Montfort, and N.K. Whiteman 2014, Mol. Biol. Evol. 31: 2441-2456. https://doi.org/10.1093/molbev/msu201; Hall, T.A., 1999, Nucleic Acids Symp. Ser. 41: 95-98. https://doi.org/10.14601/Phytopathol_Mediterr-14998u1.29; Huang, B., 2009, Omics 13: 325-330. https://doi.org/10.1089/omi.2009.0045; Huelsenbeck, J.P., and F. Ronquist 2001, Bioinformatics 17: 754-755. https://doi.org/10.1093/bioinformatics/17.8.754; Kircher, H.W., W.B. Heed, J.S. Russell, and J. Grove 1967, J. Insect Physiol. 13: 1869-1874. https://doi.org/10.1016/0022-1910(67)90023-6; López-Olmos, K., T.A. Markow, and C.A. Machado 2017 J. Mol. Evol. 84: 285-294. https://doi.org/10.1007/s00239-017-9798-4; Lovell, S.C., I.W. Davis, W.B. Arendall III, P.I.W. Bakker, J.M. Word, M.G. Prisant, J.S. Richardson, and D.C. Richardson 2003, Proteins 50: 437-450. https://doi.org/10.1002/prot.10286; Low, W.Y., S.C. Feil, H.L. Ng., M.A. Gorman, C.J. Morton, J. Pyke, M.J. McConville, M. Bieri, Y.F. Mok, C. Robin, P.R. Gooley, M.W. Parker, and P. Batterham 2010. J. Mol. Biol. 399: 358-366. https://doi.org/10.1016/j.jmb.2010.04.020; Low, W.Y., H.L. Ng, C.J. Morton, M.W. Parker, P. Batterham, and C. Robin 2007, Genetics 177: 363-1375. https://doi.org/10.1534/genetics.107.075838; Manfrin, M.H., R.A. DeBrito, and F.M. Sene 2001, Ann. Entomol. Soc. Am. 94: 333-346. https://doi.org/10.1603/0013-8746(2001)094[0333:SAEOTD]2.0.CO;2; Manfrin, M.H., and F.M. Sene 2006, Genetica 126: 57-75. https://doi.org/10.1007/s10709-005-1432-5; Markow, T.A., 2019, Curr. Opin. Insect. Sci. 31: 139-145. https://doi.org/10.1016/j.cois.2019.01.006; Matzkin, L.M., T.D. Watts, B.G. Bitler, C.A. Machado, and T.A. Markow 2006, Mol. Ecol. 15: 4635-4643. https://doi.org/10.1111/j.1365-294X.2006.03102.x; Matzkin, L.M., 2008, Genetics 178: 1073-1083. https://doi.org/10.1534/genetics.107.083287; Matzkin, L.M., 2014, Adv. Exp. Med. Biol. 781: 233-247. https://doi.org/10.1007/978-94-007-7347-9_12; McClellan, D.A., and K.G. McCracken 2001, Mol. Biol. Evol. 18: 917–925. https://doi.org/10.1093/oxfordjournals.molbev.a003892; Padró, J., D.N.D. Panis, J. Vrdoljak, P.M. Carmona, B. Colines, E. Hasson, and I.M. Soto 2018, Evol. Biol. 45: 170-181. https://doi.org/10.1007/s11692-017-9441-8; Pagadala, N., K. Syed, and J. Tuszynski 2017, Biophys Rev. 9: 91-102. https://doi.org/10.1007/s12551-016-0247-1; Panis, D.N., J. Padró, P. Furió-Tarí, S. Tarazona, P.S.M. Carmona, I.M. Soto, H. Dopazo, A. Conesa, and E. Hasson 2016, Mol. Ecol. 25: 4534-4550. https://doi.org/10.1111/mec.13785; Pereira, M.A.Q.R., C.R. Vilela, and F.M. Sene 1983, Cien. Cult. 35: 1313-1319; Pettersen, E.F., T.D. Goddard, C.C. Huang, G.S. Couch, D.M. Greenblatt, E.C. Meng, and T.E. Ferrin 2004, J. Comput. Chem. 25: 1605-1612. https://doi.org/10.1002/jcc.20084; Posada, D., and K.A. Crandall 1998, Bioinformatics 14: 817-818. https://doi.org/10.1093/bioinformatics/14.9.817; Rambaut, A., A.J. Drummond, D. Xie, G. Baele, and M.A. Suchard 2018, Syst. Biol. 01: 1-5. https://doi.org/10.1093/sysbio/syy032; Saisawang, C., J. Wongsantichon, and A.J. Ketterman 2012, Biochem. J. 442: 181-190. https://doi.org/10.1042/BJ20111747; Saisawang, C., and A.J. Ketterman 2014, PloS ONE 9: e109518. https://doi.org/10.1371/journal.pone.0109518; Sali, A., L. Potterton, F. Yuan, H.V. Vlijmen, and M. Karplus 1995, Proteins 23: 318-326. https://doi.org/10.1002/prot.340230306; Santos, M.H., E. Hasson, FM. Sene, and M.H. Manfrin 2009, Dros. Inf. Serv. 92: 44-56; Soto, E.M., J. Goenaga, J.P. Hurtado, and E. Hasson 2012, Evol. Ecol. 26: 975-990. https://doi.org/10.1007/s10682-011-9531-5; Soto, I.M., V.P. Carreira, C. Corio, J. Padró, E.M. Soto, and E. Hasson 2014, PloS ONE 9: e88370. https://doi.org/10.1371/journal.pone.0088370; Soto, I.M., E.R. Hasson, and M.H. Manfrin 2008, Biol. J. Linn.

Soc. 95: 655-665. https://doi.org/10.1111/j.1095-8312.2008.00980.x; Soto, I.M., M.H. Manfrin, F.M. Sene, and E. Hasson 2007, Ann. Entomol. Soc. Am. 100: 490-496. https://doi.org/10.1603/0013-8746(2007)100[490:VADTIC]2.0.CO;2; Shulgin, A.T., 1979, J. Psychedelic Drugs 11: 41-52. https://doi.org/10.1080/02791072.1979.10472091; Starha, R., 1996, Biochem. Syst. Ecol. 4: 85-86. https://doi.org/10.1016/0305-1978(95)00097-6; Starha, R., A. Chybidziurova, and Z. Lacny 1999, Biochem. Syst. Ecol. 27: 839-841. https://doi.org/10.1016/S0305-1978(99)00019-8; Stintzing, F.C., and R. Carle 2005, Mol. Nutr. Food Res. 49: 175-194. https://doi.org/10.1002/mnfr.200400071; Swanson, W.J., R. Nielsen, and Q. Yang 2003, Mol. Biol. Evol. 20: 18-20. https://doi.org/10.1093/oxfordjournals.molbev.a004233; Tidon-Sklorz, R., and F.M. Sene 2001, Iheringia, Sér. Zool. 90: 141-146. https://doi.org/10.1590/S0073-47212001000100014; Turner, W.J., and J.J. Heyman 1960, J. Org. Chem. 25: 2250-2251. https://doi.org/10.1021/jo01082a623; Turra, A.F., F.J.B. Marçal, I.P. Baretta, O.S. Takemura, and A. Laverde-Júnior 2007, Health Sciences Archives – UNIPAR. 11: 9-14; Thompson, J.D., D.G. Higgins, and T.J. Gibson 1994, Nucleic Acids Res. 22: 4673-80. https://doi.org/10.1093/nar/22.22.4673; Wolf, L.K., 2009, Chem. Eng. News 87; Woolley, S., J. Johnson, M.J., Smith, K.A. Crandall, and D.A. McClellan 2003 Bioinformatics 19: 671-672. https://doi.org/10.1093/bioinformatics/btg043; Yang, Z., R. Nielsen, N. Goldman, and A.M.K. Pedersen 2000, Genetics 155: 431-449. https://doi.org/10.1093/genetics/155.1.431.

Studies on longevity and climbing assay in *Drosophila melanogaster.*

Vijaykumar, R., B.S. Srinath, and N. Shivanna.* Department of Zoology, Karnatak University Dharwad, India; *Email: drnshivanna@rediffmail.com

Abstract

The longevity and the climbing assay with increased density of virgin, mated, and increased number of one sex with a single opposite sex was analyzed in *D. melanogaster*. It revealed that the longevity of virgin single fly is more than the increased number of flies per bottle as well as mated flies. The longevity decreased less than 50% with increased density and mating. When one of the sex is kept constant and the other sex flies increased, the life span decreased more than 50% of days in all the flies compared to single flies. The climbing assay that is distance covered by virgin male, virgin female, mated male, and mated female is gradually decreased from 11 days aged to 31 days aged flies for all the distances. The time taken to reach maximum distance is less for 11 days aged flies than the 31 days aged flies, whereas 11 days aged flies stayed for maximum time at the distance of more than 20 cm compared to 21 and 31 days aged flies. This shows that the younger flies reached very fast and stays more time against the negative geotaxis than the older flies.

Introduction

Aging is a process which influences the life of every organism. It is a biological process of gradual decline of biological functions and also a multi-factorial phenomenon regulated by a combination of genetic and environmental factors. It is delayed by modulating the biological processes (Kulkarni *et al*., 2020; Jing *et al*., 2022).

Longevity has been studied for many years on different organisms like *Drosophila melanogaster, Bombyx mori, Saccharomyces cerevisiae*, *Caenorhabditis elegans,* and so forth, on oxidative stress, oxidative insults, and locomotion (Balasubramani *et al*., 2014), effects of resveratrol in lifespan extension (Song *et al*., 2021), lipid metabolism, oxidant regulation (Mirisola and Longo, 2022), and influence of Insulin signaling pathway (Xu *et al*., 2022) with single factors revealed that the life span of the above organisms.

Behavioral assays like locomotor activities, circadian rhythm, sleep patterns, and cognitive functions can be useful to study aging-related activities (Yadav *et al*., 2016). Model systems like *Drosophila melanogaster* help to study variation in exercise response and are ideally suited to different exercise systems

like negative geotaxis behavior (climbing assay), their efficiency to move to the top (Watanabe and Riddle, 2019, 2021). Negative geotaxis (startle-induced vertical movement) is a frequently used index of locomotor behavior for quantifying *Drosophila* health due to an age-dependent decrease in climbing speed (Simon *et al*., 2006; Spierer *et al*., 2021). Pathological changes could detect the locomotive defects by several days (Feany and Bender, 2000).

The influence of chemicals on longevity and climbing assay in *D. melanogaster* was analyzed taking one assay or factor at a time (Bass *et al*., 2007; Raj *et al*., 2017; Rajak *et al*., 2017; Bednarova *et al*., 2020; Musachio *et al*., 2020; Zhang *et al*., 2021; Watanabe and Riddle, 2021).

But none of the studies have compared different aspects and ages on longevity and climbing assay of virgin and mated flies. Hence a systematic study was designed to analyze longevity and the climbing assay (varied distances and time) with increased density of virgin, mated, and increased number of one sex with a single opposite sex was systematically analyzed.

Materials and Methods

Drosophila *stock culture and maintenance*

Drosophila melanogaster (Oregon-K) species was collected from Drosophila Stock Center, Department of Zoology, University of Mysore. India, and they were cultured in wheat cream agar medium prepared as per the procedure described by Shivanna *et al.* (1996) and maintained at constant temperature of 22 ± 1ºC with relative humidity of 70-80%.

Longevity assay

Newly-eclosed flies (1 day old) were separated and reared in a fresh culture medium containing wheat cream agar medium seeded with yeast solution, with increased number (density 1-10). Flies were transferred to fresh bottles for every 2-3 days and the numbers of dead flies were recorded. The total number of days taken until the death of the last fly was noted (male, female, mated male, and mated female, single male with increased female, and single female with increased male). For each experiment 10 replicates were maintained for each sex and density.

Climbing assay of flies

Flies reared separately were fed with yeast for 11, 21, and 31 days and were used for the climbing assay. After attaining specific days they were transferred to a measuring cylinder (marked < 5, 5, 15, 20, and > 20 cm height). The measuring cylinder was tapped thrice to gather the flies at the bottom. The number of flies and time taken by flies to climb the distance of about < 5, 5, 15, 20, > 20 cm mark was recorded. The assay was repeated three times with an interval of 30 min between each trial. For each sex, ten replicates containing 10 flies/bottle were measured. Data of longevity and climbing assay were subjected to statistical analysis using SPSS software 21.0 version.

Results

Longevity assay was performed to know the influence of sex and densities on lifespan extension of flies. The longevity of *D. melanogaster* flies was studied, and the mean values were recorded with increased density from 1 to10 flies (Table 1). Average virgin male longevity of 1 fly per bottle is 38.82 days whereas the longevity of 10 flies per bottle is 22.57 days. Female longevity of 1 fly per bottle is 36.0 days and for 10 flies per bottle is 19.39 days. The longevity of male flies with equal number of females left for mating of one fly each per bottle is 35.3 days and for 10 flies per bottle is 20.97 days. The longevity of female flies with equal number of flies of one fly each per bottle is 31.1 days whereas for 10 flies per bottle is 19.27 days (Figure 1). This revealed that the longevity decreased less than 50% with increased density and mating compared to single flies.

The longevity of male with single female left for mating of one fly each per bottle is 31.4 days and for increased male (10) flies and one female per bottle is 13.59 days. Whereas the female with increased male left for mating of one fly each per bottle is 28.1 days and 10 female flies per bottle is 12.9 days. The longevity of

single male with increased female left for mating of one fly each per bottle is 32 days and for 10 female flies per bottle is 17.6 days. The longevity of increased female with single male left for mating of one fly each per bottle is 29.2 days and for 10 female and single male flies per bottle is 15.75 days (Table 1 and Figure 2). This result revealed that when one of the sexes is kept constantly and the other sex flies when increased, the life span decreased more than 50% of days compared to single flies. The statistical analysis showed that the difference of longevity between one fly per bottle and ten flies per bottle is significant in virgin as well as mated male and female flies (Table 2).

Table 1. Mean ± S.E of longevity assay of virgin, mated, and increased flies with increased density of *Drosophila melanogaster*.

Density	1	2	3	4	5	6	7	8	9	10
Virgin Male	38.82 ± .07	35.95 ± 2.71	34.79 ± 1.63	35.11 ± 2.20	34.24 ± 2.96	33.86 ± 2.22	29.79 ± 2.24	28.27 ± 1.42	24.474 ± 2.2	22.57 ± 2.06
Virgin Female	36.0 ± 2.49	34.1 ± 1.38	33.98 ± 2.29	33.07 ± 2.76	32.66 ± 2.06	30.89 ± 2.08	27.14 ± 2.54	24.59 ± 1.31	20.16± 1.16	19.39 ± 1.71
Mated male	35.3 ± 1.38	32 ± 2.0	31.43 ± 1.78	30.81 ± 0.97	29.7 ± 1.24	28.91±1.27	26.5 ± 2.00	25.38 ± 2.23	24.65 ± 2.22	20.97 ± 1.3
Mated female	31.1 ± 1.58	30. ± 1.06	28.42 ± 1.47	25.87 ± 1.44	24.2 ± 2.63	23.66 ± 3.19	21.32 ± 1.38	21.16 ± 2.14	20.12 ± 1.72	19.27 ± 1.73
Increased males (with single female)	31.4 ± 2.08	29.25 ± 1.25	26.2 ± 2.54	24.958 ± 1.28	23.835 ± 2.60	20.24 ± 1.35	18.047 ± 2.07	17.992 ± 1.32	16.63 ± 1.20	13.59 ± 0.58
Single female (with increased males)	28.1 ± 2.16	25.3 ± 1.59	23.6 ± 1.49	21.9 ± 1.96	20.9 ± 2.1	19.2 ± 1.35	17.9 ± 2.01	15.1 ± 0.88	15.1 ± 1.25	12.9 ± 0.79
Increased females (with single male)	29.2 ± 2.57	27.25 ± 1.41	25.84 ± 2.28	24.62 ± 1.89	23.32 ± 1.30	21.347 ± 2.13	19.578 ± 1.45	18.261 ± 1.43	18.62 ± 1.142	15.75 ± 1.61
Single male (with increased females)	32 ± 2.06	30 ± 3.02	28.8 ± 2.73	25.2 ± 2.64	24.3 ± 0.81	22.9 ± 2.1	21.6 ± 0.87	19.1 ± 1.1	19.6 ± 1.42	17.6 ± 1.77

Table 2. The Log rank χ^2 and Wilcoxon χ^2 values of the survival data of flies.

Sex	Log Rank χ^2	Wilcoxon χ^2
Virgin male	45.923	51.794
Virgin Female	86.272	79.691
Mated male	49.026	53.543
Mated female	35.927	36.938
Increasing males (with single female)	90.234	80.001
Single female (with increased males)	72.294	70.375
Increased females (with Single male)	49.571	47.614
Single male (with increased females)	50.626	41.016

*Significant at P< 0.01, df = 9

The distance covered by virgin male, virgin female, mated male, and mated female is maximum for 11 days aged than 31 days aged flies for all the distances and the time taken to reach maximum distance is less whereas it stayed for maximum time by the 11 days aged fly compared to 21 and 31 aged flies. This shows that the young flies reach very fast and stay more time against the negative geotaxis than the old flies (Figure 3 and 4).

Discussion

Present work revealed that virgin male lived more than mated male, increased male with single female and single male with increased female. Mated males had lower starvation resistance than virgin males (Service, 1989). Virgin female lived more than all other counterparts of female. Females life span is less on concentrated food of 15% sugar and yeast (SY) compared with those on less concentrated food (5% SY)

(Linford *et al*., 2013). Reduced fecundity and increased longevity may have a positive connection to climbing efficiency in flies (Staats *et al*., 2018).

The climbing assay revealed that the majority of male flies reached the maximum distance with less time but the female, mated male, and mated female flies showed drastic decrease in number and increase in time to reach the maximum distance. As the age increased (11, 21, and 31), climbing ability also decreased

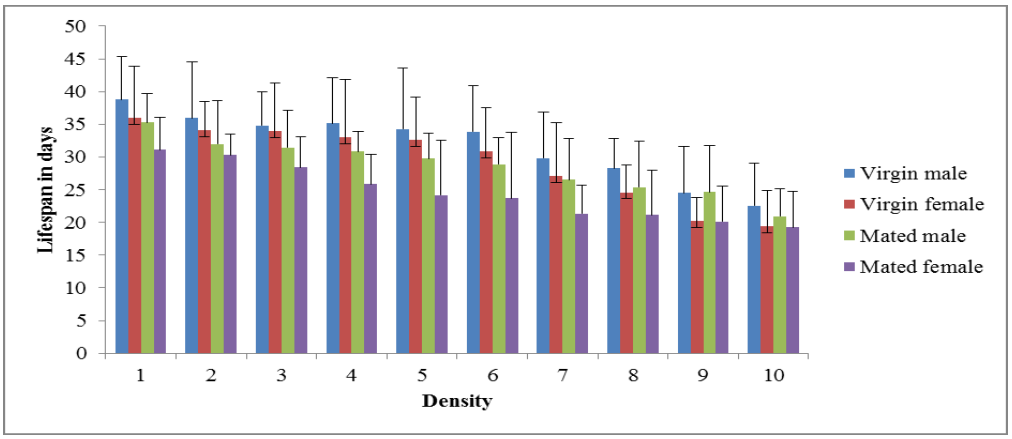

Figure 1. Longevity of virgin male, virgin female, mated male, and mated female with increased density (1-10).

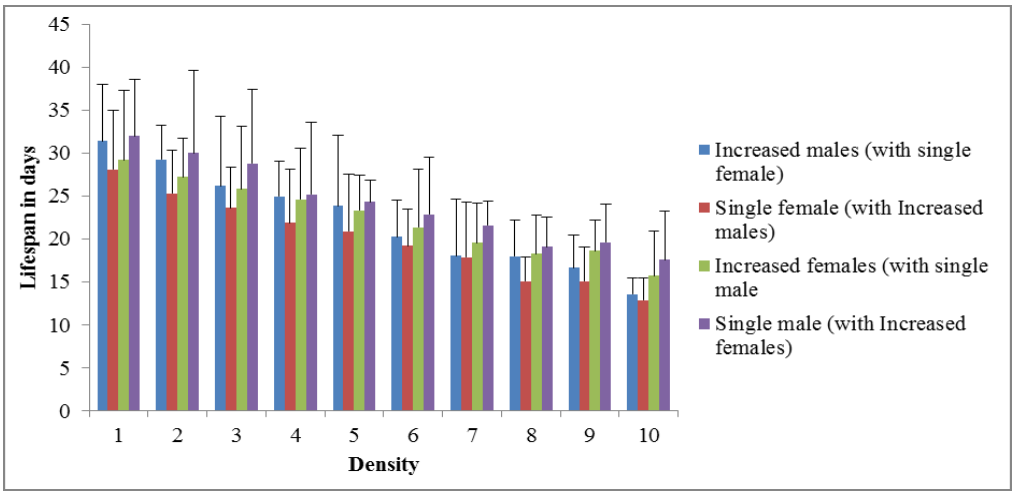

Figure 2. Longevity of increased males and female with constant female and male flies with increased density (1-10).

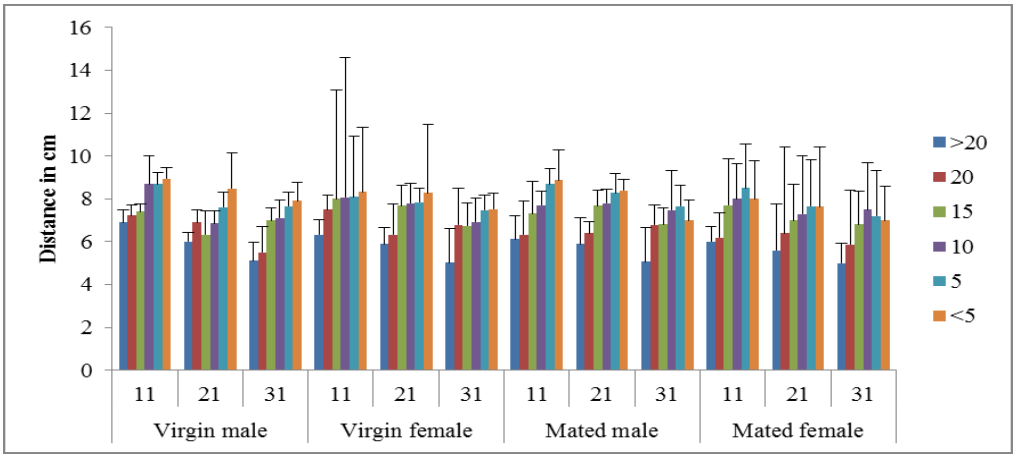

Figure 3. Distance travelled by the different aged flies.

(Figures 3 and 4). Similar observations were made by Perveen *et al*. (2021). They found increasing age significantly reduced the climbing activity in flies treated with sodium fluoride as compared to normal (control) flies. When treated with chemicals like Lamotrigine (6 mg/ml) for 4 week old flies showed reduction in locomotion than 1 week old flies (Avanesian, *et al*., 2010). In 40 days old flies in standard food (control) reduced physiological function with age (Men *et al*., 2022). Reduced climbing ability was reported in fruit flies with age (Wang *et al*., 2010).

The present study revealed that longevity decreased less than 50% with increased density and mating. When one of the sexes is kept constant and the other sex flies increased, the life span decreased more than 50% of days in all the flies compared to single flies. The climbing assay showed that the younger flies reached very fast and stay more time against the negative geotaxis than the older flies.

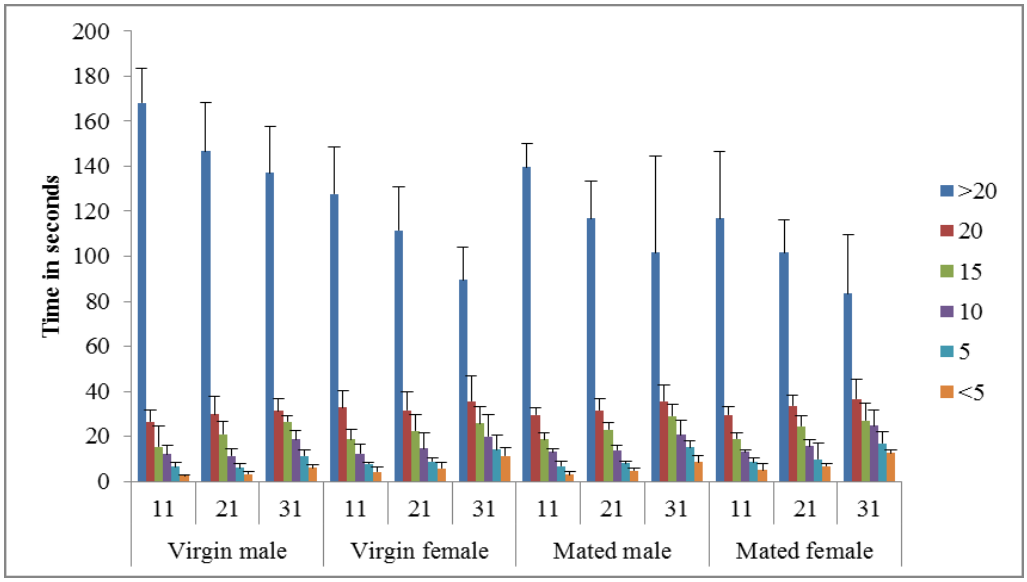

Figure 4. Time taken by different aged flies to climb the distances.

Acknowledgments: Authors thank the Chairman, Department of Zoology, Karnatak University, Dharwad, for providing necessary facilities. One of the authors (VR) thanks Backward class welfare department, Govt. of Karnataka for financial assistance.

References: Avanesian, A., B. Khodayari, J.S. Felgner, and M. Jafari 2010, Biogerontology 11(1): 45-52; Balasubramani, S.P., J. Mohan, A. Chatterjee, E. Patnaik, S.K. Kukkupuni, U. Nongthomba, and P. Venkatasubramanian 2014, Front. in Pub. Health 2: 1-9; Bass, T.M., D. Weinkove, K. Houthoofd, D. Gems, and L. Partridge 2007, Mech. of Ageing and Dev. 128(10): 546-552; Bednarova, A., M. Kropf, and N. Krishnan 2020, Ecotoxicol. Environ. Saf. 188: 1-8; Feany, M.B., and W.W. Bender 2000, Nature 404: 394-398; Jing, J.L., T.Y, Ning, F. Natali, F. Eisenhaber, and M. Alfatah 2022, Cells, 11(5): 1-14; Kulkarni, A.S., S. Gubbi, and N. Barzilai 2020, Cell Metab. 32(1): 15-30; Linford, N.J., C. Bilgir, J. Ro, and S.D. Pletcher 2013, J. Vis. Exp. 7(71): 1-9; Men, T.T., D.T. Khang, N.T. Tuan, and D. Trang 2022, Food sci. Technol. 42: 1-7; Mirisola, M.G., and V.D. Longo 2022, Cells 11: 1-16; Musachio, E.A.S, S.M. Araujo, V.C. Bortolotto, C.S. de Freitas, M.M.M. Dahleh, M.R. Poetini, E.F. Jardim, L.B. Meichtry, B.P. Ramborger, R. Roehrs, G.G. Petri, and M. Prigol 2020, Food. Chem. Toxicol. 137: 1-9; Perveen, S., S. Kumari, H. Raj, and S. Yasmin 2021, JoBAZ. 82: 1-9; Raj, A., P. Shah, and N. Agrawal 2017, PLoS ONE 12(5): 1-14; Rajak, P., M. Dutta, S. Khatun, M. Mandi, and S. Roy 2017, J. Haz. Mat. 321: 690-702; Service, P.M., 1989, J. of Ins. Physiol. 35(5): 447-452; Shivanna, N., G.S. Siddalingamurthy, and S.R. Ramesh 1996, Genome 39: 105-111; Simon, A.F., T.L. Debbie, and E.K. David 2006, Mech. of Ageing Dev. 127(7): 647-651; Song, J., L. Lian, H. Kaige, M. Shuang, T. Yongxi, T. Xiaoling, and D. Fangyin 2021, J. Pharmcol. Ana. 11(3): 374-382; Spierer, A.N., Y. Denise, Z. Chen-Tseh, and M.R. David 2021, J. Exp. Biol. 224(2): 1-6; Staats, S., K. Luersen, A.E. Wagner, and G. Rimbach 2018, J. Agri. Food Chem. 66(15): 3737-3753; Wang, R., Y. Ding, R. Liu, L. Xiang, and L. Du 2010, Fru. Veg. Cer. Sci. Biotech. 4: 77–87; Watanabe, L.P., and N.C. Riddle 2019, J. Applied. Physiol. 27(2): 482-490; Watanabe, L.P., and N.C. Riddle 2021, Sci. Rep. 11(1): 1-13; Xu, T., T.

Mingfang, L. Rong, X. Xiaoyun, P. Siyi, and T. Wu 2022, Food and Func. 13: 9893-9903; Yadav, A., D. Kaustubh, and S. Himanshu 2016, PLoS ONE 11(9): 1-20; Zhang, H.H., Y.C. Xie, H.J. Li, J.C. Zhuo, and C.X. Zhang 2021, Genes 12: 379.

Survey of Drosophilidae fauna in an interior Atlantic Forest fragment in Southeastern Brazil reveals the occurrence of the invasive *Zaprionus tuberculatus.*

Mateus, R.P.*, and L.P.B. Machado. Laboratório de Genética e Evolução, Departamento de Ciências Biológicas, UNICENTRO – Universidade Estadual do Centro-Oeste, Guarapuava-PR, Brazil. *Corresponding author: rogeriopmateus@gmail.com.

Introduction

The Brazilian Southeast region is the second largest and the most developed region of the country. Because of agricultural and urban expansion, the majority of the original vegetation in this region was excerpted. Currently, only 2.2 Mha (million hectare) consist of areas of permanent protection with natural vegetation, which 80% is legally protected in both private and public properties (Sparovek *et al.,* 2015).

The *Drosophila* fauna of the São Paulo state is well known (Tidon-Sklorz and Sene, 1999; Medeiros and Klaczko, 2004; Mateus *et al.,* 2006; Torres and Madi-Ravazzi, 2006; Schmitz and Valente, 2019). The assessment of variations in spatial and temporal diversity patterns can contribute to the understanding of biodiversity regulation processes (Schluter and Ricklefs 1993). In this context, drosophilids have been often suggested as appropriate bioindicator models in studies about the level of environment disturbance (Parsons, 1991; Avondet *et al.,* 2003; Mata *et al.,* 2008, 2010), especially regarding the presence and abundance of exotic species (Ferreira and Tidon, 2005; Gottschalk *et al.,* 2007; Poppe *et al.,* 2012; Cavasini *et al.,* 2014).

Several examples of exotic flies invasion in Brazil have being reported, such as *D. malerkotliana* (Val and Sene, 1980), *Zaprionus indianus* (Vilela, 1999; Mateus *et al.,* 2020), *Drosophila suzukii* (Vilela and Mori, 2014), and *Drosophila nasuta* (Vilela and Goñi, 2015). In 2020, another exotic drosophilid species, *Zaprionus tuberculatus*, already recognized as invasive (CABI 2021), was registered for the first time in Brazil. Cavalcanti *et al*. (2022) collected this species in the Brazilian Savanna and detected an increase of its abundance after the invasion.

Considering this, and that the arrival of a new introduced species could reduce the diversity of drosophilids in the Neotropics, this work aimed to survey the drosophilid fauna in a fragment of Atlantic forest in the interior of the São Paulo state (Brazil), in order to: 1) evaluate the conservation status of a Permanent Environment Protection Area; and 2) to verify the possible occurrence of the invasive *Z. tuberculatus* in this region, where fruit plantations could have the production affected by this species.

Material and Methods

The *Drosophila* fauna was collected in a Permanent Environment Protection Area (PEPA) of the São Paulo State University (UNESP), Bauru-SP (22°21'29.36"S, 49°0'43.99"W – Figure 1). For three days, the adult flies were attracted to fermented banana and orange in open traps, dispersed no closer than 5 m from each other, hung on branches at ± 1.5 m height from the ground. After this period, the flies were captured with entomological nets, put in glass vials with culture medium, and taken to the laboratory alive. The non-*repleta* species were screened based on their distinct pigmentation and morphology patterns (Freire-Maia and Pavan, 1949; Frota-Pessoa, 1954; Markow and O'Grady, 2006). The females of the first group were put individually in glass vials to generate isofemale lines, and the offspring were used to identify the parental female species. The only female that produced no descendants is shown as unidentified as the diagnostic characteristic is the

male aedeagus (Vilela, 1983). The cryptic species of the *willistoni* group were grouped as "*D. willistoni* group".

Table 1. Absolute (*A*) and relative (*r*) abundances for females and males of each Drosophilidae species collected in the Permanent Environment Protection Area of the São Paulo State University (UNESP), Bauru-SP – Brazil.

Species	Subgenus	Group	Females		Males		Total	
			A	r	A	*r*	A	r
Genus *Drosophila*								
D. ararama	*Drosophila*	*annulimana*	1	0.00125	-	-	1	0.00125
D. polymorpha	*Drosophila*	*cardini*	-	-	1	0.00125	1	0.00125
D. guaru	*Drosophila*	*guarani*	2	0.0025	-	-	2	0.0025
D. immigrans	*Drosophila*	*immigrans*	10	0.0125	25	0.03125	35	0.04375
D. mercatorum	*Drosophila*	*repleta*	1	0.00125	2	0.0025	3	0.00375
D. paranaensis	*Drosophila*	*repleta*	1	0.00125	-	-	1	0.00125
repleta group[1]	*Drosophila*	*repleta*	1	0.00125	-	-	1	0.00125
D. mediopunctata	*Drosophila*	*tripunctata*	1	0.00125	-	-	1	0.00125
D. mediostriata	*Drosophila*	*tripunctata*	1	0.00125	-	-	1	0.00125
D. montium	*Sophophora*	*montium*	-	-	1	0.00125	1	0.00125
D. prosaltans	*Sophophora*	*saltans*	4	0.005	3	0.00375	7	0.00875
D. sturtevanti	*Sophophora*	*saltans*	18	0.0225	9	0.01125	27	0.03375
D. capricorni	*Sophophora*	*willistoni*	1	0.00125	-	-	1	0.00125
D. willistoni group[2]	*Sophophora*	*willistoni*	438	0.5475	240	0.3	678	0.8475
Genus *Scaptodrosophila*								
S. latifasciaeformis		*latifasciaeformis*	2	0.0025	3	0.00375	5	0.00625
Genus *Zaprionus*								
Z. indianus	*Zaprionus*	*vittiger*	16	0.02	18	0.0225	34	0.0425
Z. tuberculatus	*Zaprionus*	*tuberculatus*	1	0.00125	-	-	1	0.00125
Total			498	0.6225	302	0.3775	800	1

[1] Females of cryptic species of the *Drosophila repleta* group;
[2] Cryptic species of the *D. willistoni* group that were not identified.

Results and Discussion

The collection on the Atlantic forest PEPA in Bauru/SP resulted in a total of 800 identified flies, distributed among at least 16 species, belonging to three drosophilid genera: *Drosophila,* showing the highest relative abundance (95%), followed by *Zaprionus* (4,375%) and *Scaptodrosophila*, with the lowest abundance (0.625%) and represented only by the *S. latifasciaeformis* species.

The most abundant genus, *Drosophila*, had representatives of two subgenera, *Drosophila* (5.75%) and *Sophophora* (89.25%), 10 groups and at least 13 different species (Table 1). The *Drosophila* subgenus showed the highest richness (6 groups and 8 species). The *Sophophora* subgenus presented 3 groups and at least 5 species. This richness distribution between subgenera has been observed in other studies (Sene *et al.,* 1981; Tidon-Sklorz and Sene, 1995; Tidon-Sklorz and Sene, 1999; Medeiros and Klaczko, 2004; Mateus *et al.,* 2018; Mateus *et al.,* 2021). The *Sophophora* subgenus was represented almost completely by specimens of the indigenous *D. willistoni* group (~95% within subgenus).

Among the species collected, eleven were indigenous and five were exotic. Gottschalk *et al*. (2007) stated that the number of native species is not an advisable measure to indicate the impact of urban growth in the Brazilian Atlantic forest. They proposed two parameters for this purpose: 1) the abundance and number of exotic species; 2) the abundance of the *D. willistoni* subgroup. Cavasini *et al.* (2014) analyzed two highland *Araucaria* forest fragments, a phytophysiognomy of the Atlantic forest distributed in the south and southeast regions of Brazil, and concluded that they are at an intermediate state of conservation based on the high abundance of *D. willistoni* subgroup species and the high abundance *D. kikkawai*, an exotic species. In our

case, the five exotic species showed low abundance, accounting for only 9.5% of the total flies collected, with only two species, *D. immigrans* and *Z. indianus*, showing relative abundance higher than 4%. Moreover, species of the *D. willistoni* group represented more than 84% of the sample. Therefore, it seems that this Atlantic forest fragment is reasonably well conserved.

Figure 1. Satellite image (Goggle Earth Pro software) of the location of *Drosophila* fauna collection in the Permanent Environment Protection Area (PEPA) of the São Paulo State University (UNESP), Bauru-SP – Brazil.

The *Zaprionus* genus has a high ability to disperse. For example, *Z. indianus* probably arrived in Brazil in the São Paulo state (Vilela, 1999) at the end of 1998 (Mateus *et al.,* 2020). In 2008, it already had reached Argentina (Lavagnino *et al.,* 2008), and in 2013 it was detected in Canada (Renkema *et al.,* 2013). More than 20 years after arriving in the Neotropical region, *Z. indianus* has been already collected from 41 species of fruits (Valadão *et al*., 2019).

Another important result that must be pointed out from our results is the collection of *Z. tuberculatus*. This is the record of this invasive species after its invasion in Brazil, reported by Cavalcanti *et al*. (2022). It was collected together with *Z. indianus*, a species that has been categorized as a pest in Brazil (Vilela, 1999; Roque *et al*., 2017). Cavalcanti *et al*. (2022) stated that the association of *Z. tuberculatus* with a pest species, such as the case of *Z. indianus* in the collected area, could boost its negative impacts, as its oviposition could be enabled in already damaged fruits (Amiresmaeili *et al*., 2019). Several studies have detected *Z. tuberculatus* larvae in fruits (Balmès and Mouttet, 2019, Kamel *et al*., 2020) or adults in vineyards and orchards (Chireceanu *et al*., 2015, Zengin, 2020). Therefore, this species has the potential to become a pest to soft skin fruit plantations, despite it has been considered only a secondary pest and it is not anymore on the EPPO Alert List (EPPO, 2020).

Keywords: Community, Atlantic forest biome, Neotropical region, invasive species.

Acknowledgments: We are thankful to M.C. Ferreira for technical assistance, and to Dr. Fernanda Henriques, Director of the Bauru Campus of the São Paulo State University (UNESP) for authorizing the collection at the UNESP's Permanent Environment Protection Area.

References: Amiresmaeili, N., C. Jucker, S. Savoldelli, and D. Lupi 2019, J. Entomol. Acarol. Res. 51: 8-15; Avondet, J.L., R.B. Blair, D.J. Berg, and M.A. Ebbert 2003, Environ. Entomol. 32: p. 347-358; Balmès, V., and R. Mouttet 2019, EPPO Bull. 49: 122-126; CABI 2021, Invasive species compendium. (https://www.cabi.org/isc/datasheet/117928/ - accessed 15 December 2022); Cavalcanti, F.A., L.B. Ribeiro, G. Marins, G.S. Tonelli, S.N. Báo, A. Yassin, and R. Tidon 2022, Annals Entomol. Soc. Am. 115: 267-274; Cavasini, R., M.L.T. Buschini, L.P.B Machado, and R.P. Mateus 2014, Braz. J. Biol. 74: 761-768; EPPO

2020, Mini datasheet on *Zaprionus tuberculatus*. (Diptera: Drosophilidae). (https://gd.eppo.int/download/doc/1437_minids_ZAPRTU.pdf/ - accessed 15 December 2022); Ferreira, L.B., and R. Tidon 2005, Biodiv. Conserv. 14: p. 1809-1821; Freire-Maia, N., and C. Pavan 1949, Cultus. 1: 3–66; Frota-Pessoa, O., 1954, Arq. Museu Paran. 10: 253–330; Gottschalk, M.S., D.C. De Toni, V.L.S. Valente, and P.R.P. Hofmann 2007, Neotrop. Entomol. 36: 848-862; Kamel, M.B.H., Z.B. Cheik, S. Zouari, L. Mdellel, and V. Balm 2020, EPPO Bull. 50: 307-310; Lavagnino, N.J., V.P. Carreira, J. Mensch, E. Hasson, and J.J. Fanara 2008, Rev. Soc. Entomol. Argent. 67: 189-192; Markow, T.A., and P.M. O'Grady 2006, Academic Press/Elsevier; Mata, R.A., M. Mcgeoch, and R. Tidon 2008, Biodiv. Conserv. 17: p. 2899-2916; Mata, R.A., M. Mcgeoch, and R. Tidon 2010, Braz. J. Nat. Conserv. 8: p. 60-65; Mateus, R.P., M.L.T. Buschini, and F.M. Sene 2006, Braz. J. Biol. 66: 719-729; Mateus, R.P., L.P.B. Machado, and D.P. Simão-Silva 2018, Stud. Neotrop. Fauna Environ. 53: 152–161; Mateus, R.P., E.M. Moraes, and L.P.B. Machado 2020, Dros. Inf. Serv. 103: 29-31; Mateus, R.P., M.C. Ferreira, and L.P.B. Machado 2021, Dros. Inf. Serv. 104: 30-34; Medeiros, H.F., and L.B. Klaczko 2004, Biota Neotropica 4: 1-12; Parsons, P.A., 1991, Global Ecol. Biogeog. 1: p. 77-83; Poppe, J.L., V.L.S. Valente, and H.J. Schmitz 2012, Pap. Avul. Zool. 52: p. 185-196; Renkema, J.M., M. Miller, H. Fraser, J-PH. Légaré, and R.H. Hallett 2013, Scientific Note J. Ent. Soc. Ont. 144: 125-130; Roque, F., C. Matavelli, P.H.S. Lopes, W.S. Machida, C.J. Von Zuben, and R. Tidon 2017, Ann. Entomol. Soc. Am. 110: 521-527; Schmitz, H.J., and V.L.D.S. Valente 2019, Pap. Avul. Zool. 59: e20195945; Schluter, D., and R.E. Ricklefs 1993, In: Ricklefs, R.E., and D. Schluter, editors, Chicago (IL): The University of Chicago Press, p. 1–10; Sene, F.M, M.A.Q.R. Pereira, C.R. Vilela, and N.M.V. Bizzo 1981, Dros. Inf. Serv. 56: 118–121; Sparovek, G., A.G.O.P. Barretto, M. Matsumoto, and G. Berndes 2015, Environ. Sci. Technol. 49: 10285-10293; Tidon-Sklorz, R., and F.M. Sene 1995, Iheringia, Sér. Zool. 78: 85–94; Tidon-Sklorz, R., and F.M. Sene 1999, In: Brandão, C.R.F., and E.M. Cancello, editors, São Paulo (SP), FAPESP, p. 247-261; Torres, F.R., and L. Madi-Ravazzi 2006, Iheringia, Sér. Zool. 96: 437-444; Val, F.C., and F.M. Sene 1980, Pap. Avul. Zool. 33: 293-298; Valadão, H., C.E.B. Proença, M.P. Kuhlmann, S.A. Harris, and R. Tidon 2019, Ecol. Entomol. 44: 721-737; Vilela, C.R., 1999, Dros. Inf. Serv. 82: 37-39; Vilela, C.R., 1983, Rev. Bras. Entomol. 27: 1–114; Vilela, C.R., and L. Mori 2014, Rev. Bras. Entomol. 58: 371-375; Vilela, C.R., and B. Goñi 2015, Rev. Bras. Entomol. 59: 346-350.

Zaprionus tuberculatus was collected in the metropolitan region of São Paulo, state of São Paulo, Brazil.

Montes, Luan F., and Carlos R. Vilela. Departamento de Genética e Biologia Evolutiva, Instituto de Biociências, Universidade de São Paulo, São Paulo - SP, Brazil. Corresponding author: 10740700@usp.br and crvilela@ib.usp.br

The invasive species *Zaprionus tuberculatus* Malloch, 1932, has been recorded in Brasília (Federal District) since early 2020 as reported late last year by Cavalcanti *et al.* (2021). Here, we report for the first time the collection of one female *Zaprionus tuberculatus* in the Metropolitan Region of São Paulo, Brazil. The single fertilized female specimen was identified among a total of 37 Drosophilidae flies collected from 1-6 April 2022 in a two-story house in the Cerâmica district of São Caetano do Sul (23º37'52''S, 46º34'09''W), state of São Paulo, Brazil, by the first author and A.F. Montes. Most of the flies were aspirated from the walls of an adjacent outdoor area belonging to the house, followed by those collected from kitchen and then from bathroom. It is important to point out that approximately 90 m from the collection area there is a greengrocery. The collected flies were kept in banana-agar-brewer yeast medium (Goñi and Vilela, 2016) at uncontrolled room temperature until their identification and isolation on April 7th, and since then at 18 ± 1ºC. When the isolated flies were transferred to new culture vials, one tiny ball of live baker's yeast was placed over the medium surface.

In decreasing order of abundance the 37 flies were: *Drosophila melanogaster* Meigen, 1830 (15 males, 11 females), *D. ananassae* Doleschall, 1858 (1 male, 2 females), *D. simulans* Sturtevant, 1919 (1 male,

2 females), *D. cardini* Sturtevant, 1916 (1 female), *D. hydei* Sturtevant, 1921 (1 female), *D. mercatorum* Patterson and Wheeler, 1942 (1 female), *Zaprionus indianus* Gupta, 1970 (1 female), and *Z. tuberculatus* (1 female). Additionally, several imagoes (males and females of F_1 generation) that emerged from the food medium of the collection vials were identified as *D. kikkawai* Burla, 1954, indicating that at least one fertilized female of such species was collected. After being anesthetized, the two *Zaprionus* females were isolated aiming to obtain isofemale lines. Initially, the single *Zaprionus tuberculatus* female laid nine eggs (observed on April 9th) but just one larva hatched (observed on April 11th) and developed into a male imago (Figure 1A,C) that was backcrossed to his mother on May 5th establishing an isofemale line coded M89F1. Unfortunately, the single *Z. indianus* female laid *ca*. 25 eggs from which no larva hatched. However, as it happened with *D. kikkawai*, an undetermined number of *Z. indianus* imagoes emerged from the food medium of the collection vials and were used to establish a multifemale line coded M89M1. As stated by Yassin and David (2010), when cultures of *Zaprionus* spp. are crowded, the mature larvae climb up the bottle and often escape through the plug, and die from desiccation. We have observed that this larval behavior is more pronounced in *Z. tuberculatus* than in *Z. indianus*. It was also noticed that the pupal death increases if pupariation occurs in the space between the plug and the vial neck. To avoid crowding, the mature flies of *Z. tuberculatus* were kept for less than 24 h on the oviposition substrate.

The two females belonging to the genus *Zaprionus* were identified to species level using the key to European invasive species of *Zaprionus* by Bächli *et al.* (2004), through the analysis of the ornamentation of profemur (Figure 1C,D). Once the two strains were established, our identifications could be confirmed through the additional analyses of their fronts and eggs following Tsacas *et al.* (1977), Yassin and David (2010), and Cavalcanti *et al.* (2021). *Z. tuberculatus* (Figure 1A) bears a clear-cut mid-frontal longitudinal white stripe from ocellar triangle to ptilinal suture. *Z. indianus* specimens (Figure 1B) are mostly devoid of such mid-frontal white stripe. The relative length and width of the two pairs of the egg respiratory filaments differ between the two invasive *Zaprionus* species. In *Z. tuberculatus*, the apical pair of egg filaments is shorter and thinner than the basal pair that is clearly longer and much thicker (Figure 1E). In *Z. indianus* (Figure 1F), the two pairs of egg filaments are only slightly different regarding their length and width.

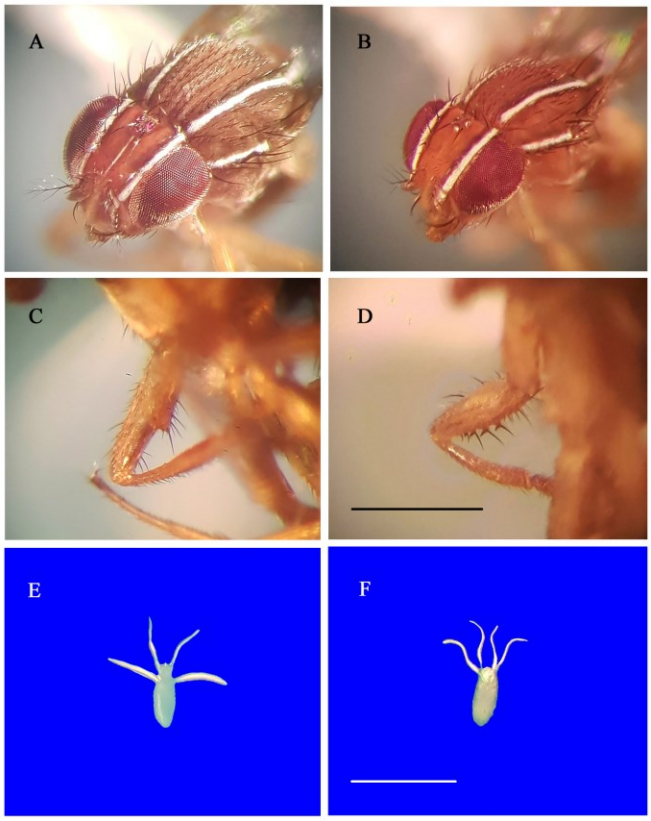

Figure 1. *Zaprionus tuberculatus* (A, C, E), male, generation F_1, isofemale line M89F1: A, head (with clear-cut mid-frontal white stripe) and thorax, oblique dorsal view; C, right profemur, anterior view (note the prominent ventral tubercle bearing a strong seta apically); E, egg, dorsal view. *Zaprionus indianus* (B, D, F), male, multifemale line M89M1: B, head (without clear-cut mid-frontal white stripe) and thorax, oblique dorsal; D, left profemur, posterior view (note the ventral row of four L-shaped pairs of a strong seta adjacent to and divergent with a stiff setula); F, egg, dorsal view. Scale bars = 0.5 mm. A-D to the same scale, E and F to the same scale.

The Paleotropical genus *Zaprionus* currently (XII.2022) comprises 58 species, 46 of which belong to *Zaprionus* subgenus and are endemic to the Afrotropical Region (Yassin and David, 2010). So far, three out of the 46 Afrotropical species became

or are on the way of becoming invasive species in tropical and/or temperate climate of other biogeographical regions: *Zaprionus indianus*, *Z. tuberculatus*, and *Z. ghesquierei* Collart, 1937. The three invasive species of *Zaprionus* are generalists with regard to their breeding sites (Chassagnard and Kraaijeveld, 1991) as, according to Lachaise and Tsacas (1984), *Z. indianus* (cited as *Z. collarti* Tsacas, 1980 [junior synonym] emerged from 71 species of fruits, *Z. tuberculatus* from 20, and *Z. ghesquierei* from 24 (but refer to Yassin and David, 2010, for up-to-date table and further details). Apparently, the first species invaded the American continent around late 1998 (Vilela, 1999; Vilela and Goñi, 2015) and the second around early 2020 (Cavalcanti *et al.*, 2021), respectively. Although the latter has not been recorded yet in the continental America, but considering it has been collected in Cyprus and mainland Turkey (Chassagnard and Kraaijeveld, 1991), and Hawai'i (O'Grady *et al.*, 2002), we predict it is just a matter of time before *Z. ghesquierei* will be found in the Americas. So, New World researchers surveying drosophilids must be aware of this possibility, paying special attention to the presence of a conspicuous white spot at scutellum tip and the absence of spines on the profemur, typical of *Z. ghesquierei*, while identifying specimens of invasive *Zaprionus* species.

Cavalcanti *et al.* (2021) considered that it is impossible to determine the entry route and the origin of the "propagule" of the invasive species *Z. tuberculatus* collected in Brasília's urban parks and surrounding natural Savanna Biome. However, as it was proposed for *Z. indianus* by Vilela (1999), they raised the possibility of an accidental transportation of immatures of imagoes of the invasive species from some country to South America by airplanes or ships.

Another alternative would be that fertilized female(s) escaped from stocks of *Z. tuberculatus* maintained by Stock Centers in the Americas, and eventually became established in the wild. By the way, on 16.VIII.2016 and 06.XII.2016, we had been informed by Dr. Rodrigo Cogni (e-mail pers. comm.) that one strain of *Z. tuberculatus* (#50001-0001.05) [collection site not informed], coming from the *Drosophila* Species Stock Center (then at University of California, San Diego, USA), was being maintained and used by his laboratory researchers at the Department of Ecology of the IB-USP (Cidade Universitária "Armando de Salles Oliveira" [CUASO] São Paulo, SP, Brazil) at least as early as July 2016. Later on, the same strain was used in the MSc project of Camila Souza Beraldo (Beraldo, 2018, unpublished thesis). However, we could not confirm the latter hypothesis after checking again the 247 voucher specimens of a total of 252 males plus females previously identified by A.S. Rampasso and Vilela (2017) as *Zaprionus indianus* that emerged out of 105 fallen fruits of three ornamental plant species (*Inga vera* Willd. subsp. *affinis* (DC.), *Psidium cattleianum* Sabine, and *Syzygium cumini* (L.) Skeels), and collected on January 31st 2017 in the gardens of the CUASO, west São Paulo city. They indeed have their profemur ornamentation typical of *Z. indianus* (Figure 1D) as previous assumed based only on the presence of four white longitudinal stripes on dorsal mesonotum. Anyway, to shed some light on the entry route of the *Z. tuberculatus* collected in Brasília, it would be desirable to check again the voucher specimens identified as *Z. indianus* from drosophilid surveys in the Americas, collected from baited traps or emerged from ornamental or native fruits, especially those conducted after July 2016.

In short, voucher specimens of *Zaprionus tuberculatus* and its sibling *Zaprionus indianus* Gupta, 1970, can be easily distinguished from each other based on morphological grounds such as the presence or absence of one clear-cut mid-frontal white stripe (Figure 1A, B) and the type of profemur ornamentation (Figure 1C, D).

Whether or not *Z. tuberculatus* has the potential to become a new pest of the cultured figs in the Americas is something that deserves to be analyzed. Aware that the fig crop season of the cultivar roxo-de-valinhos has just begun, we bought a styrofoam tray containing five figs wrapped in PVC transparent food film, crop from Valinhos municipality (SP), supposedly having *Zaprionus* ssp. larvae, in an open market downtown São Paulo City on December 11, 2022, aiming to identify the emerged species. In the lab, the figs were longitudinally cut and placed in 1/4L glass vials over wet vermiculite and kept at 22 ºC. So far (December 27), the following imagoes emerged: one female of *Z. tuberculatus* and one female of *Z. indianus* (22.XII), two females and one male of *Z. tuberculatus* plus six females and one male of *Z. indianus* (23-24.XII), three females and five males of *Z. indianus* (25.XII), one female and one male of *Z. indianus* (26.XII), and two males of *Z. indianus* (27.XII). However, as the decaying figs released too much water the vials became too wet and moldy, most of the larvae died, and so did most of the pupae putatively belonging to *Z. tuberculatus* probably due to their more prominent behavior of pupariating in the space between the plug and

the vial neck. It seems that better results could be achieved by using dried (instead of wet) vermiculite and only 1/4 of a longitudinally sliced fig per 1/4L glass vial.

Voucher specimens from strains M89F1 (*Z. tuberculatus*) and M89M1 (*Z. indianus*) as well as of both species emerged from Valinhos' figs will be deposited at the Museu de Zoologia, Universidade de São Paulo.

The domiciliary collections described above were part of the optional discipline named Practical Genetics for Basic Education of the Biological Sciences Course of the Universidade de São Paulo. At first, enrolled students are asked to cook a conventional banana-agar culture medium to be used to transport *Drosophila* specimens collected from inside their residences to the lab class. Then, they made their own aspirator and were trained to use them to sample flies from culture vials. The main goal of the activity is to survey the *Drosophila* specimens occurring indoors, mainly in kitchens, in the Metropolitan Region of São Paulo and to try to establish isofemale lines of the model organism *Drosophila melanogaster*, supposedly the most abundant species occurring at home. Once obtained, male or female virgins isolated from the isofemale lines are crossed individually with three selected, and easily scored at naked eyes, wing mutants (*apterous*, *taxi*, and *vestigial*). After analyzing three generations following Mendel's scheme, the students will be able to determine their inheritance patterns (autosomal recessive for the three mutations).

Acknowledgments: We are grateful to F. Flauzino for technical assistance and to 2022 Practical Genetics for Basic Education discipline team: Dr. D.S. Scheepmaker (faculty member) and four students (C. D'Elia, L. Pacheco, S. Komatsu, and M. Ribeiro) for different reasons.

References: Bächli, G., C.R. Vilela, S.A. Escher, and A. Saura 2004, Faun. Ent. Scand. 39: 1-362; Beraldo, C.S., 2018, Variação na susceptibilidade do hospedeiro a diferentes patógenos: um estudo experimental e filogenético de *Drosophila*-vírus, unpublished MSc thesis, São Paulo; Cavalcanti, F.A.G.S., L.R. Ribeiro, G. Marins, G.S.S.S. Tonelli, S.N. Báo, A. Yassin, and R. Tidon 2021, Ann. Entomol. Soc. Am. 115(3): 267-274; Chassagnard, M.Th., and A.R. Kraaijeveld 1991, Annls. Soc. ent. Fr. (N.S.) 27(4): 495-496; Goñi, B., and C.R. Vilela 2016, Zoologia 33(6): 1/13-13/13; Lachaise, D., and L. Tsacas 1984, Breeding-sites in Tropical African Drosophilids. In: *The Genetics and Biology of* Drosophila, v. 3d, (Ashburner, M., H.L. Carson, and J.N. Thompson, Jr., eds.) Academic Press, London. pp. 221-332; O'Grady, P.M., J.W. Beardsley, and W.D. Perreira 2002, Bishop Mus. Occ. Pap. 69: 34-35; Rampasso, A.S., and C.R. Vilela 2017, Fruits from three ornamental plants as breeding sites of invasive and native Drosophilidae (Diptera) in the capital of the State of São Paulo, Brazil, X Symposium on Ecology, Genetics and Evolution of *Drosophila*, Nov. 6-9, Ouro Preto, Brazil, Poster; Tsacas, L., J. David, R. Allemand, G. Pasteur, M.T. Chassagnard, and S. Derridj 1977, Annls. Soc. ent. Fr. (N.S.) 13(2): 391-415; Vilela, C.R., 1999, Dros. Inf. Serv. 82: 37-39; Vilela, C.R., and B. Goñi 2015, Mosca-africana-do-figo, *Zaprionus indianus* Gupta. In: Pragas introduzidas no Brasil: insetos e ácaros (Vilela, E., and R.A. Zucchi, eds.). pp. 173-196. FEALQ, Piracicaba, Brazil; Yassin, A., and J.R. David 2010, ZooKeys 51: 33-72.

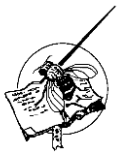

The effect of social isolation on the viability during the development of *Drosophila melanogaster.*

Del Pino, Francisco, Tamara Solari Lagos, Patricia Solís Aravena, Carlos Monje Myrik, and Eduardo Alvarez. Human Genetics Program, ICBM, School of Medicine, University of Chile.

Abstract

This study seeks to find a possible relationship between social isolation and the viability of *Drosophila melanogaster*, for which two groups of flies are bred; one was developed in isolation and the other in community. The results show that the social isolation significantly decreases the viability of *D. melanogaster.*

Introduction

Social isolation refers to an environmental factor that implies the development of a specimen without the presence of other individuals from the same species, and viability refers to the effective probability that an organism can survive.

A relationship between social isolation and viability has been found both in *Drosophila melanogaster* as well as in other species, through the manipulation of environmental factors that relate to the interaction between conspecifics. This possible relationship could be due to multiple causes, among them is the justified explanation in the genetic bases of living beings, where the concept of epigenetics[1] plays an important role. Multiple studies have established a relationship between epigenetic alteration and environmental exposure (Gartstein and Skinner, 2018), in which it has been shown that factors from the environment, such as the presence of mechanosensory stimuli, modulate the development of organisms (Ardiel and Rankin, 2010), because of the generation of cellular mechanisms that regulate gene expression.

The present study aims to demonstrate that there is an association between isolation during development and a significant decrease in viability in *Drosophila melanogaster*. It also seeks to determine in which of the stages of development the presence of conspecifics is crucial for the viability of the individuals.

[1] Epigenetics corresponds to the study of changes in gene expression that do not involve a modification in the DNA sequence and that can be reversible (Bedregal *et al*., 2010).

Materials and Methodology

Species and strain used

An isofemale strain of *D. melanogaster*, Canton-S strain is used, which comes from a common parent whose descendants were crossed with each other for 15 generations to rule out the variable of genetic information in the interpretation of the results, allowing to establish the influence of the environment as the variable that affects viability.

Medium preparation

Petri dishes of 4 centimeters in diameter and 1.5 centimeters in height are used, previously sterilized, lined up to half (approximately 0.8 centimeters) with Burdick culture medium (Burdick, 1954) colored with Gourmet brand dye (following the instructions of the brand, 1 drop every 100 grams of medium approximately), at a temperature between 23ºC and 24ºC (optimal temperature for the development of *D. melanogaster*).

Data collection

Two groups of *D. melanogaster* Canton-S are used for this study;

- Group 1; 60 capsules with 1 isolated egg each.
- Group 2; 4 capsules with 30 eggs grouped in each one.

After the hatching of the eggs, the larvae are transported to flasks with the same amount of Burdick's medium. Every 24 hours, viability is recorded as the flies progress in their development; the number of eggs that hatch, larvae that pupate, and pupae that become an adult is recorded. The time limit considered for the count of viable specimens varies according to the stage; (1) hatching of the egg: 24 hours, (2) transition from larva to pupa: 120 hours, and (3) transition from pupa to adult: 5 days. Any specimen that does not go to the next stage, or does so after this established time, is not considered viable.

Statistical design

A comparison of the proportions is made by using the chi-square statistical test (χ^2), considering a p-value < 0.05. The dependent and independent variables correspond to viability (viable/unviable) and the social environment (isolated/grouped), respectively.

Results

When viability tests were performed in the grouped (non-isolated) and isolated groups, the following results were obtained by stage of development:

As summarized in Figure 1, in both groups the viability is affected mainly in the transition from egg to larva and from larva to pupa.

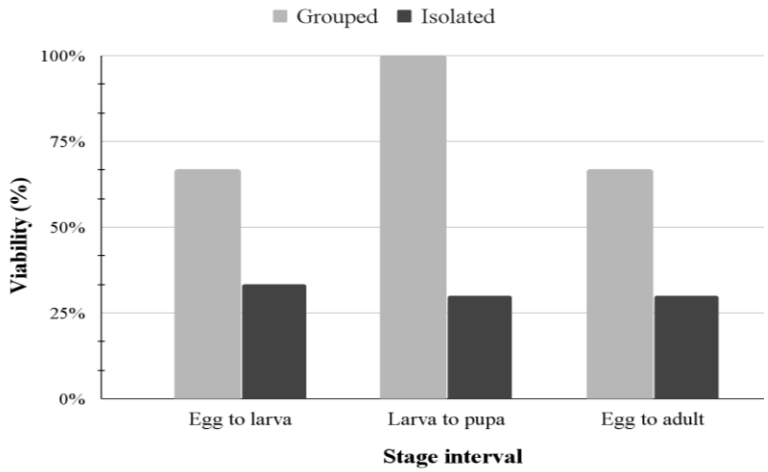

Figure 1. Percentage of viability egg to larva and larva to pupa of both groups. The percentage of viability observed in the pupal to adult period is omitted because it is equal to 100% in both groups.

Table 1. Number of total specimens according to developmental stage.

Group	Number of specimens according to stage (% viability)			
	Egg	Larva	Pupa	Adult
Grouped	120	80 (~ 66%)	80 (100%)	80 (100%)
Isolated	60	20 (~ 33%)	18 (90%)	18 (100%)

Table 2. Values obtained for X^2 for each transition period between stages using 3.84 as the critical value (p-value < 0.05). In the case of the pupa to adult transition, the calculation of X^2 is not done.

	(X^2)	P Value	H. null (H0)	H. alternative (H1)
Egg to larva	18	0	Rejected	Accepted
Larva to pupa	6	0.014	Rejected	Accepted
Egg to adult	21.6	0	Rejected	Accepted

Statistical analysis

For the analysis of the results, each stage is evaluated separately. The alternative hypothesis H1 is defined as the one that establishes that there is an association between viability and isolation; on the other hand, the null hypothesis states that there is no association between these variables.

The alternative hypothesis is accepted when analyzing the viability data for the transition from egg to larva, from larva to pupa and from pupa to adult. The analysis of the transition from pupa to adult is not performed since the results are in agreement with those expected.

Discussion and Conclusions

In view of the results obtained, it is concluded that social isolation is associated with the viability of *D. melanogaster* flies. However, the strength of association has a greater magnitude in earlier stages of development, observing a bigger difference between the results obtained from the transition from egg to larva, than from larva to pupa and from pupa to adult. In summary, it is concluded that the influence of stimuli between conspecifics is more relevant in early stages. Although, it is to be expected that 100% of the eggs in any of the groups will not hatch, if a lower viability is observed in the isolated eggs.

This raises the question of whether the eggs communicate, and the way in which it is done, so we propose to study the mechanisms involved (and their nature) in viability, in the context of social isolation.

References: Ardiel, E.L., and C.H. Rankin 2010, Pediatric Child Health 15(3): 153-156; Bedregal, P., B. Shand, M.J. Santos, and P. Ventura-Juncá 2010, Rev. Med. Chile 138: 366-372; Burdick, A.B., 1954, Dros. Inf. Serv. 28: 170; Gartstein, M.A., and M.K. Skinner 2018, CUP 30: 1269–1303.

Geographic distribution of inversions of *Drosophila ananassae*: Latitudinal cline in the frequency of *In(2L)A* of Muller's element E.

Tomimura, Yoshihiko[1], Yoshiko N. Tobari[2], and Muneo Matsuda[3,2]*. [1]Shiba Gakuen, Minato-ku, Tokyo, Japan; [2]The Research Institute of Evolutionary Biology, Tokyo, Japan; [3]Department of Biology, School of Medicine, Kyorin University, Tokyo, Japan; *Corresponding author: email: matsudam@ks.kyorin-u.ac.jp

Introduction

Drosophila ananassae is one of eight cosmopolitan species of *Drosophila* (*melanogaster, simulans, ananassae, funebris, immigrans. hydei, replete,* and *busckii)* that occur in all six zoogeographic regions. *D. ananassae* is thought to have spread with cultivated pineapple (ananassae) (Patterson and Stone, 1952). Of the eight pantropical species, the widely distributed inversion polymorphisms of *D. melanogaster*, *D. immigrans*, *D. hydei* and *D. busckii* are few, and the inversion polymorphisms of *D. simulans* and *D. replete* have not been observed. However, *D. ananassae* (Tomimura *et al*., 1993; Matsuda *et al*., 2009) and *D. busckii* (Krivshenko, 1963) are high-frequency inversion polymorphs. Based on these findings, about the wildly distributed "cosmopolitan species", Dobzhansky (1970) pointed out that populations from remote and climatically different countries carry the same chromosomal variants, often with similar frequencies. However, the relationship between environmentally dependent cosmopolitan species and inversion polymorphisms is unclear.

Das *et al*. (2004) showed strong evidence of population size expansion in ancestral populations in Southeast Asia, based on analysis of nucleotide variation using ten neutral loci of *D. ananassae*. Schug *et al*. (2007, 2008) found high levels of variation in genetic structure among all populations of *D. ananassae*, indicating differential sex discrimination ability across the species' range. However, Tomimura *et al*. (1993) found three cosmopolitan inversions of *In(2L)A*, *In(3L)A*, and *In(3R)A* in *D. ananassae* in populations from almost the entire range of the species, from East Africa, India, Southeast Asia, Papua New Guinea, and South Pacific Islands to Brazil. We found the three cosmopolitan inversions in populations almost globally. This uniform inversion distribution seems to contradict the evidence for genetic differentiation of species colonization shown by premating isolation analysis and microsatellite analysis.

Studies have reported latitudinal trends in inversion frequencies in *Drosophila* species, for example, in *D. melanogaster* (Mettler *et al*., 1977; Arauz *et al*., 2011; Inoue and Watanabe, 1977, 1979; Knibb *et al*., 1981; Rako *et al*., 2006) and *D. subobscura* (Krimbas and Powell, 1992; Bayon *et al*., 2001). However, in 45 populations of *D. ananassae* from Kanyakumari, Tamil Nadu (8.07°N) to Jammu, Kashmir (34.08°N), India, the simple correlation between frequencies of the three cosmopolitan inversions of latitude, longitude, and

Table 1 Numbers of strains of *Drosophila ananassae* used in this study.

Locality [a]	longitude	latitude	No. of strains studied	Collection	
				Year	Collector
Mbengwi, Cameroon	10.00E	6.01N	2	2004	Arizona Stock
Oku, Cameroon	10.25E	6.15N	1	2004	Arizona Stock
Mbalang-Djalingo, Cameroon	13.44E	7.19N	1	2004	Arizona Stock
Maroua, Cameroon	14.19E	10.36N	1	2004	Arizona Stock
Yokadouma, Cameroon	15.03E	3.31N	1	2004	Arizona Stock
Kisangani, Congo	15.19E	0.31N	1	2005	Arizona Stock
Gisakura, Rwanda	29.52E	2.26S	1	2005	Arizona Stock
Namulonge, Uganda	32.17E	1.22N	2	2005	Arizona Stock
Chiang Mai, Thailand	98.39E	18.47N	19	2002	A. Das
Bangkok, Thailand	100.28E	13.43N	14	2002	A. Das
Kuala Lumpur, Malaysia	101.41E	3.08N	5	2002	A. Das
Mahasarakam, Thailand	104.04E	16.11N	5	2002	M. Ito
Phnom Penh, Cambodia	104.55E	11.33N	44	2002	A. Das
Bogor, Indonesia	106.47E	6.35S	29	2001	M. Kimura
Bogor, Indonesia	106.47E	6.35S	23	2008	M. Kimura
Jakarta Java, Indonesia	106.50E	6.12S	1	2004	C.S. Ng
Kota Kinabalu, Malaysia	116.06E	5.58N	8	2002	A. Das
Kota Kinabalu, Malaysia	116.06E	5.58N		2008	M. Kimura
Lombok, Indonesia	116.21E	8.30S	1	2001	M. Kimura
Sabah, Malaysia	116.47E	5.25N	1	2006	K. Akutsu
Manila, Philippines	120.58E	14.35N	13	2002	A. Das
Taipei, Taiwan	121.33E	22.02N	1	2006	S. Prigent
Iriomotejima, Japan	123.44E	24.19N	1	2008	Y. Tomimura
Cebu, Philippines	123.53E	10.27N	20	2002	A. Das
Ishigakijima, Japan	124.11E	24.23N	1	1998	M. Watada
Miyakojima, Japan	125.16E	24.48N	2	1995	M. Watada
Miyakojima, Japan	125.16E	24.48N	1	1999	M. Watada
Kumejima, Japan	126.46E	26.20N	13	2000	F. Hihara
Naha Okinawa, Japan	127.40E	16.12N	55	2008	Kondo & Yafuso
Naze Kagoshima, Japan	127.58E	28.23N	6	1998	M. Watada
Ogasawara Tokyo Japan	142.09E	27.07N	1	1999	Y. Fuyama
Honolulu Hawaii, U.S.A	157.51W	21.18N	3	2005	Y. Tomimura
Nayarit, Mexico	104.50W	21.45N	1	2004	Arizona Stock
Thomasville Georgia, U.S.A	83.58W	30.52N	1	2003	Arizona Stock
Marathon Florida, U.S.A	81.05W	24.42N	1	2002	Arizona Stock
Ubatuba, Brazil	45.05W	23.26S	42	2007	B. Goni
Donde, Guinea	13.01W	12.01N	1	2005	Arizona Stock
Kade, Ghana	0.50W	6.05N	2	2004	Arizona Stock
Total			322		

[a] Localities are shown from Africa to South America along with longitude

altitude was not significant (Singh and Singh, 2007). We considered that the main habitat areas of the species, including its core, Southeastern and peripheral populations, should be further investigated to confirm this report.

Following the report by Tomimura *et al*. (1993) of salivary gland chromosomal variation in *D. ananassae* and related species, we obtained samples from a number of localities covering the range of the species to confirm the frequency of inversions and heterozygosity. In this study, we analyzed the frequency of cosmopolitan inversions in natural populations and the correlations between inversion frequency and longitude and latitude. We discuss the evolutionary processes that maintain the cosmopolitan inversions, including data from previous studies (Tomimura *et al*., 1993).

Materials and Methods

We used strains of single female origin collected from six zoogeographic regions, excluding the Palearctic zone. The habitats of *D. ananassae* used in this study are shown Table 1. The population ranges in longitudinal order from 10.00°E to 142.09°E/157.51°W to 0.50°E, and the habitat ranges from 23.26°S to 30.52°N. *D. ananassae* is widespread in subtropical and tropical regions almost globally. The number of strains of *D. ananassae* used in this study is shown in Table 1.

At least eight female larvae from each female-derived strain were examined cytologically. Chromosome 4 is mostly heterochromatin and usually buried at the chromosome center. Chromosome rearrangements were determined and described using a reworked photomap (Tobari *et al*., 1993).

Table 2. Geographical distribution of inversions and translocations of *D. ananassae* used in both previous and present data.

Locality	paracentric inversions							N[b]	*
	XL	XR	2L	2R	3L	3R	Others		
Mbengwi, Cameroon	ST	ST	ST, A	ST	ST, A	ST, A		2	
Oku, Cameroon	ST	ST	ST	ST	ST	ST, J		1	
Mbalang-Djalingo, Cameroon	ST	ST	ST, A	ST, O	ST, A	ST, J		1	
Maroua, Cameroon	ST	ST	ST, A	ST, O	A	ST		1	
Yokadouma, Cameroon	ST	ST	ST	ST	ST	ST, J		1	
Kisangani, Congo	ST	ST	ST, A	ST	A	ST, A		1	
Gisakura, Rwanda	ST	ST	ST	ST	ST, A	ST		1	
Namulonge, Uganda	ST	ST	ST, A	ST	ST, A	ST		2	
Nairobi, Kenya	ST	ST	ST	ST	ST, A	ST, A		2	*
Mombasa, Kenya	ST	ST	ST, A	ST, F	ST, A	ST, A		7	*
La Nicoliere, Mauritius	ST	ST	ST, A	ST	ST, A	ST, A		2	*
Mysore, India	ST	ST	ST, A	ST	ST, A	ST, A		27	*
Coimbatore, India	ST	ST	ST, A	ST	ST, A	ST, A	*In(3LR)H, In(3LR)I*	11	*
Hyderabad, India	ST	ST	ST, A	ST	ST, A	ST, A	*In(3LR)G*	25	*
Madras, India	ST	ST	ST	ST	ST, A	ST, A		2	*
Kandy, Sri Lanka	ST	ST	ST, A	ST	ST, A	ST, A		3	*
Calcutta, India	ST	ST	ST, A	ST	ST, A	ST, A		32	*
Shwebo, Myanmer	ST	ST	ST	ST	ST, A	ST		1	*
Mandalay, Myanmer	ST	ST	ST, A, N	ST	ST, A	ST, A		7	*
Yangon, Myanmer	ST	ST	ST, A	ST	ST, A	ST		1	*
Chiang Mai, Thailand, 2002	ST	ST	ST, A	ST	ST, A	ST, A		19	
Chiang Mai, Thailand, 1971, 1979	ST	ST	ST, A, B, K	ST	ST, A	ST, A	*In(3LR)C*	120	*
Bangkok, Thailand	ST	ST	ST	ST	ST, A	ST, A		14	
Penang, Malaysia	ST	ST	ST, A	ST	ST, A	ST, A		1	*

Kuala Lumpur, Malaysia, 2002	ST	ST	ST, A	ST	ST, A	ST, A		5	
Kuala Lumpur, Malaysia, 1971	ST	ST	ST, A, M	ST	ST, A	ST, A		28	*
Mahasarakam, Thailand	ST	ST	ST, A, K	ST	ST, A	ST, A		5	
Bukit Timer, Singapore	ST	ST	ST, A, B	ST	ST, A	ST, A		17	*
Phnom Penh, Cambodia	ST	ST	ST, A, B	ST	ST, A	ST, A, O[ac]		44	
Bogor, Indonesia, 2001	ST	ST	ST, A, B, C, J	ST, D	ST, A	ST, A		29	
Bogor, Indonesia, 2008	ST	ST	ST, A, B, J	ST, D	ST, A	ST, A, O[ac]		23	
Jakarta, Indonesia	ST	ST	ST, A	ST	ST, A	ST, A		1	
Kuching, Sarawak, Malaysia	ST	ST	ST, A	ST, E	ST, A	ST, A		1	*
Miri, Sarawak,	ST	ST	ST, B	ST	ST, A	ST, A		1	*
Burunei Town, Burunei	ST	ST	ST, A, B	ST	ST, A	ST, A		2	*
Kota Kinabalu, Malaysia, 2002	ST	ST	ST, A, B	ST	ST, A	ST, A		8	
Kota Kinabalu, Malaysia, 1971, 1979	ST	ST	ST, A, B	ST	ST, A	ST, A		16	*
Lombok, Indonesia	ST	ST	ST, A	ST	A	ST, A		1	
Sabah, Malaysia	ST	ST	ST, B, J	ST	ST	ST		1	
Sandakan, Sabah, Malaysia	ST	ST	ST, A	ST	ST, A	ST, A		3	*
Palawan, Philippines	ST	ST	ST, A	ST	ST, A	ST, A		21	*
Manila, Philippines	ST	ST	ST, A	ST	ST, A	ST, A	*In(3LR)J*[b]	13	
Los Banos, Philippines	ST	ST	ST, A, B	ST	ST, A, F	ST, A		22	*
Taipei, Taiwan	ST	ST	ST, A	ST	A	ST		1	
Taiwan, Taiwan	ST	ST	ST, A	ST	ST, A	ST, A		13	*
Iriomotejima, Japan	ST	ST	A	ST	A	A		1	
Cebu, Philippines	ST	ST	ST, A	ST	ST, A	ST, A		20	
Ishigakijima, Japan	ST	ST	ST, A	ST	A	ST		1	
Miyakojima, Japn, 1995	ST	ST	ST, A	ST	ST, A	ST		2	
Miyakojima, Japan, 1999	ST	ST	ST, A	ST	ST, A	ST, A		1	
Kumejima, Japan	ST	ST	ST, A	ST	ST, A	ST, A		13	
Naha, Okinawa, Japan	ST	ST	ST, A	ST	ST, A	ST, A		55	
Nago, Okinawa, Japan	ST	ST	ST, A	ST	ST, A	ST, A		16	*
Naze, Okinawa, Japan	ST	ST	ST, A	ST	ST, A	ST, A		6	
Ogasawara, Tokyo, Japan	ST	ST	ST, A	ST	A	ST		1	
Guam, Marianas	ST, A	ST	ST, A, B, C	ST, A, B	ST, A	ST, A	*In(2LR)B*	42	*
Wau, Papua New Guinea	ST	ST	ST, A, B, J, O, P	ST, H	ST, A	ST, A	*In(3LR)F*	23	*
Lae, Papua New Guinea	ST	ST	ST, A, B, D, J, L	ST, G	ST, A	ST, A, H, J		23	*
Port Moresby, Papua New Guinea	ST	ST	ST, A, B	ST, J	ST, A, H	ST, A, F		25	*
Ponape, Caroline	ST	ST	ST, B, C	ST, A	ST	ST, A		26	*
Noumea, New Caledonia	ST, AT	ST	ST, A	ST	ST, A	ST, A	*In(2LR)C*	10	*
Nauru, Nauru	ST	ST	ST, A, B, C	ST, A, B	ST, I	ST, B	*T(X;2)B*	32	*
Lautoka, Fiji	ST	ST	ST, A, B	ST, I	ST, A	ST, A, J		40	*
Tongatapu, Tonga	ST	ST	ST, A	ST	ST, A, G	ST, A, J		34	*
Vava'u, Tonga	ST	ST	ST, A, B	ST	ST, A	ST, A, J		38	*
Pago Pago, Samoa	ST	ST	ST, B	ST	ST, A	ST, A, J		29	*
Honolulu, Hawaii, U.S.A. 2005	ST	ST	ST, A, B	ST	ST, A	ST, A		3	
Honolulu, Hawaii, U.S.A., 1981	ST	ST	ST, A, B	ST	ST, A	ST, A		24	*
Nayarit, Mexico	ST	ST	A	ST	A	ST		1	
Thomasville, U.S.A.	ST	ST	ST, A	ST	ST	ST		1	
Marathon, U.S.A.	ST	ST	ST, A	ST	A	ST, A		1	
Ubatuba, Brazil, 2007	ST	ST	ST, A	ST, M, N, O	ST, A	ST, A		42	
Ubatuba, Brazil, 1986	ST	ST	ST, A	ST, M, N, O	ST, A	ST, A		23	*
Donde, Guinea	ST	ST	ST, A	ST	ST	ST		1	
Kade, Ghana	ST	ST	ST, A	ST, O	ST, A	ST		2	

Results and Discussion

O'Grady *et al*. (2001) suggest that salivary gland chromosome data are highly consistent with DNA sequence data and are more informative than nucleotide data when placed in a simultaneous analysis framework. Classical *Drosophila* studies have used chromosome inversions to understand phylogeny and speciation. DNA sequence information can be combined with classical data to determine phylogeny and speciation. Our results suggest many points of agreement between DNA sequence and inversion data.

Inversion polymorphism

Table 2 shows the geographical distribution of *D. ananassa*e inversions and translocations, consistent with published data (Tomimura *et al*., 1993). In natural populations, eight unique pericentric inversions and one translocation have been identified. These data confirm the high mutation rate and instability of chromosomes in nature, as described by Kikkawa (1938), a pioneer in the study of *D. ananassae*.

Three cosmopolitan inversions, namely *In(2L)A*, *In(3L)A*, and *In(3R)A*, were observed in all populations, where three or more strains of one female origin were examined. In addition, non-cosmopolitan inversions were observed in many populations. *In(2R)O* was observed in Cameroon, Africa, and Ubatuba, Brazil, South America. This indicates that West African *D. ananassae* migrated to Southwest America or *vice versa*. *In(2L)J* was found in Bogor (Indonesia), Sabah (Malaysia), and Papua New Guinea. This indicates that *In(3R)J* is a new inversion found in both Phnom Penh (Cambodia) and Bogor (Indonesia).

We cannot ignore the possibility that the genetic significance of the high inversion polymorphism found globally, where this species is found, is mainly related to a selective advantage in heterozygous adaptation. The reason for the rapid spread of identical inversions, leading to cosmopolitan inversions, may play a role in the widespread expansion of the species' habitat, making it a cosmopolitan species. Lowey and Willis (2010) reported that extensive chromosomal inversion polymorphism contributes to local adaptation and reproductive isolation.

Frequency of three cosmopolitan inversions and the latitudinal cline

Tobari (pers. comm.) found that the frequency of inversions of *D. melanogaster* varies seasonally in the Odate population of Japan, with the frequency of inversions increasing toward winter. These data suggest that genetic factors in and around the inversion region contribute to thermotolerance. In addition, latitudinal frequency clines of inversion polymorphisms in *D. melanogaster* are often observed in several countries (Mettler *et al.*, 1977; Knibb *et al.*, 1981; Knibb, 1982; Leumeunier and Aulard, 1992). Especially, *In(3R)P* shows clinal variation along latitudinal gradients on several continents (Anderson *et al*., 2005; Kennington *et al*., 2006; Rhul, *et al*., 2015). Kapun *et al*. (2016) suggested that *In(3R)P* inversion clines are maintained by spatially- and perhaps temporally-varying selection, but the underlying selective mechanisms remain poorly understood.

In this study, the frequencies of three cosmopolitan inversions of *D. ananassae*, *In(2L)A*, *In(3L)A*, and *In(3R)A*, were analyzed for all populations studied (37 populations). The cytological analyses of strains were done within 10 years after collection. The inversion frequencies were calculated as shown in Table 3. The frequency of *In(2L)A* in each population ranged from 0% to 100%, with an average of 36%. The frequency of *In(3L)A* in each population ranged from 0% to 100%, with a mean of 61%. The frequency of *In(3R)A* in each population ranged from 0% to 100%, with a mean of 25%. *In(2L)A*, a significant simple correlation (r = 0.5452, df = 35, $P < 0.05$), but no significant correlation with latitude was found for the other two inversion frequencies (r = 0.2453 for *In(3L)A* and r = 0.1046 for *In(3R)A*).

Based on chromosomal homology, polytene chromosome band sequences, and nucleotide sequences, both 3R in *D. melanogaster* and 2L in *D. ananassae* were found to be Muller's element E (Paterson and Stone, 1952; Schaeffer *et al*., 2008). Moreover, we found a latitudinal cline of *In(2L)A* in a natural population of *D. ananassae*. However, the latitudinal relationship of *In(2L)A* frequency observed in this study is not consistent with the results of Indian populations (Singh and Singh, 2007). The study on the frequency of inversions in 45 Indian populations, ranging from the south (8.08N) to the north (34.08N), revealed that the frequency of *In(2L)A* was 48.9%–97.6% and was not significantly correlated with latitude. Differences in collection period

Table 3. Frequencies of three cosmopolitan inversions, *In(2L)A*, *In(2R)A*, and *In(3L)A*, of 43 populations of *D. ananassae*.

Symbol	Population	No. of strains observed	No. of individuals	*In(2L)A* Frequency	*In(3L)* Frequency *A*	*In(3R)A* Frequency	latitude	longitute	*
1	Mbengwi	2	26	0.42	0.19	0.12	6.01N	10.00E	
2	Oku	1	4	0.00	0.00	0.00	6.15N	10.25E	
3	Mbalang-Djalirgo	1	6	0.33	0.58	0.00	7.19N	13.44E	
4	Maroua	1	16	0.59	1.00	0.00	10.36N	14.19E	
5	Yokadouma	1	6	0.00	0.00	0.00	3.31N	15.03E	
6	Kisangani	1	8	0.63	1.00	0.06	0.31N	25.11E	
7	Gisakura	1	9	0.00	0.39	0.00	2.26N	29.02E	
8	Namulonge	2	23	0.37	0.48	0.00	1.22N	32.17E	
9	Chiang Mai	19	158	0.01	0.43	0.68	18.47N	98.39E	*
10	Bangkok	14	126	0.00	0.23	0.16	13.43N	100.28E	*
11	Kuala Lumpur	5	41	0.16	0.91	0.38	3.08N	101.41E	*
12	Mahasarakam	5	99	0.14	0.10	0.16	16.11N	103.18E	*
13	Phnom Penh	44	402	0.28	0.64	0.44	11.33N	104.55E	*
14	Bogor(2001)	29	225	0.13	0.60	0.60	6.35S	106.47E	
15	Bogor(2008)	23	185	0.20	0.64	0.46	6.35S	106.47E	*
16	Jakarta	1	10	0.30	0.75	0.50	6.12S	106.50E	
17	Kota Kinabalu	8	66	0.14	0.88	0.35	5.58N	116.06E	*
19	Lombok	1	9	0.61	1.00	0.11	8.30S	116.40E	
20	Sabah Malaysia	1	3	0.00	0.00	0.00	5.25N	116.47E	
21	Manila	13	95	0.05	0.71	0.28	14.35N	120.58E	*
23	Taipei	1	12	1.00	1.00	0.00	22.02N	121.32E	
26	Iriomotejima	1	12	1.00	1.00	1.00	24.19N	123.49E	
28	Cebu	20	103	0.06	0.50	0.45	10.27N	123.53E	*
29	Ishigakijima	1	10	0.75	1.00	0.00	24.23N	124.11E	
31	Miyakojima	2	19	0.45	0.37	0.05	24.48N	125.16E	
32	Miyakojima	1	12	0.71	0.38	0.71	24.48N	125.16E	
33	Kumejima	13	111	0.63	0.86	0.30	26.20N	126.46E	*
34	Naha	55	349	0.74	0.86	0.40	26.12N	127.40E	*
35	Naze	6	56	0.54	0.84	0.25	28.23N	129.29E	*
36	Ogasawara	1	14	0.50	1.00	0.00	27.07N	142.09E	
37	Honolulu	3	21	0.17	0.26	0.21	21.18N	157.51W	
38	Nayarit	1	12	1.00	1.00	0.00	21.45N	104.5W	
39	Marathon	1	9	0.67	0.00	0.00	24.42N	81.05W	
40	Thomasville	1	11	0.36	0.73	0.09	30.52N	80.40W	
41	Ubatuba	42	446	0.44	0.62	0.29	23.26S	45.05W	*
42	Donde	1	9	0.28	0.00	0.00	12.01N	13.01W	
43	Kade	2	15	0.47	0.77	0.10	6.05N	0.50W	

may explain the discrepancy between our results. Das *et al*. (2004) found that the pattern of DNA variation in Asian populations was best explained by adaptive mutations that swept through geographically localized populations. The migration routes of *D. ananassae* from Sunderland appear to be consistent with those of humans in the region. The pattern of migration of *D. ananassa*e, based on nucleotide variation, appears to be

similar to the latitudinal direction of the reverse frequency of *In(2L)A*. Although it is unclear whether the linkage of *D. ananassae* with *In(2L)A* is due to local adaptations to temperature or migration from the center to the periphery, it is interesting that *D. melanogaste*r and *D. ananassae*, which are thought to have differentiated 10–15 million years ago, have the same chromosome elements (3R in *melanogaste*r and 2L in *ananassae*) and the same relationship between chromosome mutation frequency and latitude.

Table 4. Frequencies of heterozygote and F-statistic of each chromosome arm of *D. ananassae*.

			2L				3L				3R			
Population	No. of strains	No. of Individual	f(A)	Ob(Het)	E(Het)	F	f(A)	Ob(Het)	E(Het)	F	f(A)	Ob(Het)	E(Het)	F
Ubatuba	42	446	0.44	0.38	0.49	0.22	0.62	0.39	0.47	0.17	0.29	0.31	0.42	0.26
Bogor	23	185	0.20	0.31	0.32	0.05	0.64	0.38	0.46	0.18	0.46	0.44	0.50	0.11
Kuala Lumpur	5	41	0.16	0.32	0.27	-0.19	0.91	0.17	0.16	-0.09	0.38	0.17	0.47	0.64
Kota Kinabalu	8	66	0.14	0.17	0.25	0.32	0.88	0.12	0.21	0.43	0.35	0.33	0.45	0.27
Cebu	20	103	0.06	0.08	0.11	0.29	0.50	0.50	0.50	0.01	0.45	0.56	0.49	-0.14
Phnom Penh	44	402	0.28	0.37	0.40	0.09	0.64	0.38	0.46	0.18	0.44	0.41	0.49	0.18
Bangkok	14	126	0.00	0.00	0.00	0.00	0.23	0.37	0.35	-0.03	0.16	0.15	0.27	0.45
Manila	13	95	0.05	0.08	0.10	0.16	0.71	0.36	0.42	0.14	0.28	0.24	0.40	0.40
Mahasarakam	5	99	0.14	0.19	0.24	0.19	0.10	0.14	0.18	0.22	0.16	0.18	0.27	0.33
Chiang Mai	19	158	0.01	0.01	0.01	-0.01	0.43	0.46	0.49	0.07	0.68	0.38	0.44	0.13
Naha	55	349	0.74	0.34	0.38	0.13	0.86	0.20	0.25	0.18	0.40	0.37	0.48	0.22
Kumejima	13	111	0.63	0.50	0.47	-0.08	0.86	0.16	0.23	0.31	0.30	0.33	0.42	0.21
Naze	6	56	0.54	0.39	0.50	0.21	0.84	0.29	0.27	-0.06	0.25	0.25	0.38	0.33
Total	267	2237	0.32	0.24	0.27	0.36	0.63	0.30	0.34	-0.22	0.39	0.34	0.48	0.28
Average			0.25	0.24	0.27	0.10	0.63	0.29	0.25	0.14	0.37	0.32	0.43	0.27

f(A): frequency of inversion. Ob(Het): observed heterozygote frequency. E(Het): expected heterozygote frequency, F: F-statistics

Heterozygosity for inversions

Thirteen populations (9,10,11,12,13,15,17,21,28,33,34,35,41) were selected (Table 4), excluding populations with a small number of strains (< 5), from which strains were established from single females and immediately used, and the frequency of inversions. The 13 populations studied showed a significant correlation coefficient between the frequency of *In(2L)A* and latitude only ($r = 0.7151$, df = 11, $P < 0.001$).

Further, we calculated heterozygosity and F-statistics. The average frequency of inversion for each cosmopolitan was found to be 26%, 63%, and 35% for *In(2L)A*, *In(3L)A*, and *In(3R)A*, respectively. The values of heterozygosity for *In(2L)A*, *In(3L)A*, and *In(3R)A* were 0–0.50, 0.12–0.50, and 0.17–0.56, respectively. F-values for *In(2L)A*, *In(3L)A*, and *In(3R)A* ranged from −0.19 to 0.32, −0.09 to 0.43, and −0.14 to 0.64, respectively. The heterozygosity for the 2L, 3L, and 3R chromosome arms was high, averaging 0.26–0.63, and the average F-statistic for the inversion polymorphisms ranged from 0.11 to 0.26. Despite the variation in F-statistics among the populations studied, the structure of each population seems to be in Hardy–Weinberg equilibrium for the three cosmopolitan inversions.

Dobzhansky and Sturtevant (1938) argued that mating frequency increases inversion heterozygotes, which may be of selective value in relation to heterosis effects. In *D. ananassa*e, male recombination is a common phenomenon (Moriwaki *et al*., 1973; Goni *et al*., 2012) and is different from that in other *Drosophil*a species. In *D. ananassae*, when crossing over occurs within a paracentric inversion loop, male meiosis results in the formation of dicentric and accentuated chromosome fragments (Goni *et al*., 2012). The effect of inversion polymorphism on population fitness may differ between species without and with meiotic male crossing over, and *D. ananassae* may be a suitable model for investigating the role of inversion polymorphism in natural population structures. Although *D. melanogaster* is a cosmopolitan species with a worldwide geographical distribution, studying how population isolation and semi-isolation affect genome evolution is challenging. However, Schug *et al*. (2007, 2008) reported that populations of *D. ananassa*e appear to be semi-isolated, and understanding local geographical isolation would be valuable. Our population genetic studies using chromosomal polymorphisms and DNA sequences provide evidence that the genetic structure of this species is important (Stephan *et al*., 1998; Das *et al*., 2004; Baines *et al*., 2004).

Heterozygosity and F-statistics in each cosmopolitan inversion (2L, 3L, and 3R) in populations where more than five strains were studied showed high mean heterozygosity between 0.18 and 0.33 and constant F-statistics. These populations were found to be in Hardy–Weinberg equilibrium. In *D. ananassae*, three cosmopolitan inversions, namely *In(2L)A*, *In(3L)A*, and *In(3R)A*, are highly polymorphic and are maintained in *D. ananassae* habitats worldwide. This increases the probability of chromosomal aberrations due to male mating. Heterozygous conditions and structural heterozygosity of factors controlling male recombination are also thought to increase the frequency of male recombination, which is likely to be deleterious. However, why male recombination factors and inversion polymorphisms are maintained in natural populations is unknown. We speculate that inverted heterozygotes are highly adaptive, as shown by the fitness analyses of Tobari (1964), Kojima and Tobari (1967), and Tobari and Kojima (1968), and factors of male recombination modifiers should be linked to their inverted regions. We propose that these population structures are maintained by strong balanced selection, such as heterosis or frequency-dependent selection, as reported by Tobari and Kojima (1967).

References: Anderson, A.R., A.A. Hoffmann, S.W. Mackechinie, and P.A. and Umia 2005, Molecular Ecology 14: 851-858; Arauz, P.A., P.B. Francese, A. Latorre, L. Serra, and F. Mastres 2011, Genetica 139: 1477-1486; Baines, J.F., A. Das, S. Mousset, and W. Stephan 2004, Genetics 168: 1987-1998; Balanyá, J., J.M. Oller, R.B. Huey, G.W. Gilchrist, and L. Serra 2006, Science 313: 1773-1775; Das, A., S. Mohanty, and W. Stephan 2004, Genetics 168: 1975-1985; Dobzhansky, T., 1970, *Genetics of the Evolutionary Process*. Columbia Univ. Press, New York, USA; Dobzhansky, T., and A.H. Sturtevant 1938, Genetics 23: 28-64; Goni, B., M. Matsuda, M. Yamamoto, C. Viela, and Y.N. Tobari 2012, Genome 55: 505-511; Inoue, Y., and T.K. Watanabe 1977, A. Rep. Natn. Inst. Genet., Mishima 27: 74; Inoue, Y., and T.K. Watanabe 1979, The Japanese Journal of Genetics 54: 69-82; Kennington, W.J., L. Partridge, and A.A. Hoffmann 2006, Genetics 172: 1655-1663; Kikkawa, H., 1938, Genetica 20: 458-516; Knibb, W.R., 1982, Genetica 58: 213-221; Knibb, W.R., J.G. Oakeshott, and J.B. Gibson 1981, Genetics 98(4): 833-847; Krivshenko, J.D., 1963, Genetics 48: 1239-1258; Kojima, K.I,, and Y.N. Tobari 1969, Genetics 61: 201-209; Kojima K.I, and Y.N. Tobari 1969b, Genetics 63: 639-651; Lemeunier, F., and S. Aulard 1992, Inversion polymorphism in *Drosophila melanogaster*. In: *Drosophila Inversion Polymorphism.* (Krimbas, C.B., and J.R. Powell, eds.). CRC Press; Boca Raton: pp. 339-405; Kapun, M., D.K. Fabian, J. Goudet, and T. Flatt 2016, Mol. Evo. Biol. 33: 1317-1336; Matsuda, M., C.S. Ng, M. Doi, A. Kopp, and Y.N. Tobari 2009, Fly 3: 157-169; Mettler, L.E., R.A. Voelker, and T. Mukai 1977, Genetics 87: 169-176; O'Grady, P.M., R.H. Baker, C.M. Durando, W.J. Etges, and R. DeSalle 2001, BBC Evol. Biol. 1: 6; Patterson, J.T., and W.S. Stone 1952, *Evolution in the Genus* Drosophila. New York: The Macmillan Company; Rane, Rahul V., L. Rako, M. Martin Kapun, Siu F. Lee, and A.A. Hoffmann 2015, Molecular Ecology 24: 2423; Rako, L., A.R. Anderson, C.M. Sgro, A.J. Stocker, and A.A. Hoffmann 2006, Genetica 128: 373-384; Schaeffer, S.W., A.U. Bhutkar, B.F. McAllister, M. Matsuda, L.M. Matzkin, P.M. O'Grady, C. Rohde, V.L.S. Valente, M. Aguadé, W.W. Anderson, Edwards, A.C.L. Garcia, J. Goodman, J. Hartigan, E. Kataoka, R.T. Lapoint, E.R. Lozovsky, C.A. Machado, M.A.F. Noor, M. Papaceit, L.K. Reed, S. Richards, T.T. Rieger, S.M. Russo, H. Sato, C. Segarra, D.R. Smith, T.F. Smith, V. Strelets, Y.N. Tobari, Y. Tomimura, M. Wasserman, T. Watts, R. Wilson, K. Yoshida, T.A. Markow, W.M. Gelbart, and T.C. Kaufman 2008, Genetics 179: 1601-1655; Schug, M.D., S.G. Smith, A. Tozier-Pearce, and S.F. McEvey 2007, Genetics 175*: 1429-1440; Schug, M.D., J.F. Baines, A. Killon-Atwood, S. Mohanty, A. Das, S. Grath, S.G. Smith, S. Zargham, S.F McEvey, and W. Stephan 2008, Mol. Ecol. 17: 2706-2721; Singh, P., and B.N. Singh 2007, Genet. Res. 89: 191-199; Stephan, W., L. Xing, D.A. Kirby, and J.M. Braverman 1998, Proc. Natl. Acad. Sci. U.S.A. 95: 5649-5654; Tobari, Y.N., 1964, Evolution 18: 343-348; Tobari, Y.N., and K.I. Kojima 1967, Genetics 57: 179-188; Tomimura, Y., M. Matsuda, Y.N. Tobari, M.L. Cariou, J.L. Da Lage, W. Stephan, and C.H. Langley 1993, In: Drosophila ananassae*: Genetical and Biological Aspects*. (Tobari, Y.N., ed.), Japan Scientific Societies Press and Karger, Tokyos: 139-138.

Contributions to Drosophila Information Service are accepted throughout the year for publication in the annual issue. Deadline for the annual issue is 31 December.

Neural-Gal4 and control UAS-responding transgenes in longevity assays in *Drosophila*.

Keats, Melissa F., and Brian E. Staveley. Department of Biology, Memorial University of Newfoundland, St. John's, Newfoundland and Labrador, Canada A1C 5S7; telephone (709) 864-4317; telefax (709) 864-3018; Corresponding author: Dr. Brian E. Staveley; email address: bestave@mun.ca

Introduction

The *UAS-Gal4* system is well established as a powerful tool for controlling expression of transgenes in *Drosophila melanogaster* (Brand and Perrimon, 1993; Busson and Pret, 2007). This system makes use of the yeast *Gal4* transcription factor and its perceived inactivity in *D. melanogaster*. However, the expression of *Gal4* can affect the phenotype of *D. melanogaster*. Such is the case when *GMR-Gal4* homozygotes display a highly disorganized ommatidial array and higher levels of apoptosis compared to heterozygotes (Kramer and Staveley, 2003). It is, therefore, important to use negative controls, such as *UAS-lacZ* and examine the role that benign transgenes may play in phenotypic expression.

RNAi-mediated gene knockdown is used in the *UAS-Gal4* system to determine loss-of-function phenotypes. However, non-specific phenotypes (false positives) may result from off target affects (Kondo *et al.,* 2009; Langer *et al.,* 2010; Jonchere and Bennett, 2013). In the past our research group has evaluated *UAS-GFP-RNAi* expression in a subset of neurons in *Drosophila* to find a significant reduction in lifespan (Chavoshi-Jolfaei and Staveley, 2020). Therefore, when using *RNAi*, negative controls should be analyzed. *UAS-LUC-RNAi* is one proposed control which involves *RNAi* specified for the luciferase protein from fireflies. Here we demonstrate that it appears to be a suitable control responder transgene for longevity assays.

The identification of *Gal4* directing transgenes (or "drivers"), which have potential to increase lifespan, is ideal for enhanced longevity assays. *TH-Gal4* shows increased lifespan when driving *Pink1* overexpression, as well as *Ref(2)P* inhibition (Todd and Staveley, 2012; Hurley and Staveley, 2021). *D42-Gal4* shows increased lifespan in many instances, such as driving overexpression of *G6PD*, *dTOR*, and *hSOD1* (Parkes *et al.*, 1998; Legan *et a.l*, 2008; Mockett and Nobles, 2013). Here, we demonstrate if *OK6-Gal4*, *C380-Gal4* and *Repo-Gal4* appear to be suitable conditionally directing transgenes for enhanced longevity assays.

Methods and Materials

Drosophila melanogaster *stocks and culture*

The *Drosophila* stocks utilized here, *UAS-lacZ* (BDSC-1776); *UAS-LUC-RNAi* (BDSC-31603); *D42-Gal4* (BDSC-8816); *TH-Gal4* (BDSC-8848); *OK6-Gal4* (BDSC-64199); *Repo-Gal4* (BDSC-7415); and *C380-Gal4* (BDSC-80580) were obtained from the Bloomington Stock Center at the University of Indiana (Indiana, USA). Flies were maintained on standard cornmeal, molasses, yeast, and agar media treated with propionic acid and methylparaben to prevent fungal growth. Stocks were kept at room temperature (20 ± 2°C).

Drosophila *Crosses*

Critical class males were obtained by crossing females from *D42-Gal4*, *TH-Gal4*, *OK6-Gal4*, *Repo-Gal4* and *C380-Gal4* to either *UAS-lacZ*$^{4\text{-}1\text{-}2}$ or *UAS-LUC-RNAi* males. Both crosses and critical class males were maintained at 25°C throughout the biological assays.

Longevity Assays

Critical class males were collected and placed into standard plastic vials in cohorts of no more than 20 flies. Every two days post isolation, the number of dead flies in every vial was scored until all had perished. Fresh food was supplied every 4-6 days or after any deaths occurred. Graph Pad Prism 9.4.1 was used to

generate survival curves and conduct Log-Rank (Mantel-Cox) tests to determine statistical significance. Bonferroni correction was used when making multiple comparisons.

Table 1. Log-rank statistical analysis of longevity of flies with both *UAS-lacZ* and *UAS-LUC-RNAi* directed by several tissue specific *Gal4* lines.

Genotype	Number of Flies	Median Survival (Days)	Chi-square Value	P-value	Significance
Repo-Gal4/ UAS-lacZ	134	46	N/A	N/A	N/A
Repo-Gal4/ UAS-LUC-RNAi	296	47	0.03041	0.8616	No
D42-Gal4/ UAS-lacZ	169	54	N/A	N/A	N/A
D42-Gal4/ UAS-LUC-RNAi	189	60	72.20	<0.0001	Yes
TH-Gal4/ UAS-lacZ	139	52	N/A	N/A	N/A
TH-Gal4/ UAS-LUC-RNAi	122	62	48.64	<0.0001	Yes
OK6-Gal4/ UAS-lacZ	218	58	N/A	N/A	N/A
OK6-Gal4/ UAS-LUC-RNAi	352	56	1.769	0.1835	No
C380-Gal4/ UAS-lacZ	138	44	N/A	N/A	N/A
C380-Gal4/ UAS-LUC-RNAi	135	44	0.05181	0.8199	No

Results and Discussion

UAS-LUC-RNAi does not diminish longevity

The expression of *UAS-LUC-RNAi* under the direction of *Repo-Gal4* (glial-specific), *OK6-Gal4* (motor neuron-specific), and *C380-Gal4* (motor neuron-specific) yielded no significant difference in longevity when compared to *UAS-lacZ*. When crossed to *TH-Gal4* (dopaminergic neuron-specific) and *D42-Gal4*, expression of *UAS-LUC-RNAi* showed an increase in longevity. Therefore, this may be a suitable *RNAi* control.

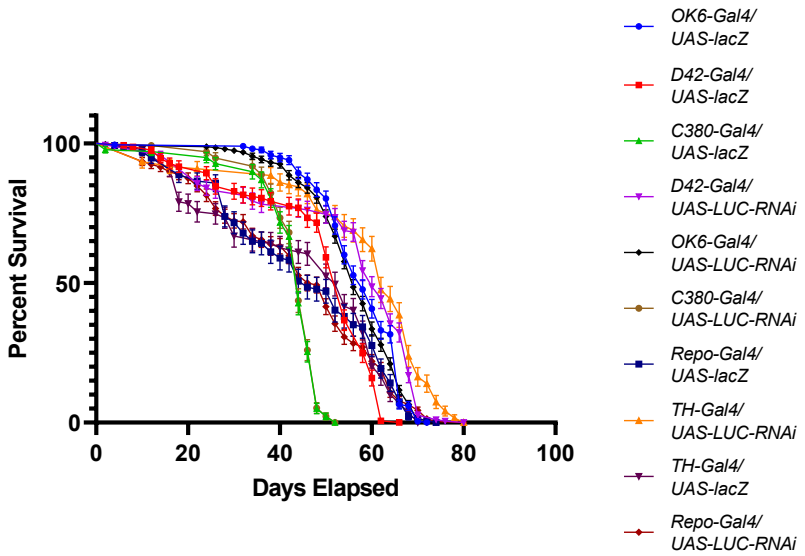

Figure 1. Longevity of critical class males when responder genes *UAS-lacZ*$^{4\text{-}1\text{-}2}$ and *UAS-LUC-RNAi* are placed under the control of several tissue-specific directing transgenes.

Repo-Gal4 does not seem to contribute to enhanced longevity

The median survival of *UAS-lacZ* crossed to *Repo-Gal4* was significantly lower (46 days) when compared to *D42-Gal4* (54 days), *TH-Gal4* (52 days), and *OK6-Gal4* (58 days). *Repo-Gal4* may not be a suitable driver for longevity assays.

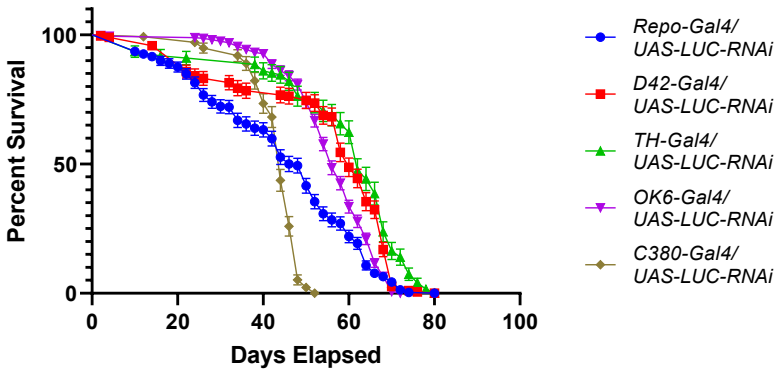

Figure 2. Longevity of critical class males at 25°C when *UAS-lacZ* is placed under the control of several drivers. *OK6-Gal4* yielded the highest median lifespan (58 days), while *C380-Gal4* showed a severely diminished median lifespan (44 days).

C380-Gal4 does not contribute to enhanced longevity

The expression of *UAS-lacZ* under the direction of *C380-Gal4* appears to sensitize flies to degeneration. When comparing *C380-Gal4* to the other motor neuron-specific drivers, *D42-Gal4* and *OK6-Gal4*, there was a statistically significant decrease in longevity (median 44 days). This result is not unlike those seen for previous studies which have used *C380-Gal4* to drive gene expression (Wilkinson *et al.*, 2021). This suggests that *C380-Gal4* not be used in longevity assays. However, there may be use for *C380-Gal4* if attempting to model severe cases of neurodegeneration.

Table 2. Log-rank statistical analysis of longevity of flies with *UAS-Gal4* expression driven by several tissue specific *Gal4* lines. Significance was determined with Bonferroni correction.

Genotype	Number of Flies	Median Survival (Days)	Chi-square Value	P-value	Significance (Bonferroni)
Repo-Gal4/ UAS-lacZ	134	46	N/A	N/A	N/A
D42-Gal4/ UAS-lacZ	169	54	2.188	0.1390	No
TH-Gal4/ UAS-lacZ	139	52	0.004968	0.9438	No
OK6-Gal4/ UAS-lacZ	218	58	23.26	0.0001	Yes
C380-Gal4/ UAS-lacZ	138	44	28.03	0.0001	Yes
D42-Gal4/ UAS-lacZ	169	54	N/A	N/A	N/A
TH-Gal4/ UAS-lacZ	139	52	2.243	0.1342	No
OK6-Gal4/ UAS-lacZ	218	58	53.32	0.0001	Yes
C380-Gal4/ UAS-lacZ	138	44	120.6	0.0001	Yes
TH-Gal4/ UAS-lacZ	139	52	N/A	N/A	N/A
OK6-Gal4/ UAS-lacZ	218	58	22.62	0.0001	Yes
C380-Gal4/ UAS-lacZ	138	44	53.67	0.0001	Yes
OK6-Gal4/ UAS-lacZ	218	58	N/A	N/A	N/A
C380-Gal4/ UAS-lacZ	138	44	269.1	0.0001	Yes

OK6-Gal4 median lifespan is similar to TH-Gal4 and D42-Gal4

When crossed to *UAS-lacZ*, the drivers *D42-Gal4*, *TH-Gal4*, and *OK6-Gal4* had similar median lifespans. There was no statistical difference between that of *D42-Gal4* and *TH-Gal4*. However, *OK6-Gal4* showed a small but statistically significant increase in lifespan compared to both *D42-Gal4* and *TH-Gal4*. Therefore, *OK6* may be a suitable driver for longevity assays.

Acknowledgments: We wish to thank the Bloomington Drosophila Stock Center (University of Indiana, Bloomington, USA) for providing *Drosophila* lines. This research was funded by the Department of

Biology of Memorial University of Newfoundland Teaching Assistantship and a Memorial University of Newfoundland School of Graduate Studies Fellowship to MFK and by the Memorial University Seed Fund and by a Natural Science and Engineering Council of Canada (NSERC) Discovery Grant to BES.

References: Brand, A.H., and N. Perrimon 1993, Development 118: 401–415; Busson, D., and A.-M. Pret 2007, Methods Mol. Biol. 397: 161–201; Chavoshi-Jolfaei, M.S., and B.E. Staveley 2020, Dros. Inf. Serv. 103: 68-73; Hurley, E.P., and B.E. Staveley 2021, BMC Res. Notes 14: 53; Jonchere, V., and D. Bennett 2013, PLoS ONE, 8,e70489; Kondo, S., M. Booker, and N. Perrimon 2009, Genetics 183: 1165–1173; Kramer, J.M., and B.E. Staveley 2003, Genet. Molecular Res. 2: 43–47; Langer, C.C., R.K. Ejsmont, C. Schönbauer, F. Schnorrer, and P. Tomancak 2010, PLoS ONE, 5, e8928; Legan, S.K., I. Rebrin, R.J. Mockett, S.N. Radyuk, V.I. Klichko, R.S. Sohal, and W.C. Orr 2008, J. Biol. Chem. 283: 32492–32499; Mockett, R.J., and A.C. Nobles 2013, J. Gerontol. A Biol. Sci. Med. Sci. 68: 1157–1169; Parkes, T.L., A.J. Elia, D. Dickinson, A.J. Hilliker, J.P. Phillips, and G.L. Boulianne 1998, Nat. Genet. 19: 171–174; Todd, A.M., and B.E. Staveley 2012, Genet. Molecular Res. 11: 1497–1502; Wilkinson, E.C., E.L. Starke, and S.A. Barbee 2021, Front. Genet. 12: 762012.

Free flight odor tracking to the *cis*-Vaccenyl acetate pheromone in *Drosophila melanogaster* males.

Houot, Benjamin[1,2], Claude Everaerts[1], and Jean-François Ferveur[1]*. [1]Centre des Sciences du Goût et de l'Alimentation, UMR6265 CNRS, UMR1324 INRA, Université de Bourgogne Franche-Comté, 6, Bd Gabriel, 21000 Dijon, France; [2]Present address: Institut Gustave Roussy, 114 rue Edouard-Vaillant 94805 Villejuif Cedex France; *Correspondence to jean-francois.ferveur@u-bourgogne.fr.

Introduction

cis-Vaccenyl acetate (*c*VA) is a pheromone involved in the induction of several behaviors both at a long distance (aggregation) and at a close distance (courtship and aggressive male-male behaviors). The studies reporting the attractive effect of *c*VA at a long distance either used *c*VA directly extracted from male glands (ejaculatory bulbs where *c*VA is exclusively produced; Bartelt *et al.,* 1985a; Guiraudie-Capraz *et al.,* 2007), or natural *c*VA combined with food-derived volatile molecules (Das *et al.,* 2017; Schaner *et al.,* 1987). However, other compound(s) secreted by male reproductive tissues could synergistically act with *c*VA, as in *D. virilis* (Bartelt *et al.,* 1985b). In another experiment, pure synthetic *c*VA was tested in combination with food processed by flies, in a wind tunnel (Cazalé-Débat *et al.,* 2019). However, in these studies, food- and cuticular hydrocarbon-derived compounds resulting of oxidation and/or of fly microbiota activity could partly or totally alter *c*VA effect. Here, we tested the effect of synthetic *c*VA either alone (dissolved in a solvent) or combined with plain food (not degraded by fly microbiota) in a wind tunnel. We also controlled the effect of three solvents currently used to dissolve cVA.

Material and Methods

Male flies were screened 2 to 6 hours after emergence under light CO_2 anaesthesia and kept at 24 ± 0.5°C isolated until the test. Experiments were conducted with starving flies to stimulate upwind flight attraction (Lebreton *et al.,* 2012). Basically, the night before the test, flies were individually kept in a glass vial only containing a piece of cotton wool moistened with 90 µL of distilled water at 25°C. Four days old male flies were individually tested in the wind tunnel (wind speed = 0.4 m/s). Each fly was introduced with a mouth aspirator into an acclimation chamber (consisting of an acrylic tube; ∅ = 5 mm) separated by a gate from the inside of the wind tunnel. After 3 min acclimation, focal flies were allowed to reach the part of the tube opening inside the wind tunnel. We measured five free flight parameters: (*i, ii*) the frequencies to take

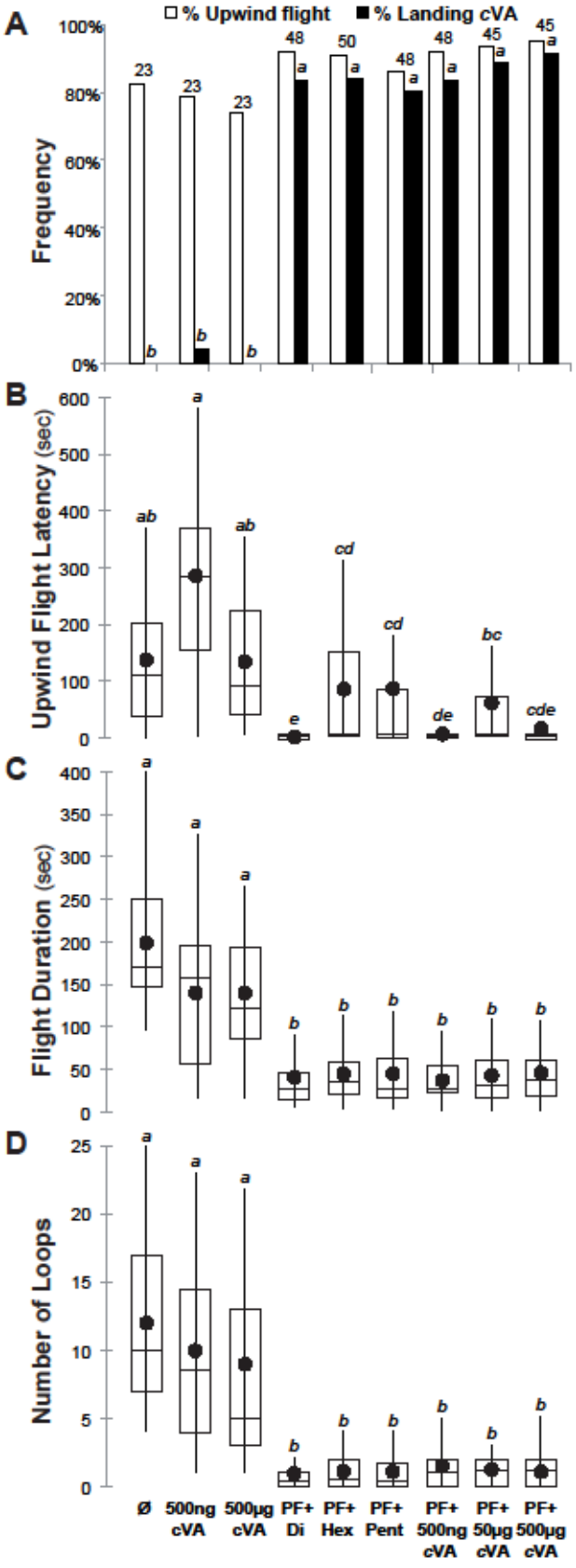

Figure 1. Free flight and landing frequencies in single male flies tested in a wind tunnel to various chemical sources including *cis*-Vaccenyl acetate (*c*VA). (**A**) Histograms represent the frequency of flies taking upwind flight (empty bars; calculated from the total number of flies tested: see top of each histogram bar), and landing on each chemical source (filled bars). In these flies, we measured (**B**) upwind flight latency, (**C**) flight duration (both in seconds), and (**D**) number of loops inside the tunnel before landing. The chemical sources tested are indicated below the graphs (from left to right): empty control (ø), 500 ng or 500 µg cVA dissolved in dichloromethane (Di) and deposited on a filter paper, plain food (PF) with Di, Hexane (Hex) or Pentane (Pent) solvents, and 500 ng, 50 µg or 500 µg cVA dissolved in Di and deposited on PF. Differences between upwind flight frequencies and between landing frequencies (shown in **A**) were tested with the Wilks G^2 likelihood ratio test completed with a computation of significance by cell (Fisher's exact test): significant differences are indicated by different letters at $\alpha < 0.05$. « Upwind flight latency », « flight duration » and « number of loops » data are shown as box-whisker plots. Each bar of the box-plot represents the 50% median data (or second and third quartile; the median value is shown as a small horizontal bar; the mean as a dot), while the two thin vertical bars ("whiskers") down and up the box represent the 25% lower and 25% higher data distribution (fourth and first quartiles), respectively. These data (**C, D, E**) were assayed with a Kruskall-Wallis test. For each parameter, significant differences are indicated by different letters at level $p < 0.05$.

upwind flight and to land on the platform with the chemical source tested, (*iii*) the latency to take upwind flight, (*iv*) the flight duration (= difference between the latency to land and the latency to take upwind flight), and (*v*) the number of loops performed by each fly before landing on the chemical source. Each chemical source to be tested was deposited on a small Whatman filter paper patch (length = 3.5 cm; width = 1.5 cm. The effect of solvents, and of cVA dissolved in solvent added in food or not, was tested after solvent complete

evaporation. We only show data obtained with male flies since female data were incomplete. Moreover, flies which did not take upwind flight before 10 min were discarded.

Results and Discussion

In all the tests (Figure1A), males showed similarly high frequencies to take upwind flight (75-95%). However, tests involving plain food either mixed with *c*VA or with one of the three solvents induced similar high landing frequency (80-90%). Differently, males very rarely landed on the platform with nothing (ø = blank control) or only *c*VA (500 ng/500 µg).

The comparison of upwind flight latency between the nine chemical sources also revealed marked differences (Figure1B). Plain laboratory food either mixed with *c*VA or with a solvent generally induced a faster response than *c*VA alone or the blank control. Note that the dichloromethane solvent added to food induced a very fast – quasi-instantaneous – upwind flight response. The comparison of flight duration also showed a clear separation between experiments with laboratory food (short flight duration) and those involving *c*VA alone or the blank control (longer flight duration; Figure1C). The number of loops showed a similar divergence between flies of these two experimental groups (with/out food; Figure 1D). This difference may explain the variation of flight duration.

In conclusion, our experiment reveals that *c*VA alone (dissolved in a solvent) had no effect on *D. melanogaster* male free flight behavior. Differently, laboratory food induced a clear attraction in male flies, and their response was not altered by the addition of increasing doses of *c*VA.

References: Bartelt, R.J., A.M. Schaner, and L.L. Jackson 1985a, J. Chem. Ecol. 11: 1747-1756; Bartelt, R.J., L.L. Jackson, and A.M. Schaner 1985b, J. Chem. Ecol. 11: 1197-1208; Cazalé-Débat, L., B. Houot, J.P. Farine, C. Everaerts, and J.F. Ferveur 2019, Sci. Rep. 9: 14917; Das, S., F. Trona, M.A. Khallaf, E. Schuh, M. Knaden, B.S. Hansson, and S. Sachse 2017, Proc. Natl. Acad. Sci. U.S.A. 114: E9962–E9971; Guiraudie-Capraz, G., D.B. Pho, and J.M. Jallon 2007, Integrative Zoology 2: 89-99; Lebreton, S., P.G. Becher, B.S. Hansson, and P. Witzgall 2012, J. Insect Physiol 58: 125-129; Schaner, A.M., R.J. Bartelt, and L.L. Jackson 1987, J. Chem. Ecol. 13: 1777-1786.

A search for *Tofu*, the mutation compensating for the loss of functional *BEAF*.

McKowen, J. Keller[1], and C.M. Hart[2]. Upper Iowa University[1] Department of Biology and Chemistry, 605 Washington St. Fayette, Iowa. Louisiana State University[2] Department of Biology A310 Life Science Annex Baton Rouge, Louisiana.

Abstract

Compensatory mutations offer clues to deciphering the role of a particular protein. Here we investigate an unknown compensatory, present in the *BEAF*^{NP6377} fly line, which we call *Tofu*. This mutation, when isolated, can rescue the ovary defect phenotype seen by earlier knockout experiments of *BEAF*. We employ both classical genetics and genomic sequencing to attempt to identify the mutation. We find evidence that points to mutations in a polycomb repressive element controlling the Ribbon gene, which may lead to aberrant overexpression. Ribbon has a similar DNA binding motif and overlaps with many BEAF binding sites. These mutations which may cause ectopic expression of the Ribbon gene are strong candidates for *Tofu*.

Introduction

BEAF is an insulator binding protein of *Drosophila melanogaster* that mainly binds the promoter region of housekeeping genes (Cuvier *et al.,* 1998; Jiang *et al.,* 2009; Zhao *et al.,* 1995). The *BEAF* gene is located on the second chromosome. It is composed of three exons and expressed as two isoforms: 32A and 32B. Each isoform has a unique DNA binding region coded by exons 1 and 2, respectively. The third exon

contains interacting domains and is shared by both isoforms (Hart *et al.,* 1997). Previously, our lab generated and characterized a nonfunctional allele of *BEAF* by (a) eliminating the ATG start codon of both the 32A and 32B specific exons and (b) introducing two tandem stop codons into the shared exon, $BEAF^{AB\text{-}KO}$ (*ABKO*). Flies homozygous for the *ABKO* allele are sickly, display a mild rough eye phenotype, and have defects in oogenesis. Ovaries of *ABKO* flies have malformed egg chambers, displaying variable phenotypes that are most apparent at stage eight of oogenesis. The outcome of these defects is that very few mature oocytes are produced. This phenotype leads to a sharp loss in the fecundity of this fly line (Roy *et al.,* 2007a).

A separate mutant allele, $BEAF^{NP6377}$ (*NP6377*), was generated by inserting a Gal4 enhancer trap element containing a mini-white marker gene, *P(GawB)*, into the first shared exon of the 32A and 32B isoforms (Hayashi *et al.,* 2002). This *NP6377* line was used in a study that attributed the striking phenotypes of neoplastic growth and recessive larval lethality to the loss of BEAF, which was not observed in our mutant lines (Gurudatta *et al.,* 2012). Skeptical of these findings, we obtained the *NP6377* line to test for second site mutations. We attempted to rescue the phenotypes using a trans-gene of *BEAF*. If the phenotypes are caused by non-functional BEAF, a *BEAF* trans-gene should rescue back to wild type. *ABKO* allele phenotypes were rescued by a trans-gene, but *NP6377* was still recessive larval lethal. The lines were crossed in a complementation test. Since they were independently generated second site mutations they would be heterozygous in the progeny. The test showed a rescue of the recessive lethal and neoplastic growth phenotypes, suggesting they were not a consequence of the loss of BEAF. *NP6377/ABKO* flies were viable. The defect in fertility caused by the lack of BEAF was apparently suppressed by a dominant mutation. *ABKO/ABKO* (*Tofu KO*) and *NP6377/NP6377* (*Tofu NP)* lines were created through meiotic recombination of the *ABKO* and *NP6377* lines. The recombinant lines lacked functional BEAF and the recessive lethal mutations, but they retained the dominant enhancer of fertility mutation (Hart, 2014). In an attempt to locate the mutation we call *Tofu,* we employed two methods: high-throughput genomic DNA sequencing and classical genetic mapping via meiotic recombination.

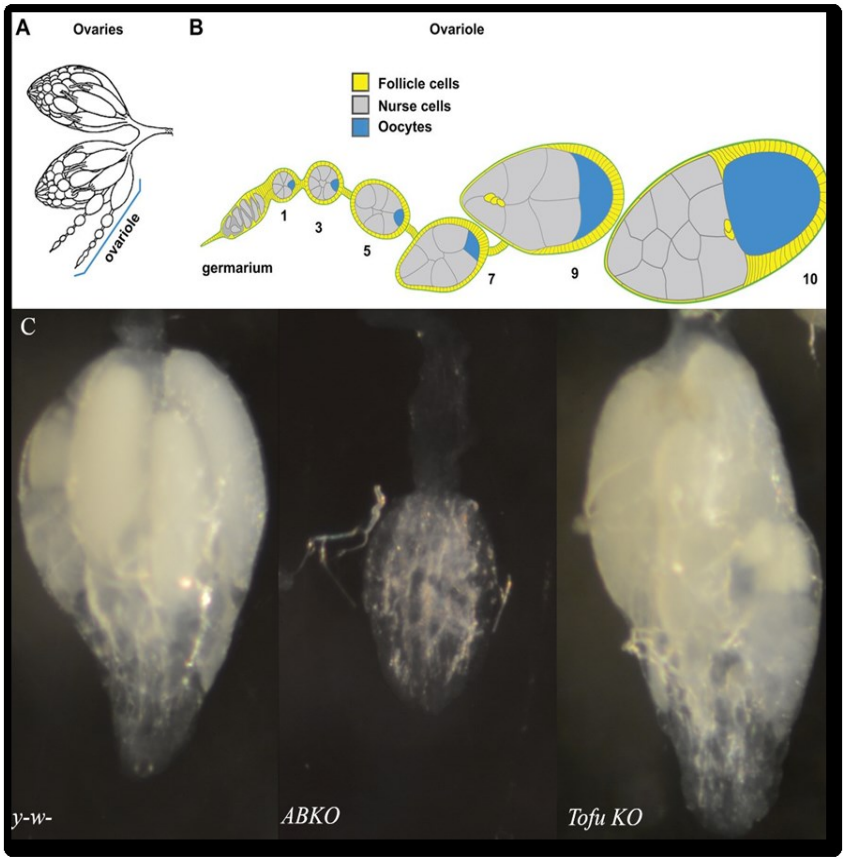

Figure 1. A: Line drawing of typical fly ovary morphology. Ovaries are composed of several ovarioles which produce oocytes. B: Oocyte development proceeds from the stem cells in the germarium as egg chambers which can be classified as stages by phenotype. C: Ovary phenotypes of y-w-, ABKO, and Tofu KO flies. Tofu KO ovaries have mature eggs, but are atypical. (A&B reproduced with permission from Andersen and Horne-Badovinac, 2016).

Materials and Methods

Fly stocks

Flies were maintained on standard cornmeal, yeast, and sugar medium with Tegosept. *BEAF^{NP6377}/CyO GFP* fly stocks were kindly provided by Victor Corces. *BEAF$^{AB\text{-}KO}$/G30* fly stocks were previously generated by our lab (Roy *et al.,* 2007b). *BEAF$^{Tofu\ NP}$* and *BEAF$^{Tofu\ KO}$* were created by meiotic recombination of *BEAF$^{AB\text{-}KO}$* and *BEAF^{NP6377}* (Hart, 2014). Baylor P mapping kit lines, *Actin 5C-Gal4*, *UAS-dpp*, and balancer chromosome lines were obtained from the Bloomington Stock Center.

Fly genotyping

To detect the *ABKO* allele, we designed a genotyping primer set consisting of three primers. The 3' BEAF-stop+89-3 primer was common to each set. The BEAF-mut-5 primer has 3' homology with the introduced stop codon of the *ABKO* allele. The BEAF-wt-Bam-5 has 3' homology to the WT *BEAF* allele. Each primer set was used to genotype flies. Genotyping was done using PHIRE tissue direct master mix.
BEAF-wt-Bam-5: GACATCATATACAGCGAGGATCC
BEAF-mut-Bam-5: AAGGACATCATATACAGCGAGTAATG
BEAF-stop+89-3: TTACGACACGCTGATTTGCC

DNA preparation for sequencing

50 third instar wandering larvae from *y-w-, ABKO/CyO-GFP, NP6677/CyO-GFP, Tofu KO,* and *Tofu NP* lines were harvested. Larvae homozygous for *BEAF* knockout alleles were screened by lack of GFP expression from the *ABKO/CyO-GFP,* and *NP6677/CyO-GFP* lines. Larvae were homogenized in 500 µL of Buffer A (10 mM Tris-Cl (pH 7.5), 60 mM NaCl, 10 mM EDTA, 150 µM spermine, 150µM spermidine, 200 µg/mL Proteinase K). Then 500 µL of Buffer B (200 mM Tris-Cl (pH 7.5), 30 mM EDTA, 2% SDS, 200 µg/mL Proteinase K) was added, and the samples were incubated for one hour at 37°C. Samples were then purified by phenol extraction, followed by phenol-chloroform-isoamyl alcohol (25:24:1) extraction, and then chloroform extraction. Samples were finally cleaned by ethanol precipitation and dissolved in 10 mM Tris.

Illumina sequencing

Genomic DNA was submitted to the Roy J. Carver Biotechnology Center at the University of Illinois at Urbana. Libraries were prepared for each sample. Paired end sequencing was done using an Illumina HiSeq2500 instrument.

Data analysis

Raw reads were obtained as paired fastq files. Read quality was analyzed using FASTQC (Andrews, 2010). Reads were aligned to the dmel r6.09 genome using bowtie2. Samtools was used to assess alignment quality and compress sam alignments into bam format. Variant calling was done using the GATK toolkit (Auwera *et al.,* 2013; DePristo *et al.,* 2011; McKenna *et al.,* 2010). Variant call files (VCF) were compared using bedtools (Quinlan, 2014). Protein coding changes were called with SnpEff (Cingolani *et al.,* 2012). SNP density was visualized as bigwig files using 2000bp windows. Data for recombination rates in 2R was kindly provided by Josep Comeron and converted to bigwig for visualization. File conversion was done using unix commands, kent utilities (Kent *et al.,* 2010), bedTools, and deepTools (Ramírez *et al.,* 2016). Data were displayed using IGV (Robinson *et al.,* 2011).

Results

Identification of Tofu chromosome

We performed a segregation analysis to identify the chromosome that contains *Tofu.* This is done by crossing the line carrying the mutation with balancer chromosomes and tracking the phenotypes of the mutant allele along with marker alleles of the balancers. A balancer chromosome has undergone inversions to such an extent that it will not homologously pair with a typical chromosome. They typically contain dominant allele markers and recessive lethal alleles. *CyO* is a balancer of chromosome 2 and contains a dominant marker

mutation that gives flies a curly wing phenotype. *TM3* is a balancer of chromosome 3 and contains a dominant marker mutation that gives flies a stubby bristle phenotype. Male flies (XY) can be used to track mutations on the X chromosome. We performed a series of segregation crosses to determine the chromosome on which *Tofu* resides.

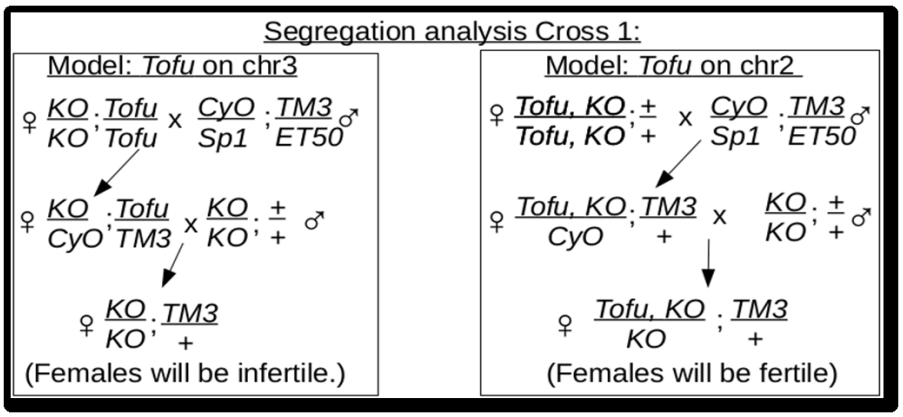

Figure 2. Diagram of a segregation cross for chromosomes 2 and 3. An identical mating strategy is divided into models of expected results.

In the first cross (Figure 2), we mated *Tofu KO* flies with a double balancer line *CyO/Sp1;TM3/ET50*. Virgin female progeny from this cross were mated to homozygous *ABKO* males. Females from this cross with the *TM3* chromosome were isolated with *y-w-* males and scored for fertility. If *Tofu* is on chromosome 3, it would become segregated from TM3 and the flies would be infertile. If it is on chromosome 2, the files would be fertile. If it is on chromosome X or 4, fertility would be around 50%. We assayed 200 flies from the cross and found a fertility rate of 53%. This indicates *Tofu* is not on chromosome 3, but it does not strongly support association with chromosome 2.

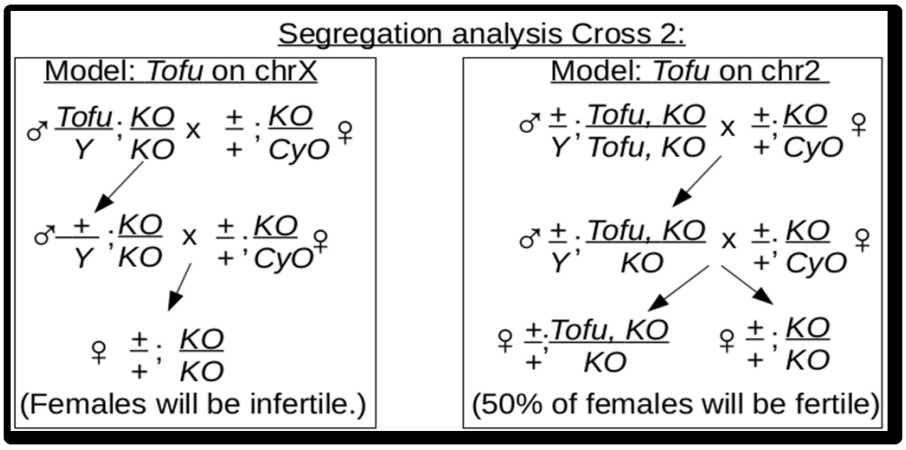

Figure 3. Diagram of a segregation cross for chromosomes X and 2. An identical mating strategy is divided into models of expected results.

In a second cross (Figure 3), we mated males of the *Tofu KO* line to *ABKO/CyO* virgin females. The chromosome X will be segregated from male progeny of this cross because male flies receive the maternal X chromosome. Male progeny from this cross were again mated with *ABKO/CyO* virgin females. If *Tofu* is on chromosome X, it would have been segregated, and the female progeny would be infertile. If it is on chromosome 2, 50% of female progeny would be fertile. We assayed 200 female progeny from the second cross and found a fertility rate of 52%. This indicates *Tofu* is not on chromosome X and suggests it is associated with chromosome 2.

Genomic sequencing

To find the *Tofu* mutation, we used genomic sequencing to compare mutations among fly lines. We collected genomic DNA from five lines: *y-w-, ABKO*, *NP6377*, and the two lines generated from recombination: *Tofu NP* and *Tofu KO*. *NP6377, Tofu NP,* and *Tofu KO* have the *Tofu* mutation, while *y-w-* and

ABKO do not. We planned to identify variants from the reference genome for each line and cross compare variants according to the *Tofu* phenotype in order to find the causal mutation.

We sequenced the genomes using Illumina to generate paired end reads of about 150bp at a genome coverage of over 40 reads per base. In this process, the DNA is fragmented into short segments around 200-800bp in length. Forward and reverse adapter sequences are ligated to the fragments, and the reverse adapter has a sequence attached to the flow cell. The fragment is sequenced from the forward primer, and each base is detected and recorded as it is synthesized. Then, the process is repeated on the opposite strand with the reverse primer. This results in high-confidence base calling, which is needed for variant detection (Bentley *et al.,* 2008). After quality checking and adapter trimming, we aligned the reads to the dm6 genome release for *D. melanogaster* using bowtie2. The alignment process matches the short reads to a pre-computed reference genome. Reads belonging to a pair are coordinated. Paired read sequencing ensures high accuracy, and a non-mapping sequence between read pairs can indicate an insertion mutation relative to the reference sequence (Langmead *et al.,* 2009; Li *et al.,* 2009).

After alignment, we called variants by comparing each experimental sequence to the reference genome. To do this, we used a suite of programs in the genome analysis toolkit GATK. Using GATK, we generated variant call files (VCFs) which detail the location and variation for every diversion found from the reference. Changes to a single base are single nucleotide polymorphisms (SNP). Extra bases (insertions) and missing bases (deletions) are lumped together as INDELs. For simplicity of discussion, INDELs are included with SNP variants and together are referred to as SNPs, though they differ biologically. Each line examined had over 700,000 SNPs from the reference genome. After cross comparing, we found 62,045 SNPs that fit the pattern for *Tofu* among the lines sequenced. Of these, 1,202 were localized to chromosome 2, on which we determined the mutation must reside by the use of balancer chromosomes. The number of SNPs that fit the *Tofu* pattern on chromosome 2 was small compared to other chromosomes. We reasoned this was due to artificial and natural selection of the *Tofu* mutation on that chromosome.

We used SnpEff to predict the effect of the SNPs on protein synthesis and found 587 of the SNPs on chromosome 2 would cause miss-sense or frame-shift mutations. This number was still far too high to test each mutation in transgenic flies. However, we could select candidates from this list to test based on gene ontology.

Mapping by meiotic recombination

To narrow down a region that contains *Tofu* and thus limit our candidate SNPs, we tried a classic fly genetics technique: the meiotic mapping or genetic linkage assay. The assay takes advantage of homologous recombination of the chromosomes during meiosis. This assay is improved by the fact that meiotic homologous recombination is prevented in male flies, occurring only during oogenesis. Thus, we can limit any crossing over event to a single female fly. During recombination, matching regions in the chromosome are randomly exchanged. The closer together genes are located along the chromosome, the more likely they are to remain together after the exchange takes place. By tracking phenotypes of these genes in the resulting generation, one can calculate a recombination frequency between the genes. If the recombination frequency is less than 50%, the genes are close enough together to be considered linked. Smaller recombination frequencies indicate closer distance (Bridges, 1935; Morgan, 1911; Sturtevant, 1913).

Calculating recombination rates depends on tracking an observable phenotype. *Tofu* is a dominant mutation that restores fertility in the absence of functional BEAF. The *ABKO* and *Tofu KO* lines have a non-functional allele of the *white* gene, giving them white eyes (*w*-). For mapping, we used fly lines from the Baylor P mapping kit. These are *w*- lines with a *white* trans-gene *P[w+]* inserted into the 2nd chromosome at a known cytological location (Zhai *et al.,* 2003). To track the *Tofu* phenotype, we first had to replace the wild type *BEAF* allele of the *P[w+]* lines with *ABKO* so that the *P[w+]* lines would have nonfunctional BEAF. To produce the *P[w+] KO* lines (red eyes), homozygous *ABKO* males were mated to homozygous *P[w+]* virgin female flies. All progeny from the cross were heterozygotes, and meiotic recombination of the *P[w+]*and *ABKO* alleles may occur in the female's oocytes. Red eyed virgin females were selected from this cross and mated with a balancer of the second chromosome line *CyO/Sp1*. In parallel crosses, a single virgin *P[w+]/ABKO* female and two *CyO/Sp1* males were mated. Red eyed females from each cross were isolated in the pupal stage and allowed to eclose. Red eyed females with curly wings were mated to their siblings with

the same phenotype. Once larvae were apparent in the vial, a male sibling was genotyped for the *ABKO* allele using PCR and restriction analysis as described in Roy *et al*. (2007). Once recombination was confirmed, the *P[w+], KO/CyO* populations were kept as a stable line and named according to their cytological location (*e.g*., 27E6).

P[w+], KO lines were mated with *Tofu KO* (white eyes). From this cross, virgin female *P[w+], KO / Tofu KO* flies (red eyes) were mated with *ABKO/ABKO* males (white eyes). If recombination between the alleles did not occur, the resulting female progeny would be *P[w+], KO/ABKO* (red eyes, infertile), and *Tofu KO/ABKO* (white eyes, fertile). A recombination frequency less than 50%, would link the locus of the *white* trans-gene from the mapping lines to *Tofu*.

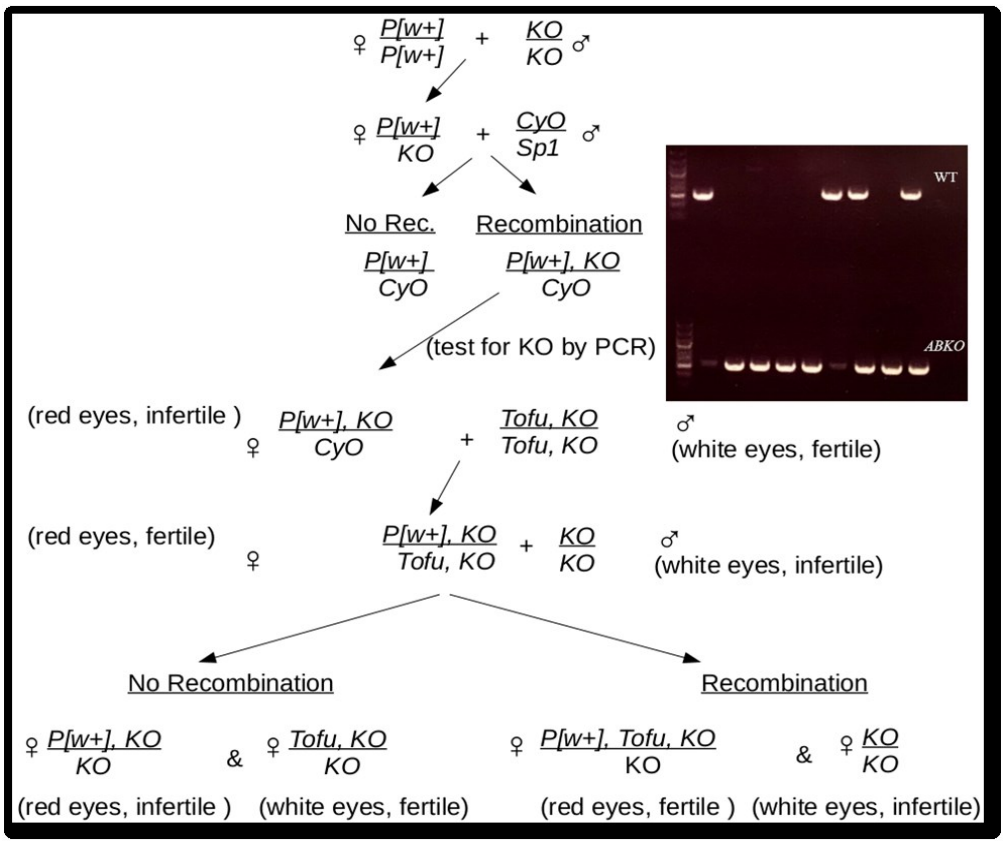

Figure 4. Diagram of recombinant mapping strategy. Flies were segregated based on eye color and individual females were scored for fertility. Insert shows an example PCR genotype result.

The phenotype of *Tofu* is restored female fertility in the absence of functional BEAF. *Tofu* is a dominant mutation, so it can be scored in the F2 progeny where it will be absent or heterozygous. To observe the phenotype of enhanced fertility, we crossed F1 flies with ABKO, which lack a functional copy of BEAF, and then scored the ability of female F2 progeny to lay eggs. We began by selecting red and white eyed female F2 progeny and isolating them in a single vile with a *y-w-* male. After one week, the vials were scored for fertility on the presence or absence of larvae. The intensity of labor and resources required for scoring individual flies this way limited the numbers we could feasibly score, which we held to 200 per cross (100 with white eyes, 100 with red).

If *Tofu* is genetically linked to a *P[w+]* element, then the rate at which the two alleles combine would be less than a random chance of 50%. This would result in (a) less fertile, red eyed flies and (b) more fertile, white eyed flies in the scoring generation. If we look at only the red eyed flies, the data from these crosses implicates cytological regions 27E6, 30C1, 35B1, 35D2, 36E3, and 47A11 as possibly linked regions. These results, however, were not confirmed by a reciprocal white eyed infertile/fertile ratio but were instead quite similar to red. We reasoned that the data from this experiment were unreliable. This may be due to genetic interaction in our flies that we are unaware of, which could decrease the general health and fertility of the flies. Another possibility is that single pair mating results in unhealthy conditions in the fly vials, increasing mortality and decreasing fertility. Scoring fertility is tricky because it can be affected by environmental conditions as well as genetics. Fertility rates are easily underestimated. Single female crosses are especially susceptible to environmental conditions, because the low number of larvae in the media makes it more

susceptible to problems like bacterial or fungal growth.

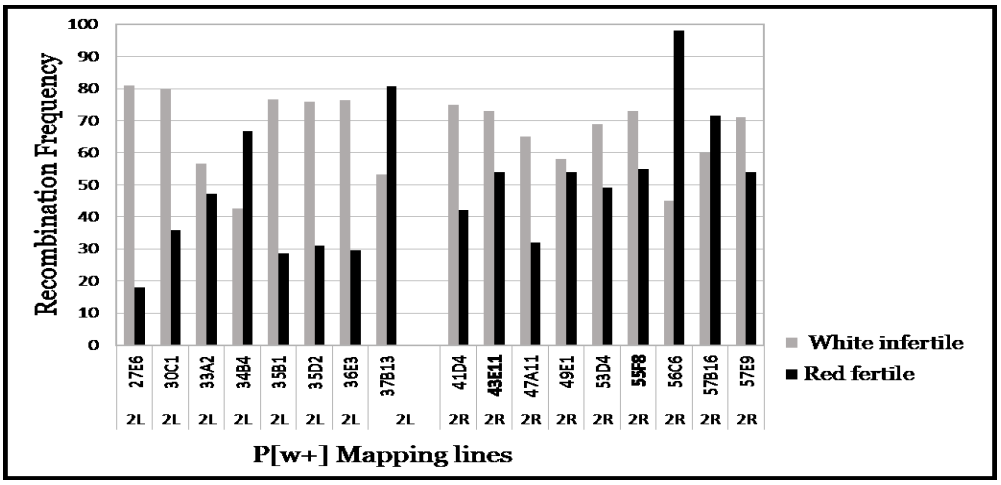

Figure 5. Results of recombinant mapping of Tofu and the P[w+] lines.

We made an early effort to map the left arm of chromosome 2 (2L), because *Tofu* seemed to separate easily from *BEAF* via recombination. Since the *BEAF* gene is in the middle of 2R, we reasoned *Tofu* was likely be on the other arm. However, our linkage assay suggested that 'far apart' can be closer together than we assumed. A recessive marker mutation speck (sp) which is found in the 60B12-60C1 region on 2R is relatively close to *BEAF* at 51C2. This mutation is present in our *ABKO* and *Tofu KO* lines, but not in the NP lines. After crossing *Tofu NP* to a line containing *sp* we found the alleles combined easily. In a subsequent cross shown in Figure 6, we were able to separate the alleles at similar rate of 48%. These observations suggested that regions on 2R could contain *Tofu*.

Our results did not support any linked regions, so, we attempted to determine the recombination rate of the two *P[w+], KO* lines nearest to *BEAF*, 49E1 and 53A4. In this cross, we measured the rate at which the *P[w+]* marker would separate from *BEAFABKO*. We first mated the *P[w+], KO* lines to *y-w-* flies. The F1 females from this cross were mated to a balancer line. F2 progeny were genotyped for the WT and *ABKO* alleles of *BEAF* using PCR. Both regions demonstrated linkage to *BEAF* with the closer region, 49E1, separating from *BEAF* at a rate of 7.6% and 53A4 separating at a rate of 11.3%. The results confirmed our ability to identify linked regions, confirming the failure of our fertility assay resulted from problems accurately scoring fertility.

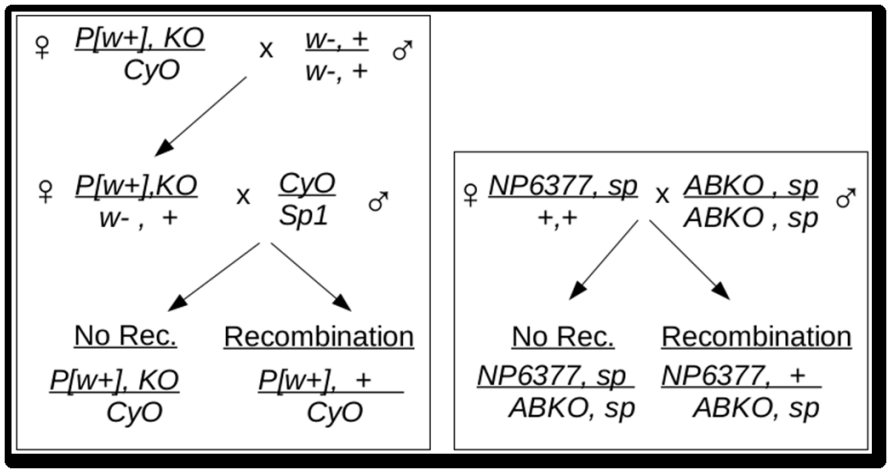

Figure 6. Diagram of cross strategies for the separation of alleles from BEAF. Left: Separation of P[w+] transgene. Recombination was scored by PCR genotyping of the ABKO allele. Right: Separation of sp allele from the NP6377 allele. Flies were scored on presence of sp phenotype.

Reanalysis of SNPs

Tofu NP and Tofu KO were generated by meiotic recombination between NP6377 and ABKO. Tofu was transferred between these fly lines, so nearby variants should be linked to Tofu. According to this line of reasoning, the Tofu mutation should lie in the middle of a variant dense region, so we plotted the Tofu candidate variants on the integrated genome browser (IGV). While there are several pockets of variant dense

regions, one region on 2R is enriched with variants. It contains (a) 954 of the 1203 candidate SNPs on the second chromosome and (b) 256 of the 587 SNPs that changed protein coding sequence. I refer to this region as the "SNP island" (Figure 7).

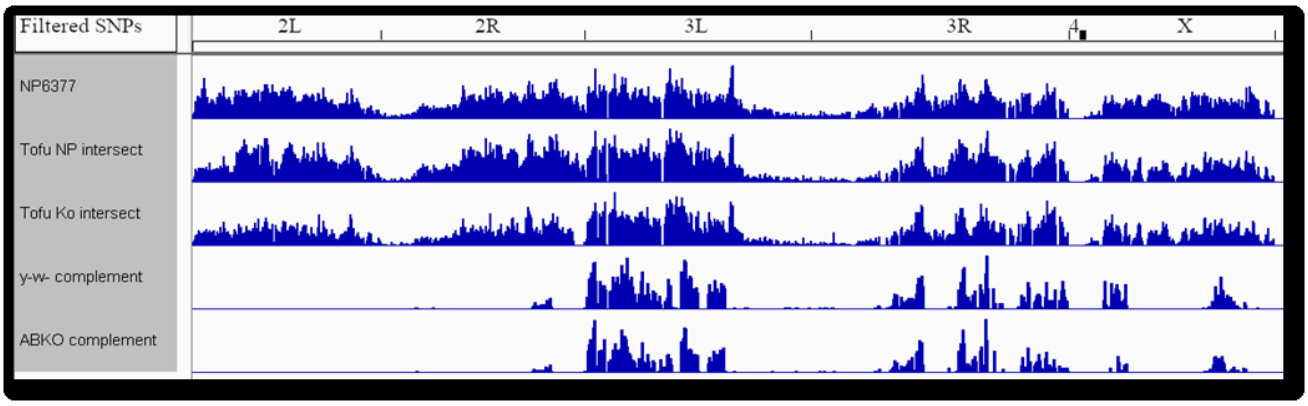

Figure 7. SNP density visualization. The SNPs are filtered from top down, the top row represents an unfiltered VCF and the bottom row are candidate SNPs for Tofu.

The SNP island corresponds to cytological regions 55F8-57C3. The original p-element fly lines we used were outside of this region, so we obtained *P[w+]* insertion lines at regions within the SNP island 56C6 and 57B16 (Figure 5). The results were confounding, because they suggest recombination may be encouraged between these regions, rather than suppressed. It is possible the *Tofu* mutation is being propagated by mismatch repair pathways, resulting in gene conversion (Borts *et al.,* 2000). The process of mismatch repair uses homologous recombination, and mismatch repair proteins can prevent recombination from occurring if the DNA is not sufficiently complementary (Do and LaRocque, 2015). Active transcription can promote recombination (Grimm *et al.,* 1991). Due to the influence of transcription and homology, recombination loci are not random along the genome. Instead, they initiate at specific sites called "hotspots" and are inhibited at "coldspots" (Boulton *et al.,* 1997). An effort was made to assess recombination rates along the *Drosophila* genome, and the data are illustrated in Figure 8 (Comeron *et al.,* 2012). If the *Tofu* mutation strongly activates transcription, recombination of this region should also increase.

The original focus of the SNP analysis was to identify gain-of-function protein coding mutations that rescue the loss of functional *BEAF*. Protein coding mutations, however, usually result in reduced function of the protein, while a regulatory mutation is more likely to increase function. Unfortunately, regulatory mutations are often difficult to predict because they do not alter the gene coding sequence. The limited knowledge of transcription factor binding specificity makes it difficult to predict if an SNP will alter a factor's binding affinity at that site. Additionally, enhancer-promoter specificity is not well characterized for most genes, making it difficult to predict which genes are affected by a given enhancer. Regulatory regions can act from great distances to alter the expression of target genes, but because this is not well characterized for most genes, only mutations in nearby (cis) regulatory regions are feasible for analysis at this time. A mutation that disrupts the function of a silencer would be the most likely to cause a gain of function in which an intact protein gains the ability to function in an atypical context. Therefore, we searched for silencer elements that contain an SNP as regulatory candidates. A previous study of polycomb response elements (PREs) predicted 537 PREs based on chromatin analysis (Nègre *et al.,* 2011). We found only two predicted PREs with candidate SNPs on the second chromosome, and both are within the SNP island region of 2R. One is upstream of the gene *Act57B*, while the other is upstream of the *ribbon* gene.

Our lab previously performed a co-immunoprecipitation of BEAF from *Drosophila* embryos and by mass spectrometry, identified 93 co-immunoprecipitated factors with significant peptide signals. We searched for SNPs in the gene body of these proteins and found that 10 of the potential *BEAF* interaction partners had an SNP: *bl, CG30122, CG4038, hrb27c, lola, me31b, prp19, rib, sdha,* and *spindly*. If these proteins interact

with BEAF, they likely regulate at least some of the same genes as BEAF, increasing the chance they compensate for loss of BEAF and are stronger candidates for *Tofu*.

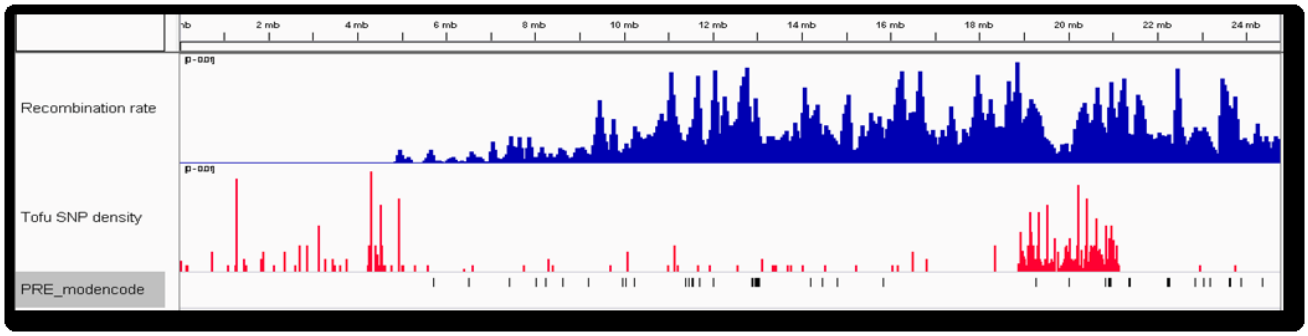

Figure 8. IGV screenshot of chromosome 2R showing recombination rates (blue), SNP distribution of Tofu candidates (red), and putative PREs (black). Recombination rates were determined by Comeron *et al*. (2012).

These analyses suggest the mutation of the PRE upstream of the *ribbon* gene is the strongest *Tofu* candidate. It lies within the SNP dense region of the *Tofu* candidate SNPs. Furthermore, it was found to potentially interact with BEAF by CO-IP and mass spectrometry analysis. The predicted PRE directly upstream of its promoter is mutated, which could cause more pervasive expression of the protein. The H3K27me3 histone mark is associated with Polycomb silencing and can be found at the PRE upstream of *ribbon* in ChIP-seq data from ovaries (SRX177656). This indicates *ribbon* is silenced in the wild type ovary. A literature search of ribbon revealed it is involved in gonad development (Silva *et al.,* 2016). It has other developmental roles in Malpighian tubules, salivary glands, hindgut, tracheae and head (Jack and Myette, 1997). ChIP-seq data of ribbon from salivary glands revealed a similar DNA binding consensus motif to that of *BEAF*: CGATA(Cuvier *et al.,* 1998; Hart *et al.,* 1997; Loganathan *et al.,* 2016; Zhao *et al.,* 1995). These findings from the literature further strengthen the idea that ribbon could replace the function of BEAF.

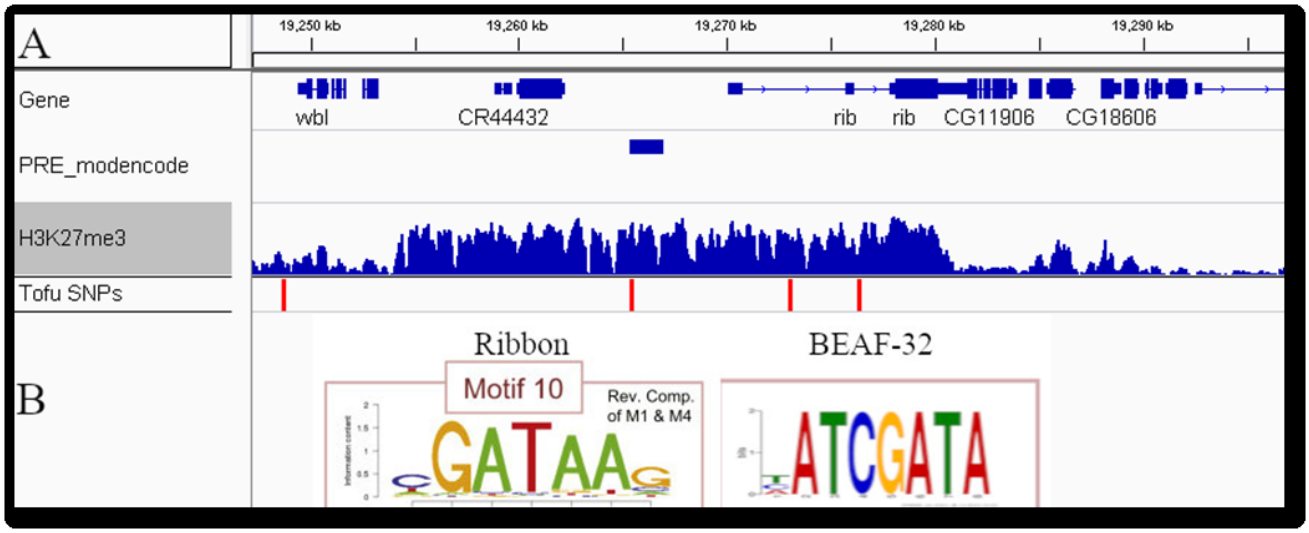

Figure 9. A: IGV screenshot of the candidate PRE upstream of the ribbon gene. The histone mark H3K27me3 associated with polycomb repression was collected from ovaries SRX177656. B: A comparison of BEAF and Ribbon consensus motifs identified by MEME analysis of ChIP-seq peaks. The ribbon motif is from Loganathan *et al*. (2016). The BEAF motif called from S2 cells SRX3486677.

Discussion

In retrospect, our genomic sequencing did not sample enough populations containing the *Tofu* mutation. Genome wide association studies in humans use many genomes from individuals to identify SNPs associated with a trait. These studies include a minimum of 2,000 individuals in each group, often exceeding 100,000 (Spencer *et al.,* 2009; Tam *et al.,* 2019). Our analysis was limited to 5 genomes of pooled populations, and this likely limited our ability to screen SNPs. However, similar pooled sequencing strategies have been employed successfully in *Drosophila* (Blumenstiel *et al.,* 2009).

Our original focus for *Tofu* candidates were SNPs with a predicted protein coding change. The strategy we had in mind was to select several candidates that had moderate or severe protein coding changes and clone the mutant alleles into *ABKO* flies. Rescue of fertility by a trans-gene would be a conclusive test for *Tofu* candidates. With 587 potential candidates on chromosome 2 with protein coding mutations, none of them were striking candidates with similar functions to BEAF. For this reason, we employed meiotic mapping to narrow down the list of candidates.

Our attempts at mapping were mostly unsuccessful, due to the difficulty of scoring fertility. Eventually we realized SNP density would indicate the *Tofu* mutation, which cut the number of protein coding SNPs to 256, still a high number. Looking at potential interacting partners of BEAF, and the inspection of regulatory elements led us to *ribbon*. If the PRE mutation upstream of *ribbon* is indeed preventing silencing of the gene, this should be detected by a relative increase in *ribbon* mRNA levels in *Tofu* flies. We plan to screen embryos for atypical expression patterns of *ribbon* via FISH in the *Tofu KO* line as compared to the wild type *y-w-* using *BEAF* expression as a control.

References: Borts, R.H., S.R. Chambers, and M.F.F. Abdullah 2000, Mutat. Res. Mol. Mech. Mutagen. 451: 129–150. https://doi.org/10.1016/S0027-5107(00)00044-0; Boulton, A., R.S. Myers, and R.J. Redfield 1997, Proc. Natl. Acad. Sci. 94: 8058–8063. https://doi.org/10.1073/pnas.94.15.8058; Bridges, C.B., 1935. SALIVARY CHROMOSOME MAPSWith a Key to the Banding of the Chromosomes of Drosophila Melanogaster. J. Hered. 26, 60–64. https://doi.org/10.1093/oxfordjournals.jhered.a104022; Cingolani, P., A. Platts, L.L. Wang, M. Coon, T. Nguyen, L. Wang, S.J. Land, X. Lu, and D.M. Ruden 2012, Fly (Austin) 6: 80–92. https://doi.org/10.4161/fly.19695; Comeron, J.M., R. Ratnappan, and S. Bailin 2012, PLOS Genet. 8: e1002905. https://doi.org/10.1371/journal.pgen.1002905; Cuvier, O., C.M. Hart, and U.K. Laemmli 1998, Mol. Cell. Biol. 18: 7478–7486. https://doi.org/10.1128/MCB.18.12.7478; Do, A.T., and J.R. LaRocque 2015, Sci. Rep. 5: 17601. https://doi.org/10.1038/srep17601; Grimm, C., P. Schaer, P. Munz, and J. Kohli 1991, Mol. Cell. Biol. 11: 289–298. https://doi.org/10.1128/MCB.11.1.289; Hart, C.M., K. Zhao, and U.K. Laemmli 1997, Mol. Cell. Biol. 17: 999–1009. https://doi.org/10.1128/MCB.17.2.999; Jack, J., and G. Myette 1997, Genetics 147: 243–253; Loganathan, R., J.S. Lee, M.B. Wells, E. Grevengoed, M. Slattery, and D.J. Andrew 2016, Dev. Biol. 409: 234–250. https://doi.org/10.1016/j.ydbio.2015.10.016; Morgan, T.H., 1911, Science 34: 384–384. https://doi.org/10.1126/science.34.873.384; Nègre, N., C.D. Brown, L. Ma, C.A. Bristow, S.W. Miller, U. Wagner, P. Kheradpour, M.L. Eaton, P. Loriaux, R. Sealfon, Z. Li, H. Ishii, R.F. Spokony, J. Chen, L. Hwang, C. Cheng, R.P. Auburn, M.B. Davis, M. Domanus, P.K. Shah, C.A. Morrison, J. Zieba, S. Suchy, L. Senderowicz, A. Victorsen, N.A. Bild, A.J. Grundstad, D. Hanley, D.M. MacAlpine, M. Mannervik, K. Venken, H. Bellen, R. White, M. Gerstein, S. Russell, R.L. Grossman, B. Ren, J.W. Posakony, M. Kellis, and K.P. White 2011, Nature 471: 527–531. https://doi.org/10.1038/nature09990; Silva, D., K.W. Olsen, M.N. Bednarz, A. Droste, C.P. Lenkeit, E. Chaharbakhshi, E.R. Temple-Wood, and J.C. Jemc 2016, PLOS ONE 11: e0167283. https://doi.org/10.1371/journal.pone.0167283; Spencer, C.C.A., Z. Su, P. Donnelly, and J. Marchini 2009, PLoS Genet. 5: https://doi.org/10.1371/journal.pgen.1000477; Sturtevant, A.H., 1913, J. Exp. Zool. 14: 43–59. https://doi.org/10.1002/jez.1400140104; Tam, V., N. Patel, M. Turcotte, Y. Bossé, G. Paré, and D. Meyre 2019, Nat. Rev. Genet. 20: 467–484. https://doi.org/10.1038/s41576-019-0127-1; Zhai, R.G., P.R. Hiesinger, T.-W. Koh, P. Verstreken, K.L. Schulze, Y. Cao, Y., H. Jafar-Nejad, K.K. Norga, H. Pan, V. Bayat, M.P. Greenbaum, and H.J. Bellen 2003, Proc. Natl. Acad. Sci. 100: 10860–10865. https://doi.org/10.1073/pnas.1832753100; Zhao, K., C.M. Hart, and U.K. Laemmli 1995, Cell 81: 879–889. https://doi.org/10.1016/0092-8674(95)90008-X.

Updated list of drosophilid species recorded in the Brazilian Savanna.

Ribeiro, L.B.[1], F.A.G.S. Cavalcanti[1], J.P.C. Viana[1], J.M. Amaral[2], S.C. Costa[3], and R. Tidon[1,2]. [1]Programa de Pós-Graduação em Ecologia, Instituto de Biologia, Universidade de Brasília, Brasília, DF, Brazil; [2]Departamento de Genética e Morfologia, Instituto de Biologia, Universidade de Brasília, Brasília, DF, Brazil; [3]Departamento de Biologia, Faculdade de Filosofia, Ciências e Letras de Ribeirão Preto, Universidade de São Paulo, Ribeirão Preto, SP, Brazil; Email: rotidon@unb.br

Introduction

The Brazilian Savanna, known locally as the Cerrado, covers about 2 million km^2 and is the second largest biome in South America. It is considered the most biodiverse savanna in the world (Oliveira and Marquis, 2002), and its vegetation comprises a structural gradient ranging from grasslands to forests, whose canopy height can reach 15–20 m (Ratter *et al.,* 1997). The Cerrado is subject to intense land use changes, with approximately 45% of its native vegetation having been converted to anthropogenic use (Souza *et al.,* 2020; Mapbiomas, 2021). Because of the high degree of endemism and extensive environmental alteration, it is considered as a hotspot of biodiversity (Myers *et al.,* 2000).

The drosophilid fauna of this region was first studied in the 1940´s through sporadic collections (*e.g.*, Dobzhansky and Pavan, 1950). The first regular collections of these insects occurred in the late 1990's and are concentrated in the Federal District, where a monitoring program is still ongoing (Tidon *et al.,* 2003; Tidon, 2006; Marques *et al.*, 2022). More recently other research groups have also investigated drosophilid communities established in other areas of the biome (Blauth and Gottschalk, 2007; Costa *et al.,* 2021).

The last list of drosophilids in the Brazilian Savanna was provided by Roque *et al.* (2015), and new records have been published since then. In this study, we compiled the available information on drosophilids collected in the Brazilian Savanna to expand this list.

Material and Methods

We searched for references recording species of Drosophilidae for localities in the ISI Web of Knowledge (www.webofknowledge.com), Google Scholar (scholar.google.com), TaxoDros (Bächli, 2022, www.taxodros.uzh.ch), and the Brazilian platform Curriculum Lattes, which contains publication lists of most researchers working in Brazil. We used the terms *Drosophila*, Drosophilidae, drosophilid, Cerrado and Brazilian Savanna. Drosophilid records found in this search were added to the list compiled by Roque *et al.* (2015).

Results and Discussion

From the list provided by Roque *et al.* (2015), which included 129 records, we excluded two species. *Rhinoleucophenga mymercophaga* Vidal and Vilela was removed, because it was recorded in a savanna vegetation in São Paulo State (Vidal and Vilela, 2015), located in a transitional area between the Cerrado and Atlantic Forest biomes. The second excluded species, *R. angustifrons* Malogolowkin, was originally recorded by Roque and Tidon (2008), but a re-analysis by Poppe *et al.* (2016) suggests that it is likely a *Leucophenga* Mik specimen. Here, we also identified the previously undetermined species of the genus *Diathoneura* as *D. brasiliensis* Duda.

In addition to the changes already mentioned, we have added 11 drosophilid species to the previous list. Five of them are neotropical and belong to the subfamily Drosophilinae: *Drosophila piratininga* Ratcov and Vilela*, D. aldrichi* Patterson*, Scaptomyza vittate* (Coquillett) (in Roque *et al.,* 2016), *D. mediosignata* Dobzhansky and Pavan (in Valadão *et al.,* 2010), and *D. saltans* Sturtevant (in Roque and Tidon, 2013). Four

species, representing three genera not previously recorded in the Brazilian Savanna, belong to the subfamily Steganinae: *Hyalistata cerradensis* Costa, Pirani & Oliveira, *H. emas* Costa, Pirani & Oliveira*, Pseudiastata brasiliensis* Costa Lima (in Costa *et al.,* 2022), and *Mayagueza lopesi* Costa, Pirani & Oliveira (in Costa *et al*., 2021). Finally, two non-neotropical species were also added: *Drosophila nasuta* Lamb (Leão *et al*., 2017) and *Zaprionus tuberculatus* Malloch (Cavalcanti *et al.,* 2022). Thus, there are currently 138 drosophilid species recorded in the Brazilian Savanna (Table 1).

Table 1. List of the drosophilid species recorded in the Brazilian Savanna, arranged by classification. Species exotic to the Neotropical Region are market with "(E)", and those not recorded in the list provided by Roque *et al*. (2015) are marked with "#".

Species of Subfamily Drosophilinae	
Genus *Drosophila*	
Subgenus *Dorsilopha*	
***busckii* group**	*D. busckii* Coquillett (E)
Subgenus *Drosophila*	
***annulimana* group**	*D. annulimana* Duda
	D. aragua Vilela and Pereira
	D. arapuan da Cunha and Pavan
	D. ararama Pavan and da Cunha
	D. arauna Pavan and Nacrur
***aureata* group**	*D. aureata* Wheeler
***bromeliae* group/ *bromeliae* subgroup**	*D. bromelioides* Pavan and da Cunha
***calloptera* group**	*D. atrata* Burla and Pavan
	D. calloptera Schiner
	D. quadrum (Wiedemann)
	D. schildi Malloch
***canalinea* group**	*D. annulosa* Vilela and Bachli
	D. canalinea Patterson and Mainland
	D. piratininga Ratcov and Vilela #
***cardini* group/ *cardini* subgroup**	*D. cardini* Sturtevant
	D. cardinoides Dobzhansky and Pavan
	D. neocardini Streisinger
	D. neomorpha Heed and Wheeler
	D. polymorpha Dobzhansky and Pavan
***coffeata* group**	*D. coffeata* Williston
	D. fuscolineata Duda
	D. pagliolii Cordeiro
***dreyfusi* group**	*D. camargoi* Dobzhansky and Pavan
	D. dreyfusi Dobzhansky and Pavan
***guarani* group/ *guaramunu* subgroup**	*D. griseolineata* Duda
	D. guaraja King
	D. maculifrons Duda
***guarani* group/ *guarani* subgroup**	*D. guaru* Dobzhansky and Pavan
	D. ornatifrons Duda
***immigrans* group/ *immigrans* subgroup**	*D. immigrans* Sturtevant (E)
	D. nasuta Lamb (E) #
***pallidipennis* group**	*D. pallidipennis* Dobzhansky and Pavan
***repleta* group/ *fasciola* subgroup**	*D. coroica* Wasserman
	D. ivai Vilela
	D. mapiriensis Vilela and Bachli
	D. moju Pavan
	D. onca Dobzhansky and Pavan
	D. papei Bachli and Vilela
	D. querubimae Vilela
	D. rosinae Vilela
***repleta* group/ *hydei* subgroup**	*D. hydei* Sturtevant
***repleta* group/ *mercatorum* subgroup**	*D. mercatorum* Patterson and Wheeler

	D. paranaensis Barros
***repleta* group/ *mulleri* subgroup**	*D. aldrichi* Patterson #
	D. antonietae Tidon-Sklorz and Sene
	D. borborema Vilela and Sene
	D. buzzatii Patterson and Wheeler
	D. gouveai Tidon-Sklorz and Sene
	D. meridionalis Wasserman
	D. nigricruria Patterson and Mainland
	D. serido Vilela and Sene
	D. seriema Tidon-Sklorz and Sene
***repleta* group/ *repleta* subgroup**	*D. eleonorae* Tosi *et al*.
	D. neorepleta Patterson and Wheeler
	D. pseudorepleta Vilela and Bachli
	D. repleta Wollaston
	D. zottii Vilela
tripunctata* group/ subgroup *I	*D. neoguaramunu* Frydenberg
tripunctata* group/ subgroup *II	*D. cuaso* Bachli, Vilela and Ratcov
	D. medioimpressa Frota-Pessoa
	D. mediopunctata Dobzhansky and Pavan
	D. mediosignata Dobzhansky and Pavan #
	D. paraguayensis Duda
	D. roehrae Pipkin and Heed
	D. unipunctata Patterson and Mainland
tripunctata* group/ subgroup *III	*D. bandeirantorum* Dobzhansky and Pavan
	D. bifilum Frota-Pessoa
	D. mediopicta Frota-Pessoa
	D. mediostriata Duda
	D. mesostigma Frota-Pessoa
	D. paramediostriata Townsend and Wheeler
	D. trapeza Heed and Wheeler
tripunctata* group/ subgroup *IV	*D. albirostris* Sturtevant
	D. nappae Vilela, Valente and Basso-da-Silva
***virilis* group/ virilis subgroup**	*D. virilis* Sturtevant (E)
Ungrouped species	*D. caponei* Pavan and da Cunha
	D. impudica Duda
Subgenus *Phloridosa*	*D. denieri* Blanchard
	D. lutzii Sturtevant
Subgenus *Siphlodora*	*D. flexa* Loew
Subgenus *Sophophora*	
***melanogaster* group/ *ananassae* subgroup**	*D. ananassae* Doleschall (E)
	D. malerkotliana Parshad and Paika (E)
***melanogaster* group/ *melanogaster* subgroup**	*D. melanogaster* Meigen (E)
	D. simulans Sturtevant (E)
***melanogaster* group/ *suzukii* subgroup**	*D. suzukii* (Matsumura) (E)
***montium* group/ *kikkawai* subgroup**	*D. kikkawai* Burla (E)
***saltans* group/ *cordata* subgroup**	*D. neocordata* Magalhaes
***saltans* group/ *elliptica* subgroup**	*D. neoelliptica* Pavan and Magalhaes
***saltans* group/ *saltans* subgroup**	*D. austrosaltans* Spassky
	D. prosaltans Duda
	D. pseudosaltans Magalhaes
	D. saltans Sturtevant #
***saltans* group/ *sturtevanti* subgroup**	*D. sturtevanti* Duda
***willistoni* group/ *bocainensis* subgroup**	*D. bocainensis* Pavan and da Cunha
	D. bocainoides Carson
	D. capricorni Dobzhansky and Pavan
	D. fumipennis Duda
	D. nebulosa Sturtevant
	D. parabocainensis Carson
***willistoni* group/ *willistoni* subgroup**	*D. paulistorum* Dobzhansky and Pavan
	D. equinoxialis Dobzhansky
	D. tropicalis Burla and da Cunha

	D. willistoni Sturtevant
Genus *Diathoneura*	*Diathoneura brasiliensis* Duda #
Genus *Hirtodrosophila*	
***hirticornis* group**	*H. morgani* (Mourao, Gallo and Bicudo)
Ungrouped species	*H. pleuralis* (Williston)
	H. subflavohalterata (Burla)
Genus *Mycodrosophila*	*M. projectans* (Sturtevant)
Genus *Neotanygastrella*	*N. tricoloripes* Duda
Genus *Scaptodrosophila*	*S. latifasciaeformis* (Duda) (E)
Genus *Scaptomyza*	
Subgenus *Mesoscaptomyza*	*S. nigripalpis* Malloch
	S. vittata (Coquillett) #
Genus *Zaprionus*	
Subgenus *Zaprionus*	
***vittiger* group**	*Z. indianus* Gupta (E)
***tuberculatus* subgroup**	*Z. tuberculatus* Malloch (E) #
Genus *Zygothrica*	
***aldrichii* subgroup**	*Z. microeristes* Grimaldi
***dispar* subgroup**	*Z. dispar* (Wiedemann)
	Z. prodispar Duda
Ungrouped species	*Z. apopoeyi* Burla
	Z. poeyi (Sturtevant)
Species of Subfamily Steganinae	
Genus *Amiota*	Undetermined species
Genus *Hyalistata*	*H. cerradensis* Costa, Pirani & Oliveira #
	H. emas Costa, Pirani & Oliveira #
Genus *Leucophenga*	
Subgenus *Leucophenga*	*L. bimaculata* (Loew)
	L. montana Wheeler
	L. maculosa (Coquillett in Johnson)
	L. ornativentris Kahl
	L. varia (Walker)
Genus *Mayagueza*	*M. lopesi* Costa, Pirani & Oliveira #
Genus *Pseudiastata*	*P. brasiliensis* Costa Lima #
Genus *Rhinoleucophenga*	
Subgenus *Pseudophortica*	*R. obesa* (Loew)
Without subgenus	*R. lopesi* Malogolowkin
	R. matogrossensis Malogolowkin
	R. montensis Junges & Gottschalk
	R. nigrescens Malogolowkin
	R. personata Malogolowkin
	R. punctulata Duda
	R. tangaraensis Junges & Gottschalk

Updating the list of drosophilid species recorded in an area is important because it provides a real understanding of the biodiversity of that area. In the case of drosophilids, which are considered good models for ecological studies (Mata *et al*., 2010), updated records may also raise new questions about the structure and function of their communities. For example, most species of the subfamily Steganinae have peculiar life habits (*e.g*., predators, parasites, and feeders on animal tissues or secretions); however, this subfamily is still poorly known in Brazil (Ashburner, 1981; Bächli, 2022). The number of drosophilid species recorded in the Brazilian Savanna is still rising, suggesting that this biome demands more collection efforts. To expand the species list, it is necessary to diversify collection methods, improve taxonomic keys for neotropical drosophilids, and maintain inventories.

New arrivals of invasive species also deserve special attention. *Drosophila nasuta*, native to the Indo-Pacific region, was first detected in the Brazilian Cerrado in December 2013 and has since increased its abundance (Leão *et al.,*2017) and geographic distribution in other biomes (Montes *et al.*, 2021; Medeiros *et al*., 2022). *Zaprionus tuberculatus* was collected in the Brazilian Savanna in 2020, marking the first time this afrotropical species has been recorded in the Americas (Cavalcanti *et al.;* 2022). This species can cause economic damage to fruits, especially when associated with other drosophilid pests (Amiresmaeili *et al.,* 2019). Our results highlight and reinforce the importance of monitoring drosophilid communities and updating species lists, as this information supports the development of conservation and agricultural strategies.

Acknowledgments: We are thankful to the Universidade de Brasília. This research was granted by the Conselho Nacional de Desenvolvimento Científico e Tecnológico (CNPq), and Coordenação de Aperfeiçoamento de Pessoal de Nível Superior (CAPES).

References: Amiresmaeili, N., C. Jucker, S. Savoldelli, and D. Lupi 2019, J. Entomol. Acarol. Res. 51: 8–15; Ashburner, M., 1981, In: *The Genetics and Biology of* Drosophila, Vol. 3: 395–429; Bächli, G., 2022, TaxoDros. *The database on Taxonomy of Drosophilidae*, http://taxodros.uzh.ch/; Blauth, M.L., and M.S. Gottschalk 2007, Dros. Inf. Serv. 90: 90-96; Cavalcanti, F.A., L.B. Ribeiro, G. Marins, G.S. Tonelli, S.N. Báo, A. Yassin, and R. Tidon 2022, Ent. Soc. of America. 115(3): 267-274; Chaves, N.B., and R. Tidon 2008, Rev. Bras. Ent. 52: 340-348; Costa, S.C., G. Pirani, and S.S. Oliveira 2021, Zootaxa 5068(2): 287-294; Costa, S.C., G. Pirani, and S.S. Oliveira 2022, Zootaxa 5116(3): 334-350; Dobzhansky, T., and C. Pavan 1950, J. Anim. Ecol. 19: 1-14; Leao, B.F.D., F. Roque, P.H.M. Deus, and R. Tidon 2017, Dros. Inf. Serv. 100: 65-69; Mata, R.A, M. McGeoch, and R. Tidon 2010, Nature Conserv. 8(1): 60–65; Marques, N.S, R.B. Machado, L.M.S. Aguiar, L. Mendonça-Galvão, R. Tidon, E.M Vieira, O.J. Marini-Filho, and M. Bustamante 2022, Perspect. Ecol. Conserv. 20(2): 69–78; Medeiros, H.F., M.P. Monteiro, A.W.B. Caçador, C.M. Pereira, C.D.L.B. Praxedes, M.B. Martins, M.A. Montes, and A.C.L. Garcia 2022, Neotrop. Entomol. 51: 493–97; Montes, M.A., C.H.C.B. Neves, A.F. Ferreira, M.D.F.S. dos Santos, J.I.F.P. Quintas, G.D.Â. Manetta, P.V. de Oliveira, and A.C.L. Garcia 2021, Neotrop. Entomol. 50: 571–78; Myers, N., R.A. Mittermeier, C.G. Mittermeier, G.A.B. da Fonseca, and J. Kent 2000, Nature 403: 853-858; Oliveira, P.S., and R.J. Marquis 2002, *The Cerrados of Brazil. Ecology and Natural History of a Neotropical Savanna*. Columbia University Press; Paula, M.A., P.H.S. Lopes, and R. Tidon 2014, Dros. Inf. Serv. 97: 113-115; Poppe, J.L., V.L.S. Valente, J.P.J. Santos, and M.S. Gottschalk 2016, Zootaxa 4208(3): 261-281; Projeto MapBiomas - Coleção 7 *da Série Anual de Mapas de Uso e Cobertura da Terra do Brasil*, accessed on 20 December 2022 from http://mapbiomas.org; Ratter, J.A., J.F. Ribeiro, and S. Bridgewater 1997, *The Brazilian Cerrado vegetation and threats to its biodiversity*. Ann. Bot. 80: 223–230; Roque, F., and R. Tidon 2008, Dros. Inf. Serv. 91: 94-98; Roque, F., R.A. da Mata, and R. Tidon 2013, Biodivers. Conserv. 22(3): 657-672; Roque, F., L. Mencarini, and R. Tidon 2015, Dros. Inf. Serv. 98: 70-74; Roque, F., L. Mencarini, B.F.D. Leao, M.N. Delgado, and R. Tidon 2016, Dros. Inf. Serv. 99: 48-49; Souza Jr, C.M., J.Z. Shimbo, M.R. Rosa, *et al.* 2020, Remote Sensing 12(17): 2735; Tidon, R., D.F. Leite, and B.F.D. Leão 2003, Biol. Conserv. 112(3): 299-305; Tidon, R., 2006, Bio. Jour. Lin. Soc. 87(2): 233-247; Valadão, H.O., J.V. Hay, and R. Tidon 2010, Int. J. Ecol. 1: 1-7; Vidal, M.C., and C.R. Vilela 2015, Ann. Entomol. Soc. Am. 108(5): 932-940.

Downregulation of transmembrane O-Mannosyltransferases targeting cadherins makes 'waves' in the *Drosophila* central nervous system axonal tracts.

Koff, Melissa, Morgan Thomas, Huey Wong, and Vlad Panin. Department of Biochemistry and Biophysics, Texas A&M University, College Station, TX 77843. panin@tamu.edu

Abstract

A recently discovered family of O-manosyltransfearses termed TMTCs was shown to add O-linked mannose to cadherins. *TMTC* mutations were found to be associated with brain malformations and neurological disorders, suggesting that TMTCs play important roles in the nervous system. However, the biological roles of TMTCs remain poorly understood. TMTCs are well-conserved in animals, from *Drosophila* to humans, which suggests that *Drosophila* can serve as a model to elucidate TMTC functions. In this study, we focus on *Drosophila TMTC1-3*. We found that, during larval stages, *TMTC1* and *2* are expressed predominantly in the nervous system, showing broad and prominent expression throughout brain hemispheres and the ventral ganglion. We analyzed mutant phenotypes of these genes, which uncovered that the mutants have a distorted, wave-like pattern of the longitudinal axions. We found that *TMTC3* knockout results in similar axonal waving, while the most severe phenotype was detected when RNAi-mediated knockdown was combined with a *TMTC3* deficiency. Our data suggest that the *TMTC* genes have partially redundant functions in the nervous system and potentially regulate Cadherin-N activity. Taken together, our results contribute to elucidating the function of TMTCs in the *Drosophila* nervous system and have potential implications for uncovering similar mechanisms in humans.

Introduction

Recently discovered noncanonical protein O-mannosyltransferases TMTCs (Transmembrane O-Mannosyltransferases Targeting Cadherins) add O-linked mannose to cadherins, protocadherins, and some other proteins; however, the biological functions of TMTC-mediated O-mannosylation remain poorly understood (Larsen *et al.,* 2019). Cadherins are a large family of calcium-dependent transmembrane glycoproteins which are crucial for cell adhesion. They play essential roles in many biological processes across metazoan organisms, including neural development, tumor suppression, and epithelial maintenance. Mutations in cadherins lead to a range of congenital diseases, from neurological abnormalities to cancer (van Roy and Berx, 2008; Brasch *et al.,* 2012). Although O-mannose has been found on cadherins within important functional domains, the *in vivo* function of these modifications remains unclear (Larsen *et al.,* 2019). Notably, *TMTC* mutations were found to be associated with brain malformations and neurological disorders, which suggests that TMTCs play important roles in nervous system development, possibly by affecting the function of neural cadherins (Larsen *et al.,* 2019). In humans, the disruption of *TMTCs* results in a motley of human disease phenotypes; the most severe of which is Cobblestone lissencephaly, a rare central nervous system disorder characterized by defects in neuronal migration, resulting in abnormal brain development and other developmental defects (Farhan *et al.,* 2017). TMTC1-4 proteins are hypothesized to have non-fully overlapping substrate specificities: TMTC 1-4 have been proposed to modify different strands within the cadherin EC (Extra Cellular) domain, while working in a partially redundant manner (Larsen *et al.,* 2019). Interestingly, the absence of O-mannose on cadherin, caused by a loss of TMTC3 activity, resulted in a decreased cellular adhesion but did not affect cadherin stability or localization within the cell (Graham *et al.,* 2020). These findings were obtained *in vitro*; however, *in vivo* functions of TMTCs remain poorly understood.

Here, we focus on *Drosophila* TMTC1, TMTC2, and TMTC3 and their functions in the developing nervous system. Using previously generated Trojan GAL4 exon gene trap alleles, we revealed that, during larval stages, TMTC1 and 2 are expressed predominantly in the nervous system, showing broad and prominent

expression throughout brain hemispheres and the ventral ganglion. We also used these Gal4 alleles and RNAi-mediated knockdown to analyze the mutant phenotype of TMTC1-3 genes. Our analyses revealed that *TMTC* mutants have defects in the morphology of the main axon tracts in the larval brain. Our results suggest that TMTC-mediated O-mannosylation is necessary for proper neuroarchitecture in the developing brain, while possibly affecting Cadherin-N (CadN) function.

Materials and Methods

Drosophila *stocks and alleles*

TMTC1 and *2 Gal4* insertion alleles (BDSC 76620 & 66854) were obtained from the Bloomington Stock Center. They were generated in a large-scale mutagenesis approach using the Trojan *GAL4* exon gene trap strategy based on the MiMIC technology (Lee *et al.,* 2018) and contain an insertion that inactivates the gene and simultaneously generates GAL4 expressed in the gene's endogenous pattern. Homozygous individuals from these lines served as mutants for experiments. For RNAi experiments, the following lines were used: *UAS-TMTC3-IR1* (v33248), *UAS-TMTC3-IR2 (v110199),* (VDRC collection, Vienna Stock Center), *Df(2R)Exel6072* and *C155-Gal4* (obtained from the Bloomington Drosophila Stock Center).

Immunohistochemistry

3rd instar larvae of desired genotypes were dissected, fixed, and immunostained according to previously published protocols (Baker *et al.,* 2018). The primary antibody, mouse anti-FasII (Developmental Studies Hybridoma Bank), was used at a 1:10 dilution. Secondary antibody, anti-mouse Cy3 (Jackson Immunoresearch) was used at a 1:250 dilution. Following the immunostaining, the CNS was dissected and mounted on slides in Vectashield mounting medium with DAPI (Vector Laboratory). Digital images were obtained using a Zeiss Axioplan 2 fluorescent microscope with an ApoTome module for optical sectioning. AxioVision and ImageJ software were used for image processing.

Results and Discussion

Using the advantages of the *Drosophila* model, we have elucidated the expression of TMTC 1 & 2 in the developing larvae central nervous system. We utilized flies that have a transgenic insertion of a gene-trap Trojan GAL4 cassette within a coding intron of these genes (Lee *et al.,* 2018). The cassette results in the expression of GAL4 under the control of the regulatory sequences associated with the genes, while also creating a mutant allele. This method allows for both the expression and phenotype analyses of these genes. Using *UAS-CD4-tdGFP* as a fluorescent reporter activated by Gal4 expression, we show that *TMTC1* and *2* are broadly expressed in an overlapping pattern in the larval ventral ganglion and hemispheres of the central nervous system (Figure 1).

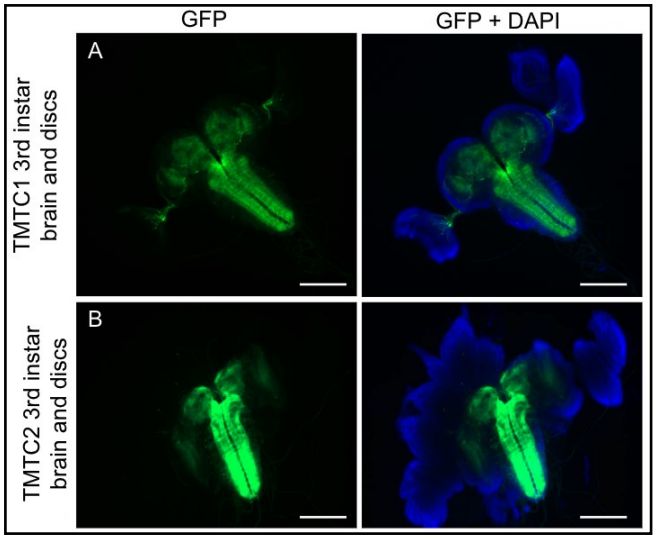

Figure 1. Expression of TMTC1 and TMTC2 revealed by CD4-GFP as a fluorescent marker. Central nervous system expression of TMTCs in the 3rd instar larval brain. A.) *Drosophila* 3rd instar CNS and accompanying discs, expressing TMTC1. B.) *Drosophila* 3rd instar CNS and accompanying discs, expressing TMTC2. Scale bars 100 μm.

Utilizing the same fly line containing the Trojan Gal4 gene-trap cassette, we selected homozygous TMTC1 and TMTC2 mutant larvae for further analysis of the central nervous system. Fasciclin-2 (FasII) is a well-studied orthologue of human NCAM, Neural Cell Adhesion Molecule, and is a major player in axonal pathfinding and fasciculation. FasII mediates homophilic adhesion and is expressed in axons that form bindles and major axonal tracts in the ventral ganglion. Examining homozygous TMTC1-Gal4 and TMTC2-Gal4 mutant brains by immunostaining for Fasciclin-2 expressing axons revealed "waving" defects of major axonal tracts in the larval ventral ganglion (Figure 2). While the general development of these axonal bundles does not appear to be abolished in *TMTC 1* or *2* mutants, their morphology is strikingly abnormal. Interestingly, in the majority of the brains examined, this axon waving phenotype is limited to dorsal medial and central intermedial tracts (Figure 2).

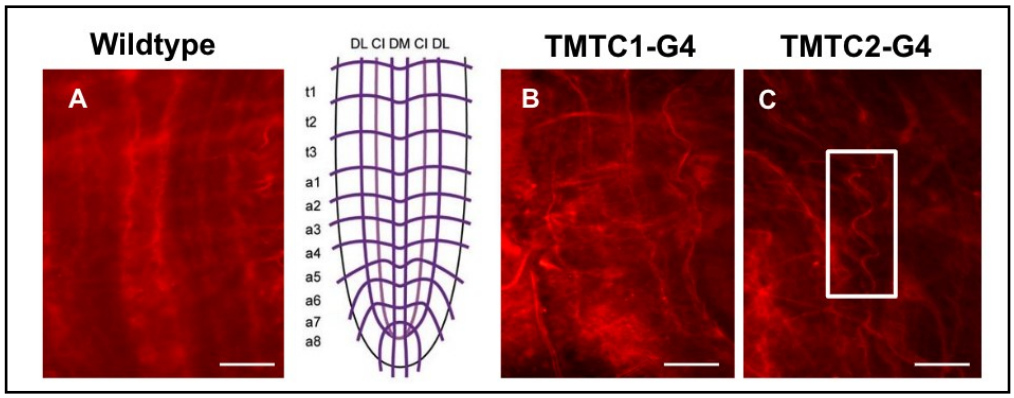

Figure 2. TMTC1 and TMTC2 affect the morphology of main axonal tracts in the 3rd instar larval brain, suggesting that TMTC-mediated O-mannosylation is important for N-Cadherin functions required for proper neuroarchitecture in the developing brain. All images are oriented A.) Wildtype larval brain showing normal FasII expressing tracts. (right) idealized schematic of FasII expressing tracts, thoracic and abdominal neuromeres (t1-3, a1-8). Longitudinal connections are referred to relative to their position: dorso-ventral (D: dorsal, C: central, V: ventral) and medio-lateral (M: medial, I: intermedial, L: lateral) adapted from (M. Vömel, 2008) B.) TMTC1-Gal4 homozygous mutant showing a mildly disturbed FasII staining. C.) TMTC2-Gal4 homozygous mutant exhibiting a 'wave' in the C1 tract, outlined in a white square. Scale bars 50 µm.

Finally, we knocked down *TMTC3* by the *UAS-RNAi* approach using of a strong pan-neuronal driver, *C155-Gal4*, which induced an axon waving phenotype similar to that detected in *TMTC1&2* mutants (Figure 3). Using RNAi constructs of different effectiveness (Farhan *et al.,* 2017) we found that the severity of the axon waving phenotype increased with the effectiveness of TMTC3 knockdown. The most severe phenotype was detected in the genotype combining a strong RNAi-mediated knockdown with one copy of *TMTC3* deficiency, suggesting that the strength of the phenotype is directly related to the level of *TMTC3* activity and, possibly, to the amount of TMTC3-mediated O-mannosylation in the CNS.

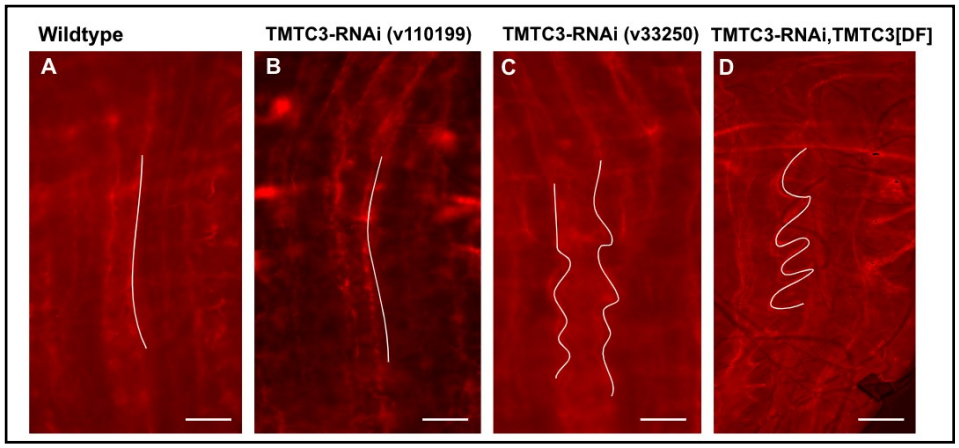

Figure 3. Using a strong pan-neuronal driver we see that the 'wave' phenotype increases in severity along with a more effective knock-down of TMTC3. A.) Wildtype brain exhibiting normal FasII staining, a white line highlights a DM tract. B.) Using an RNAi construct that is only ~20% effective at knocking down TMTC3

mRNA does not display a phenotype, and appears similar to wildtype. A white line highlights a DM tract. C.) A more effective (~80%) RNAi construct produces a wave phenotype in both DM tracts. D.) Strong RNAi construct combined with a chromosomal deletion that encompasses TMTC3, resulting in a more effective knockdown, shows a severe phenotype. A white line highlights a DM tract. Scale bars 50 μm.

Here we show that TMTC mutant or deficient brains analyzed by FasII staining exhibit a 'wavy' phenotype of select longitudinal axonal tracts of the ventral ganglion (Figures 2 and 3). We observed this new phenotype in both *TMTC1*^{Gal4} and *TMTC2*^{Gal4} mutants and RNAi-mediated knockdown of *TMTC3*, suggesting that the *TMTC* genes have partially redundant functions in the nervous system. A possible mechanism underlying this effect on axonal tracts may be the involvement of TMTCs in modulating of Cadherin-N (CadN), a prospective target of TMTCs. CadN mutants do not survive past embryonic stages; however, embryonic FasII staining of *CadN* mutants shows a similar albeit a less pronounced defect of longitudinal axonal tracts in the ventral ganglion (Iwai *et al.,* 1997). Rescue experiments and the analysis of genetic interactions between *TMTCs* and *CadN* will need to be performed to confirm the specificity of the phenotype and elucidate its relation to CadN function.

Acknowledgments: We thank members of the Paninlab for helpful discussion of the project and advice on experimental approaches. We are grateful to Adnan Halim and his research group for useful discussions, suggestions and ideas related to this study. This work was supported in part by grants from the National Institutes of Health (NIH/NS09940), Texas A&M-CONACYT Foundation (2012-037S), and the Texas A&M AgriLife Institute for Advancing Health Through Agriculture to V.P.

References: Baker, R., N. Nakamura, I. Chandel, B. Howell, D. Lyalin, and V.M. Panin 2018, J. Neurosci. 38: 1850-1865; Brasch, J., O.J. Harrison, B. Honig, and L. Shapiro 2012, Trends Cell Biol. 22: 299-310; Farhan, S.M.K., K.C.J. Nixon, M. Everest *et al*. 2017, Hum. Mol. Genet. 26: 4278-4289; Graham, J.B., J.C. Sunryd, K. Mathavan *et al*. 2020, Mol. Biol. Cell 31: 167-183; Iwai, Y., T. Usui, S. Hirano, R. Steward, M. Takeichi, and T. Uemura 1997, Neuron 19: 77-89; Larsen, I.S.B., Y. Narimatsu, H. Clausen, H.J. Joshi, and A. Halim 2019, Curr. Opin. Struct. Biol. 56: 171-178; Lee, P.T., J. Zirin, O. Kanca, W.W. Lin *et al*. 2018, Elife 7: e35574; van Roy, F., and G. Berx 2008, Cell Mol. Life Sci. 65: 3756-3788.

Guide to Authors

Drosophila Information Service prints short research, technique, and teaching articles, descriptions of new mutations, and other material of general interest to *Drosophila* researchers. The current publication schedule for regular issues is annually, with the official publication date being December. The annual issue will include material submitted during the calendar year. The submission deadline for each annual issue will be 31 December of the publication year, but articles are accepted at any time. Submissions should be in MS Word. .

Submission: Proofs will not be sent to authors unless there is some question that needs to be clarified. The editor reserves the right to make minor grammatical, spelling, and stylistic changes if necessary to conform to DIS format and common English usage. Tables may be slightly reformatted to conform to DIS style. Color illustrations now appear in color in both the printed version (from: www.lulu.com) and on our journal web site (www.ou.edu/journals/dis).

Citation of References: Citation should be by name and date in the text of an article (Smith, 1989; Jin and Brown, 1990; Waters *et al*., 1990). At the end of the article, references should be listed **alphabetically** by senior author, listing all authors with initials, date, journal, volume, and page numbers. Titles will not be included except for books, unpublished theses, and articles in press. An example format is:

Green, R.L., 1998, Heredity 121: 430-442.

Waters, R.L., J.T. Smith, and R.R. Brown 1990, J. Genet. 47: 123-134.

Note the initials are before each name except for the senior author.

Manuscripts and inquiries should be sent to James Thompson, Department of Biology, University of Oklahoma, Norman, OK 73019. Telephone (405)-325-4821; email jthompson@ou.edu; FAX (405)-325-7560.

Printed copies of Drosophila Information Service
can be obtained from www.lulu.com.

Edith M. Wallace (1881?-1964): A Belated Eulogy to an Unsung Heroine of Science.

Otto, P.A. Department of Genetics and Evolutionary Biology, Institute of Biosciences, University of Sao Paulo, Rua do Matao 277 room 344, 05508-090 Sao Paulo SP, Brazil; email otto@usp.br

A summary at an internet ancestry site reveals that Edith M. Wallace was born in the state of Massachusetts in 1879 and died in Los Angeles, California, in 1964 at the age of 85; another site includes information as to her burial place (Edgewood Cemetery at 107 Amherst St. in Nashua, New Hampshire). All the other sites with information about her, however, state that the New Englander lived for 83 years, from 1881 to 1964. It is known that she took the Zoology course at the Marine Biological Laboratory (Woods Hole, Mass.) in 1902, graduating the following year from Mt. Holyoke College, a liberal arts women's college in South Hadley, Mass. She then obtained a master's degree in Biology at Clark University in Worcester, Mass., and taught at colleges in Ohio and Maine before signing on with Thomas Hunt Morgan at Columbia University in 1908 (1,2,3,4).

The photograph (Figure 1, above), taken by Alfred Huettner around 1920, shows Miss Wallace seated looking at the camera (4). [Legend for Figure 1: Edith M. Wallace. Photo originally obtained from the www site https://hpsrepository.asu.edu/handle/10776/12945. Presently the image is kept at the Marine Biological Laboratory sites https://twitter.com/mblhistory/status/991292683304996864?lang=en and https://darchive.mblwhoilibrary.org/handle/1912/22613?show=full.]

Although trained as a biologist, she was hired as a technician, possibly because at the time the prospect of a career in science for a woman was a somewhat unrealistic one; this was also the case with two other women (Eleth Cattell and Sabra Tice), who were hired by Morgan as technicians despite their Biology college education, as pointed out by Kohler in his book "Lords of the Fly." Being a first-class illustrator, Miss Wallace worked as the group's artist in addition to being Morgan's personal technician, funded by the Carnegie Institution of Washington (though no record of this could be found). After working at Columbia for twenty years, in 1928 she accompanied Morgan when his group moved to the California Institute of Technology (Caltech) in Pasadena, where she worked until her formal retirement in 1944. Caltech records attest that she was employed and funded by the institution (3,5,6).

She continued working at Caltech for some years after her retirement, but by that time she no longer drew or painted flies; her work consisted in organizing and filing Morgan's and Sturtevant's papers. Very little, in fact practically nothing, is known about both her personal life and career with Morgan's group, except for the outstanding illustrations she has left us. Around the time of her retirement she lived alone in Pasadena, where she built a solid friendship with Dr. Edward and Mrs. Pamela Lewis. Mrs. Lewis was already an accomplished artist on her own right, whom Miss Wallace taught the technique of painting with watercolors. Miss Wallace used to visit the couple regularly on Sunday evenings when they listened to classical music and the radio together (7,8,9,10).

The numerous *Drosophila* black-and-white text illustrations and the dozens of watercolor plates that she meticulously produced decorate, embellish, and effectively break the boring routine (for the non-specialist in *Drosophila* genetics) of phenotype description of gene mutations in the three volumes of "Contributions to the Genetics of *Drosophila melanogaster*" by Morgan and Bridges and in the book "The Genetics of *Drosophila*" by Morgan and his main collaborators Bridges and Sturtevant (11,12,13,14).

Most *Drosophila* black-and-white text illustrations (black India ink on ivory artist's board) and watercolor plate paintings on Canson paper produced by Miss Wallace seem to have been produced before she moved to Caltech. Not surprisingly for such a self-effacing woman, her name appears practically only at the foot of the watercolor plates, humbly informing that she drew [E. M. Wallace Del(ineavit)] or painted them [E. M. Wallace Pinx(it)]. No explicit reference is made to her as author of the many text drawings and some plate paintings in the publications mentioned before. She illustrated Sturtevant's book "The North American Species of *Drosophila*" as well, published in 1921. Since she was employed by Morgan as a technician, it seems that he was the proprietary owner of all her art production. This suggestion is reinforced by the following statement, taken from the preface of Sturtevant and Beadle's book "An Introduction to Genetics", published in 1939: "Professor T.H. Morgan has kindly permitted the use of a number of figures prepared by Miss Edith M. Wallace, among which are the frontispiece and the plate of *Drosophila* eye colors" (15,16).

Figure 2. Edith M. Wallace at Caltech (around 1936). Photograph obtained from a composite illustration on page 60 of the October 1936 issue of Modern Mechanix.

The popular newsstand magazine "Modern Mechanix," which was founded in 1928 and survived until 2001, published in its October 1936 issue an article honoring some (six) women that excelled in science, among them Miss Wallace. The caption of her photograph (reproduced in Figure 2) reads: "For 27 years Miss Edith M. Wallace has spent her days drawing mutations of the vinegar fly. She is pictured at her laboratory in Pasadena (California)." She was then in her fifties and this seems to have been the only public recognition ever published about her and her career, in addition to the preface note cited above in Sturtevant and Beadle's book (17).

In the 1960s many of the original *Drosophila* drawings made by Miss Wallace and kept at Caltech were sent by Caltech's Prof. Edward (Ed) B. Lewis (Caltech PhD graduate, 1995 Nobel Prize in Medicine and Physiology, and a former student of Sturtevant) to Prof. Daniel (Dan) Lindsley (then working at the Oak Ridge National Laboratory and also a Caltech PhD graduate and former student of Sturtevant) for inclusion in Lindsley and Grell's 1968 (2nd Ed., 1972) Red Book ("Genetic Variations of *Drosophila melanogaster"*). The figures had been used also in the book by Bridges and Brehme ("The Mutants of *Drosophila melanogaster"*), a forerunner (1944) of the more detailed Red Book. They were reused in the second, enlarged edition of the Red Book by Lindsley and Zimm ("The Genome of *Drosophila melanogaster*", 1992), an updated version

incorporating novelties from molecular genetics. These publications are among the first to cite the origin of many of her illustrations when previously unpublished ("Edith M. Wallace, unpublished"); her name is also mentioned as the discoverer of the mutation, as is the case of the famous *apterous* phenotype. Professor Lindsley then passed the original illustrations to Professor Michael Ashburner (Cambridge University in the U.K.), who ultimately returned them to Caltech. More recently, Caltech created an internet page with increasing (but still sparse) information honoring Miss Wallace and put together a relatively large archive containing her material, part of which has been carefully scanned and disposed to interested researchers (3,18,19,20).

It is believed that some of Miss Wallace's original material has been lost. For instance, when Sturtevant's office (where some of her original illustrations were kept) was hastily emptied after his death, in 1970, to accommodate a newly hired professor, some of its material was found and swiftly retrieved from garbage bins (in the rain!) by a post-doc at Caltech. Dr. Lindsley intended to contact this geneticist in order to bring the original material back to Caltech, but apparently passed away before accomplishing this. In any case, some extra original material seems to have survived somewhere besides that stored at Caltech, and practically all her illustrations survive on the publications made by the Morgan group and by Sturtevant (3,7,21).

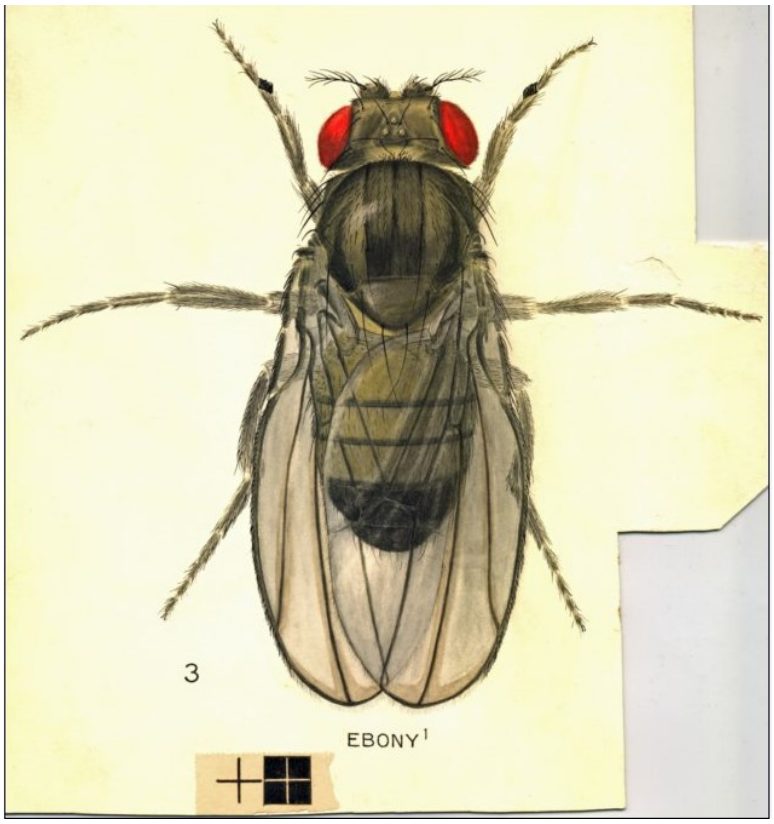

Figure 3. *Drosophila melanogaster*, *ebony* male, original watercolor painting by Miss Edith M. Wallace stored at the Caltech Archives (identification number EMW 4.1-1). Also shown at the foot of the figure is a detail of the illustration, exhibiting the incredible level of microscopic detailing achieved by her.

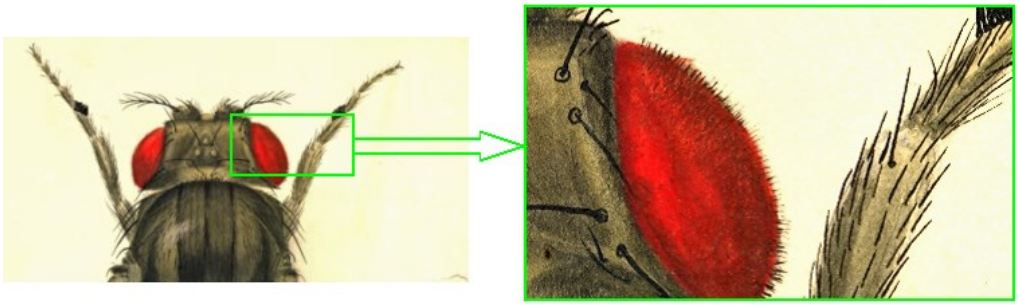

Figure 4. *Drosophila melanogaster*, male carrier of the mutation *bithorax III*. Original black ink illustration by Miss Edith M. Wallace stored at the Caltech Archives (identification number EMW 1.2-1).

Figure 5. *Drosophila melanogaster*, male mutant carrier of the phenotype *bent wing*. Original black ink illustration by Miss Edith M. Wallace stored at the Caltech Archives (identification number EMW 1.2-2).

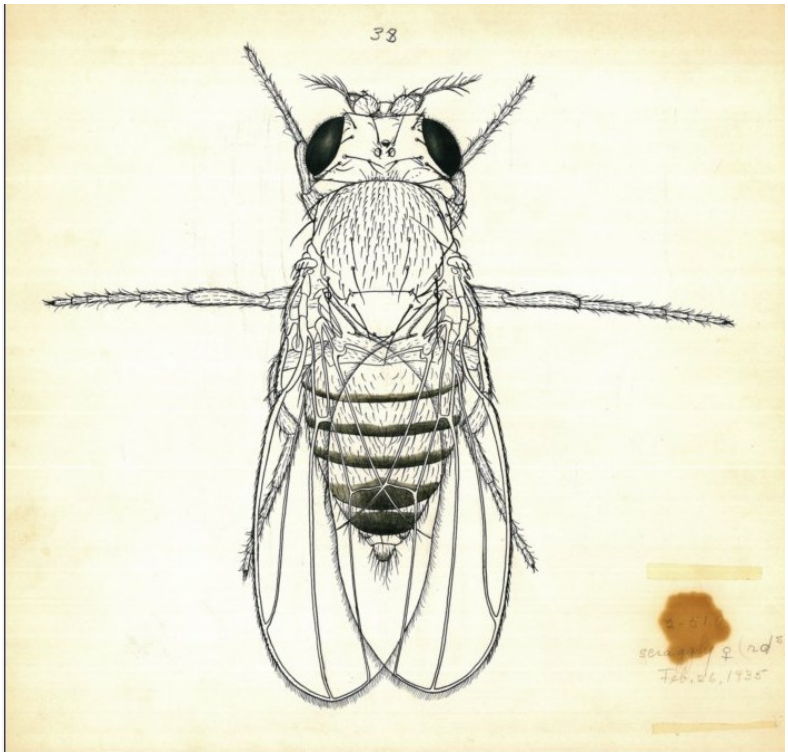

Figure 6. *Drosophila melanogaster*, female carrier of the mutation *scraggly*. Original black ink illustration by Miss Edith M. Wallace stored at the Caltech Archives (identification number EMW 1.5-1).

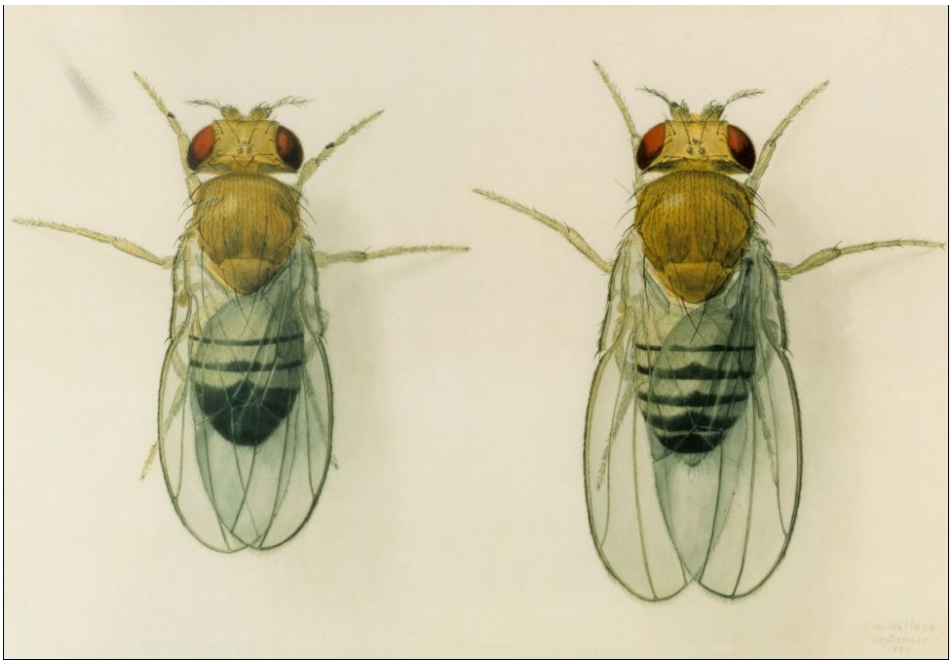

Figure 7. *Drosophila melanogaster*, male & female with the wild type (normal) phenotype. Original watercolor painting by Miss Edith M. Wallace stored at the Caltech Archives, Fine Art Series section (identification number 70.1-2).

The India ink figure drawings and watercolor plate paintings produced by Miss Wallace have an extraordinary microscopic level of detail and constitute a classical example of high-quality scientific illustration. A few of them, whose images (scanned from original material) were obtained from the Caltech Archives, can be seen below. The image showing a carrier of the ebony phenotype, for example, appears with an amplified section of a small part of the watercolor painting to bring into focus the astonishing level of detail and the incredible care of Miss Wallace in accomplishing this.

Acknowledgments: Due to the virtual absence of data about Miss Wallace, the eulogy/biography presented here is a sort of compilation entirely processed (almost literally) from very scarce (and sometimes imprecise) information scattered on several sites on the Web and complemented with data obtained from informal (usually by email) personal correspondence (dating back some thirty years) with important drosophilists, some of whom (especially Drs. Dan Lindsley and Ed Lewis) knew Miss Wallace personally but at a time when she was advanced in age and no longer did any *Drosophila* drawings and paintings. Some ideas were discussed with or suggested by Drs. James Crow (including the subtitle "unsung heroine of science") and Dan Lindsley. A small part of this correspondence, dating from twenty or more years ago, was lost, and, just like all the persons mentioned above, had the same fate as the rest of the information on Miss Wallace. Some pertinent information could be drawn from the Web sites of the Caltech and Marine Biological Laboratory archives, from Kohler's book "Lords of the Fly" and from both editions of Lindsley's "Red Book". I would also like to thank Mrs. Loma Karklins (archivist at Caltech) for her patient, kind, and competent assistance in guiding me through the intricacies of getting to the original *Drosophila* images and Mrs. Lilian Dluhosch, my wife, for helping me with the English language usage.

References: The numbers below correspond to information used in the preparation of the article and can be found grouped at the end of each paragraph of the eulogy.

(1) https://www.ancestry.ca/genealogy/records/edith-m-wallace-24-22qg578

(2) https://peoplelegacy.com/edith_m_wallace-5n3O5m

(3) https://archives.caltech.edu/news/wallace.html

(4) https://darchive.mblwhoilibrary.org/handle/1912/22613;https://twitter.com/mblhistory/status/991292683304996864?lang=en

(5) Kohler RE, Lords of the fly, University of Chicago Press, Chicago, 1994

(6) personal email correspondence w/ Carnegie Institution

(7) personal email correspondence w/ Dr. Daniel Lindsley

(8) personal email correspondence w/ Dr. Edward Lewis

(9) personal regular mail and email correspondence w/ Dr. James Crow

(10) http://www.fruitfly.org:9005/lewis/Site/Back_files/Metamorphosis.pdf

(11) Morgan TH, Bridges CB, Sex linked inheritance in *Drosophila*, Carnegie Institution, Washington, 1916

(12) Bridges CB, Morgan TH, The second chromosome group of mutant characters, Carnegie Institution, Washington, 1919

(13) Bridges CB, Morgan TH, The third chromosome group of mutant characters, Carnegie Institution, Washington, 1923

(14) Morgan TH, Bridges CB, Sturtevant AH, The genetics of *Drosophila*, Bibliographia Genetica 2, N. Nijhoff, Gravenhage, 1925 (reprinted by Garland Pub., 1988)

(15) Sturtevant AH, The North American Species of *Drosophila*, Carnegie Institution, Washington, 1921

(16) Sturtevant AH, Beadle GW, An Introduction to Genetics, W. B. Saunders, Philadelphia, 1939

(17) http://blog.modernmechanix.com/women-win-honors-in-science/

(18) Lindsley DL, Zimm GG, The genome of *Drosophila melanogaster*, Academic Press, San Diego, 1992

(19) Lindsley DL, Grell EH, Genetic Variations of *Drosophila melanogaster*, Carnegie Institution, Washington, 1968 (2nd Ed. 1972)

(20) Bridges CB, Brehme KS, The mutants of *Drosophila melanogaster*, Carnegie Institution, Washington, 1944

(21) anonymous communication at the University of Wisconsin in the early nineties

Professor J.P. Gupta
13th July 1939 – 6th May 2021

A tribute to the five decades of work done in Drosophilidae taxonomy under the guidance of Late Prof. J.P. Gupta in India.

Fartyal, Rajendra Singh[1]*, Pragya Topal[1], Sonali Khali[1], Kishor Kumar[2], Kanita[1], Durga Rawat[1], and A.K. Singh[3]. [1]Fly Laboratory, Department of Zoology, HNB Garhwal University, Srinagar Garhwal- 246174, Uttarakhand, India; [2]G.B. Pant National Institute of Himalayan Environment, Himachal Regional Center, Mohal-Kullu, 175 126, Himachal Pradesh, India; [3]Department of Zoology, Institute of Science, Banaras Hindu University, Varanasi - 221005, UP, India; [*]Corresponding author: fartyalrs@gmail.com

Abstract

Prof. (Dr.) J.P. Gupta has contributed greatly to the research on Drosophilidae, and the Taxonomy of India will always be grateful for that. The field of taxonomy will always be debited to him for creating the checklist of Indian Drosophilidae and his work in keeping the taxonomy alive with his asset monograph "*A Monograph on Indian Drosophilidae 2005*". An updated and newly discovered species checklist is presented in this article as a tribute to his work.

The genus *Drosophila* in particular, and the Drosophilidae family as a whole, have long played a significant role in the study of genetics and evolution. In the previous couple of decades, *Drosophila* has developed into an astonishingly adaptable experimental organism in almost every field of biology including genetics, molecular biology, population genetics, neural biology, and evolutionary biology (Bellen *et al*., 2010). *Drosophila* was initially used for genetic research by William Ernest Castle. Together with several colleagues, he conducted a thorough investigation into inbreeding and selection, which was published in 1906. *Drosophila* became known to geneticist Prof. T.H. Morgan through Castle's influence, and later this species served as the subject of Morgan's research (Snell and Reed, 1993). As is clear from the literature, Schiner began taxonomic studies of drosophilid species in the Indian peninsula as early as 1868 when he reported the discovery of *Drosophila insulana* (now *Leucophenga insulana*) on Nicobar Island. After a sizable period gap, M. Bezzi described *Drosophila repleta* from Calcutta as a new record (Sturtevant, 1921). Later O. Duda, J.R. Malloch, and A.H. Sturtevant described a few other new species and new records from India. Prof. S.P. Ray-Chaudhuri and Prof. D.P. Mukherjee were the first Indian researchers to describe new species from India. Under the guidance of Prof. S.P. Ray-Chaudhuri, Dr. J.P. Gupta conducted significant fieldwork in several environmentally fascinating regions of Uttar Pradesh and also had the chance to look at a few minor samples from Orissa and the Andaman and Nicobar Islands.

A checklist of genera and subgenera.

Sub Family Steganinae		
Genus	Subgenus	No. of species
Acletoxenus Von Frauenfeld		1
Amiota Loew		1 (1)
Phortica Schziner	*Sinophthalmus* Coquillett	1
	Phortica	6 (2) (1)
	Ashima	1 (1)
Cacoxenus Loew	*Gitonides* knab	8 (1) (1)
Leucophenga Mik	*Leucophenga* Mik	30 (3) (5) (6) (1*)
Paraleucophenga Hendel		3 (1) (1)
Pararhinoleucophenga Duda		1
Stegana Meigen	*Stegana* Meigen	4 (2)
	Steganina Wheeler	1 (1)
	Oxyphortica	1 (1) *
Total		58 (9) (9) (9)

Sub Family Drosophilinae		
Genus	Subgenus	No. of species
Chymomyza Czerny		1
Colocasiomyia de Meijere		1
Dettopsomyia Lamb		1
Dichaetophora Duda		2
Drosophila fallen	*Dorsilopha* Sturtevant	1
	Drosophila Fallen	74 (24) (10) (7) 2*
	Sophophora Sturtevant	73 (11) (4)
	Siphlodora Patterson & Mainland	3
	Dudaica Strand	1
	Incertae sedis	3 (1)
Hirtodrosophila Duda		16 (3) (1) (3) 3*
Impatiophila Fu and Gao		11 (11*)
Scaptodrosophila Duda		34 (22) (1)
Liodrosophila Duda		10 (4) (1)
Lissocephala Malloch		3
Lordiphosa Basden		11 (4) (4)
Microdrosophila Malloch	*Micro Drosophila*	9 (5) (1)
	Oxystylopetra Duda	3 (3)
Mulgravea Bock		2 (1)
Mycodrosophila Oldenberg	*Promyco Drosophila* Okada	1 (1)
	Myco Drosophila Oldenberg	6 (3)
Phorticella Duda		1
Scaptomyza Hardy	*Parascaptomyza* Duda	5
	Scaptomyza	4 (1) (1)
Zaprionus Coquillett	*Zaprionus*	1 (1)
	Anaprionus Okada	6 (2)
Gitona Meigen		1
Hypselothyrea de Meijere.	*Deplanothyrea* Okada	4 (3)
	Hypselothyrea de Meijere	2
TOTAL	290 (88) (19) (26)	
RED: Prof. JP GUPTA; YELLOW: Prof. B.K. Singh; GREEN: Dr. R.S. Fartyal		

Prof. Gupta pursued research on the area of *Drosophila Systematics and Evolutionary Genetics*. He has described over 90 new drosophilid species from India. He will always be regarded as the leader of Indian *Drosophila* Taxonomy and one of the world's top *Drosophila* taxonomists. Over 100 of his original research papers, reviews, and articles have been published in reputable national and international publications with excellent citation rates. Professor Gupta oversaw the dissertations of nine Ph.D. candidates. After retiring, he wrote a monograph titled "A Monograph on Indian Drosophilidae 2005," in which he shared the knowledge he had accumulated over the previous five decades with other drosophilids researchers who are still actively working in the field. He was invited to work on the Systematics of Malaysian Drosophilid species as visiting scientist to create the species inventory by the University of Kebangsaan, Malaysia.

Acknowledgment: The authors acknowledge financial support by HNB Garhwal University fellowship to Ms. Pragya Topal, Ms. Kanita, and Ms. Durga Rawat.

References: Bellen, H.J., C. Tong, and H. Tsuda 2010, 100 years of Drosophila research and its impact on vertebrate neuroscience: A history lesson for the future. Nature Reviews Neuroscience 11(7): Article 7. https://doi.org/10.1038/nrn2839; Gupta, J.P.. 2005, *Monograph on Indian Drosophilidae*. Journal of Scientific Research Banaras Hindu University 51(1): 1-252; Snell, G.D., and S. Reed 1993, William Ernest Castle, Pioneer Mammalian Geneticist. Genetics 133(4): 751-753; Sturtevant, A.H., 1921, *The North American Species of* Drosophila. Carnegie Institute of Washington Publication 301: 1-141.

"… if anything is endangered in India or world it is our Drosophila taxonomists."

- R. S. Fartyal

The North American *Drosophila* Board

The Board's duties include overseeing community resource centers and addressing other research and resource issues that affect the entire *Drosophila* research community. The Board also administers the finances for the annual North American *Drosophila* Research Conference and its associated awards, and it chooses the organizers and the site of the annual meeting. The Board consists of nine regional representatives and four international representatives, who serve 3-year terms. The three elected officers are President, President-Elect, and Treasurer. The three most recent Presidents continue participation on the Board as Past-Presidents. In addition, the Board has *ex officio* members who represent *Drosophila* community resources or centers. For more information about the Board and the summaries of the annual Board meetings, see the FlyBase web site.

Drosophila Board

President:	Michelle Arbeitman (2023)	michelle.arbeitman@med.fsu.edu
President-Elect:	Harmit Malik	hsmalik@fredhutch.org
Past President:	Tin Tin Su (2022)	tin.su@colorado.edu
Past President:	Mariana Wolfner (2021)	mariana.wolfner@cornell.edu
Past President:	Mark Peifer (2020)	peifer@unc.edu
Treasurer:	Jessica Treisman	jessica.treisman@med.nyu.edu

Regional Representative:

Name	Region	Year	
Liz Rideout	Canada	2024	elizabeth.rideout@ubc.ca
Brian Lazzaro	Great Lakes	2024	bl89@cornell.edu
Nadia Singh	Mountain	2023	nsingh@uoregon.edu
Wu Min Deng	Southeast	2024	wumin@bio.fsu.edu
Blake Riggs	California	2025	riggs@sfsu.edu
Tânia Reis	Heartland	2024	tania.reis@ucdenver.edu
Alexey Veraksa	New England	2023	alexey.veraksa@umb.edu
Hakeem Lawal	Mid-Atlantic	2025	hlawal@desu.edu
Rachel Smith-Bolton	Midwest	2024	rebolton@illinois.edu

Primarily Undergraduate Institution Representative:

Justin DiAngelo	2023	jrd5671@psu.edu

International Representatives:

Kieran Harvey	Australia/Oceania	2023	kieran.harvey@monash.edu
Mousumi Mutsuddi	Asia	2025	mousumi@bhu.ac.in
Daria Siekhaus	Europe	2025	daria.siekhaus@ist.ac.at
John Ewer	Latin America	2025	john.ewer@uv.cl

Postdoctoral and Student Representatives:

Lydia Grmai	Postdoc Representative	2023	lgrmai1@jhu.edu
Ana-Maria Raicu	Student Representative	2023	raicuana@msu.edu

Ex Officio

Norbert Perrimon	FlyBase	perrimon@receptor.med.harvard.edu
Susan Russo Gelbart	FlyBase	russo@morgan.harvard.edu
Brian Calvi	FlyBase	bcalvi@indiana.edu
Susan Celniker	BDGP	celniker@fruitfly.org
Kevin Cook	Bloomington Stock Center and Nomenclature Committee	kcook@bio.indiana.edu
Cale Whitworth	Bloomington Stock Center	calewhit@iu.edu
Patrick O'Grady	Drosophila Species Stock Center, Cornell	pmo43@cornell.edu
Jim Thompson	DIS	jthompson@ou.edu
Hugo Bellen	Bloomington Stock Center Advisory Committee & P element project	hbellen@bcm.tmc.edu
Allan Spradling	P-element project	spradling@ciwemb.edu
Stephanie Mohr	Director, DRSC/TRiP, Harvard	smohr@genetics.med.harvard.edu
Jonathan Zirin	Asst. Director, DRSC/TRiP, Harvard	jzirin@genetics.med.harvard.edu
Scott Hawley	Nomenclature Committee	rsh@stowers-institute.org
Lisa Meadows	VDRC	lisa.meadows@vbcf.ac.at
Masanobu Itoh	DGRC, Kyoto	mitoh@kit.ac.jp
Toshiyuki Takano-Shimizu	DGRC, Kyoto	fruitfly@kit.ac.jp
Chuck Langley	At Large	chlangley@ucdavis.edu
Brian Oliver	FlyBase Advisory Board	brian.oliver@nih.gov
Andrew Zelhof	DGRC, Bloomington	azelhof@indiana.edu

Genetics Society of America

Hugo Bellen	GSA Board of Directors
Suzy Brown	Senior Director
Tracy DePellegrin	Executive Director